Simulated Dynamic Pricing for Transport System Optimization

---

vorgelegt von
Dipl.-Ing. Ihab Kaddoura
geboren in Berlin

an der Fakultät V – Verkehrs- und Maschinensysteme
der Technischen Universität Berlin
zur Erlangung des akademischen Grades
Doktor der Ingenieurwissenschaften
Dr.-Ing.

genehmigte Dissertation

Tag der wissenschaftlichen Aussprache: 30.10.2019

Promotionsausschuss:
Prof. Dr. Oliver Schwedes (Vorsitzender)
Prof. Dr. Kai Nagel (Gutachter)
Prof. Dr.-Ing. Regine Gerike (Gutachterin)
Prof. Dr.-Ing. Bert Leerkamp (Gutachter)

Berlin 2019

Acknowledgements

This dissertation was funded in part by the German Research Foundation (DFG) within the projects *Investigating the use of simulated dynamic pricing to optimize transport systems (Project number 277809470)* and *An agent-based evolutionary approach for the user-oriented optimization of complex public transit systems (Project number 257622540)*, and in part by the German Federal Ministry of Transport and Digital Infrastructure (BMVI) within the project *Spatially and temporally detailed evaluation and optimization of automated and connected mobility concepts for public transport (AVÖV, FKZ 16AVF2160)*, and also by Stiftung Mercator within the project *New Emscher Mobility (NEMO)*.

I would like to express my sincere gratitude to Kai Nagel for offering me the opportunity to work in this exciting field of research, his valuable advice and guidance throughout each stage of this dissertation.

I am also very thankful to the following people for their helpful input, insightful comments and fruitful discussions: Alejandro Tirachini, Amit Agarwal, Andreas Neumann, Benjamin Kickhöfer, Billy Charlton, Daniel Röder, Dominik Grether, Dominik Ziemke, Gernot Liedtke, Gregor Leich, Janek Laudan, Joschka Bischoff, Kai Martins-Turner, Lars Kröger, Marcel Rieser, Michal Maciejewski, Michael Zilske, Theresa Thunig, and Tilmann Schlenther.

My thanks also go to Andrea Stillarius and Jakub Wilk for their constant administrative and technical assistance. I would also like to thank the staff members at the Institute of Mathematics who maintained the compute servers.

Last but not least, I am greatly indebted to my family, in particular to my wife, Omayma, and my parents, Saada and Dieter, for always supporting and encouraging me, and my three daughters for their patience and inspiration.

Table of Contents

List of Figures

List of Tables

Abstract

This thesis investigates the use of simulated dynamic pricing for the optimization of transport systems. Pricing strategies are developed and incorporated into an agent-based transport simulation framework which allows for a real-world application, complex user reactions and a detailed analysis of the pricing scheme's effects, including person-specific wins and losses. A mechanistic approach is developed which calculates dynamic and road-specific prices to be added to each user's generalized travel cost in order to provide corrected incentives to transport users and improve the overall transport system.

The first part addresses the simulation-based computation of congestion prices. Optimal user-specific bus fares are estimated by simulating user interactions and delay effects within the public transport system at a microscopic level. For road traffic, two congestion pricing approaches are developed and investigated. The first one directly builds on the Pigouvian taxation principle and computes marginal external congestion costs based on the queuing dynamics at the bottleneck links; resulting toll payments differ from agent to agent depending on the position in the queue, and the affected users' values of travel time savings. The second approach uses control-theoretical elements to adjust toll levels depending on the congestion level in order to reduce or eliminate traffic congestion; resulting toll payments are the same for all travelers per time bin and road segment. The second part of this thesis describes the computation of noise damages and prices. An activity-based and dynamic average and marginal noise cost pricing approach is presented which accounts for the within-day dynamics of varying population densities in different areas of the city. The simulation experiments indicate that the pricing approach can be used to improve the overall system welfare and to derive traffic control strategies. The third part of this thesis elaborates on the interrelation of external effects, in particular road traffic congestion, noise and air pollution. Simulation experiments are carried out for different assumptions regarding transport users choice dimensions which are found to have a crucial effect on the simulation outcome. The fourth part of this thesis addresses optimal pricing strategies in regard to the prospect of future mobility concepts. Applying the congestion pricing methodology to the Shared Autonomous Vehicle (SAV) mode highlights the importance of also controlling the private car mode in order to improve a city's transport system.

Zusammenfassung

Die vorliegende Arbeit untersucht den Einsatz simulierter dynamischer Preise für die Optimierung von Verkehrssystemen. Es erfolgt die Entwicklung und Einbindung verschiedener dynamischer Bepreisungsstrategien innerhalb einer agenten-basierten Verkehrssimulation, mit der sich reale Fallstudien untersuchen, komplexe Nutzerreaktionen abbilden sowie detaillierte Wirkungsanalysen einschließlich personenspezifischer Gewinner-Verlierer-Analysen durchführen lassen. Ein mechanistischer Ansatz wird entwickelt, der mittels dynamischer und straßen-spezifischer Preise, die zu den generalisierten Kosten individueller Reisender hinzugefügt werden, die Anreizwirkung so korrigiert, dass sich der Zustand des gesamten Verkehrssystems verbessert.

Der erste Teil der Arbeit behandelt die simulationsgestützte Berechnung von Staupreisen. Optimale nutzer-spezifische Busfahrpreise werden abgeschätzt, indem Wechselwirkungen zwischen Nutzern und Wartezeiten innerhalb des öffentlichen Verkehrs mikroskopisch simuliert werden. Für den Straßenverkehr werden zwei Ansätze zur Bepreisung von Stau entwickelt und untersucht. Der erste Ansatz baut direkt auf dem Konzept der Pigou-Steuer auf und berechnet externe Staugrenzkosten basierend auf der Warteschlangen-Dynamik an Engpässen. Resultierende Mautzahlungen variieren von Agent zu Agent je nach Position innerhalb der Warteschlange sowie individuellem Zeitwert der verzögerten Personen. Der zweite Ansatz nutzt einen regelungstechnischen Ansatz zur Berechnung einer dynamischen Maut zur Reduzierung bzw. Eliminierung von Stau. Resultierende Mautzahlungen sind pro Zeitintervall und Straßenabschnitt konstant für alle Nutzer. Der zweite Teil der Arbeit thematisiert die simulationsgestützte Berechnung von Lärmschäden sowie -preisen zwecks Internalisierung. Es wird ein aktivitätenbasierter und dynamischer Ansatz zur Bepreisung von Durchschnitts- und Grenzkosten vorgestellt, der zeitlich und räumlich variierende Bevölkerungsdichten in unterschiedlichen Teilen der Stadt berücksichtigt. Die Simulationsexperimente zeigen, dass der Bepreisungsansatz zur Steigerung der Gesamtwohlfahrt sowie Ableitung von Verkehrsmanagementstrategien genutzt werden kann. Der dritte Teil der Arbeit legt den Fokus auf die Wechselwirkung von externen Effekten, insbesondere Stau, Lärm und Luftschadstoffen. Es werden Simulationsexperimente für verschiedene Annahmen bzgl. der Wahlmöglichkeiten von Verkehrsnutzern durchgeführt, welche einen entscheidenen Einfluss auf die Simulationsergebnisse haben. Der vierte Teil der Arbeit befasst sich mit optimalen Bepreisungsstrategien mit Blick auf zukünftige Mobilitätskonzepte. Die Anwendung der Staubepreisungsmethodik auf eine Fallstudie mit geteilten autonomen Fahrzeugen unterstreicht die Wichtigkeit der zusätzlichen Regulierung des motorisierten Individualverkehrs zur Verbesserung des städtischen Verkehrssystems.

CHAPTER 1

Introduction

1.1 Motivation

Being stuck in traffic is not only frustrating but also comes at a high cost for the economy and for society as a whole. Aside from the significant amount of time which is lost in traffic congestion (see, e.g., Reed and Kidd, 2019), a less fluent traffic flow increases fuel consumption and exhaust emissions. Transport-related environmental impacts such as noise and air pollution are growing public health issues causing diseases and premature deaths (see, e.g., Krzyzanowski et al., 2005; WHO Europe, 2011; Walton and et al, 2015). With more than 25,000 fatalities and more than 1.4 million injured people per year in the European Union, road traffic accidents make up a significant proportion of societal costs (European Commission, 2018). Despite these negative impacts, transport remains a vital component of daily life. The ability to travel from one place to another forms the basis of several economic and social activities. A major challenge in transport planning is to incorporate the negative impacts of transport such as environmental effects into the rebalancing of transport supply and transport demand. Traffic management may help in utilizing the existing transport supply in the most efficient way. Pricing poses an incentive-based approach to manage traffic and additionally provides a revenue stream that may be used for reinvestments in the public sector.

The remainder of this chapter is structured as follows. Sec. 1.2 addresses the basic relevant economic concepts of external effects and pricing. Sec. 1.3 provides the research questions posed in this thesis. In Sec. 1.4, the general research approach is presented, including the key features of the agent-based and dynamic pricing approach. An overview of the applied simulation framework is provided in Sec. 1.5. The outline of this thesis and overview of simulation experiments and applied case studies are given in Sec. 1.6.

1.2 The Concept of External Cost Pricing

The following paragraphs provide some edited excerpts from the introductory sections of the following chapters. For a more detailed literature review of transport-related external effects and pricing studies, please refer to, e.g., Sec. 4.1, Sec. 6.1 or Sec. 8.1.

External Effects Transport users do not only invest their own time and money, but impose so-called external costs such as congestion, air pollution, noise, or accidents on other individuals within the transport sector or outside the transport sector. External costs are not borne by the causing individual and are, thus, not considered in the individual's decision making process (see, e.g., Verhoef, 2001). Several studies indicate that traffic congestion makes up the largest part of the transport related external costs (see, e.g., Maibach et al., 2008; Small and Verhoef, 2007; de Borger et al., 1996; Parry and Small, 2009). Further important contributions to the total external costs are air pollution, noise and accidents (Nash, 2003; Parry and Small, 2005; Maibach et al., 2008). The environmental effects, in particular air pollution and noise, are usually categorized into local damages (e.g., carcinogenic exhaust gases, noise) and global effects (greenhouse gases, e.g., carbon dioxide (CO_2)) (Beckers et al., 2007). Depending on the time of day (e.g., peak-time vs. off-peak), spatial structure (e.g., urban vs. rural area, densely vs. sparsely populated area), available modes of transportation (e.g., Public Transport (PT) vs. car) and vehicle fleet composition (e.g., electric vs. combustion engine) as well as the monetization approach and resulting cost rates, each external effect's contribution to the total external costs may vary. This highlights the importance for a case-specific and differentiated investigation of external effects.

Using Pricing to Improve the Transport System If the transport users had to compensate for their external costs, they might change their behavior, e.g., use other transport routes, other times of day, switch to environmentally friendlier vehicles or modes, travel less or even move closer to their work place. The concept of pricing can be understood as a decentralized (or market-based) tool to change individual travel behavior towards an overall improved transport system (see, e.g., Maibach et al., 2008; Small and Verhoef, 2007). The idea to charge a toll that is equal to the marginal external costs, also referred to as *internalization of (marginal) external effects*, goes back to Pigou (1920) based on the theoretical foundations laid by Marshall (1920). Pigou (1920) addresses the change in people's behavior towards a higher system efficiency by imposing a toll that is equal to the marginal external costs. The assumption is that the toll would make users take into account their contribution to the external costs, for example additional travel times that they impose on other travelers or the increase in noise damages that they impose on residents along the road. Consequently, an individual should only travel when his or her own benefit of being at the trip destination is larger than the sum of the own costs (private costs) *and* the damages imposed on others (external costs).

For static congestion, the economic standard model based on Pigou (1920), depicted in Fig. 1.1, considers a single Origin-Destination (OD) pair and assumes all trips to take place in a single time-independent interval. The market equilibrium (point E) is described by the intersection of the demand curve $d(q)$ and the marginal private cost $mpc(q)$, where q denotes the traffic volume and q_E denotes the traffic volume in the market equilibrium. The system optimum (point O) is described by the intersection of the demand curve $d(q)$ and the marginal social cost function $msc(q)$, resulting in the optimal traffic volume q_O. In the case of the existence of external costs, the $mpc(q)$ and $msc(q)$ curve differ. In that case, the generalized user costs provide failing incentives and the market equilibrium results in a welfare loss (marked by the shaded area). Applying the concept of Pigouvian taxation (also referred to as 'Marginal Social Cost (MSC) Pricing'), external costs are internalized by adding the optimal toll $\tau = msc(q_O) - mpc(q_O)$ to the transport users' private costs which then corrects for the failing incentives and shifts the market equilibrium towards the system optimum. The demand curve $d(q)$ describes the transport users' marginal benefits and is given by the users' willingness-to-pay for the trip. Very often, this concept is explained using the terms *average cost* instead of $mpc(q)$ and *marginal cost* instead of $msc(q)$ (see, e.g., Button, 1993).

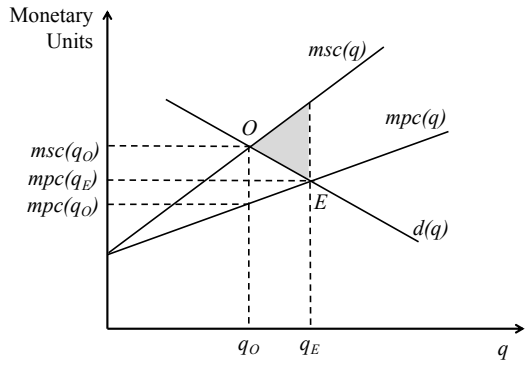

Figure 1.1: Static market diagram: MSC vs. Marginal Private Cost (MPC)

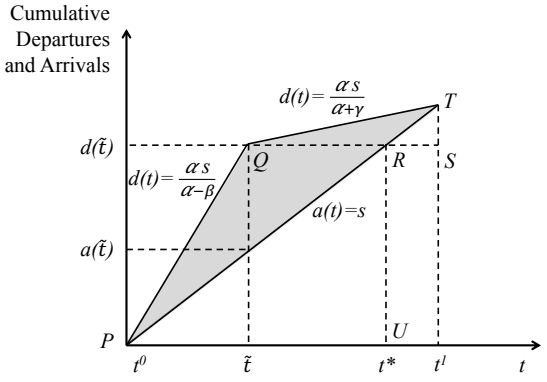

Figure 1.2: Vickrey's dynamic bottleneck model

For dynamic traffic congestion, a prominent example for optimal pricing is the bottleneck scenario, presented by Vickrey (1969) and depicted in Fig. 1.2 based on Arnott et al. (1990). Vickrey's

scenario considers a single OD which only consists of a single bottleneck that has to be passed in order to get from the origin to the destination. $d(t)$ denotes the cumulative departures at time t. $a(t)$ are the cumulative arrivals which corresponds to the capacity of the bottleneck denoted by s. All individuals have a desired arrival time of t^*. At time t^0 the first individual departs and the queue starts to evolve. At time t^1 the queue has dissolved and all individuals have arrived at their destination. The individual departing at $\tilde{t}$ arrives punctually at t^*, individuals departing at $t < \tilde{t}$ arrive too early, individuals departing $t > \tilde{t}$ arrive too late. The total early arrival time is PRU, the total late arrival time is RTS. The slope of $d(t)$ results from s, the marginal cost of traveling α, the marginal cost of early arrival β and the marginal cost of late arrival γ. The vertical distance between $d(t)$ and $a(t)$ is the number of queued individuals and the horizontal distance between $d(t)$ and $a(t)$ is the queuing time (or travel time). Similar to the static market diagram shown in Fig. 1.1, the generalized user costs provide failing incentives and the user equilibrium yields a welfare loss which amounts to the total queuing time PQT (marked by the shaded area). In contrast to Fig. 1.1, the optimal toll is capable of fully eliminating the queue and resulting time losses at the bottleneck. The optimal toll is time-dependent and increases linearly from t^0 to a maximum value at t^*, and then decreases linearly to 0 at t^1. This tolling scheme induces a departure rate (inflow of vehicles) which is equal to the capacity of the bottleneck. From the user perspective, waiting time is traded for toll payments, leaving the users as well off as before. From the government's perspective, a revenue stream is generated that can be used to make some or all people better off. In that study, the network is to a very high degree stylized, and congestion is considered to occur in form of a queue at the bottleneck. User reactions to the tolling scheme are found to modify the distribution of departure times such that the traffic inflow to the bottleneck is reduced to its capacity, thus eliminating the queue. Since this scenario can be solved analytically, it has been studied widely in the transport economics literature and several extensions are applied, e.g., heterogeneous Values of Travel Time Savings (VTTS) (Vickrey, 1973) or demand elasticity Arnott et al. (1993). Arnott et al. (1993, p. 166) observe that "private cost and marginal social cost are determined by the pattern of congestion over the entire period of use, and not, as is assumed in the standard analysis, by the number of users over some portion of the period", implying that, once schedule delay costs are included, it is no longer possible to cut the time period of interest into several time slots and determine the optimal toll in them independently. Arnott et al. (1993, p. 166) also point out that "Marginal social cost should be computed *mutatis mutandis*, not *ceteris paribus*; that is, marginal social cost is computed incorrectly if one adds a commuter and computes the increase in social cost from doing so, without allowing other drivers to adjust their departure times.", implying that an iterative approach might be useful if the problem cannot be solved analytically.

Pricing in Practice There are several limitations for the real-world implementation of an optimal pricing scheme as implied by theory. A toll which changes every second or from one road segment to the next poses several difficulties. The pricing scheme may be too complex to be understood by the transport users who consequently cannot adjust their travel behavior accordingly. Furthermore, a complex tolling scheme may be technically difficult to implement or yield high toll collection costs. A vehicle-specific or road usage-based pricing scheme may as well be related to privacy issues. Therefore, several studies address practice-oriented solutions to control traffic that can easily be implemented in the real world (Verhoef, 2001; Proost and van Dender, 2001; Small and Verhoef, 2007; Tirachini and Hensher, 2012). In addition, there is often severe opposition against pricing by the population (Schade and Schlag, 2000).

Common tolling schemes for road traffic are area-pricing (e.g., London) or cordon-pricing (e.g.,

Stockholm) (Beckers et al., 2007; Eliasson and Jonsson, 2011). Advanced pricing strategies may combine time dependent tolling (peak pricing), vehicle-specific price categories, and different rates for different transport routes as for instance applied in Singapore (MoT, 2019). A more simple and widely used approach is to impose a tax on fuel ("energy tax") or the vehicle itself, e.g., based on the engine capacity or CO_2 emission per km. With respect to PT, a common approach is the use of time and zone dependent fares as for instance applied in London (anytime vs. off-peak tickets, TfL, 2019) or Berlin ("10-Uhr-Karte", BVG, 2019). Different technologies such as camera systems, Dedicated Short Range Communication or satellite-based systems may be used for a differentiated collection of tolls or fares. Most on-demand transport services (see, e.g., Uber, 2019; Lyft, 2019) charge higher fares due to increased demand during peak times.

All of the existing pricing schemes have a different (wanted or unwanted) control effect addressing different choice dimensions of transport users. In general, vehicle taxes may provide an incentive to buy a more environmental friendly vehicle or even switch to alternative modes of transportation. Peak pricing may motivate transport users to travel off-peak and avoid the rush hour. In contrast, localized schemes (e.g., cordon-pricing, area-pricing or road-specific tolling) rather provide an incentive to change routing decisions or even transport mode decisions for trips from, to or within certain areas.

1.3 Research Questions

Starting from a more general perspective, the first research question addresses the overall functionality of the proposed pricing methodology: Is simulated dynamic pricing a useful approach for the optimization of transport systems? In this context, the next research question explores both the effectiveness and effects of the pricing methodology: How do congestion pricing or noise pricing change travel behavior and is there a positive impact on the overall system welfare? The following research question directly builds on the previous one and addresses the interrelation of different external effects: How are congestion, noise and air pollution correlated with each other; or, what impact does the pricing of a single external effect have on the others? A further research question investigates the design of the simulation-based pricing methodology: What are the implications for the design of a pricing strategy resulting from a simulation framework which allows for real-world case studies and stochastic user behavior? Additionally, varying assumptions regarding transport users' travel behavior are tackled: How do simulation results change if transport users' mode choice decisions are incorporated into the transport model? Finally, optimal pricing strategies are addressed in the context of innovative modes of transportation: How may simulated dynamic pricing contribute to an improvement of the transport system in regard to the prospect of Shared Autonomous Vehicles (SAVs)?

1.4 Research Approach

This thesis investigates the use of simulated dynamic pricing for the optimization of transport systems. Pricing strategies are incorporated into a simulation framework which allows for a real-world application, complex user reactions and a detailed analysis of the pricing scheme's effects, including person-specific wins and losses. A simple mechanistic approach is developed which builds on the basic concepts of optimal pricing theory (Sec. 1.2). The approach calculates dynamic and road-specific prices to be added to each user's generalized travel cost. This cost correction may be

interpreted as a price to be charged from the transport user, but it can just as well be interpreted as a computational device to move the system to a better operating point. Iterations of these models, where in each iteration some synthetic travelers react to the charges, should then lead to a better and potentially to the optimal solution. This approach has recently become possible with the advent of powerful computers and powerful person-oriented traffic simulation software. The approach is applied within the activity-based and agent-based dynamic simulation framework Multi-Agent Transport Simulation (MATSim) (see Sec. 1.5). The core idea is to keep track of all relevant external effects which are imposed on other transport users (e.g., delays), on residents (e.g., noise, carcinogenic air pollutants) and on the global population (greenhouse gas emissions) at a very sophisticated level of detail. More precisely, external effects may be calculated (i) for each road segment, (ii) for each time step, and (iii) even for each traveler. The advantages of the innovative simulation-based approach are listed below.

- Using an **agent-based approach** allows to (i) calculate external effects for each traveler or vehicle type separately and (ii) convert these effects into prices which take into account heterogeneity in demand, such as different VTTS or vehicle types.
- The traffic simulation which is used by the simulation framework makes reasonable compromises between the computational performance and the level of detail. Therefore, the presented approach allows for large-scale networks, a sophisticated representation of the demand side, e.g., multiple origin-destination points and **real-world application**.
- The applied **traffic simulation** is based on a queue model developed by Gawron (1998) which accounts for flow and storage constraints. The combination of these two means that congestion becomes a history-dependent effect, with the result that optimal prices in different time slots are no longer independent from each other (see Arnott et al., 1990).
- The prices are added to the individual's generalized travel cost to induce changes in user behavior. In order to predict these user reactions correctly, it is therefore crucial to account for all relevant choice dimensions. The simulation framework which is used in this research project applies an evolutionary approach to model **complex user reactions**, such as route choice, mode choice and departure time choice. By applying a random utility based approach the simulation framework also accounts for unobserved attributes and randomness in user behavior.
- The external effects are imposed on other travelers (e.g., congestion, local air pollutants) as well as individuals at home, work and other activity locations (e.g., noise, local air pollutants). Applying an activity-based simulation framework allows for a detailed consideration of the **affected individuals** in order to quantify the exposure costs and set the price level.

The attraction of the pricing approach lies in the fact that optimal prices may be derived locally – by just pricing the external costs – and if this is done everywhere, the system by itself moves towards a better state. However, as pointed out in Sec. 1.2, real-world pricing can rarely be designed exactly as implied by theory. Even if pricing itself is not considered as a viable real-world policy option, the developed methods will help by providing a benchmark of what could be achieved, and by providing guidance in which direction the system would need to be changed in order to realize those gains. The simulation results may help in assessing how the transport system would change if the pricing approach was implemented in practice. Importantly, the approach may be used to obtain hints on where to concentrate efforts to improve the system and how to trade off conflicting goals, for example between noise impacts and time losses. The prices may also be considered as theoretical cost correction terms to improve the transport system and may be incorporated into (intermodal)

routing applications. Furthermore, Autonomous Vehicles (AVs) create new opportunities in the context of traffic control. Instead of providing route recommendations or price incentives to humans, complex traffic management strategies may directly control the operation of AVs. In particular, dynamic vehicle routing and dispatch strategies may aim for the maximization of the overall system welfare by taking into consideration the time- and road-specific marginal external costs. This offers a crucial advantage over existing pricing schemes which aim at a change in human travel behavior.

1.5 Simulation Framework: Multi-Agent Transport Simulation (MATSim)

This section provides a brief overview of the activity-based transport simulation MATSim which is used and extended in this thesis. MATSim is an open-source software developed under the terms of the GNU General Public License (`https://www.gnu.org/licenses/`), version 2 or later, published by the Free Software Foundation (`https://fsf.org`). The core code and several extensions are available on GitHub (`https://github.com/matsim-org/matsim`). The software structure follows a modular design which allows for an easy replacement or extension of the default functionality. The overview of MATSim provided in this section refers to the simulation setup which is most relevant for this thesis. The following is a combined and edited version of MATSim related descriptions in several articles that have been previously published, see, e.g., Kaddoura and Nagel (2016b, 2019, 2018); Kaddoura et al. (2017c); Kaddoura (2015), and Neumann et al. (2016); Kaddoura et al. (2015a) for the description related to PT, or Kaddoura et al. (2018) for the description related to SAVs.

In MATSim, each transport user is simulated as an individual agent. The agents' initial behavior has to be provided in the form of travel plans describing the daily activity patterns (e.g., home-work-shopping-home), the activity locations, the activity end times and information about the trips between these activities. The initial travel behavior is then modified applying an evolutionary iterative approach. In each iteration, (1) the travel plans are executed (Traffic simulation), (2) scored (Evaluation) and (3) modified (Learning). (1) represents the agents' physical behavior; (2) and (3) describe the agents' mental behavior.

1. **Traffic Simulation** All travel plans are simultaneously executed and the transport users interact in the simulated physical environment. Traffic congestion and vehicle movements are simulated applying a queue model (Gawron, 1998). Each road segment (link) is modeled as a *First In First Out* queue with certain attributes, i.e, a free speed travel time t_{free}, a flow capacity c_{flow} which limits the outflow (in the literature often referred to as 'bottleneck congestion', see, e.g., van den Berg, 2011), and a storage capacity $c_{storage}$ which limits the number of vehicles on a link and causes spill-back. Each time step, typically 1 second (*sec*), the state of each link's queue is updated. A vehicle is only moved from link l_1 to link l_2 if (i) the free speed travel time (given by the freespeed and length of link l_1) has passed, (ii) the inverse of the flow capacity has passed since the last vehicle left link l_1, and (iii) there is space on link l_2. Individual movements of agents can be aggregated to traffic flows that are found to be consistent with the fundamental diagram (see, e.g., Agarwal et al., 2015).

   MATSim also simulates the interaction of **PT** users, transit vehicles and road traffic. The transit schedule provides all planned PT operations. Transit vehicles may be delayed by (i) other road users and (ii) PT users. Transit vehicles are included in the traffic flow simulation, thus, buses and cars may compete for the same limited road capacity. Each stop can be

configured to either block the traffic or to allow overtaking whenever a bus stops. Depending on the vehicle type, i.e., the number of doors, and the assumption regarding simultaneous or sequential boarding/alighting, transit vehicles may be delayed by passengers at transit stops. In case a vehicle is fully loaded, additional boardings are denied and passengers will have to wait for the next transit vehicle. Vehicles of one transit line can serve different tours. Consequently, the delay of one vehicle can be transferred to the following tour. In the case of a delay, the driver will try to follow the schedule by shortening dwell times (if no person wants to alight or board) as well as slack times. For a detailed description of MATSim's PT dynamics, see Rieser (2010) and Rieser (2016).

The simulation of **SAVs** is based on an existing module for dynamic vehicle routing problems (Maciejewski, 2016; Maciejewski et al., 2017) and an existing module for the simulation of taxis or SAVs (Bischoff and Maciejewski, 2016a). SAV users need to order an SAV once they have left their activity location, wait for an available SAV to arrive, get on the SAV and get off the SAV at the destination. SAVs interact with each other and other vehicles, e.g., Conventional (driver-controlled) private Cars (CCs), and may get stuck in traffic.

2. **Evaluation** For each agent, the executed plan is evaluated based on agent-specific predefined behavioral parameters and utility functions. A plan's deterministic utility (often referred to as 'score') typically consists of two parts: (i) the generalized travel cost or trip-related disutility (e.g., travel time, monetary payments) and (ii) the utility gained from performing activities:

$$V_{p,i} = \sum_{a=1}^{A} \left(V_{p,a}^{act} + V_{p,a}^{trip} \right) , \tag{1.1}$$

where $V_{p,i}$ is the person p's total utility (deterministic part) for a given plan i; A is the total number of activities; $V_{p,a}^{act}$ is the (positive) utility earned for performing activity a; and $V_{p,a}^{trip}$ is the (usually negative) utility earned for traveling to activity a. Activities are assumed to wrap around the 24-h-period, that is, the first and the last activity are stitched together. In consequence, there are as many trips between activities as there are activities. The first part typically considers the mode of transportation, the travel time, waiting, access and egress times and monetary costs (e.g., operation costs, fares, tolls). The latter part is based on the approach by Charypar and Nagel (2005) where the marginal gain is typically positive but decreases with the duration spent at the activity location:

$$V_{p,a} = \beta^{perf} \cdot t_a^{typ} \cdot \ln \left(t_{p,a}^{perf} / t_{0,a} \right) , \tag{1.2}$$

where $t_{p,a}^{perf}$ is the time person p performs activity a, t_a^{typ} is an activity's *typical duration*, β^{perf} is the marginal utility of performing an activity at its typical duration, and $t_{0,a}$ is defined as

$$t_{0,a} = t_a^{typ} \cdot \exp(-1) , \tag{1.3}$$

see Horni et al. (2016, Sec. 97.4.2) for a discussion of this setting. Further activity-related constraints can easily be incorporated. An activity can only be performed during opening times. If an agent arrives at an activity location before or after the activity is open, the early or late arrival penalty results from the opportunity cost of time which is approximately equivalent to β^{perf}. Additionally, there may be a late arrival penalty β^{late} which comes on top of the opportunity cost of time if an agent arrives after the *latest arrival time* which can be specified for each activity. Depending on the agent-specific travel plans, in particular the

number and types of activities, agents are differently pressed for time, resulting in different VTTS.

3. **Learning** For the majority of agents, the plan to be executed in the next iteration is chosen based on a multinomial logit model. During the phase of choice set generation, some agents generate new travel plans by cloning an existing plan and changing parts of the cloned plan. The following provides an overview of the agents' basic choice dimensions which may be enabled separately or simultaneously.
   - **Route Choice:** Based on the link-specific costs in the previous iterations such as travel times and toll payments, an agent's new transport route (sequence of links between one activity location and another one) is identified applying a least-cost path approach. To increase the diversity of identified transport routes, a random term may be added to the link-specific costs.
   - **Mode Choice:** Agents randomly choose from the set of available modes (e.g., car, PT, walk, bicycle, taxi) to replace the mode of an existing trip or (sub-)tour (e.g., the trip from home to work and the trip back home). Available modes may be specified for different agents or subpopulations.
   - **Departure Time Choice:** Activities' end times (departure times) are shifted by a random time period within a predefined maximum range. Typically, the predefined maximum time shift range is set to 2 h.

   The newly generated travel plan will then be executed in the next iteration. Typically, the maximum number of travel plans per agent is limited, thus, the plan with the worst performance is discarded and plans that result in a higher utility are kept in the agent's choice set.

A repetition of these steps enables the agents to improve and obtain plausible travel plans, and the simulation results stabilize. Assuming that the set of each agent's travel plans represents a valid choice set, the system state is an approximation of the stochastic user equilibrium (Nagel and Flötteröd, 2012). Further details of the simulation framework MATSim are for example given in Horni et al. (2016).

1.6 Outline

The thesis is structured as follows. Part I addresses the simulation-based computation of congestion prices in the PT mode (Ch. 2) and car mode (Ch. 3, Ch. 4). Part II describes the computation of noise damages (Ch. 5) and noise prices (Ch. 6, Ch. 7). In Part III, prices are set accounting for several external effects (congestion and noise in Ch. 8; congestion, noise and air pollution costs in Ch. 9). Part IV addresses optimal pricing strategies for SAVs. Finally, Ch. 11 provides an overall conclusion and outlook. The thesis comprises selected studies conducted in different projects over a period of several years. The newly developed methodology was continuously extended and applied to different case studies. Tab. 1.1 provides a summary of the simulation experiments carried out in this thesis, including the applied scenario (or case study) and considered choice dimensions of transport users.

Table 1.1: Simulation experiments carried out in this thesis

		Scenario	Choice dimensions
	Part I: Congestion Pricing		
Ch. 2	Internalization of Public Transport Delays	Multi-Modal Corridor	mode + time
Ch. 3	Agent-based Congestion Pricing with Heterogeneous with Heterogeneous VTTS	Berlin (Neumann et al., 2014)	route
Ch. 4	Congestion Pricing in a Real-world Oriented Agent-based Simulation Context	Vickrey's bottleneck	time
Ch. 4	Congestion Pricing in a Real-world Oriented Agent-based Simulation Context	Berlin (Ziemke et al., 2019)	route route + time + mode
	Part II: Noise Pricing		
Ch. 5	Activity-based and Dynamic Calculation of Road Traffic Noise Damages	Berlin (Neumann et al., 2014)	-
Ch. 6	Average Noise Cost Pricing	Berlin (Neumann et al., 2014)	route
Ch. 7	Marginal Noise Cost Pricing	Berlin (Neumann et al., 2014)	route
	Part III: Simultaneous Pricing of Several External Effects		
Ch. 8	Simultaneous Internalization of Traffic Congestion and Noise Costs	Berlin (Neumann et al., 2014)	route
Ch. 9	Simultaneous Internalization of Congestion, Noise and Air Pollution Costs	Munich (Agarwal and Kickhöfer, 2016)	route route + mode
	Part IV: External Cost Pricing in a World of Shared Autonomous Vehicles		
Ch. 10	External Cost Pricing in a World of Shared Autonomous Vehicles	Berlin (Ziemke et al., 2019)	route + time + mode

Part I

Congestion Pricing

CHAPTER 2

Internalization of Public Transport Delays

This chapter addresses optimal price setting for the PT mode. A methodology is presented which directly builds on the simulation of user interactions at a microscopic level. User-specific fares are set based on the marginal delay effect which occurs in form of prolonged in-vehicle and waiting times. This chapter is an edited version of a previously published paper (Kaddoura et al., 2015b) in which the description of the multi-modal corridor and simulation setup is partly based on Kaddoura et al. (2015a).

2.1 Introduction and Problem Statement

In the transport sector congestion, air pollution, noise and accidents are sources of inter- or intra-sectoral external costs leading to welfare losses and an inefficient market equilibrium (van Essen et al., 2008, see also Sec. 1.2). Marginal social cost pricing means setting generalized prices equal to the sum of marginal producer costs, marginal private user costs and marginal external costs. By charging the optimal fare, external effects are internalized and taken into account by users. Thus, the right incentives are given to achieve market efficiency and maximize social welfare.

Since theoretical first best conditions do not exist in reality (e.g., due to underpriced competing modes, difficult computation, unfeasible application), second best solutions are required (Verhoef, 2001; Proost and van Dender, 2001; Small and Verhoef, 2007). Insights from the first best solution may help to develop a second best pricing strategy. Furthermore, the first best solution can be used as a theoretical benchmark for the evaluation of other measures.

In this chapter, the general PT marginal cost pricing principle is introduced in MATSim, in which passenger-specific first-best fares can be calculated even in large scale scenarios. This is the first model that considers microscopic user-by-user bus fares, calculated with the objective to maximize social welfare. Accounting for time-dependency and queue formation allows for simulating the interaction of activity scheduling decisions and PT pricing. Three sources of external delays are accounted for when calculating the effect of an extra passenger taking the bus: (i) delay for passengers on-board, (ii) delay for passengers waiting at downstream stops and (iii) extra waiting time for passengers unable to board a full bus. Depending on the total delay imposed on other passengers, a user-specific fare is computed. In this study, other externalities such as crowding costs and road congestion are excluded. The microscopic price differentiation is compared against the classical flat fare rule in order to analyze differences in terms of revenue, optimal frequency of service and social welfare. In reality, charging an individual-specific fare for each trip would be difficult to implement and could even be considered unethical. Therefore, temporal and spatial effects are analyzed by calculating average fares for each user-specific pricing scenario, which may be used as a starting point for more practical (second-best) pricing schemes, for instance, charging users anonymously according to time of day and location of boarding (and perhaps also location of disembarking). Importantly, the approach is useful to analyze the relationship between optimal pricing and trip length at a microscopic level, an issue previously addressed with analytical models by Mohring (1972); Turvey and Mohring (1975); Kraus (1991), as discussed in the next section. A numerical example provides insights on the sensitivity of the user-specific optimal bus fare to travel distance and to the headway between vehicles, in which the relevance of introducing user-specific bus fares – as opposed to optimal flat fares – is evident.

Most studies on transport externalities focus on the private transport sector. Congestion is usually the largest part of all external costs in peak periods, whereas in off-peak periods other externalities such as pollution and accidents have been found to be at comparable levels with congestion (de

Borger et al., 1996; Parry and Small, 2009). In the context of urban PT modes, external effects among PT users are investigated to a lesser extent (Maibach et al., 2008; Prud'homme et al., 2012). Nash (2003) addresses the urban rail sector and relates delays to the traffic volume by regression, finding delay effects to be the most significant external effect. A number of recent survey-based studies find that crowding externalities can be a substantial part of total travel costs (Wardman and Whelan, 2011; Prud'homme et al., 2012; Haywood and Koning, 2013). While most discomfort studies address in-vehicle crowding, some studies also include crowding in access-ways and platforms (Lam et al., 1999; Douglas and Karpouzis, 2005). Several authors have incorporated external effects in analytical models that usually account for delays due to capacity constraints, boarding and alighting passengers, the disutility of crowding and congestion effects among vehicles at bus stops or train stations (see, e.g., Mohring, 1972; Turvey and Mohring, 1975; Kraus, 1991; Parry and Small, 2009; de Palma et al., 2015a; Tirachini, 2014; Tirachini et al., 2014). Turvey and Mohring (1975) analyze delay effects induced by boarding and alighting passengers to (i) passengers inside the bus and (ii) passengers waiting at a transit stop who will enter the bus either further along the route or at the same stop behind agents who get on and off the bus. However, the authors explain, in case of random passenger arrival patterns at transit stops, the second effect disappears on average. That is because agents with shorter waiting times compensate for agents with a longer waiting time.

The only external effect considered in Mohring (1972) are delays that boarding and alighting passengers impose on passengers who are inside a transit vehicle. In this case, the optimal fare increases as a function of the number of passengers inside a transit vehicle because those passengers experience an extra delay when a new passenger gets on or off a vehicle. For the case of a feeder route, Mohring (1972) finds marginal cost to be inversely related to the trip length because when buses approach the Central Business District (CBD) they increase in passenger number. However, Turvey and Mohring (1975) point out that this rule does not hold for the case of limited vehicle capacities and the probability of fully loaded buses causing passengers not to be able to board the first arriving bus. That is, short-distance passengers may not be able to board a bus full of longer-distance passengers. Along the same lines, Kraus (1991) found that when including an external discomfort cost, long-distance sitting passengers impose a discomfort cost on short-distance passengers who are unable to find a seat, and therefore, are forced to stand.

Beyond analytical models, marginal social cost pricing on PT has not received much attention in activity-based simulations, which are less simplifying and more applicable to real-world scenarios. Analytical models usually ignore more complex user reactions, i.e., time adaptation, and the situation of coordinated arrival patterns in which passengers schedule their arrival according to a published timetable of services (see Jansson (1993) for a model with coordinated arrival patterns). Whereas the cost of prolonged in-vehicle times as well as the disutility of crowding and discomfort are addressed by several authors, external waiting cost resulting from boarding and alighting passengers is less intensively discussed. In Kaddoura et al. (2015a) flat bus fares are optimized applying a simulation-based grid search approach, finding delay effects due to passenger transfers and capacity constraints to have a major impact on the social welfare and optimal pricing structure. The present study takes up these findings and addresses the setting of optimal PT pricing by investigating the marginal cost imposed by PT users on other users, at a microscopic user-by-user level. Results in terms of social welfare, distribution of optimal fares and optimal frequency of service can be used as a benchmark for the analysis of other pricing policies such as flat fares.

2.2 Methodology: Agent-based Computation of Marginal External Delay Effects

This study enhances MATSim by implementing a marginal social cost pricing approach. On an agent-based level external effects, marginal delays and number of affected users, are traced back to their origin. These *ceteris paribus* external effects are internalized by charging the equivalent monetary amount from the agent who is causing the delay effects. This approach neglects the fact that transport users may adapt to the monetary payments, for example by departing earlier or later. An optimal pricing scheme, in contrast, would follow a *mutatis mutandis* approach and account for the users' reactions in order to avoid delays or monetary payments (see, e.g., Arnott et al., 1993; Button, 2004, see also Ch. 4). Similar to the Queue based Congestion Pricing (QCP) described in Sec. 4.3.1, from iteration to iteration, users are enabled to change their travel behavior, marginal external effects are recomputed and prices updated. Hence, for multiple iterations, the pricing approach accounts for the users' changes in travel behavior.

Of all existing external effects (see Sec. 1.2) this study focuses on delay effects among users within the PT mode. That is, road congestion and interferences between buses and cars are excluded (see Sec. 2.3.1) and the disutility of traveling (in-vehicle time) is independent from crowding effects inside the transit vehicles or the seat availability (see Tab. 2.3). As slack times are used to catch up on delays, operating costs are constant and only depend on the number of buses. Hence, marginal operating cost per passenger is 0 Australian Dollar (AUD) and the optimal user-specific fare is equal to the external cost only. External effects which are considered in this study either prolong in-vehicle times or waiting times. Sources for externalities are capacity constraints and delays induced by boarding/alighting passengers.

Effect 1: In-vehicle time delays due to boarding and alighting passengers
Assuming a scheduled minimum dwell time of 0 sec, transit vehicles will be delayed when agents are boarding or alighting. Therefore travel times, i.e., in-vehicle-times, increase with the number of agents who get on and off the bus. **An agent who is boarding imposes a delay of the average boarding time (1 sec) on each agent inside the transit vehicle.** To give an example, for two passengers inside a vehicle the total external effect amounts to 2 sec (see Fig. 2.1). Thus, the equivalent monetary amount that is charged to the causing agent amounts to $VTTS_{v,pt} \times \frac{2}{3600} h$. In this setup bus drivers are not able to catch up on delays except during slack times at the route endpoints when there is no passenger inside the vehicle.

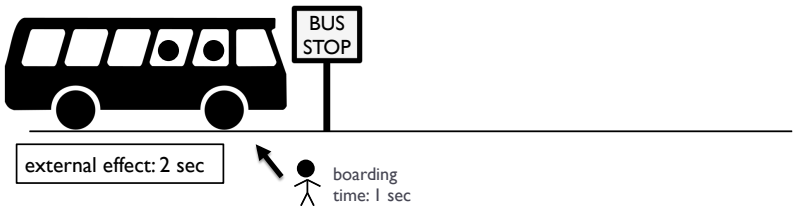

Figure 2.1: External effect 1

Effect 2: Waiting time delays due to boarding and alighting passengers
As referred to in Sec. 2.1, another external effect is discussed in context of passengers who get on and off buses. In case travelers' arrival patterns at transit stops are coordinated, meaning the users

try to reach the stop shortly before a bus arrives, there may be users with **prolonged waiting times due to other passengers who are boarding or alighting**. As the agents are assumed to adapt to the schedule, this effect does not cancel out on average as is the case for random passenger arrivals in Turvey and Mohring (1975). Nevertheless, the agents' adaptation to bus departures is not perfect and some agents will also benefit from delayed buses. These positive external effects are ignored in this approach. Therefore, the calculation of waiting time delays due to boardings/alightings is an upper limit of the actual delays. If an agent delays the bus by 1 *sec* and for instance three agents are waiting at a transit stop further along the route, the total external effect amounts to 3 *sec* (see Fig. 2.2). Hence, the external cost which is charged to the causing agent amounts to $VTTS_{w,pt} \times \frac{3}{3600} h$. However, agents are able to adapt their arrival times at transit stops according to the delay of transit vehicles. To give an example, 600 boarding agents delay a vehicle by 10 *min*. The waiting time of a passenger further along the route may be less than the delay of the arriving bus, for instance 1 *min*. In that case, the external effect imposed on that passenger amounts to the waiting time only. The causing agents do not have to pay for the total delay of the transit vehicle but only for the external effect. Therefore, the actual waiting time is divided by the vehicle delay to derive a factor ($\frac{1\ min}{10\ min} = 0.1$) to calculate the delay effect that each causing agent has to pay for.

Effect 3: Waiting time delays due to capacity constraints

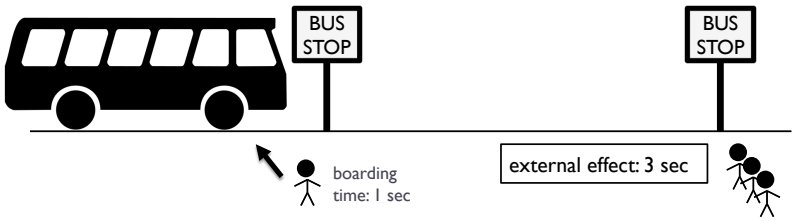

Figure 2.2: External effect 2

If transit vehicles are fully loaded and boardings are denied, the passengers' waiting times increase. In this case, the agents inside the transit vehicle impose a negative external effect on the agent(s) who are not able to enter the bus. The external delay effect depends on when the next transit vehicle is arriving at the transit stop. For example, if the next transit vehicle arrives 600 *sec* later, the total external effect amounts to 600 *sec* (see Fig. 2.3). The passengers of the vehicle that denied boarding have to pay $VTTS_{w,pt} \times \frac{600}{3600} h$ in total. Assuming all agents in the transit vehicle cause this externality, each agent in the bus is charged an equal partial amount. In case boarding is denied a second time, the agents in the second bus pay for the interval until the third bus arrives at the transit stop, and so forth. In case of bus bunching, overtakings may cause a positive external effect since left behind passengers are able to get on a bus that is faster than the previous bus. In this setup, buses do not overtake each other.

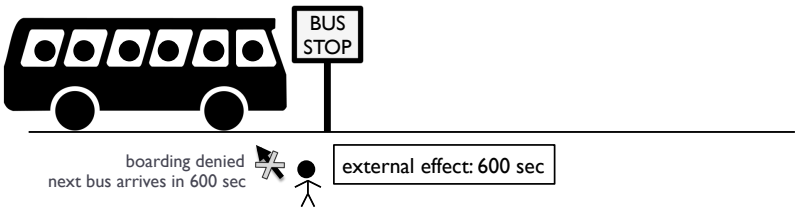

Figure 2.3: External effect 3

2.3 Case Study: Multi-Modal Corridor

2.3.1 Scenario Setup

Supply Similar to Kaddoura et al. (2015a), the supply side consists of a multi-modal corridor with a total length of 20 km along which all transport users' activities are located. From 4 a.m. until midnight, the corridor is served by a constant number of identical buses that are operated by a single company. Transit stops are located at a regular distance of 500 m along the corridor. Assuming a walk speed of 4 km/h, access and egress times depend on the beeline distance between transit stop and activity location. For the simulation experiments described in this chapter, bus capacities are set to 100 passengers per vehicle and the minimum dwell time at each transit stop is set to 0 sec, thus the bus only stops at transit stops if passengers intend to board or alight. Buses are assumed to decelerate when approaching bus stops regardless if passengers will board/alight or not. That is, the deceleration and acceleration time at bus stops is constant for all transit stops and therefore included in the average bus speed. Considering an average bus speed of 30 km/h, a slack time of 20 min when reaching a corridor's endpoint and ignoring passenger transfers amounts to a cycle time of 2 h. As transit vehicles are delayed by passengers, actual cycle times and headways differ from the planned schedule. Bus door operation mode is serial so that alighting precedes boarding. For each vehicle the average boarding time is set to 1 sec per person[1] and alighting times to 0.75 sec per person. Delayed transit vehicles will try to follow the schedule by shortening slack times. For the alternative car mode, the free-flow speed is set to 50 km/h. In order to focus on dynamic delay effects within the PT mode, interferences between cars and buses are excluded and roads are not affected from congestion. Therefore, car travel times only result from the distance between two activity locations and the free-flow speed.

Demand The demand side consists of 20,000 travelers with randomly distributed activity locations along the corridor. The activity patterns are split into two types: "Home-Work-Home" (35% of all travelers, peak demand) and "Home-Other-Home" (65% of all travelers, off-peak demand). Initial departure times for bus users (both activity patterns) is shown in Fig. 2.4.

2.3.2 Choice Dimensions and Simulation Setup

Choice Dimensions Agents are enabled to switch between PT and car or to adapt their departure times.

[1] Assuming 2 doors per vehicle and 2 sec for each person and door, obtained with a boarding system with contactless card fare payment (Wright and Hook, 2007)

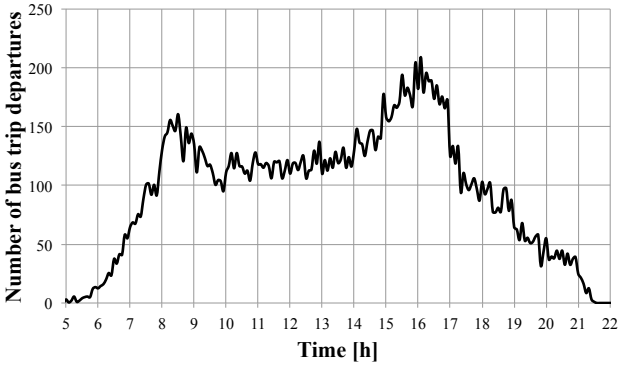

Figure 2.4: Initial departure time distribution for bus users, car mode is similar

Utility Functions and Parameters The total utility (deterministic part) that an executed plan gets is the sum of the (positive) utility earned for performing an activity and the (usually negative) trip-related utility (see Sec. 1.5). In this chapter, the functional form of the travel related utility functions is as follows:

$$\begin{aligned} V_{pt,i,j} &= \beta_{v,pt} \cdot t_{i,v,pt} + \beta_{w,pt} \cdot t_{i,w,pt} + \beta_{a,pt} \cdot t_{i,a,pt} + \beta_{e,pt} \cdot t_{i,e,pt} + \beta_c \cdot c_{i,pt} \\ V_{car,i,j} &= \beta_0 + \beta_{tr,car} \cdot t_{i,tr,car} + \beta_c \cdot c_{i,car} \ , \end{aligned} \tag{2.1}$$

where V is the systematic part of utility for person j on her trip to activity i. It is computed in "*utils*" and mode dependently as indicated by the indices *car* and *pt*. The travel time $t_{i,tr,car}$ and monetary distance costs $c_{i,car}$ are considered as attributes of a car trip to activity i. For PT trips, in-vehicle time $t_{i,v,pt}$, waiting time $t_{i,w,pt}$, access time $t_{i,a,pt}$, egress time $t_{i,e,pt}$ and monetary costs $c_{i,pt}$ are considered.

Table 2.1: Activity attributes

Activity	Typical Duration	Opening Time	Closing Time
Home	12 *h*	undefined	undefined
Work	8 *h*	6 a.m.	8 p.m.
Other	2 *h*	8 a.m.	8 p.m.

Parameters Behavioural parameters for the utility function are based on an Australian study by Tirachini et al. (2014). Estimated parameters[2] and VTTS are depicted in Tab. 2.2. The estimated value for $\beta_{e,pt}$ yields a VTTS for egress of 53.23 AUD/h which is implausibly high. Since egress times are — in the present scenario — constant, $\beta_{e,pt}$ is set to be equal to the access time parameter $\beta_{a,pt}$. Splitting the time related parameters into opportunity costs of time and an additional mode specific disutility of traveling (Kickhöfer et al., 2011, 2013), leads to the parameters in Tab. 2.3 which match the MATSim framework.

While car users in reality have to find a parking lot and also need to walk from the parking lot to the desired activity location, in the model they can directly enter and leave their vehicles at the activity location and immediately start an activity. To compensate for a too attractive car mode,

[2]Estimated parameters are flagged by a hat.

Table 2.2: Parameters and VTTS based on Tirachini et al. (2014)

$\hat{\beta}_{tr,car}$	−0.96	[*utils*/*h*]
$\hat{\beta}_{v,pt}$	−1.14	[*utils*/*h*]
$\hat{\beta}_{w,pt}$	−1.056	[*utils*/*h*]
$\hat{\beta}_{a,pt}$	−0.96	[*utils*/*h*]
$\hat{\beta}_{e,pt}$	−3.3	[*utils*/*h*]
$\hat{\beta}_{c}$	−0.062	[*utils*/*AUD*]
$\hat{\beta}_{act}$	n.a.	
$VTTS_{tr,car}$	15.48	[*AUD*/*h*]
$VTTS_{v,pt}$	18.39	[*AUD*/*h*]
$VTTS_{w,pt}$	17.03	[*AUD*/*h*]
$VTTS_{a,pt}$	15.48	[*AUD*/*h*]
$VTTS_{e,pt}$	53.23	[*AUD*/*h*]

Table 2.3: Parameters and VTTS used in MATSim

$\beta_{tr,car}$	0	[*utils*/*h*]
$\beta_{v,pt}$	−0.18	[*utils*/*h*]
$\beta_{w,pt}$	−0.096	[*utils*/*h*]
$\beta_{a,pt}$	0	[*utils*/*h*]
$\beta_{e,pt}$	0	[*utils*/*h*]
β_{c}	−0.062	[*utils*/*AUD*]
β_{act}	+0.96	[*utils*/*h*]
$VTTS_{tr,car}$	15.48	[*AUD*/*h*]
$VTTS_{v,pt}$	18.39	[*AUD*/*h*]
$VTTS_{w,pt}$	17.03	[*AUD*/*h*]
$VTTS_{a,pt}$	15.48	[*AUD*/*h*]
$VTTS_{e,pt}$	15.48	[*AUD*/*h*]

the alternative specific constant β_0 for car was re-calibrated for the synthetic corridor scenario. An urban scenario is assumed in which a modal split of around 50% : 50% between car and bus is obtained if the bus service is provided with 9 *min* headway and a fare of 1.50 *AUD*. The outcome of the calibration process is an alternative specific constant for car of $\beta_0 = -0.15$. $c_{i,car}$ is calculated for every trip by multiplying the distance between the locations of activity $i-1$ and i by a distance cost rate of 0.40 *AUD*/*km*. $c_{i,pt}$ is the fare which is either a flat fee that has to be paid every time an agent boards a bus, or the sum of all user-specific prices which are paid during a trip.

Operator's Profit and Social Welfare The operator cost model that is applied in this study follows an approach for urban regions in Australia (ATC, 2006). Total operator cost C is calculated as:

$$C = (vkm \cdot c_{vkm} + vh \cdot c_{vh}) \cdot O + vNr \cdot c_{vday} \quad , \tag{2.2}$$

C is divided into three categories: vehicle-*km* vkm, vehicle-*h* vh and an overhead O factor including operating costs which are not covered in the other categories. Capital costs for vehicles result from the number of vehicles vNr engaged per day and equivalent daily capital costs c_{vday}. Unit costs per vehicle-*km* c_{vkm}, unit costs per vehicle-*h* c_{vh}, the overhead and capital costs are based on estimations by ATC (2006) for urban regions in Australia. Unit costs per vehicle-*km* and capital costs depend on the capacity (seats and standing room); a linear regression analysis yields cost functions implying capital costs between 54 and 199 *AUD*/day and unit costs between 0.62 and 1.13 *AUD*/vehicle-*km*. The number of PT trips per day T_{pt} multiplied by a constant fare f leads to daily operator's revenues. Hence, operator's profit per day $\Pi_{operator}$ can be described as follows:

$$\Pi_{operator} = T_{pt} \cdot f - C \tag{2.3}$$

User benefits are calculated as logsum term or Expected Maximum Utility for all choice sets of the users. Social welfare W is measured as the sum of operator profit and user benefits per day:

$$W = \Pi_{operator} + \sum_{j=1}^{J} \left(\frac{1}{|\beta_c|} \ln \sum_{p=1}^{P} e^{V_p} \right) \quad , \tag{2.4}$$

where β_c is the cost related parameter of the multinomial logit model or the negative marginal utility of money, J is the number of agents in the population, P is the number of plans or alternatives of individual j, and V_p is the systematic part of utility of alternative (= plan) p.

Table 2.4: Unit costs and cost functions from ATC (2006)

c_{vkm}	0.006 · capacity + 0.513 [AUD/vehicle-km]
c_{vDay}	1.6064 · capacity + 22.622 [AUD/vehicle-day]
c_{vh}	33 [AUD/vehicle-h]
O	1.21

Simulation Procedure For the first 250 iterations of demand relaxation (see Sec. 1.5), plans are modified by each choice dimension (mode/time) with a probability of 10%. The size of the agents' choice sets is set to 6 daily plans each. After 250 iterations, the agents are assumed to have a plausible set of plans, thus choice set generation is switched off. For additional 50 iterations, the agents choose among their existing daily plans according to a multinomial logit model. To allow for a fast computational performance and assuming the impact of randomness, i.e., fluctuations from iteration to iteration, to be negligible, the last iteration is considered as a representative day, and the outcome of the last iteration is used for analyzing travel behavior and social welfare.

2.3.3 Simulation Experiments

In a first experiment prices are set according to the cost resulting from prolonged in-vehicle times only (effect 1). The other external effects described above exist in the simulation but are not considered in the calculation of marginal cost fares. In a second experiment prolonged waiting times due to boarding/alighting passengers are included: prices are set according to the external in-vehicle and waiting cost resulting from boarding and alighting passengers (effect 1 and 2). Externalities due to capacity constraints exist but are not considered when setting prices. In a third experiment, all three external effects are included in calculating the optimal fare (effect 1, 2, and 3). Unless explicitly stated, marginal cost pricing means the inclusion of all three effects.

To validate the results in terms of social welfare and external delay effects, a grid search approach is used to identify the optimal fare where all users are charged by the same amount. The grid search is implemented as introduced in Kaddoura et al. (2015a). The relaxation of the initial demand (see Sec. 1.5) is embedded into an external loop in which the flat fare is systematically varied between 0 AUD and 3.0 AUD (in steps of 0.025 AUD). The marginal social cost pricing requires a single simulation run, whereas the grid search requires one simulation run for each possible PT fare. Hence, in terms of performance the marginal social cost pricing approach is much faster than the grid search optimization approach.

Both pricing strategies, user-specific and flat fares, are run for different levels of transport supply. Scheduled headways are increased by 2 min between 3 min and 13 min.

2.4 Results and Discussion

2.4.1 Social Welfare

Fig. 2.5 depicts the absolute welfare level obtained for each headway and pricing rule. As a benchmark to evaluate the effectiveness of different pricing rules, a service is considered with PT fares that amount to 0 *AUD* per trip (no pricing), yielding the lowest social welfare for all simulated headways. Charging the optimal flat fares which are found to be greater than 0 *AUD* raises social welfare, especially for larger headways and binding vehicle capacity constraints. User-specific pricing leads to an even higher social welfare than charging an optimized flat fare. That is true for all three cases, even though some of the existing externalities are excluded from setting marginal cost fares in experiment 1 and 2. Internalizing effect 1 and 2 yields a higher welfare than only internalizing effect 1, especially for larger headways and a higher average waiting time. However, for headways with passengers who are not able to board a bus due to capacity constraints, the inclusion of effect 3 has the most significant effect on social welfare.

Analyzing the distribution of bus trips over time reveals that peaks are flattened in the user-specific pricing scheme compared to the flat-pricing strategy. Since user-specific fares are higher during peak times (see later in Sec. 2.4.2) and commuters as well as non-commuters can choose their activity start and end times within wide time spans, bus users are able to shift their trip departure times in order to avoid peak periods. That is, by forcing some users to either depart off-peak or to switch to the alternative (uncongested) car mode, the efficiency within the transport system increases. Benefits from shorter in-vehicle and waiting times within the PT mode overcompensate for lower benefits resulting from users switching to car or arriving earlier or later at the activity location. Therefore, setting user-specific prices raises the social welfare if these external effects are taken into account.

A scheduled headway of 5 *min* is observed to be the optimal headway for all pricing rules except the one including external waiting cost due to fully loaded transit vehicles. When setting fares equal to all existing external effects (internalization of effect 1, 2 and 3) an overall welfare optimum is found for a headway of 9 *min*. That is, the pricing rule has an effect on the optimal level of PT supply. The observations of different welfare levels depending on headway and pricing rule

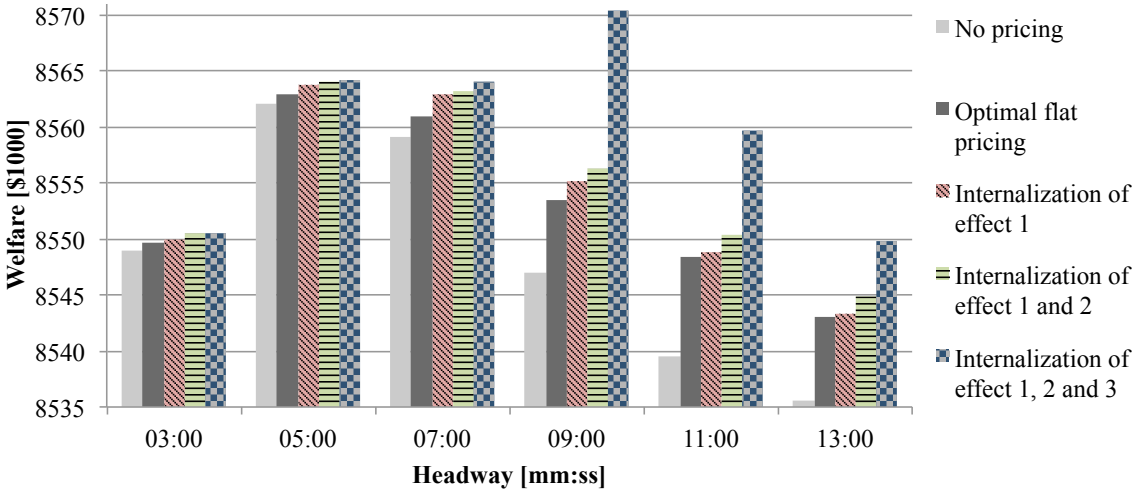

Figure 2.5: Welfare for each headway and pricing rule

are related to the number of boarding denials. Delay effects due to capacity constraints become significant for headways starting from 7 min, for smaller headways they are not significant. All pricing schemes reduce the number of boarding denials, especially when considering waiting time delays due to capacity constraints (internalization of effect 1, 2 and 3). The maximum waiting cost related to capacity constraints is found for a headway of 9 *min*. As more users will switch to the alternative car mode for larger headways the number of boarding denials decreases. Hence, for pricing strategies that do not explicitly account for capacity constraints, the welfare optimum is the largest headway without a significant number of boarding denials (5 *min*). However, in case the pricing strategy explicitly accounts for capacity constraints the welfare maximum is found for a headway yielding the maximum occurrence of boarding denials (9 *min*). A headway of 3 *min* leads to no occurrence of boarding denials, whereas for a headway of 9 *min* a maximum number of boarding denials is obtained. Therefore, these two headways are now analyzed in more detail.

Fig. 2.6 depicts the distribution of waiting times for a 3 *min* and a 9 *min* headway applying marginal social cost pricing (internalization of all effects). Waiting times that exceed the scheduled headway due to delayed vehicles or capacity constraints are not displayed. For both headways, the passengers' arrival patterns at transit stops tend to be coordinated. There are more trips with waiting times shorter than the half of the headway. However, for some trips, waiting times are observed to be longer than the half of the headway and even nearly as long as the scheduled headway. For a 3 *min* headway 4000 trips have a waiting time between 150 *sec* and 180 *sec*. For a 9 *min* headway almost 2000 trips are observed with a waiting time between 450 *sec* and 540 *sec*. For a detailed investigation of passenger arrival patterns at transit stops depending on the headway and service reliability, see Neumann et al. (2016). That indicates that for both headways there

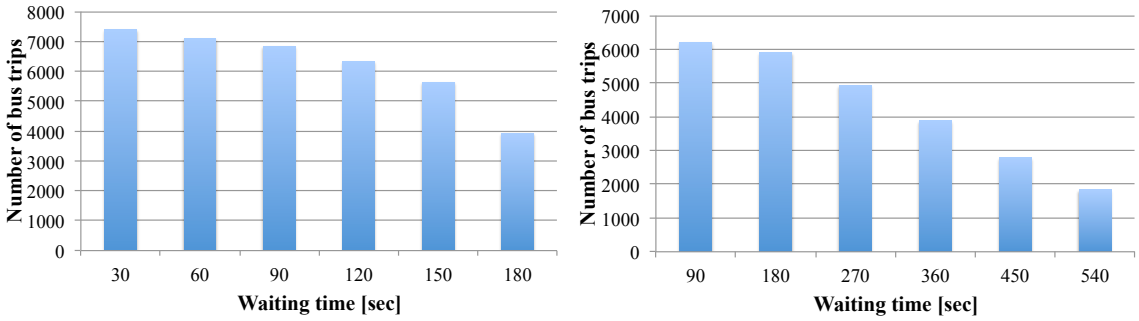

(a) 3 *min* headway **(b)** 9 *min* headway

Figure 2.6: Distribution of waiting times (internalization of all external effects)

are travelers who miss a bus by a few seconds. If a bus had arrived later, these passengers would benefit from the delay since they would be able to catch the bus they would have otherwise missed. As described in Sec. 2.2 these positive externalities are ignored in the present study and only the negative effect is accounted for when setting the prices. The distribution of waiting times confirm what was indicated by the positive effect on social welfare when including effect 2. That is, the negative effect of prolonged waiting times due to passengers getting on and off a bus outweighs the positive effect of shortened waiting times.

2.4.2 External Delay Cost

In Tab. 2.5 the average fare per PT trip is shown for each pricing rule and a headway of 3 *min* and 9 *min*, considering all trips performed during the day. For the optimal flat pricing scheme the

average fare is the flat amount that has to be paid for each bus trip. Whereas, for the user-specific pricing scheme, the average fare amounts to the average external delay cost which is charged for a PT trip. As expected, the more effects are included in setting the user-specific fares the higher the average fare per trip. As there are no occurrences of boarding denials for a 3 *min* headway, the average internalized external cost remains unaltered when including effect 3. For a 3 *min* headway, the optimal flat fare amounts to 0.73 *AUD*, setting prices according to the total external cost (internalization of all existing effects) yields an average fare of only 0.53 *AUD* (Standard Deviation (SD): 0.21 *AUD*). Charging all passengers the same optimal amount overprices PT and results in a lower number of PT users than applying marginal social cost pricing. However, for a 9 *min* headway, transit vehicle load factors and delay effects among PT users are higher which leads to an optimal flat fare of 0.78 *AUD* and an average user-specific fare of 1.69 *AUD* with a SD of 1.79 *AUD*. For this headway, optimal flat pricing seems to underprice PT service which results in more PT users compared to the user-specific pricing scheme. Total internalized external delay costs for

Table 2.5: Optimal flat fare and average user-specific fare (per bus trip; considering all trips per day)

	3 *min* headway	9 *min* headway
Optimal flat pricing	0.73 *AUD*	0.78 *AUD*
Internalization of effect 1	0.31 *AUD*	0.62 *AUD*
Internalization of effect 1 and 2	0.53 *AUD*	1.04 *AUD*
Internalization of effect 1, 2 and 3	0.53 *AUD*	1.69 *AUD*

a headway of 3 *min* amount to 20,245 *AUD*, for a headway of 9 *min* to 46,443 *AUD*. Excluding the delay cost caused by capacity constraints the external cost for a 9 *min* headway amounts to 28,509 *AUD*. Computing the externalities for the flat pricing strategy shows that, compared to the user-specific pricing strategy, the average external delay costs are higher, in particular during peak times. Depending on the number of affected users, average internalized external delay cost (all effects) range from 0 *AUD* to 1.68 *AUD* per trip for a 3 *min* headway and from 0 *AUD* to 8.89 *AUD* for a 9 *min* headway. Fig. 2.7a shows the distribution of marginal social cost fares (internalization of all effects) for a 9 *min* headway, leading to a total of 27,444 PT trips; and a 3 *min* headway with a total of 37,898 bus trips. For a 9 *min* headway, marginal social cost fares are higher because users have to wait for later vehicles due to buses operating at maximum capacity. For more than 16% of all PT trips, passengers have to pay more than 2.0 *AUD*. For the distribution of fares between 2.0 *AUD* and 8.9 *AUD*, see Fig. 2.7b.

During peak times more users are affected than off-peak. Hence, average peak prices exceed average off-peak fares as well as the obtained averages per day (see Tab. 2.5): For trips starting between 2 p.m. and 4 p.m the average internalized external delay cost is 0.60 *AUD* for a scheduled headway of 3 *min* and 2.94 *AUD* for a headway of 9 *min*. Whereas, trips after 8 p.m. cause an average effect of only 0.21 *AUD* for a 3 *min* headway and 0.42 *AUD* for a 9 *min* headway. A higher pricing during peak periods increases social welfare by causing users to switch to the alternative car mode or to adapt their activity scheduling in order to avoid peak periods (see Sec. 2.4.1).

Besides temporal aspects, externalities are analyzed focusing on spatial effects. Fig. 2.8a depicts average bus trip fares dependent on the location of boarding in one direction for a 9 *min* headway. The average internalized external cost per boarding location depends on which external effects are considered. Beginning with the first experiment, the internalization of external effect 1 only, shows

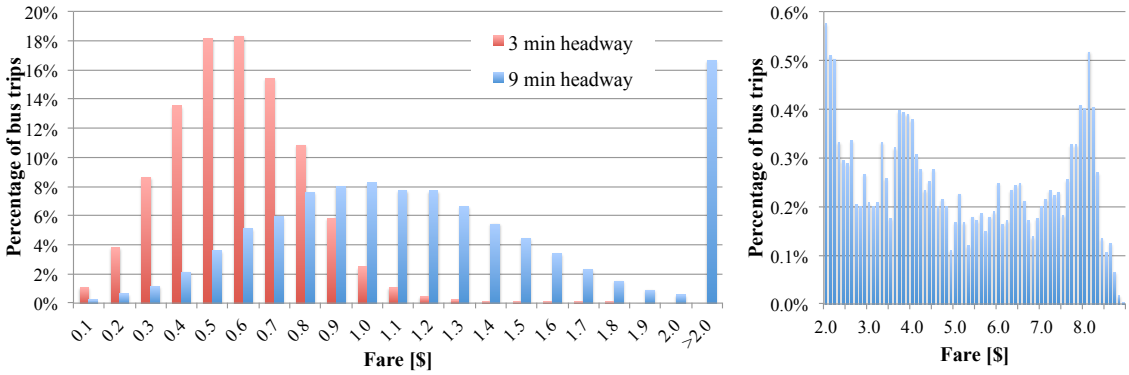

(a) 3 *min* and 9 *min* headway

(b) 9 *min* headway

Figure 2.7: Distribution of marginal social cost fares (internalization of all effects)

that average trip fares increase for passengers who board at the middle of the corridor. That is because at the beginning and the end of a transit route transit vehicle load factors are lower and thus, the probability to affect agents inside a vehicle is lower, too. Including effect 2 significantly raises the average internalized external cost per trip for agents boarding at bus stops along the first half of the transit route. That is explained by a higher number of following transit stops and therefore passengers who are affected further along the corridor. The same trend is observed for different headways, also for 3 *min* where delay effects due to capacity constraints (effect 3) are not present. As clearly shown in Fig. 2.8a adding effect 3 has a significant impact on the average internalized external cost induced by agents boarding at the first 24 transit stops. For agents who board up until transit stop 14, the average external cost-based fare increases. External cost induced by passengers boarding at the following transit stops decrease the later they get on a bus. For transit stops in the second half of the route there are fewer or no agents that cannot board a bus because of capacity constraints.

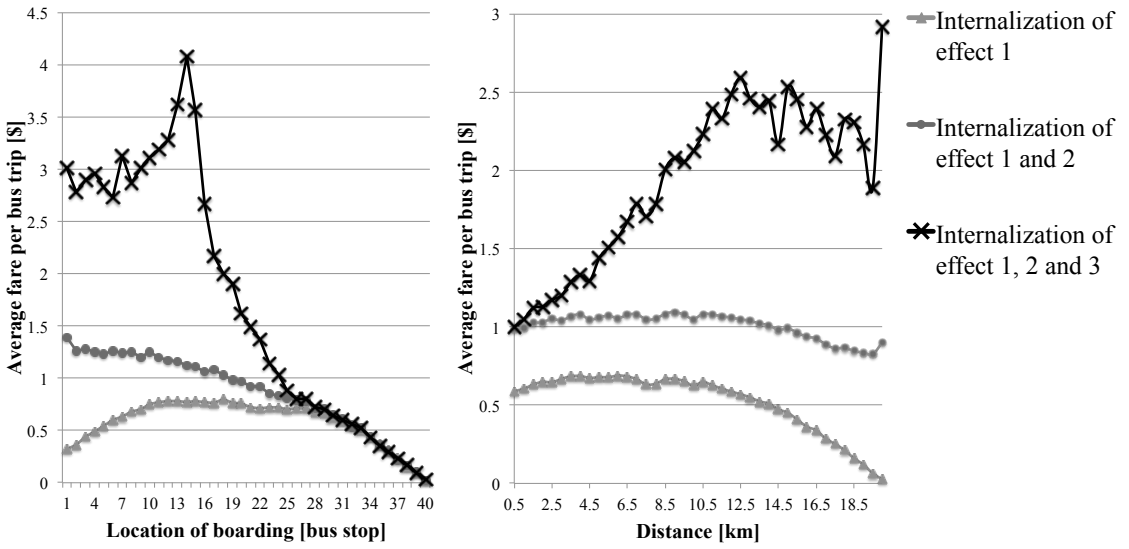

(a) Location of boarding (one way)

(b) Distance traveled

Figure 2.8: Average trip fare dependent on distance and boarding location (9 *min* headway)

Fig. 2.8b shows the average fare per travel distance for all three experiments. Internalized external cost resulting from effect 1 first slightly increases for short distances and then significantly decreases for distances larger than half of the corridor. A similar tendency is observed from Mohring

(1972) for feeder routes as passengers with longer trips board earlier and delay fewer passengers in the bus. Including effect 2 flattens decreasing average trip fares for long distance trips since passengers who board at early transit stops affect all passengers that will be entering the same transit vehicle along the route. Adding effect 3 and computing the marginal social cost fares based on all existing external delays inverts the results obtained without the capacity constraints in place: For trip distances up to 12.5 *km* average fares significantly increase with the trip length. For longer distances average fares fluctuate and slightly decrease, whereas for the maximum trip length of 20 *km* the maximum average fare is obtained. Long-distance passengers occupy seats for longer than short-distance passengers. This is in line with findings from Kraus (1991) who observes the same effect when including the disutility of discomfort and from Turvey and Mohring (1975) who consider fully loaded vehicles. Since the vehicle load factor is the crucial variable, the disutility of prolonged waiting times due to boarding denials and the disutility of discomfort resulting from crowding have conceptually a lot in common. As crowding costs increase for longer distances, the inclusion of crowding would increase the effect observed for the internalization of boarding denial costs. That is, the average fare would increase in an even steeper way as a function of trip distance than displayed in Fig. 2.8b (internalization of effect 1, 2 and 3).

2.5 Conclusion

In this study, the agent-based simulation MATSim was successfully used for the optimization of PT fares. MATSim was enhanced by implementing a marginal social cost pricing approach: External delay effects among PT users are internalized by charging the equivalent monetary amount to the causing agent. As sources for external cost, this study considers the effect of boarding/alighting passengers on in-vehicle time (effect 1), waiting time without an active capacity constraint (effect 2) and waiting time induced by an active capacity constraint (effect 3).

As expected, marginal social cost pricing yields a higher social welfare than charging an optimized flat fare. Starting from effect 1, including more external effects is found to increase the social welfare gain of applying optimized user-specific bus fares. As passengers' waiting times indicate a coordinated arrival at transit stops (following the arrival of buses), it is crucial to include the external effect of prolonged waiting times due to boarding and alighting passengers (effect 2). Adding this effect to the external effect of prolonged in-vehicle times (effect 1) increases the level of social welfare and also affects the relationship between average optimal fare and travel distance: Since passengers who board at early transit stops affect all passengers who are or will be waiting for the same vehicle along the route, average external costs are higher for early boardings. Thus, for a longer trip length, the average optimal fare decreases to a lesser extent as a function of trip distance. Once passengers are not able to board the first arriving transit vehicle due to limited capacities, social welfare rises most significantly when internalizing these delays by charging the extra waiting cost to the passengers inside the vehicle (effect 3). Including that effect increases average external cost-based prices for long distance trips and early boarding locations along the transit route. In this setup, explicitly accounting for this externality when setting user-specific fares, changes the welfare optimal headway from 5 *min* to 9 *min*. During peak periods average external cost-based fares are observed to be higher than off-peak. As a consequence, users are priced out. They either reschedule their activities and shift their trip departure times to periods with less demand or they switch to the alternative transport mode car. Benefits from a higher efficiency within the PT sector (shorter in-vehicle and waiting times) overcompensate for lower benefits of users who are priced out.

Future research studies may integrate the developed approach to a real-world case study (e.g., Berlin, see Sec. 4.5.1) and include more effects associated with PT users (e.g., the disutility of crowded vehicles). Furthermore, an integrated study may be carried out in which the methodology presented in this chapter is coupled with pricing approaches that account for additional external effects, namely road congestion and environmental effects, addressed in the following chapters.

CHAPTER 3

Agent-based Congestion Pricing

with Heterogeneous Values of Travel Time Savings

In this chapter, a road pricing scheme is presented which directly builds on the Pigouvian taxation principle (see Sec. 1.2) and computes marginal external congestion costs based on the queuing dynamics at the bottleneck links. Resulting toll payments differ from agent to agent depending on the position in the queue. The user-specific and dynamic road pricing scheme is then extended towards a consistent consideration of non-linear, user- and trip-specific VTTS. The heterogeneous VTTS are inherent to the model and result from each agent's individual time pressure. The innovative pricing and routing methodology is applied to a real-world case study of the Greater Berlin area, Germany. This chapter is an edited version of an article that has been previously published (Kaddoura and Nagel, 2016b). The in-depth description of the agent-based congestion pricing approach in Sec. 3.2.1.1 is an edited excerpt from another previously published article (Kaddoura, 2015).

3.1 Introduction and Problem Statement

In this chapter, an agent-based congestion pricing methodology is presented and extended towards a consistent consideration of heterogeneous VTTS. The applied congestion pricing methodology makes use of an iterative market mechanism: First, user-specific and dynamic tolls are computed based on the delay imposed on other travelers. Second, the transport demand is allowed to change its travel behavior to avoid these toll payments. In this study, the transport users (agents) are enabled to generate new routes based on the generalized travel cost, taking into account both the travel time and the congestion tolls. Third, each agent's daily behavior, including the transport route, is evaluated to obtain the agent's affinity to repeat that behavior, i.e, to use the same transport route in the next iterations. Hence, the VTTS is required (i) to compute congestion tolls, (ii) to identify routes which minimize (generalized) costs and (iii) to evaluate transport routes.

The approach uses the transport simulation framework MATSim (see Sec. 1.5). The VTTS which is used for evaluation (iii) is inherent to the model and results from each agent's individual schedule delay costs and time pressure. However, the VTTS which is used for tolling (i) and routing (ii), normally is assumed to be constant and equal for all agents.

As an issue of increasing interest, heterogenous VTTS have been addressed in several studies. Empirical studies reveal that the VTTS depends on certain trip-specific attributes, such as the transport mode (Hensher and Rose, 2007), trip distance (Hess et al., 2008) or traffic state (Hensher, 2001). Additionally the VTTS may vary with person-specific characteristics, such as the income (Kickhöfer et al., 2011).

Several studies address the importance of schedule delay costs. Based on Vickrey's bottleneck model (Vickrey, 1969), dynamic approaches allow for a consideration of the activity at the trip destination, to compute schedule delay costs, and to consider dynamic tolls. In several studies, the bottleneck model is extended to account for heterogenous transport users (Vickrey, 1973; de Palma and Lindsey, 2004; van den Berg and Verhoef, 2011). The level of heterogeneity is found to affect the increase in system welfare. For a larger heterogeneity in the user preferences, pricing will result in more diverse choices which reinforces the increase in system welfare (de Palma and Lindsey, 2004; Verhoef and Small, 2004).

In this study, an innovative approach is presented which accounts for true VTTS when (i) converting external delays into congestion tolls (Sec. 3.2.1) and (ii) when generating new transport routes (Sec. 3.2.2). The advantage of an iterative simulation-based approach is that complex

VTTS can be taken into account. The VTTS is considered to be non-linear, user- and trip-specific. Moreover, the VTTS is subject to destination-related constraints. The innovative pricing and routing methodology is applied to a real-world case study of the Greater Berlin area, Germany.

3.2 Methodology

3.2.1 Congestion Pricing

3.2.1.1 QCP Approach

The computation of external congestion costs builds on the queue model described in Sec. 1.5. Each time a transport user is delayed, i.e, cannot move from one link to the next one, the causing agent is identified and charged.

Conceptual Approach: Person-specific Calculation of Marginal Congestion Cost This paragraph describes the person-specific calculation of marginal congestion effects. The approach was initially presented by Kaddoura and Kickhöfer (2014) and firstly applied to a real-world case study in Kaddoura (2015). The methodological description provided in this paragraph is an edited excerpt from Kaddoura (2015).

An agent who leaves a road segment prevents all following agents from leaving that road segment for the time of c_{flow}^{-1}. This is depicted in Fig. 3.1, assuming a flow capacity of 1200 vehicles per h and three agents 1, 2 and 3 arriving at the end of the link at time step $t = 0$, $t = 1$ and $t = 2$. Accordingly, the delay effect imposed on the following agents is computed, which can be used for

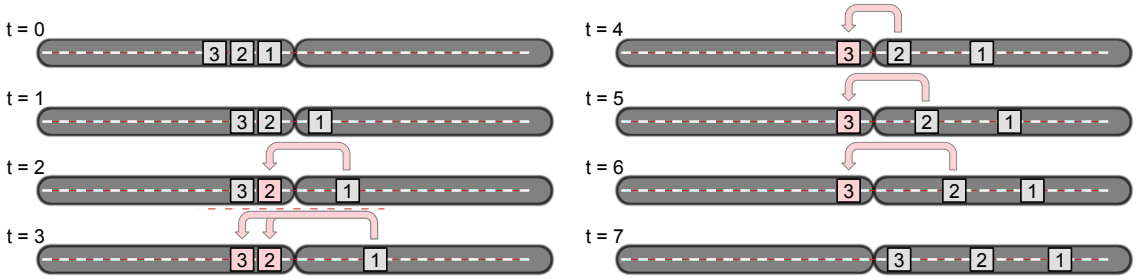

Figure 3.1: Example: Congestion effects due to the flow capacity. A red arrow indicates an external delay effect (source: Kaddoura (2015)).

setting optimal local and user-specific tolls. The first external delay effect appears at time step $t = 2$, when agent 2 cannot leave the first road segment. Since agent 1 has left the road segment and the flow capacity constraint limits the number of leaving agents per time, $c_{flow}^{-1} = 3$ *sec* have to pass until the next agent can be moved to the next road segment. At time step $t = 3$, both agents 2 and 3 are delayed by agent 1. At time step $t = 4$, agent 2 is allowed to leave the road segment, however, agent 3 is still queued. This time, agent 2 is considered as the causing agent that imposes a delay of 3 *sec* ($t = 4...6$) on agent 3. Summing up for each agent the private and external delay cost results in the following:

- Agent 1 causes 3 *sec* congestion and is not affected by any delay.
- Agent 2 causes 3 *sec* delay and is exposed to 2 *sec*.

- Agent 3 causes no delay and is exposed to 4 *sec* delay.

That is, especially for longer queues, the first agent(s) will cause more congestion than they are exposed to compared to the agents at the back of a queue. When applying a marginal congestion cost pricing scheme, depending on the cost of the alternatives (routes, transport modes, departure times), transport users will change their travel behavior to reduce the sum of the private and (internalized) external congestion cost.

As described in Sec. 1.5, the simulation framework accounts for a second capacity constraint, namely the storage capacity $c_{storage}$, which limits the number of vehicles that can be placed on a road segment. Therefore, agents may also be delayed because there is no space on the next road segment in the agent's route. In that case, the queue which results from c_{flow} of the current road segment has dissolved, and the delay results from a *downstream* road segment, i.e., the bottleneck link. That is, due to spill-back effects, external delay effects may extend over several road segments. This is visualized in Fig. 3.2, where the network consists of three road segments; the central road segment is the bottleneck link with $c_{flow} = 1200$ vehicles per h, and for the first road segment c_{flow} is unlimited. Compared to the previous example, for the bottleneck link $c_{storage}$ is set to one vehicle. Spill-back occurs in time step $t = 2$ and $t = 3$ when agent 3 cannot leave the first road

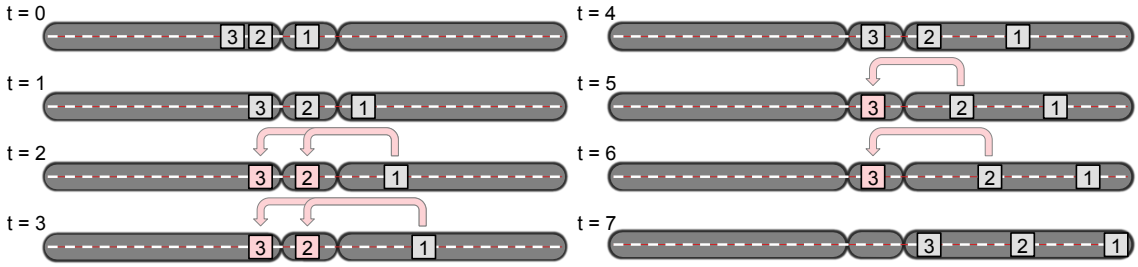

Figure 3.2: Example: Congestion effects due to the flow and storage capacity. A red arrow indicates an external delay effect (source: Kaddoura (2015)).

segment because agent 2 blocks the next link. Agent 2 in turn cannot leave the bottleneck link because of agent 1 who has previously left the bottleneck link and c_{flow} limits the flow to one agent every 3 *sec*. Therefore, agent 1 is considered as the causing agent for the spill-back related delay of agent 3.

Implementation: Person-specific Calculation of Marginal Congestion Cost The computation of marginal external effects, for both approaches, is implemented as follows. Each time an agent leaves a link and was delayed on that link, the delay is ascribed to the agents who were before in the same queue.

Additionally, in case of spill-back related delays, the delay is ascribed to the agents in a downstream link's queue. At this stage, several approaches are implemented to internalize these spill-back related delays (see Sec. 4.3.1). A reasonable compromise between computational performance and precise calculation seems to memorize the spill-back related delay if a link's queue has already dissolved (e.g., for the first link in Fig. 3.2), and then to identify the causing agent(s) in case the affected agent drives along the bottleneck link at which the queue has not yet dissolved (e.g., in time step $t = 7$ in Fig. 3.2). This is the approach that is considered in the following.

The Costs of Being Delayed The delay imposed on other travelers is converted into monetary units. Thereby, the affected agent p's cost of arriving delayed at activity a is composed of two parts:

$$c_{p,a} = c_{p,a}^{trip} + c_{p,a}^{perf} \ , \tag{3.1}$$

where $c_{p,a}^{trip}$ is the increase in generalized cost related to the trip to activity a, and $c_{p,a}^{perf}$ is the decrease in utility from having less time available to perform activity a. The trip related delay costs are

$$c_{p,a}^{trip} = d_{p,a} \cdot \left(-\beta^{travel} / \beta^{money}\right) \ , \tag{3.2}$$

where $d_{p,a}$ is the total delay of person p at activity a, β^{travel} is the normally negative marginal utility of traveling and β^{money} is the marginal utility of money. β^{travel} and β^{money} in this study are constant for all car users and trips.

For the conversion of activity related delays into monetary units, the existing approach (Kaddoura and Kickhöfer, 2014; Kaddoura, 2015) makes the approximation that users perform activities for their predefined typical durations ($t_{p,a}^{perf} = t_a^{typ}$), which means that the marginal utility is approximated as

$$\frac{\partial}{\partial t_{p,a}^{perf}} V_{p,a} \approx \frac{\partial}{\partial t_{p,a}^{perf}} V_{p,a} \Bigg|_{t_{p,a}^{perf} = t_a^{typ}} = \beta^{perf} \cdot t_a^{typ} \cdot \frac{1}{t_{p,a}^{perf}} \Bigg|_{t_{p,a}^{perf} = t_a^{typ}} = \beta^{perf} \ , \tag{3.3}$$

where $V_{p,a}$ denotes the utility gained from performing an activity, described in Eq. (1.2). However, depending on the number and types of activities in a daily plan, transport users have more or less time available to perform their activities. Hence, they are differently pressed for time, thus being delayed in traffic affects different transport users differently. Furthermore, activities have certain constraints such as opening and closing times. If the activity is still closed, being delayed may for example result in zero activity delay cost. In the existing approach, all this is ignored, and the above leads to

$$c_{p,a}^{perf} \approx d_{p,a} \cdot \left(\beta^{perf} / \beta^{money}\right) \quad . \tag{3.4}$$

In total, the marginal costs of being delayed are, for tolling purposes, assumed as

$$VTTS^{delay} = \partial c_{p,a} / \partial d_{p,a} \approx \left(-\beta^{travel} + \beta^{perf}\right) / \beta^{money} \ , \tag{3.5}$$

where $VTTS^{delay}$ is the value of travel time saving which is used to convert delays into congestion tolls. Consequently, congestion tolls payed by the causing agent may not correctly reflect the affected agent's true delay cost.

3.2.1.2 Extension 1: Non-linear and User-specific Conversion of Delays into Tolls

In this extension, delays are now converted into monetary payments accounting for the affected agent's trip-specific VTTS making the tolls reflect true external congestion costs. Total activity delay costs are computed as

$$c_{p,a}^{perf} = \left[V_{p,a}\left(t_{p,a}^{perf} + d_{p,a}\right) - V_{p,a}\left(t_{p,a}^{perf}\right)\right] / \beta^{money} \ . \tag{3.6}$$

The costs for being delayed by one time unit are computed as $c_{p,a}^{perf} / d_{p,a}$. The person and trip specific VTTS is thus approximated as

$$\begin{aligned} VTTS_{p,a}^{delay} &\approx \partial c_{p,a}^{trip} / \partial d_{p,a} + c_{p,a}^{perf} / d_{p,a} \\ &\approx -\beta^{travel} / \beta^{money} + \left[V_{q,a}\left(t_{q,a}^{perf} + d_{p,a}\right) - V_{q,a}\left(t_{p,a}^{perf}\right) \right] / \left(\beta^{money} \cdot d_{p,a}\right) \ . \end{aligned} \tag{3.7}$$

The amount payed by each causing agent q for delaying person p during the trip to activity a then is $m_{q,p,a} = d_{q,p,a} \cdot VTTS_{p,a}^{delay}$, where $d_{q,p,a}$ is the delay which the causing agent q imposes on person p during the trip to activity a.

3.2.2 Time- and Cost-Sensitive Routing

3.2.2.1 Existing Approach

The existing simulation framework generates new transport routes assuming a constant VTTS for all trips.[1] The routing relevant costs are assumed as

$$g_{q,a} = VTTS^{travel} \cdot t_{q,a} + m_{q,a} = g_{q,a}^{trip} + g_{q,a}^{perf} \ , \tag{3.8}$$

where $g_{q,a}$ is the total routing relevant cost of person q traveling to activity a; $VTTS^{travel}$ is the VTTS which is used to convert travel time into travel cost; $t_{q,a}$ is the total travel time of person q traveling to activity a; $m_{q,a}$ is the total amount payed by person q during the trip to activity a; $g_{q,a}^{trip}$ is the generalized cost related to the trip to activity a; and $g_{q,a}^{perf}$ is the opportunity cost of time (that could have been spent performing activity a). The trip related travel costs and the opportunity cost of time are

$$g_{q,a}^{trip} = t_{q,a} \cdot \left(-\beta^{travel} / \beta^{money}\right) + m_{q,a} \qquad \text{and} \qquad g_{q,a}^{perf} \approx t_{q,a} \cdot \left(\beta^{perf} / \beta^{money}\right) \ , \tag{3.9}$$

where the same approximation as in (Eq. (3.4)) was made that activities are assessed at their typical durations. Hence, in the existing routing approach, the VTTS for all agents and car trips is assumed as

$$VTTS^{travel} = \partial g_{q,a} / \partial t_{q,a} \approx \left(-\beta^{travel} + \beta^{perf}\right) / \beta^{money}. \tag{3.10}$$

However, as described in Sec. 3.2.1, the utility gained from performing an activity depends on the transport users' individual time pressure. In Eq. (3.9), this utility is assumed to be equal to β^{perf}. Hence, the routing costs, and in particular the opportunity costs of time, neglect the non-linear, user- and trip-specific VTTS which is given by Eq. (1.2) (see Sec. 1.5, Evaluation). Thus, the existing routing approach may not correctly account for the agents' trip-specific weighting of travel time and monetary costs.

[1] This statement was correct when the original version of this paper was written. In the meantime, an alternative approach using randomized VTTS was investigated by (Nagel et al., 2014). The consequences of that are investigated at the end of Sec. 3.4.

3.2.2.2 Extension 2: Non-linear and User-specific Routing

In this extension, the opportunity costs of time are computed as

$$g_{q,a}^{perf} \approx t_{q,a} \cdot \left[V_{q,a}\left(t_{q,a}^{perf} + \epsilon\right) - V_{q,a}\left(t_{p,a}^{perf}\right) \right] / \beta^{money}, \tag{3.11}$$

where $V_{q,a}(\cdot)$ is the utility person q gains from performing activity a (see Sec. 1.5, Evaluation, Eq. (1.2)); and ϵ is one time unit. In this study, ϵ is set to 1 *sec* which implies that $t_{q,a}$ and $t_{q,a}^{perf}$ is given in *sec*. Hence, the opportunity costs of time are linearized accounting for the non-linearity in Eq. (1.2). The resulting user- and trip-specific VTTS is

$$\begin{aligned} VTTS_{q,a}^{travel} &= \partial g_{q,a}^{trip} / \partial t_{q,a} + \partial g_{q,a}^{perf} / \partial t_{q,a} \\ &\approx \left[-\beta^{travel} + V_{q,a}\left(t_{q,a}^{perf} + \epsilon\right) - V_{q,a}\left(t_{p,a}^{perf}\right) \right] / \beta^{money} , \end{aligned} \tag{3.12}$$

where $VTTS_{q,a}^{travel}$ is the value of travel time savings of person q traveling to activity a.

3.3 Case Study: Berlin, Germany

3.3.1 Scenario Setup

The proposed routing and congestion pricing approach is applied to the real-world MATSim model of the Berlin metropolitan area (Neumann et al., 2014). The road network contains all major and minor roads of the Greater Berlin area. The demand side is modeled as survey-based (Ahrens, 2009) "population-representative" agents and "non-population representative" agents to include for freight, airport and tourist traffic. The transport demand was calibrated accounting for mode shares, travel times and travel distances. Compared to survey data (Ahrens, 2009) the differences in mode shares per distance are below 5% (Neumann et al., 2014).

As initial plans the executed plans of the relaxed travel demand are taken from the scenario by Neumann et al. (2014). The population size is reduced to a 10% sample and road capacities are reduced accordingly. The 10% population sample comprises a total of 598,891 agents and a total of 1,411,910 trips, with 476,198 trips within the car and Heavy Goods Vehicles (HGV) transport mode.

3.3.2 Choice Dimensions and Simulation Setup

The adaptation of demand to supply is repeated for 100 iterations. During the first 80 iterations, choice sets are generated: In every iteration, 10% of the agents are rerouted based on link- and time-specific costs in the previous iteration. Thereby, the number of travel alternatives per agent is limited to 4 plans, thus poor plans are replaced by better plans. During the final 20 iterations, choice sets are fixed and plans are selected based on a multinomial logit model.

3.3.3 Simulation Experiments

The following simulation experiments are carried out:

- In experiment 0, the existing pricing and routing methodology is applied in which the VTTS is considered to be equal for all car trips and road users.
- Experiment 1 applies the extended pricing approach (extension 1) and the existing routing approach.
- Experiment 2 applies the extended routing approach (extension 2) and the existing pricing approach.
- Finally, simulation experiment 3 combines extension 1 and 2.

The pricing experiments are compared with a simulation run without pricing which is considered as the base case.

3.4 Results and Discussion

3.4.1 Analysis of the Model-inherent Value of Travel Time Savings

In a first step, the base case is analyzed and the VTTS is calculated for each car trip non-linearly and for each user separately. The resulting distribution of the VTTS (see Fig. 3.3) reveals that for most trips the observed VTTS strongly differs from the VTTS which is assumed in the existing approach where non-linearities and user-specific differences are ignored. The median is 10 EUR/h which corresponds to the VTTS assumed in the existing approach. For 9% of all car trips, the VTTS amounts to 4 EUR/h which is the case if the opportunity cost of time is zero, e.g., if the activity at the destination is not open. However, for 30% of all car trips, the VTTS is larger than 16 EUR/h.

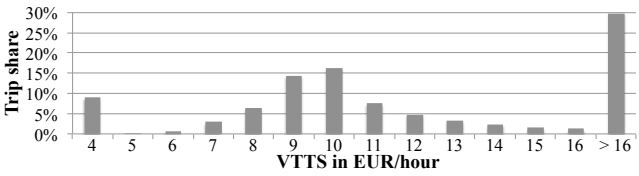

Figure 3.3: Distribution of VTTS (base case) in the scenario by Neumann et al. (2014)

3.4.2 Improved Pricing and Routing

Next, extension 1 and 2 are used to compute congestion tolls to which transport users are enabled to react by adjusting their route choice decisions. Tab. 3.1 depicts the changes in welfare relevant parameters as a result of the pricing policy. In all pricing experiments, the travel time is reduced and the system welfare, defined as the sum of toll revenues and travel related user benefits, is higher compared to the base case situation. The travel related user benefits refer to the population wide utility converted to monetary units.

In experiment 1, congestion tolls that are payed by the causing agents better reflect the affected agents' true delay cost. Since transport users are allowed to react to these tolls, delays imposed on

Table 3.1: Comparison of the pricing experiments with the base case (no pricing)

Changes in ...	Experiment 0	Experiment 1	Experiment 2	Experiment 3
travel time (car mode)	−13,800 *h*	−14,422 *h*	−15,563 *h*	−17,012 *h*
travel related user benefits (including toll payments)	−752,998 *EUR*	−1,179,869 *EUR*	−676,355 *EUR*	−1,033,819 *EUR*
toll revenues	+1,107,293 *EUR*	+1,559,639 *EUR*	+1,073,998 *EUR*	+1,484,971 *EUR*
system welfare	+354,295 *EUR*	+379,770 *EUR*	+397,643 *EUR*	+451,152 *EUR*

transport users with high VTTS are avoided and congestion costs decrease. A comparison of the different pricing approaches reveals that extension 1 (Exp. 1) improves the overall system welfare by 7% more compared to the existing approach (Exp. 0). Furthermore, in experiment 1, the toll revenues are higher compared to the existing pricing approach. This is explained by the overall higher level of the affected agents' VTTS. In turn, a higher VTTS results in a higher congestion toll to be charged from the causing agent.

In experiment 2, tolls are computed following the existing congestion pricing methodology. However, transport users are enabled to generate routes which take into account the user- and trip-specific VTTS. The improved routing approach (Extension 2) improves the overall system welfare by 12% more compared to the existing routing approach. The increase in welfare is explained by the agents' capability to identify better routes which do not only consider the trip related cost but also the expected gains from performing the activity at the destination.

In pricing experiment 3, extension 1 and 2 are combined. Congestion tolls are computed and transport users are routed accounting for the non-linear, user- and trip-specific VTTS. This pricing experiment results in the largest decrease in congestion and the highest welfare level. The welfare increases by 27% more compared to the existing approach. This is due to two effects. First, the tolls better reflect the delayed transport users' congestion cost. Second, the transport routes better reflect the agents' individual weighting of time and money.

A detailed investigation of the spatial effects in the Greater Berlin area, i.e., transport users' changes in route choice decisions, resulting from the QCP approach is provided in Ch. 8.

Randomization Nagel et al. (2014) have addressed the problem related to the router (Sec. 3.2.2) in a different way, by randomizing the VTTS before each run of the router, rather than computing an agent- and trip-specific approximation. Experiment 3 is thus repeated with the randomizing router instead of extension 2. First, the number of iterations is observed to have a crucial effect on the simulation outcome. For a total of 100 iterations, the randomizing routing approach results in a system welfare which is below the welfare level resulting from the extended routing approach without randomization (Exp. 3). In contrast, for a total of 500 iterations, the system has more time to evolve. Using the randomizing router now results in a system welfare similar to the welfare level resulting from the extended routing approach without randomization (Exp. 3). One can conclude that the randomizing router of Nagel et al. (2014) has a similar effect as extension 2 of this chapter (Sec. 3.2.2), but extension 2 of this chapter reaches similar results within a factor of five fewer iterations.

3.5 Conclusion

Overall, in this study, an innovative agent-based congestion pricing and routing approach was presented and successfully applied to a real-world case study. The study has shown that it is worth the effort to extend the routing and congestion pricing approach to account for heterogeneous VTTS which are inherent to the model and result from each agent's individual time pressure. Similar to the activity related travel cost, the proposed methodology may be applied to account for non-linear and user-specific trip related travel costs. The results of the case study reveal that the proposed methodology performs better than assuming a constant VTTS or randomizing the VTTS. The improved consistency of setting congestion toll levels, identifying transport routes and evaluating plans translates into a higher system welfare.

In the following chapter, an alternative and more real-world oriented pricing approach is developed which is compared to the QCP approach presented in this chapter. Furthermore, in the following chapter, pricing experiments are applied to a more advanced case study of the Greater Berlin area which allows for mode choice.

CHAPTER 4

Congestion Pricing in a Real-world Oriented Agent-based Simulation Context

In this chapter, a congestion pricing methodology is presented which uses control-theoretical elements to adjust toll levels depending on the congestion level. Resulting toll payments are the same for all travelers per time bin and road segment. The pricing approach is compared to the congestion pricing methodology presented in Ch. 3. The pricing approaches are applied to Vickrey's bottleneck model and the case study of the Greater Berlin area. This chapter is an edited version of an article that has been previously published (Kaddoura and Nagel, 2019).

4.1 Introduction and Problem Statement

Following the concept of marginal social cost pricing, introduced by Pigou (1920), the social welfare is maximized by setting tolls equivalent to marginal external costs (see Sec. 1.2). Hence, optimal toll setting requires knowledge about the marginal congestion cost which in turn requires knowledge about the congestion function and demand elasticity.

A possible way to model road traffic congestion is the application of a so-called capacity restraint function (CR-function) to translate the traffic volume and road-specific parameters into a travel time. Based on this approach, all travelers on the same road segment are assumed to experience the same travel cost. The above works for static situations. For dynamic situations, a possible way is to apply a queue model which accounts for dynamic traffic congestion, i.e, a queue that builds up in case the inflow rate exceeds the road segment's flow capacity (or service rate). A major difference to the static approach is that travel costs depend on the position in the queue: Travelers at the end of a queue experience higher travel times compared to travelers further ahead.

An important point is that marginal social costs have to be computed *mutatis mutandis*, and not *ceteris paribus* (see, e.g., Arnott et al., 1993; Button, 2004). That is, the computation of marginal social cost needs to account for the user reactions of all other travelers. In the case of traffic congestion, the immediate effect of an additional traveler is that total congestion costs increase and consequently *ceteris paribus* marginal congestion costs are positive. In contrast, *mutatis mutandis* marginal costs depend on the existing travel alternatives, e.g., alternative modes, routes or departure times:

1. In case for some users there is a travel alternative associated with no additional costs, existing travelers may switch to that alternative. Consequently, traffic congestion is reduced to the original level. Since total experienced travel costs are the same, *mutatis mutandis* marginal congestion costs are zero.
2. In case there is no travel alternative or all travel alternatives are associated with much higher costs, travelers are not able to adjust and traffic congestion will not decrease. Consequently, *mutatis mutandis* and *ceteris paribus* marginal congestion cost are at the same level.
3. In case for some users there is a travel alternative associated with some additional costs, existing travelers may switch to that alternative. Consequently, traffic congestion somewhat decreases. However, the overall effect of an additional traveler is that total experienced travel costs have increased. Consequently, *mutatis mutandis* marginal costs are greater than zero but below *ceteris paribus* marginal costs.

Vickrey's bottleneck model, which can be seen as the archetypical queue model, is widely used by researchers to investigate the trade off between not arriving at the desired time (schedule delay), and being delayed by traffic congestion (see Sec. 1.1). The optimal tolling scheme forces travel demand to disperse over time, traffic congestion is eliminated, and system welfare is maximized. The optimal

toll is time-variant; with linear schedule delay functions, toll levels first increase linearly from 0 at the beginning of the rush-hour to a maximum value at the desired arrival time, and then decrease linearly with time to 0 at the end of the rush-hour (Vickrey, 1969, see also Sec. 1.1). The initial model was extended in several analytical studies, e.g., to account for elastic demand (Arnott et al., 1993), simplistic networks (de Palma et al., 2004), heterogeneous travellers (van den Berg, 2011), hypercongestion (Fosgerau, 2015) or household scheduling preferences (de Palma et al., 2015b). Levinson and Rafferty (2004) present a pricing approach where transport users are charged based on the marginal congestion externality and – in contrast to standard economic theory – parts of the toll revenues are immediately used to reimburse the delayed travelers. In Levinson and Rafferty (2004), marginal congestion cost are computed as the bottleneck's service time per vehicle (the inverse of the flow capacity) multiplied with the number of following vehicles that will be queued (until the queue dissipates). Therefore, the marginal cost function is described as triangular, where the toll jumps to the maximum for the first traveler that passes the bottleneck, and then decreases linearly to zero. In their numerical illustration, where travelers are enabled to adjust their departure times in order to react to the tolling scheme, the morning peak is segmented into 5-minute intervals for which the utility for all travelers is averaged. In different tolling approaches different forms of the time-variant toll are tested. The authors find the "first-pays-most" tolling function to be effective regarding the criteria "reduction of travel delay, schedule delay, user cost, social cost and inequity". In contrast, the highest welfare is obtained for a time-variant toll which is consistent with Vickrey (1969). Verhoef (2003) investigates congestion pricing applying a car-following model, i.e, continuously varying driving speeds over time and space, including hypercongestion. Since there is no closed-form solution, a pricing rule is developed which approximates the welfare maximum. The developed pricing rule builds on the Pigouvian taxation principle transferred to the traffic congestion resulting from a car-following model. A numerical model is used to show that applying a tolling scheme based on Vickrey's bottleneck model may result in a lower welfare compared to the developed pricing rule.

Most congestion pricing studies make use of an analytical modeling approach to investigate illustrative case studies with an often simplistic network and transport demand. Simulation-based approaches allow for real-world applications with complex networks and population structures. Nagel et al. (2008) use a large-scale transport simulation to investigate the effects of a pricing scheme which investigates user-specific and time-dependent tolls by setting tolls proportionally to the time spent traveling; however, it does not iteratively optimize tolls. In the context of simulation-based evacuation studies, Lämmel and Flötteröd (2009) develop a routing strategy which approximates user- and road-specific marginal social costs and yields a reduction in total travel time. They argue that each ("causing") agent i in a queue delays every following ("affected") agent j in the same queue by a time increment of $d\tau_j$. Their implementation then includes the following approximations:

1. They assume steady state flow conditions, and therefore can approximate $d\tau_j \approx 1/\bar{q}$, where $\bar{q}$ is the steady state flow.
2. They also approximate the number of affected agents by the time difference between i and the dissolution of the queue.

The approach described in Ch. 3 takes this one step further by replacing approximation 2 by actively identifying the affected agents, and multiplying each affected agent's additional delay by its individual value of travel time savings, before allocating the resulting marginal cost to the causing agent. All these approaches have problems when the true bottleneck is not at the end of the present link but further downstream, and there are different variants in how that is treated; for a detailed description, see Sec. 4.3.1. In Agarwal and Kickhöfer (2015) and Ch. 8 the same approach

is combined with a simulation-based methodology to reduce air pollution or noise exposure costs, respectively.

One could assume that a more complex iterative traffic simulation requires a more complex computation of the optimal toll levels. For example, a time-dependent traffic simulation might require the computation of time-variant tolls; for a traffic model with user-specific VTTS, the computation of optimal toll levels might need to account for the users' variable VTTS; for more complex assumptions regarding the transport users' choice dimensions, optimal tolling might become more difficult since marginal social costs need to be computed *mutatis mutandis*, i.e, accounting for the transport users' behavioral reactions. A plausible way of dealing with more complex traffic simulations is thus to extend the computation of optimal tolls towards a higher level of detail. As described in Ch. 3, one approach is to compute link-, time- and user-specific congestion tolls based on the dynamic queuing effects at bottlenecks (see, e.g., Kaddoura and Kickhöfer, 2014; Kaddoura, 2015).

This chapter proposes an alternative approach which neglects the complex interaction of transport users at bottlenecks. This rather simple approach computes time- and link-specific congestion prices and corrects these prices from iteration to iteration applying a simple control-theoretical approach. This chapter investigates the potential and effectiveness of the proposed approach to improve the overall system welfare, and discusses advantages compared to more complex optimization approaches. In this study, Vickrey's bottleneck model is transferred to an iterative agent-based simulation approach which allows for large-scale networks and a sophisticated representation of transport demand. The model is used to develop and investigate different congestion pricing approaches. The newly developed congestion pricing approaches are compared to pre-existing congestion pricing approaches described in Ch. 3. The focus lies on the following two pricing approaches:

1. A rather simple time interval-based list pricing approach described in Sec. 4.3.2 in which marginal congestion cost and tolls are the same for all travelers in the same time interval.
2. A more complex approach which accounts for the queuing dynamics, i.e, the position in the queue and resulting delay effects, described in Sec. 4.3.1 and introduced in Ch. 3.

Simulation results are compared to Vickrey's original model. Finally, to make full use of the simulation-based methodology, the pricing approaches are applied to a real-world case study of the Greater Berlin area.

4.2 The Queue Model's Economics

To get started, let us look at the economics of a single isolated queue. For a single link and assuming all agents to enter the link simultaneously, the total travel cost function is

$$\begin{aligned} C(x) &= VTTS \cdot \left(t_{free} \cdot x + \sum_{i=1}^{x} (i-1) \cdot c_{flow}^{-1} \right) \\ &= VTTS \cdot \left(t_{free} \cdot x + \left(\frac{x^2 - x}{2} \right) \cdot c_{flow}^{-1} \right), \end{aligned} \tag{4.1}$$

where $C(x)$ is the total cost; $VTTS$ is the value of travel time savings[1]; x is the number of agents entering the link; t_{free} is the free speed travel time; and c_{flow} is the (out-)flow, which here is equal to the (out-)flow capacity since there is no spillback from downstream links. That is, first all x travellers incur the free speed travel time, t_{free}. Then, each departing vehicle consumes a time headway of c_{flow}^{-1}, meaning that the ith vehicle is confronted with an additional waiting time of $(i-1) \cdot c_{flow}^{-1}$. Evidently, $C(x)$ increases quadratically with the number of car users. Marginal and average cost are

$$MC(x) = \frac{\partial C(x)}{\partial x} = VTTS \cdot \left(t_{free} + \left(x - \frac{1}{2} \right) \cdot c_{flow}^{-1} \right) \ , \tag{4.2}$$

$$AC(x) = \frac{C(x)}{x} = VTTS \cdot \left(t_{free} + \left(\frac{x}{2} - \frac{1}{2} \right) \cdot c_{flow}^{-1} \right) \ , \tag{4.3}$$

where $MC(x)$ is the marginal travel cost and $AC(x)$ is the average travel cost.

With constant inflow, Eq. (4.1) becomes

$$C(x) = VTTS \cdot \left(t_{free} \cdot x + \left(\frac{x^2 - x}{2} \right) \cdot \left(c_{flow}^{-1} - c_{inflow}^{-1} \right) \right) \ ,$$

where c_{inflow} is the inflow rate or time headway between each agent, and traffic congestion only appears in case $c_{inflow} > c_{flow}$ (active bottleneck, see e.g., Daganzo, 1997). This just replaces c_{flow}^{-1} by $(c_{flow}^{-1} - c_{inflow}^{-1})$ in Eqs. (4.1) to (4.3), that is, the functional form of the dependence on x will not be changed.

From these equations, the following can be observed for the queue model:

- At $x = 0$, marginal and average cost are the same. For $x > 0$, marginal cost is larger than average cost which is consistent with the basic (= static) economic theory (see, e.g., Maibach et al., 2008).
- In heavily congested situations, the outflow c_{flow} might become quite small, for example because of spillback from downstream and/or a situation close to a grid lock. c_{flow}^{-1} thus would become very large, and in consequence the slopes of $MC(x)$ and $AC(x)$ would become close to vertical, and the situation would become similar to a purely capacity-limited facility, as for example described by Button (1993, Chapter 6.2).

4.3 Methodology: Simulation-based Congestion Pricing

This section describes the different congestion pricing implementations that will be investigated in this chapter. They can be grouped into two types: (i) a queue-based internalization of delays and (ii) (time) interval based list prices.

[1] In this simple illustration the VTTS is assumed to be equal for all agents on the link. However, MATSim explicitly allows for agent-specific behavioral parameters including agent-specific VTTS.

4.3.1 Queue based Congestion Pricing (QCP)

The QCP methodology computes delays at an agent-specific level based on the queuing dynamics at the bottleneck link. That is, an agent's toll depends on the position in the queue and the number of following travelers (in the same queue) as well as their VTTS.

In each iteration, marginal congestion costs are estimated based on the *ceteris paribus* effect, i.e, neglecting the agents' reactions of using alternative routes or times of the day. However, from iteration to iteration the agents are enabled to change their travel behavior in order to avoid traffic congestion or toll payments. That is, over the entire simulation process, i.e, for multiple iterations, user reactions are accounted for, and the computation of marginal congestion cost moves towards the *mutatis mutandis* principle (see, e.g., Arnott et al., 1993; Button, 2004).

Pre-existing QCP Approach The pre-existing congestion pricing methodology allocates delays to the causing agent. The basic mechanism is described below. For a detailed description of this approach, see Sec. 3.2.1.1.

- For each agent leaving the link r ("affected agent"), the link-specific delay is computed as the difference between free speed travel time and actual travel time.
- If an agent's delay is > 0 sec, iterate through link r's queue (starting with the first agent ahead and then proceeding with the next agent ahead, and so on) and let each "causing" agent pay for $c_{flow,r}^{-1}$ **until the delay is fully internalized (cost recovery)** or until the vehicle initially starting link r's queue is reached (meaning there is spill-back resulting from a downstream link; see next point).
- Spill-back related delays are taken into account as follows: For each causing agent ahead who pays for $c_{flow,r}^{-1}$, the same amount of time is deducted from the affected agent's total delay which needs to be internalized. Without any spill-back related delays, there is no remaining delay after iterating through the queue of link r. In case the delay is not fully internalized after iterating through link r's queue, the non-internalized delay is stored with the affected agent. The agent will carry it into the next link, and attempt to allocate it there to the vehicles ahead, if there is a queue at the end of that next link. This may eventually lead to the spill-back causing link, where the bottleneck is active, i.e, the link's flow capacity prevents agents from moving to the next link.

The pre-existing methodology can be considered as marginal congestion pricing with price-cap, resulting in toll revenues that correspond to the level of the congestion cost (cost recovery). Consequently, the pre-existing approach may underestimate optimal toll levels.

New QCP Approach (a) This approach is similar to the pre-existing one but goes beyond cost recovery. Instead, each agent in the queue ahead is considered as the causing agent. In contrast to the pre-existing approach, this approach may result in toll revenues that exceed total congestion costs.

- If the delay is > 0 sec, iterate through the queue of link r and let **each** agent ahead pay for $c_{flow,r}^{-1}$.
- Spill-back related delays are taken into account as follows: Non-internalized delays after iterating through the link r's queue are added to the agent's delay on the next downstream link, as in the pre-existing QCP approach.

New QCP approach (b) This approach is similar to QCP Approach (a), except that spill-back related delays are **not** additionally taken into account.

Some Discussion of the QCP Approaches One notes that the description of QCP approaches becomes quite involved. There are also many design decisions that need to be made, for example:

- Should causing agents be charged $c_{flow,r}^{-1}$, or their actual time headway? The latter feels more intuitive, but would be grossly unfair if the actually active bottleneck would be further downstream (and the causing agent maybe even take a different route). – The present investigation always allocates $c_{flow,r}^{-1}$.
- Should affected agents receive compensation for their delay, or should the toll go to some authority? The former might lead to some "bucket brigade" (Holland, 1992) flow of compensations where, say, each agent could charge the agent ahead *fully* for its delay, and the agent ahead could then charge the agent further ahead for its own delay, thus only having to pay the difference. – The present investigation takes the second alternative.
- Should delays be allocated upstream across nodes? Clearly, the actually active bottleneck might be further downstream, pointing to a "yes" answer. However, for this the algorithm would have to identify the actually active bottleneck. – The present investigation makes certain compromises here, as explained above.

4.3.2 Interval-based List Pricing (LP)

The List Pricing (LP) approach computes tolls based on the congestion level in a previous iteration. These tolls, or interval-based list prices (see, e.g., Schlechte and Tanner, 2010; Tanner and Mitusch, 2011), are computed for each link and time interval. In contrast to the QCP methodology, all agents traveling on the same link and within the same time interval face the same toll payments. As control loop feedback mechanism two different controllers, a rather simple control approach (Controller A) and a proportional-integral-derivative (PID) controller (Controller B) are embedded in the iterative simulation approach described in Sec. 1.5. Both controllers use road charges to control traffic and to decongest the transport network.

1. Initialization: Run the simulation for k^{pre} iterations without any price setting.
2. Compute the average delay per link and time interval as

$$d_{r,t,k}^{0} = \frac{\sum_{n=1}^{N_{r,t,k}} (t_{r,t,n,k}^{act} - t_{r}^{free})}{N_{r,t,k}} \ , \tag{4.4}$$

   where r denotes the link, t is the time interval, k is a counter for the price adjustment iteration, n denotes the agent, $N_{r,t}$ is the total number of agents leaving link r in time interval t, $t_{r,t,n,k}^{act}$ is the actual travel time and t_{r}^{free} is the free speed travel time.
3. A link and time interval is considered as congested if a certain threshold value is exceeded. Thus, set the average delay which is processed by the controller to

$$d_{r,t,k} = \begin{cases} 0 & \text{for } d_{r,t,k}^{0} < d^{min} \\ d_{r,t,k}^{0} & \text{for } d_{r,t,k}^{0} \geq d^{min} \end{cases} \ , \tag{4.5}$$

where d^{min} denotes the threshold value.

4. Control:

   LP Controller A: Controller A adjusts the price per link and time interval as follows:

$$m_{r,t,k} = \begin{cases} m_{r,t,k-1} + a & \text{for } d_{r,t,k} > 0 \\ max\{0, m_{r,t,k-1} - a\} & \text{for } d_{r,t,k} = 0 \end{cases}, \tag{4.6}$$

   where $m_{r,t,k}$ denotes the adjusted toll per link and time interval, $m_{r,t,k-1}$ is the previous toll, and a is the toll adjustment value.

   LP Controller B: Controller B is a discrete PID controller which adjusts the price per link and time interval as follows:

$$m_{r,t,k} = max\{0, K_p \cdot d_{r,t,k} + K_i \cdot D_{r,t,k} + K_d \cdot (d_{r,t,k} - d_{r,t,k-1})\}, \tag{4.7}$$

   where K_p, K_i and K_d denote tuning parameters, $D_{r,t,k}$ is the current integral value, $d_{r,t,k-1}$ is the previous average delay. $D_{r,t,k}$ is initially set to zero and then changed as follows: If $d_{r,t,k}$ is positive, $D_{r,t,k}$ is increased by $d_{r,t,k}$. If $d_{r,t,k}$ is zero, $D_{r,t,k}$ is decreased by deducting the unused road capacity which is computed as $w \cdot \left(\frac{T}{N_{r,t,k}} - c_{flow,r}^{-1}\right)$, where T is the time bin size of time interval t and w is a scaling factor.

5. Keep the tolls constant and let the transport demand adjust for k^{update} iterations. Thereby, enable all agents to adjust their choice sets for $k^{update} \cdot k^s$ iterations, where k^{update} is the toll update interval and k^s is the fraction of iterations during which agents are enabled to explore new travel alternatives. For the final $(1 - k^s) \cdot k^{update}$ iterations, the agents are only allowed to select from their existing choice sets based on a multinomial logit model.
6. Repeat steps 2 to 5 several times.
7. Finally, run the simulation for k^{post} iterations without adjusting the prices.

4.4 Illustrative Example: Vickrey's Bottleneck Scenario

4.4.1 Choice Dimensions and Scenario Setup

This section describes how Vickrey's bottleneck scenario (Vickrey, 1969; Arnott et al., 1990, 1993, see also Sec. 1.2) is applied in the agent-based simulation context of MATSim.

The **network** consists of three subsequent links link 1, link 2 and link 3, where link 2 is the bottleneck with a flow capacity of 1800 vehicles per hour (see Fig. 4.1). Spill-back effects are neglected. The free speed travel time from link 1 to link 3 amounts to 202 *sec*.

(0) ——link 1——> **(1)** ——link 2——> **(2)** ——link 3——> **(3)**

Figure 4.1: Illustrative scenario: Network

The **demand** is modeled as 7200 agents that each perform one trip from link 1 to link 3. The behavioral parameters α, β and γ which in Arnott et al. (1990) denote the marginal cost of traveling,

early arrival and late arrival are set as follows: $\alpha = 12$, $\beta = 6$, $\gamma = 18$ in monetary units per hour. The desired arrival time is 8.30 a.m. by setting both the activity opening and latest activity start time on link 3 to the same value. Each agent's utility is computed based on the travel time cost, the schedule delay cost and the monetary tolls. Further utility components are neglected. Demand elasticity is introduced by allowing for departure time choice. The total number of iterations is set to 500. In each iteration 5% of all agents are enabled to randomly shift their departure times within the range of 2 hours. All other agents select from their existing choice sets according to a multinomial logit model. The choice set is limited to 5 plans per agents. Further parameters are set as follows: $k^{update} = 1$ and $k^s = 1.0$, meaning tolls are updated in every iteration; $T = 300$ sec; $d^{min} = 30$ sec; $a = 1.0$ monetary units; $K_p = K_i = K_d = 0.01$; and $w = 10.0$ (for an explanation of these parameters, see Sec. 4.3.2).

4.4.2 Results

Tab. 4.1 provides the total travel time, delay, user costs (including toll payments), toll revenues and system welfare for the final iteration in the base case (no pricing) and the different congestion pricing approaches. All congestion pricing approaches are found to reduce total travel delay and to

Table 4.1: Vickrey's bottleneck scenario.

	Base case (no pricing)	LP controller A $a = 1.0$	LP controller B K_p=K_i=K_d=0.01	QCP pre-existing approach	QCP approach (a) & (b)
Total travel time [h]	4,289	459	440	3,035	767
Total delay [h]	3,885	55	36	2,631	363
Difference in user benefits including toll payments [monetary units]	n/a	−24,221	−18,725	−16,141	+19,199
Toll revenues [monetary units]	0	65,335	57,902	31,570	20,829
Difference in system welfare [monetary units]	n/a	+41,114	+39,177	+15,429	+40,028

increase system welfare. The LP approach (both controllers) and the QCP approaches (a) and (b) result in a higher increase in system welfare compared to the pre-existing QCP approach; note that QCP (a) and (b) are identical for this setup since there is no spillback.

Fig. 4.2 depicts the number of departing and en route agents per time of day (in 5-minute time bins) for the final iteration in the base case and the different congestion pricing approaches. This visualization reveals that in all congestion pricing experiments the number of en route agents is at an overall lower level compared to the base case. The LP approach (Controller A and B) approximates a uniform distribution of departures and en route agents during the morning period. In contrast, for the QCP approach the number of en route agents and departure time distribution depicts one (QCP approaches (a) and (b)) or several (QCP pre-existing approach) peaks.

Fig. 4.3 depicts the toll level per time of day for the final iteration in the different congestion pricing experiments. In the LP approach, the toll time distribution is triangular shaped. The toll first increases from 0 at around 5.30 a.m. to a maximum value of approximately 18 monetary units at the desired arrival time (8.30 a.m.) and then decreases to 0 at around 9.45 in the morning. In

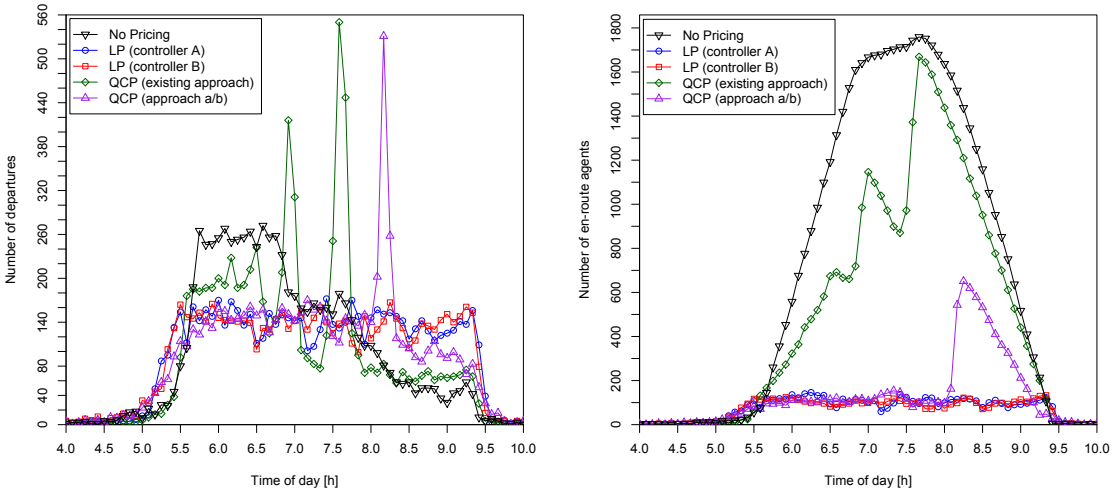

(a) Departures **(b)** En route

Figure 4.2: Number of departing and en route agents per time of day

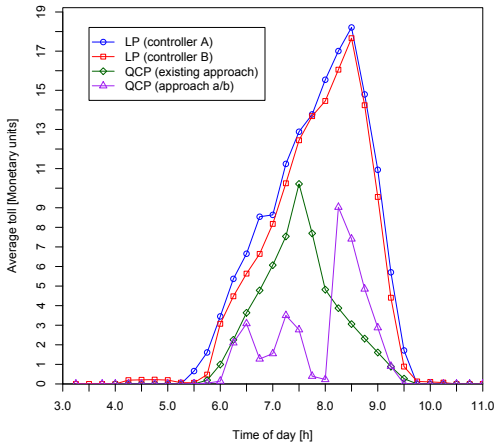

Figure 4.3: Average toll per time of day.

the pre-existing QCP approach, the average toll per time of day is at an overall lower level; with a maximum value of 10 monetary units at around 7.30 in the morning. The QCP approaches (a) and (b) result in an overall lower toll level compared to the LP approach, with several peaks.

In Fig. 4.4, the cumulative departures and arrivals are shown for the morning period. The horizontal distance between cumulative departures and arrivals describes the travel time, and the vertical distance describes the queue length. Thus, the area between the two curves indicates the level of traffic congestion which is observed to be very high in the no pricing situation, reduced for the QCP approach and very low applying LP approach.

The following lessons can be taken from these results:

- The pre-existing QCP approach is not strong enough to bring congestion down to zero (see Fig. 4.4c). This corresponds to the fact that the pre-existing QCP approach only charges up to cost recovery, whereas economic theory would demand to charge marginal cost, which is larger.

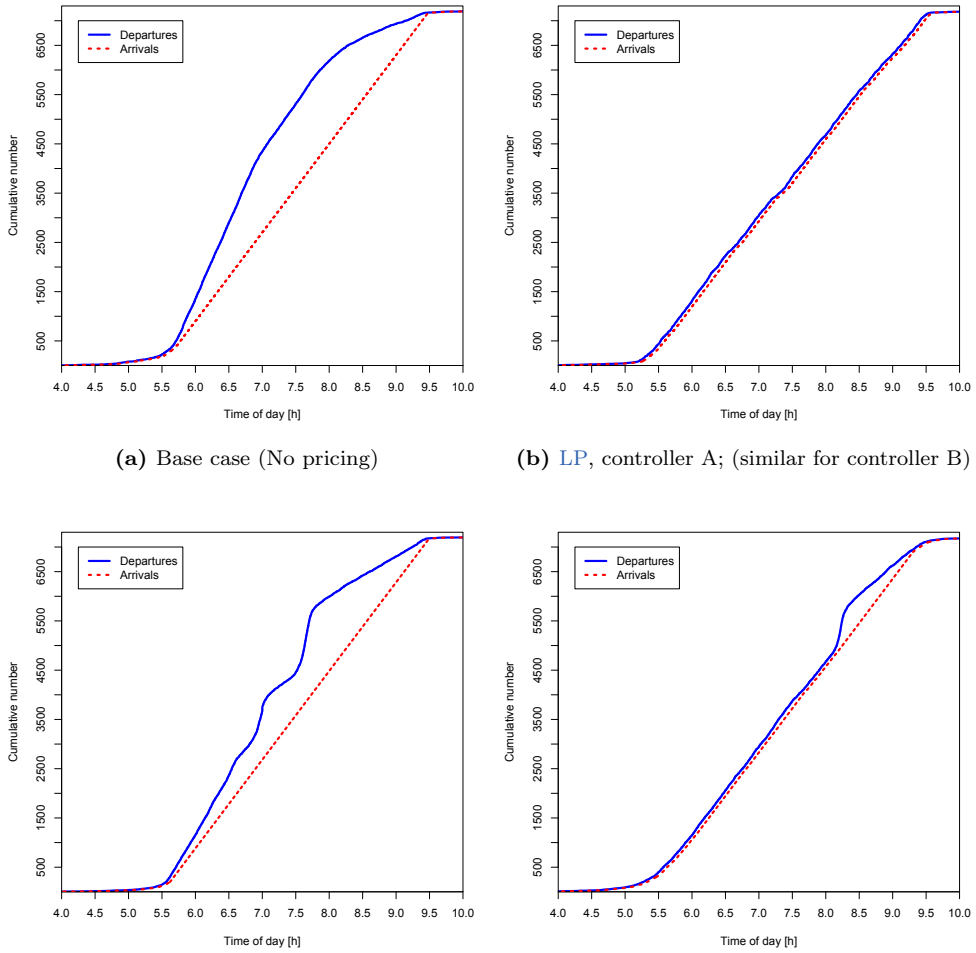

(a) Base case (No pricing)

(b) LP, controller A; (similar for controller B)

(c) QCP, pre-existing approach

(d) QCP, approach = (a) or (b)

Figure 4.4: Cumulative departures and arrivals in the final iteration

- The QCP (a) or (b) approaches have stability issues in the Vickrey scenario. The reason is that with QCP the first vehicle in a queue always pays most. In consequence, the early positions in the queue become very unattractive. The drivers react by underutilizing the capacity during these early times. The system reacts by repeatedly "breaking" the queue, thereby reducing the charges for the early vehicles (see the "QCP a/b" lines both for the toll in Fig. 4.3 and for unused capacity in Fig. 4.5). Note how, in Fig. 4.3, QCP a/b at least gets

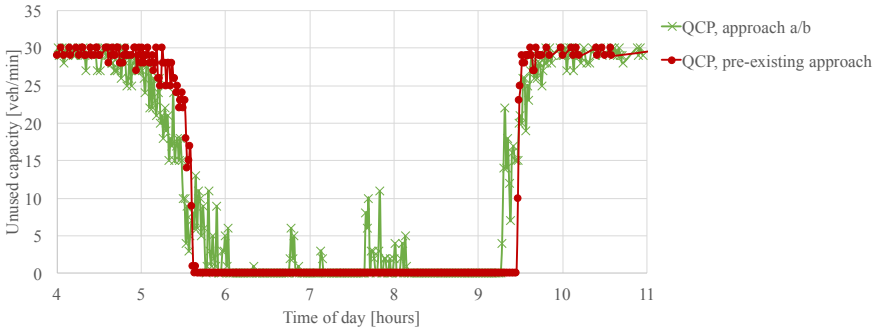

Figure 4.5: The bottleneck's unused capacity per time of day.

the position of the maximum approximately right. However, it clearly has problems getting the ramping up to that level right.

4.5 Case Study: Berlin, Germany

4.5.1 Scenario Setup

The congestion pricing approaches are applied to a real-world case study of the Greater Berlin area generated by Ziemke et al. (2019) based on the methodology developed by Ziemke et al. (2015). The transport **supply** consists of all major and minor roads in the Greater Berlin region, including all PT lines. The transport **demand** is modeled as individual agents, including commuters and non-commuters using the car, PT, bicycle, ride and walk mode. To speed up computational performance, a 10% population sample is used and the road segments' flow and storage capacities are reduced accordingly to model realistic congestion effects. Simulated traffic volumes are calibrated against hourly traffic counts for a total of 346 traffic count stations in the Berlin area. Furthermore, the simulation results are validated using System repräsentativer Verkehrsbefragungen, Mobilität in Städten (SrV) 2008 (Ahrens, 2009) and Mobilität in Deutschland (MiD) (infas and DLR, 2010) survey data accounting for, e.g., the total trip number, departure time distribution, and mode-specific trip distances and travel times. Each agent has an individual activity schedule and is differently pressed for time. Consequently, the resulting VTTS is different for each transport user (see Ch. 3). In the base case, the average VTTS per person amounts to 7.57 EUR/h with a 5% percentile of 4.53 EUR/h, a median of 6.74 EUR/h and a 95 % percentile of 16.31 EUR/h. The applied Berlin case study is publicly available via GitHub (MATSim-VSP, 2019, release version 5.2)

4.5.2 Choice Dimensions, Simulation Setup and Simulation Experiments

For different assumptions regarding transport users' choice dimensions, a selection of pricing schemes is applied to the Greater Berlin case study. In a first setup, transport users are only enabled to change their routes. In a second setup, transport users are enabled to adjust their routes, departure times and modes of transportation.

Each choice dimension is represented by a strategy which is either enabled or disabled.

- **Route choice:** A new transport route is generated based on the least cost path taking into account mean travel times and toll payments from the previous iteration(s). That is, the agents may accept a longer route, i.e, higher distance- or time-based travel costs, in order to avoid toll payments.
- **Departure time choice:** Activity end times are randomly shifted within a maximum range of two hours. That is, the agents may accept schedule delay costs and deviate from the desired activity schedule in order to avoid traffic congestion or toll payments.
- **Mode choice:** For each sub-tour (i.e, trips starting and ending at the same activity location), the transport mode is randomly set to only car, only bicycle or a random combination of PT or walking.

Note that, in MATSim, the strategies generate new alternatives. The actual selection of the alternatives is performed in a separate choice model, based on the scores of the executed plans.

In this study, the total number of iterations is set to 500. Only during the first 400 iterations choice sets are generated and the agents are enabled to generate a new travel plan based on the enabled choice dimensions. During the first 400 iterations, each strategy is applied by 5% of the transport users. All other agents select from their existing choice sets according to a multinomial logit model. In the final 100 iterations, choice set generation is disabled and all agents select from their existing choice sets. Each agent's choice set is limited to 5 plans which is considered to yield a plausible level of fluctuations in daily travel behavior from one iteration to the next one. The LP parameters are set as follows: $k^{update} = 1$ and $k^s = 1.0$, meaning tolls are updated in every iteration; $T = 900$ sec; $d_{min} = 1$ *sec*. In contrast to Vickrey's illustrative bottleneck example, the real-world Berlin case study requires a computation time of several days. Hence, to avoid a large number of parametric runs, the number of tuning parameters is reduced. K_i and K_d are set to 0, and instead the method of successive averages is used to smoothen the toll levels over the iterations.

4.5.3 Results

Resulting Toll Payments Each pricing approach results in different toll payments. Tab. 4.2 provides the average and maximum toll payments per car trip for each pricing and simulation setup. The total toll which is paid during a trip results from the congestion level on each road segment

Table 4.2: Resulting toll payments

	LP controller B $K_p = 0.003$ $K_i = K_d = 0$	QCP pre-existing approach	QCP approach (a)	QCP approach (b)
Average toll per car trip [*EUR*]				
Route choice only	0.31	0.19	0.55	0.46
Route, mode and departure time choice	0.27	0.16	0.39	0.34
Maximum toll per car trip [*EUR*]				
Route choice only	3.88	4.11	12.62	12.36
Route, mode and departure time choice	3.63	4.78	12.25	9.27

along the transport user's route from one activity to the next one. For a single road segment, toll payments may be different depending on the time of day (QCP, LP) or position in the queue (QCP). Tab. 4.2 points out that even though there is no upper limit, toll levels stay within a certain range because transport users are not willing to accept large payments and rather take a detour or switch to an alternative time or mode. This, in turn, reduces the congestion level on that road segment in that time bin which in turn reduces the toll level. In the LP approach, for example, the maximum toll per road segment (= per bottleneck) amounts to 1.75 *EUR* in the simulation experiment with route choice only and 1.25 *EUR* in the simulation experiment with route, mode and departure time choice. A comparison of the different simulation setups reveals that with mode and departure time choice, average toll payments are at a lower level compared to the route choice only case.

Aggregated Analysis Tab. 4.3 and Tab. 4.4 provide the changes in travel time, travel distance, delay, user benefits (including the negative effect of toll payments), toll revenues and system welfare of each congestion pricing approach compared to the base case (no pricing).

Table 4.3: Berlin: Route choice only (upscaled to 100%); comparison with the base case (no pricing)

	LP controller B $K_p = 0.003$ $K_i = K_d = 0$	QCP pre-existing approach	QCP approach (a)	QCP approach (b)
Change in car travel time [thousand *h*]	-49.40	-32.57	-41.61	-43.55
Change in average travel time per car trip [*sec*]	-23	-15	-19	-20
Change in car travel distance [thousand *km*]	512.32	210.97	983.38	753.21
Change in average travel distance per car trip [*km*]	0.06	0.03	0.12	0.10
Change in car delay [thousand *h*]	-64.85	-39.45	-75.43	-68.43
Change in average delay per car trip [*sec*]	-30	-18	-34	-31
Change in user benefits including toll payments [thousand *EUR*]	-2,192.26	-1,263.34	-4,251.34	-3,441.66
Toll revenues [thousand *EUR*]	2,451.33	1,466.62	4,359.18	3,611.05
Change in welfare [thousand *EUR*]	259.07	203.28	107.84	169.39

All pricing experiments are found to reduce total car travel time and delay (direct congestion effects). The LP approach yields the largest increase in system welfare and reduction in average travel time.

The pre-existing QCP approach yields lower prices compared to the LP approach. Consequently, the remaining level of congestion is larger compared to the LP approach. In contrast, the QCP approaches (a) and (b) yield a higher level of congestion prices compared to the LP approach. The reduced overall welfare gains imply that tolls here are now so high that the network utilization is below the optimum.

In the route choice only case, the total travel distance slightly increases which indicates that transport users take longer detours in order to avoid congested and/or tolled road segments. In contrast, with mode and departure time choice, the average travel distance per car trip increases even though the total car travel distance decreases. This indicates that short-distance travelers switch from car to alternative modes, while long-distance travelers remain within or switch to the car mode. Similar, the reduction in average travel time per car trip is lower compared to the simulation experiments without mode and departure time choice.

The comparison of the different choice dimensions reveals that mode and departure time choice increase the overall positive effect of the pricing schemes. With mode and departure time choice the increase in system welfare which results from the LP approach multiplies by two compared to the only route choice case.

Table 4.4: Berlin: Route, departure time and mode choice (upscaled to 100%); comparison with the base case (no pricing)

	LP controller B $K_p = 0.003$ $K_i = K_d = 0$	QCP pre-existing approach	QCP approach (a)	QCP approach (b)
Change in number of car trips (in thousands)	-554.04	-341.07	-986.31	-797.43
Change in car travel time [thousand *h*]	-293.93	-187.14	-460.91	-388.03
Change in average travel time per car trip [*sec*]	-14	-11	7	-3
Change in car travel distance [thousand *km*]	-3,492.73	-2,115.76	-6,488.22	-5,182.00
Change in average travel distance per car trip [*km*]	0.54	0.33	0.98	0.78
Change in car delay [thousand *h*]	-118.36	-81.82	-146.84	-134.75
Change in average delay per car trip [*sec*]	-48	-33	-58	-54
Change in user benefits including toll payments [thousand *EUR*]	-1,450.14	-834.71	-2,409.67	-1,996.38
Toll revenues [thousand *EUR*]	1,968.39	1,245.55	2,705.48	2,379.25
Change in welfare [thousand *EUR*]	518.26	410.84	295.81	382.87

Spatial Analysis: Traffic Congestion The spatial analysis confirms the above described reduction in traffic congestion. Fig. 4.6 depicts an inner-city motorway bottleneck situation and the resulting queues in the base case and the pricing policy (LP; Controller B; simulation experiment with route, mode and departure time choice).

Spatial Analysis: Traffic volumes Fig. 4.7 and Fig. 4.8 depict the changes in traffic volumes resulting from the pricing policy (LP, Controller B) in the simulation setup without and with mode and departure time choice. The simulation setup without mode and departure time choice reveals an overall tendency of reduced demand levels on major roads including the inner-city motorway and increased demand levels on minor roads (see Fig. 4.7). In contrast, the simulation setup with route, mode and departure time choice, traffic volumes are at an overall lower level (see Fig. 4.8) since transport users switch from car to alternative modes.

Person- and Trip-based Mode Shift Analysis In Fig. 4.9, the changes in transport modes are shown for each person and trip in the base case and the policy case (LP, Controller B; simulation setup with route, mode and departure time choice). Fig. 4.9 depicts all trips including those of transport users remaining within their previous transport mode. Fig. 4.9 reveals that for most trips, transport users remain within their previous transport mode and only a relatively small share of trips switch from car to bicycle (5%) and PT (3%).

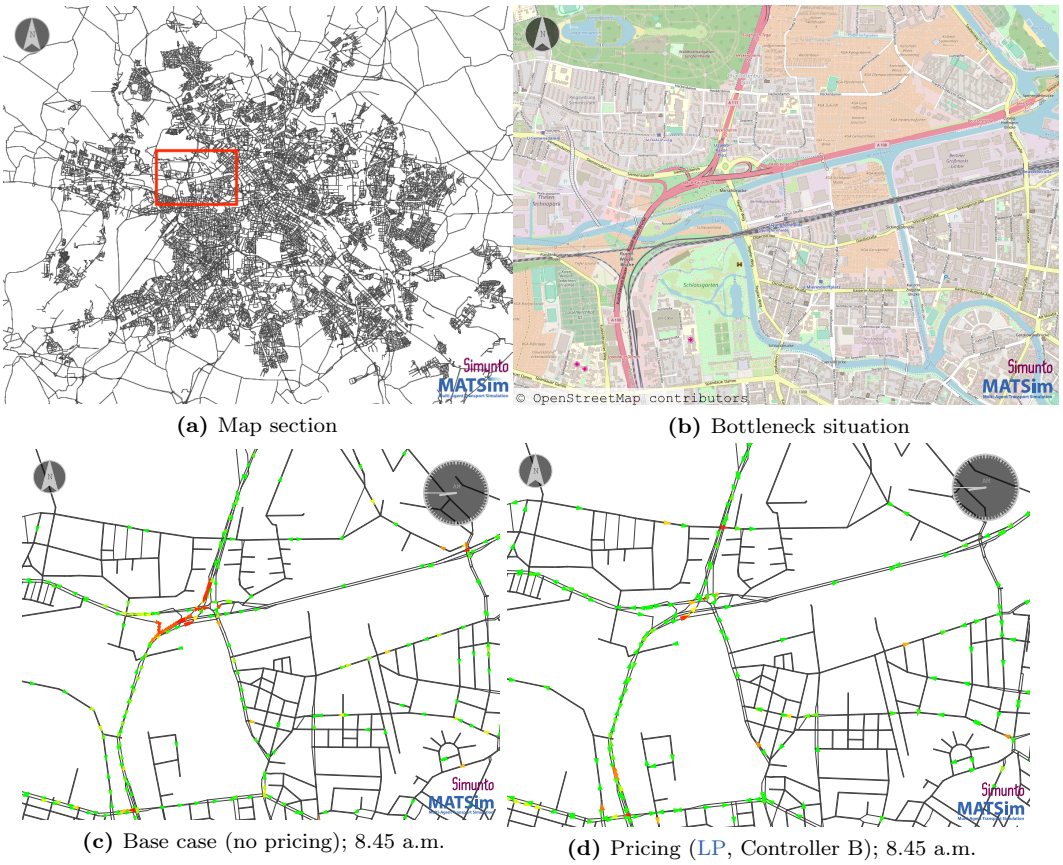

(a) Map section

(b) Bottleneck situation

(c) Base case (no pricing); 8.45 a.m.

(d) Pricing (LP, Controller B); 8.45 a.m.

Figure 4.6: An inner-city motorway bottleneck situation: Red indicates a delayed vehicle; Green indicates a non-delayed vehicle. Map layer: © OpenStreetMap contributors. (Simulation experiment with route, departure time and mode choice)

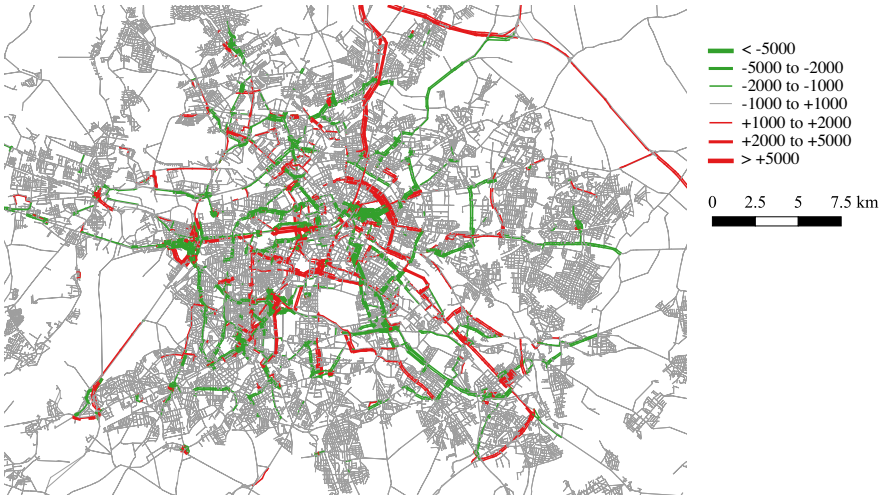

Figure 4.7: Changes in daily traffic volume resulting from the pricing scheme (LP, Controller B) only allowing for route choice. Red road segments indicate an increase in traffic; Green road segments indicate a decrease in traffic.

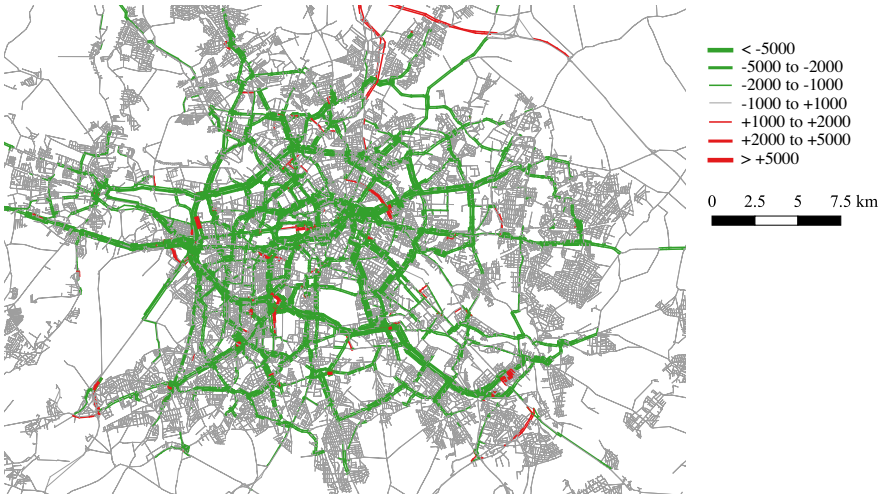

Figure 4.8: Changes in daily traffic volume resulting from the pricing scheme (LP, Controller B) allowing for route, departure time and mode choice. Red road segments indicate an increase in traffic; Green road segments indicate a decrease in traffic.

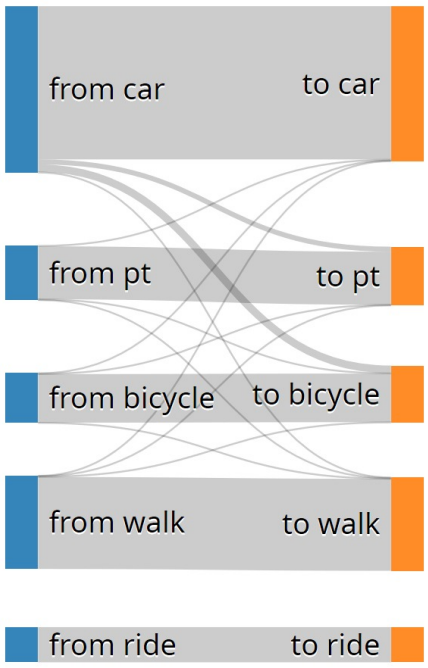

Figure 4.9: Person- and trip-specific mode switch analysis; Left: Base case; Right: Congestion pricing (LP, Controller B); Simulation experiments with route, mode and departure time choice

4.6 Discussion

The QCP approach internalizes delays directly, with each person in the queue paying for the additional delay it is causing to each person later in the queue. This has the immediate consequence that the first person in the queue has to pay most. On the other hand, it is known from, e.g., Vickrey (1969) or Arnott et al. (1990), that the optimal toll in this situation is triangular, i.e, with the first person in the queue paying little, the toll then increasing to a maximum, and then decreasing again. The reason, as Arnott et al. (1990) explain, is that internalization has to happen not *ceterus paribus*, as the QCP approach does, but *mutatis mutandis*, i.e, taking into account behavioral reactions. This results in unstable behavior: At some point, early travellers avoid tolled routes because they are too expensive. However, at this point very early travellers can use it again, since the queue will be broken at some point and thus the toll will be affordable. This entices more and more travellers to use the tolled route, until at some point the queue is no longer broken, the early travellers pay a lot, and the adaptive cycle is started again.

One might thus have speculated that QCP is approximately optimal when departure time choice and mode choice are switched off, since then the *mutatis mutandis* reaction does not seem possible. However, the simulation experiments reveal that also without mode and departure time choice, LP results in a higher system welfare compared to the QCP approach. An explanation for this may be that even without mode and departure time choice, the circular behavior described in the previous paragraph can occur, and thus the system remains strongly fluctuating, making it difficult for the adaptive agents to find a good solution. Conversely, for the real-world scenario in Sec. 4.5 with departure and mode choice enabled, the QCP approach is not as bad as one might have expected based on these thoughts. Presumably, any kind of internalization leads to improvements. Still, the LP approach is not only the most successful one here, but also to prefer because it is the simplest of the approaches that are investigated.

Both applications of the developed pricing rules show that delays are significantly reduced and the system welfare is increased. However, there is a certain amount of delay which remains. For LP-B and $K_i = K_d = 0$, there indeed has to be some remaining delay, since with these parameters Eq. (4.7) implies that delay $d = m/K_p$, where m is the toll and K_p is a positive constant. Increasing the penalty for traveling in a congested time period, e.g., by setting a (LP; Controller A) or K_p, K_i, K_d (LP; Controller B) to very high values further reduces or even eliminates traffic congestion. This, however, reduces the system welfare which is explained by a too strong reaction of the agents to avoid the congestion charges. With such drastic tolls, over many iterations, the agents maximize their individual utility by rather traveling far too early or far too late (and deviating from individually optimal activity durations) in order to avoid paying high tolls. Thus, departing during or even close to the peak time becomes unattractive.

Controller B allows for an economic interpretation. The economic theory suggests that optimal prices should reflect marginal external costs (see, e.g., Maibach et al., 2008). A proportional controller ($K_i = K_d = 0$) where travel delay is considered as the error value and where $K_p = VTTS$ may be interpreted as average congestion cost pricing. Taking into account the travel cost functions described in Sec. 4.2, K_p in the range of approximately twice the average $VTTS$ may approximate a marginal congestion pricing approach. And indeed, the average VTTS, see Sec. 4.5.1, is 7.57 $EUR/h \approx 0.0021$ EUR/sec, meaning that twice that value is similar to the value of 0.003 that was found heuristically. More theory, however, would be needed to fully untangle the relation between queueing, behavioral reaction, and toll levels.

The LP approach offers two additional advantages over the QCP approach. First, the computation

of congestion prices is much easier, which results in a better computational performance. Second, the LP approach computes link-specific tolls for a predefined time interval length, e.g., one hour, that are equal for all transport users within the same time interval. This makes the real-world application of the LP tolling scheme more feasible compared to the QCP approach where each transport user pays a different amount depending on her or his position in the queue.

Nevertheless, the LP tolling scheme only provides a first step towards the design of welfare improving pricing policies that are applicable to the real world.

The mechanism to model transport users' departure time adaptation which is applied in the Berlin and Vickrey case study randomly shifts activity end times within a certain range. The adjusted activity schedule is then tested and evaluated in the next iteration(s) (see Sec. 1.5). Since the maximum number of travel plans per agent is limited, the worst plan will be discarded. Each travel plan is then re-evaluated in the following iterations, i.e, every time it is chosen from the existing choice set and executed. That is, the learning mechanism accounts for the travel plans' reliability (see, e.g., Neumann et al., 2016). Nevertheless, the applied mechanism to model transport users' departure time adaptation follows a rather simple approach. For a more complex time adaptation approach, which applies several search rules and explicitly accounts for, e.g., uncertainty, search costs and different sources for the knowledge about departure time-specific travel conditions, see, e.g., Xiong and Zhang (2013).

4.7 Conclusion

This chapter investigates optimal congestion pricing strategies using an agent-based simulation framework which allows for real-world application and complex user behavior. Traffic congestion is simulated based on a queue model, where limited space on roads may cause spill-back and move bottlenecks upstream. Transport users iteratively adjust their travel behavior based on their experienced travel cost. Hence, the applied simulation approach goes beyond the simplifying assumptions typically made in other models in order to reduce the real-world complexity. Instead, the applied simulation approach accounts for iterative learning, stochastic user behavior, and only approximates the user equilibrium, which may be considered as closer to real world than a model where transport users behave completely rational, have a perfect knowledge about all travel alternatives, and travel behavior strictly follows the user equilibrium.

This study investigates the no closed-form solution of the optimization problem of how to set link-, time- and user-specific road charges in order to increase the overall system welfare under the above described circumstances. The literature provides some help to address this problem: Following the concept of Pigouvian taxation, road charges are optimized by setting them equivalent to the (link-, time- and user-specific) marginal external costs. By doing so, experienced travel costs are corrected and individual travel decisions are changed towards an overall higher level of efficiency. The resulting changes in the transport system depend on the assumptions regarding how transport users can react to the road charges. In the case of departure time choice and queue-based bottleneck dynamics, the literature suggests to expect traffic congestion to completely dissolve (see, e.g., Vickrey, 1969).

Unfortunately, defining the correct marginal external costs is not obvious in a time-dependent model with a queue-based traffic flow behavior. In this chapter, two pricing rules are developed and investigated. The first one directly builds on the Pigouvian taxation principle and computes

marginal external congestion costs based on the queuing dynamics at the bottleneck links; resulting toll payments differ from agent to agent depending on the position in the queue (QCP approach). The second one builds on the desired outcome and uses control-theoretical elements to adjust toll levels depending on the congestion level in order to reduce or eliminate traffic congestion; resulting toll payments are the same for all agents in the same time bin and on the same road segment (LP approach).

The pricing rules are applied to Vickrey's bottleneck model and the case study of the Greater Berlin area. The simulation experiments reveal that with and without departure time and mode choice, the rather simple LP rule results in a higher system welfare compared to the more complex, and seemingly more "correct", QCP approach. In the end, the QCP approach only approximates optimal toll levels since it computes external congestion costs *ceteris paribus*, i.e, based on the travel behavior in the current iteration, and not *mutatis mutandis*, i.e, taking into consideration the transport users' reactions. The rather complex calculation of optimal toll levels, i.e, accounting for the queuing dynamics, appears to result in large fluctuations from iteration to iteration which leads to a less stable simulation outcome. In contrast, the LP rule appears to better take into account the system's dynamics and the agents' learning behavior and produces a more stable outcome. The results also reveal that the pricing rules significantly reduce traffic congestion, however, there is still a remaining delay, even in the simulation experiments with mode and departure time choice.

Overall, this study contributes to the exploration of optimization heuristics for real-world oriented simulation approaches which allow for a complex user behavior and a high level of realism. This study also contributes to the practical implementation of pricing policies. The simulation results indicate the importance of accounting for the system's dynamics and implement a robust pricing scheme which smoothens the day-to-day traffic fluctuations, e.g., by rather slowly adjusting time-specific toll levels from one time period (day/week/month) to the next one.

Part II

Noise Pricing

CHAPTER 5

Activity-based and Dynamic Calculation of Road Traffic Noise Damages

In this chapter, an activity-based and dynamic approach is presented to analyze population exposures to road traffic noise. The contribution of this innovative approach is that (1) affected people at the workplace and places of education are incorporated and (2) the within-day dynamics of varying population densities in different areas of the city is explicitly taken into account. The proposed methodology is applied to a real-world case study of the Greater Berlin area. This chapter is an edited version of a paper that has been previously published (Kaddoura et al., 2017b).

5.1 Introduction and Problem Statement

Environmental noise is described as a growing public health problem (WHO Europe, 2011) which causes sleep disturbance, cognitive impairment, tinnitus and cardiovascular diseases (see, e.g., Ising et al., 1996; Stassen et al., 2008; WHO Europe, 2009, 2011; Babisch et al., 2013). A recent survey reveals that more than half of the population in Germany feels annoyed or disturbed by road traffic noise (Rückert-John et al., 2013). The Environmental Noise Directive of the European Union 2002/49/EC aims to reduce these effects. In order to identify priorities for action planning, an approach is defined to draw up strategic noise maps based on national computation methods and a standardized noise indicator (2002/49/EC, Appendix 1 and 2).[1] Several noise computation models have been developed in different countries, e.g., the Richtlinien für den Lärmschutz an Straßen (RLS-90) in Germany (FGSV, 1992), the CoRTN (Calculation of Road Traffic Noise) in the United Kingdom (Department of Transport, 1988), the Nordic Prediction Method in Norway, Denmark, Sweden and Finland (Nielsen et al., 1996). In a recent study by Garg and Maji (2014) a comparative review of the different calculation approaches is provided.

For the prioritization of noise control measures the computation of noise exposures to individuals is a crucial element. According to Appendix 4 of 2002/49/EC strategic noise mapping may include the presentation of a noise indicator or the exceeding of limit values, but also of estimates for the number of people or certain buildings that are exposed to noise. Eriksson et al. (2013) compare predicted and survey-based exposures and find Swedish noise maps to be useful for the assessment of residential traffic noise exposures. To indicate the exposures to the population, most noise maps include the building boundaries, however, the number of people that is exposed to certain noise levels is usually not directly shown in the map (see, e.g., SenStadt (2012b) for Berlin and DEFRA (2014) for London). Tables or charts may additionally provide estimates for the population exposures, however, theses numbers are usually spatially aggregated at city or post code level (see, e.g., SenStadt, 2012a; DEFRA, 2015).

Since certain buildings, i.e., schools and hospitals, are explicitly mentioned in 2002/49/EC, noise exposure analysis is not limited to residents at their home location. However, the data to be sent to the European Commission specified in Appendix 6 of 2002/49/EC only refers to residential noise exposures. Moreover, also the 'Good Practice Guide for Strategic Noise mapping and the Production of Associated Data on Noise Exposures' which provides recommendations regarding the computation of sound sources, noise propagation and noise immission at the receiver point, only refers to people who are affected in dwellings (WG-AEN, 2006). As a consequence, noise exposure analysis usually follows a home-based approach by estimating the number of people living in each building (see, e.g., SenStadt, 2012a; DEFRA, 2015; Gulliver et al., 2015). This also seems to be

[1] For an implementation of 2002/49/EC at national level, see, e.g., 34. BImSchV for Germany or 2006 No. 2238 for England.

the practice of many assessment approaches in which noise exposure costs are computed based on static resident numbers (see, e.g., FGSV, 1997; ITP and VWI, 2006). This makes sense for night times (see, e.g., BVU et al., 2003, pp. 187–189), whereas, during the day residents may have left their homes in order to perform other activities at different locations. Hence, the estimated noise costs or exposure analysis may lead to wrong recommendations for policy makers. Lam and Chung (2012) consider the socio-economic characteristics and find older and less educated residents in Hong Kong's private buildings to be worst affected by traffic noise. Murphy and King (2010) address the absence of a standard method for the estimation of population exposures to noise in the European Union and mention the importance of considering residents who regularly leave their home town (e.g., weekend commuters). However, the authors do not refer to residents who leave their dwelling during the day (e.g., daily commuters). Ruiz-Padillo et al. (2014) present a methodology to compute a road stretch-specific priority index to be used for action planning. This index is composed of several variables including the noise level and residential exposures. Moreover, the proposed index takes into consideration the land use, i.e., noise sensitive buildings. Tenailleau et al. (2015) discuss the definition of the considered area for the quantification of noise exposures and point out that in epidemiological research this exposure area is primarily limited to the home, i.e., the dwelling, whereas, in case outdoor exposures are considered, this area is usually extended to the relevant neighborhood. The authors conclude that noise exposures should ideally be evaluated for each individual separately to account for the differences in the daily activity and travel behavior patterns. In context of air pollution, Hatzopoulou and Miller (2010) explicitly consider the temporal and spatial variation in air quality and population by using an activity-based demand model.

The tendency that most assessment methods and strategic noise mapping approaches are limited to residential exposures seems surprising as several regulations and studies also address noise in context of other activity types. Limit values which usually refer to the A-weighted and time-averaged sound level (noise assessment level), may be used for an activity-specific evaluation of noise exposures.

In Germany, limit values for traffic noise levels during the day, defined in 16. BImSchV, are differentiated according to the land use type and depending on the time of day. For the night, limit values are reduced by 10 $dB(A)$ compared to the day, which correspond to halving/doubling the perceived loudness. Tab. 5.1 depicts limit values of the A-weighted and time-averaged traffic sound level for different land-use types based on the German 16. BImSchV. In contrast, for noise during

Table 5.1: Outdoor noise limit values based on 16. BImSchV

Land use type	Limit value (day/night)
Hospitals, schools, sanatoriums, retirement homes	57 $dB(A)$/47 $dB(A)$
Residential areas	59 $dB(A)$/49 $dB(A)$
Mixed residential/commercial areas	64 $dB(A)$/54 $dB(A)$
Commercial areas	69 $dB(A)$/59 $dB(A)$

night times, in WHO Europe (2009) a much lower outside noise level of 40 $dB(A)$ is recommended. Further activity-specific noise limits are found in context of noise protection at the workplace. In addition to noise from outside of the building (e.g., traffic noise), these regulations usually include noise sources at the workplace (e.g., machines, conversations of colleagues). Thus, provided limit values refer to the indoor sound level. An evaluation which includes the effects of annoyance and disturbance in computer workspaces describe an averaged sound level below 30 $dB(A)$ as the

optimal working environment, 30-40 $dB(A)$ as very good, 40-45 $dB(A)$ as good, 45-50 $dB(A)$ as acceptable in a commercial environment, 50-55 $dB(A)$ as inconvenient and noise levels above 55 $dB(A)$ as too high (Rau et al., 2003). DIN EN ISO 11690-1, an international standard adopted at European and national level, points in a similar direction and recommends noise limit values of 35-45 $dB(A)$ for mainly mental activities and 45-55 $dB(A)$ for repetitive office work; in classrooms, background noise levels should not exceed 30-40 $dB(A)$ (see Tab. 5.2). Since these values are indoor

Table 5.2: Indoor noise limit values based on DIN EN ISO 11690-1

Indoor type	Limit value
Conference room	30-35 $dB(A)$
Classroom, Single office	30-40 $dB(A)$
Open space office	35-45 $dB(A)$
Industrial laboratories and control rooms	35-55 $dB(A)$
Industrial workspace	65-70 $dB(A)$

noise limits, values for the outside facade may be derived by adding a value for the insulation of the building. The level of sound reduction depends on the specific characteristics of the building (e.g., wall thickness, number and size of windows), the window technology (e.g., single vs. multiple glazing) as well as personal habits (e.g., open vs. closed windows). Numbers for the sound reduction of closed windows range from 25 dB to more than 48 dB (see, e.g., DIN 4109, Beiblatt 1, p. 55–56). Open windows are described to reduce the noise level by 5 dB, partly opened windows by about 15 dB (see, e.g., RPS, 2011, Appendix 8). During night times, windows in bedrooms are found to be closed in 25% of the nights, and as average inside/outside differences 21.3 dB (single-glazed window) and 22.2 dB (double-glazed window) are given (WHO Europe, 2009). Hence, outside noise levels above 35 $dB(A)$ for open windows, and above 55 $dB(A)$ for closed windows and the worst case noise insulation, may already lead to a not optimal working environment.

There is a lack of studies on noise exposures which explicitly take into account the within-day dynamics of varying population densities in different areas of the city and incorporate people who are affected at work, university or school. This study takes up this lack of research and investigates for the case study of the Greater Berlin area the importance of dynamically considering various activity types. In a similar study, Dhondt et al. (2012) investigate the dynamic effects of air pollution exposures.

Noise computation methods require information about the traffic situation, e.g., the flow and the share of HGV per spatial and temporal unit. In order to determine the *exposures* to noise or noise *damages*, information about the population is additionally required, e.g., the number of individuals and their specific activities per spatial and temporal unit. An activity-based transport model contains both activities such as being at home, working or studying as well as trips resulting from the need to get from one activity location to another one. Thus, activity-based transport models are well suited to obtain the required input data. In this study, an activity-based and dynamic transport simulation will be coupled with a simple noise computation model which is based on the RLS-90 approach and adopts the correction term in Eq. (5.3) from Nielsen et al. (1996).

This chapter is structured as follows. Sec. 5.2 provides a methodological description of the applied simulation framework as well as the noise exposure computation model. Sec. 5.3 describes the setup of the Berlin case study which is used for the estimation of noise exposures. The results

are given and discussed in Sec. 5.4. Finally, Sec. 5.6 provides a conclusion and outlook on related future studies.

5.2 Methodology: Calculation of Noise Damages

The presented approach to compute road noise damages is based on a modular design which is visualized in Fig. 5.1. A first module computes the noise emissions based on the traffic flow, HGV

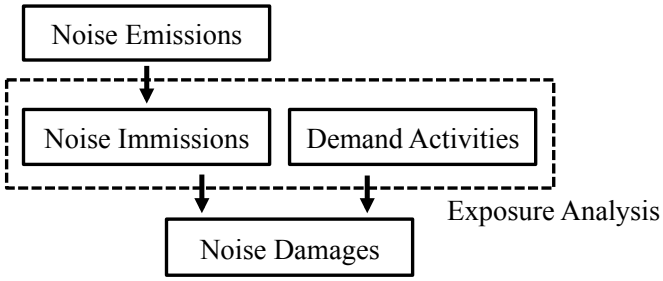

Figure 5.1: Modular design to calculate noise damages

share and the speed level. Based on these emissions and additional spatial information, a second module calculates the noise immissions for a predefined set of receiver points. A third module keeps track of each individual's activity locations as well as activity start and end times. Based on the activity information as well as the noise immissions, noise exposures may be investigated, and a forth module computes individual noise damage costs. A detailed look into each module is given in the following four sections.

5.2.1 Calculation of Noise Emissions

The calculation of noise emissions is based on the German RLS-90 approach ('Richtlinien für den Lärmschutz an Straßen', FGSV, 1992). According to this approach, in a first step, an initial average sound level is calculated for a predefined set of conditions, i.e, a free sound propagation along a horizontal distance of 25 m with a height difference of 2.25 m, a maximum speed level of 100 km/h, a smooth asphalt road surface and a gradient of less than 5%. The initial average sound level $E_{i,t}^{25}$ in $dB(A)$ for a single road segment i and a single time bin t is computed as described by Eq. (A.1) in App. A. The computation of the average sound level $E_{i,t}^{25}$ also includes the effects of HGV. In a second step, the RLS-90 methodology accounts for deviations from the initially assumed conditions. In this study, for reasons of simplification and a better computational performance, further corrections are assumed to be zero (see Sec. 5.5.2). In particular, the impact of a different road surface, road gradients larger than 5% and single reflections are ignored and $E_{i,t}^{25}$ is only corrected for the speed level:

$$E_{i,t} = E_{i,t}^{25} + D_{i,t}^{v}\,, \tag{5.1}$$

where $E_{i,t}$ denotes the resulting average noise emission level in $dB(A)$, and $D_{i,t}^{v}$ is the speed correction in $dB(A)$ described in App. A. The RLS-90 approach defines a time bin size of $T = 1\ h$. Therefore, even though the dynamic simulation approach allows for much smaller time bin sizes, in this study, the RLS-90 approach is followed and T is set to 1 h.

5.2.2 Calculation of Noise Immissions

Accounting for noise propagation and superposition, the noise emissions on the road segments are translated into resulting noise immissions at the building facades. For a better computational performance, noise immissions at the building facades are approximated by calculating a square grid of receiver points with a predefined density (see Sec. 5.4). For the analysis of the Berlin metropolitan area, in this study, the distance between the receiver points is set to 50 m. In Sec. 5.5.1, the noise immissions are computed for the building facades. The noise immission level resulting from a single road segment is calculated as follows.

$$I_{i,j,t} = E_{i,t} + D^{d}_{i,j} + D^{\alpha}_{i,j}\,, \tag{5.2}$$

where $I_{i,j,t}$ denotes the noise immission level in $dB(A)$ at receiver point j resulting from road segment i for the time bin t; $D^{d}_{i,j}$ is the correction in $dB(A)$ for air absorption (see App. A); and $D^{\alpha}_{i,j}$ denotes the length (or angle) correction in $dB(A)$. If the road segment i is a tunnel, the resulting noise immission level $I_{i,j,t}$ is 0 $dB(A)$. When calculating the distance between road segment i and receiver point j, the shortest connection is used which is either the perpendicular or the line starting at one end of the road segment. In case the perpendicular or line distance is less than 5 m, the distance is set to 5 m. The correction term $D^{\alpha}_{i,j}$ is taken from Nielsen et al. (1996) since the length of a road segment for which noise emissions are calculated should have no impact on the noise immission level at the receiver point.

$$D^{\alpha}_{i,j} = 10 \cdot \log_{10}\left(\frac{\alpha}{180}\right)\,, \tag{5.3}$$

where α is the angle of view from receiver point j to road segment i, as depicted in Fig. 5.2.

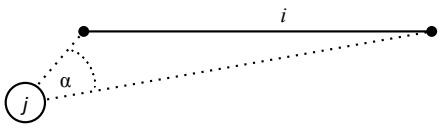

Figure 5.2: Correction for the length of the road segment

In this study, for reasons of simplification and a better computational performance, further corrections which take into account ground attenuation, multiple reflections or shielding of buildings are neglected (see Sec. 5.5.2). The superposition of average noise levels which result from several road segments is calculated applying the basic principle of energetic addition.

$$I_{j,t} = 10 \cdot \log_{10} \sum_{i} 10^{0.1 \cdot I_{i,j,t}} \tag{5.4}$$

where $I_{j,t}$ is the resulting immission level in $dB(A)$ at receiver point j, and $I_{i,j,t}$ denotes the noise immission level resulting from receiver point i which is larger than 0 $dB(A)$. For a better computational performance, in this study, only the road segments within a maximum radius of 500 m around each receiver point are taken into account, whereas the impact of road segments that are further away is neglected.

5.2.3 Calculation of Demand Activities

Applying an activity-based simulation model, individuals travel in order to get from one activity to another one. It is therefore straightforward to capture each individual's activity locations and durations throughout the day. The approach allows for different assumptions regarding which activity types are taken into account, e.g., being at home, working, performing a leisure activity. For a better computational performance, activities are considered to take place at the closest receiver point. That is, the number of individuals that may be exposed to noise is stored for each receiver point and time interval. For activities starting or ending during a time interval, the individual is partly considered, thus the number of demand units that may be exposed to noise is calculated as follows.

$$N_{j,t} = \sum_{n} \frac{a_{n,j,t}}{T} \tag{5.5}$$

where $N_{j,t}$ denotes number of demand units that may be exposed to noise at receiver point j in time interval t; n is the individual; $a_{n,j,t}$ is the duration individual n performs an activity of a considered type (e.g., only 'home' activities; 'home' or 'work' activities) at receiver point j during the time interval t; and T is the time bin size.

5.2.4 Calculation of Noise Damages

Analyzing the noise immissions $I_{j,t}$ with regard to the number of demand units $N_{j,t}$ for each receiver point and time interval, reveals how many individuals are affected and to which extent (exposure analysis). This module translates both parameters into one dimension, namely the noise damage costs.

The German Empfehlungen für Wirtschaftlichkeitsuntersuchungen an Straßen (EWS) approach (FGSV, 1997) suggests a threshold-based approach to calculate noise damage costs for the entire day and night. In order to compute noise damages for each time interval, the EWS method is applied to a consideration of smaller time intervals. The calculation is as follows.

$$C_{j,t} = \begin{cases} c^T \cdot N_{j,t} \cdot 2^{0.1 \cdot (I_{j,t} - I_t^{min})} & I_{j,t} \geq I_t^{min} \\ 0 & I_{j,t} < I_t^{min} \end{cases} \tag{5.6}$$

where $C_{j,t}$ denotes the noise damage costs at receiver point j in time interval t in monetary units; c^T is the cost rate in monetary units per $dB(A)$ that is exposed to one demand unit for the duration of T; and I_t^{min} is the threshold immission level which depends on the time of day. In this study, three different threshold immission levels are defined: 50 $dB(A)$ for time intervals during the day (6 a.m. to 6 p.m.), 45 $dB(A)$ for time intervals during the evening (6 p.m. to 10 p.m.) and 40 $dB(A)$ for time intervals during the night (10 p.m. to 6 a.m.).[2] The annual cost rate is $c^{annual} = 63.3$ EUR, based on the annual cost rate of 85 DM given in the EWS for the year 1995, converted into EUR, and updated to the year 2014 assuming an annual interest rate of 2%. The cost rate for the predefined time interval is $c^T = c^{annual} \cdot \frac{T}{(365 \cdot 24)}$.

[2] These threshold values are defined similar to the EWS. The EWS method suggests that below an immission level of 50 $dB(A)$ during the day (6 a.m. to 10 p.m.), respectively 40 $dB(A)$ during the night (10 p.m. to 6 a.m.), the damage cost are zero.

5.3 Case Study: Berlin, Germany

The activity-based approach to calculate noise damages is applied to a real-world scenario of the Greater Berlin area. The scenario which is used in this study was generated by Neumann et al. (2014, see also Sec. 3.3) who converted a trip-based model into an activity-based MATSim model. The demand side is comprised of "population-representative" agents based on a survey (see Ahrens, 2009) and "non-population representative" agents which account for additional traffic, such as freight, airport and tourist traffic based on additional data sources. The detailed spatial distribution of activities is based on land use information at the block level.

The outcome is considered as the current traffic situation which is analyzed regarding the noise damages. This study focuses on noise caused by private road users. Therefore, the traffic flow simulation only accounts for cars and HGV. The transport network contains all road types in the Berlin area, including minor roads with speed levels below 50 km/h. Other transport modes, namely PT, bike and walking, are modeled in a simplified way in which trip travel times are calculated based on the beeline distance between two activity locations. Noise which is caused by transit vehicles such as buses or streetcars, and noise resulting from other modes of transportation such as air traffic or rail transport is neglected. To improve the computational performance, the population is reduced to a sample size of 10% (approx. 600,000 agents) and the network capacity is reduced accordingly. Thus, traffic volumes have to be upscaled in order to analyze the simulation results and compute noise levels. A larger or even full population sample size is technically feasible, but the increase in model accuracy is minor compared to the additional computational power. Therefore, in most MATSim case studies, the simulated population is reduced to a sample size of 1% or 10% (Horni et al., 2016). Fig. 5.3 depicts the receiver point square grid which is used for the noise computation, the activity locations for a 10% sample size and the road network. The map section is an exemplary area in the inner-city Berlin area and includes three different area types: a rather residential area (southwest), a business district area (southeast) and a university campus (north).

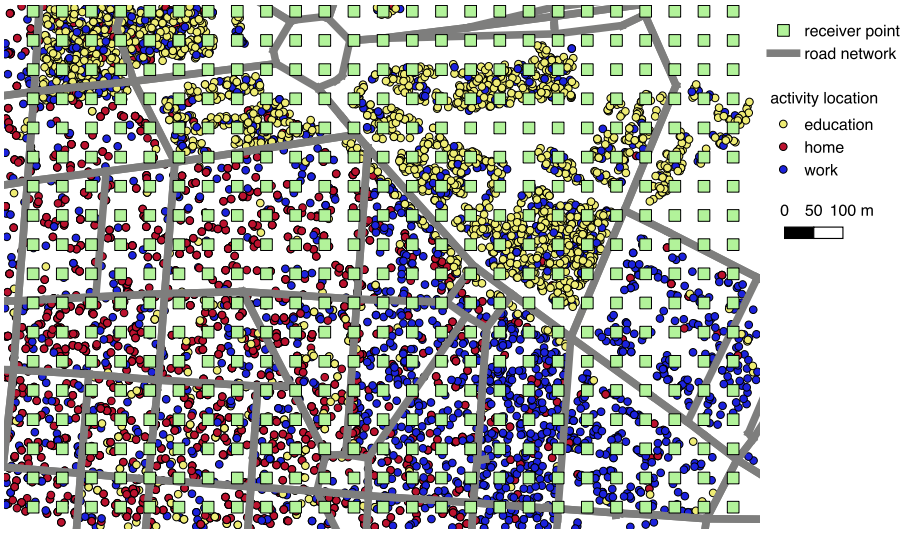

Figure 5.3: Receiver point square grid, activity locations (10% sample size) and road network; Map section: Inner-city area to the south of Ernst-Reuter-Platz, Berlin, City-West

In this study, traffic noise exposures are investigated for two different assumptions regarding the considered activity types.

1. Damage costs are only incurred for residents who are at **home**. Noise which individuals are exposed to while performing another activity type is assumed not to cause any damages and is therefore neglected.
2. Noise damage costs are incurred for residents being at **home**, and in addition, for individuals who are exposed to noise while being at **work** or their place of **education** such as kindergarten, school or university.

5.4 Results

5.4.1 Noise Immissions

At first, the investigation focuses on the noise immissions calculated for each receiver point and each time bin (see Sec. 5.2.2). Overall, the spatial plots for the Greater Berlin area seem plausible; for a validation of the model, see Sec. 5.5.1. In Fig. 5.4 the noise immissions are shown for a time bin during the morning peak (Fig. 5.4a), and for a time bin during the evening off-peak period (Fig. 5.4b). Since higher traffic volumes directly translate into higher noise levels, the overall noise immissions are higher during peak times. For both time periods, due to higher speed levels and larger traffic volumes, a higher noise immission level is observed along major roads, in particular along motorways, e.g., the inner-city southwestern motorway corridor (A115), the inner-city motorway ring road (A100), the outer-city ring road (A10). Outside of the city boundaries (depicted in black) the speed limit is higher compared to the city region. Therefore, along several roads, the noise immissions are observed to increase outside of the city region. In the city center area, noise immissions are very high for a large number of receiver points due to the higher density of major roads and superposition effects.

(a) peak time (7.00 - 8.00 a.m.) **(b)** off-peak time (9.00 - 10.00 p.m.)

Figure 5.4: Temporal comparison of noise immission levels in $dB(A)$.

5.4.2 Considered Agent Units

Noise maps such as depicted in Fig. 5.4, or more common, an average noise level which accounts for the entire day, evening and night, are an important first step towards policy making. However,

this illustration neglects the population that is exposed to the depicted noise levels. That is, policy makers will not be enabled to identify areas with an urgent need for action. To provide policy makers with further insights which may also be used to develop noise control measures, the following investigation explicitly accounts for the population, i.e., which parts of the population are affected by noise and to which extent.

Conceptually, this is done by an overlay of noise immissions and considered agent units for each receiver point and time bin. The number of agent units change during the day, and is calculated based on the number of agents that perform an activity of a considered type during the current time interval (see Sec. 5.2.3). Fig. 5.5 depicts the number of considered agent units between 10.00 and 11.00 a.m. for the two assumptions regarding the considered activity types (left-hand side: home; right-hand side: home, work, education). The inclusion of more activity types, significantly

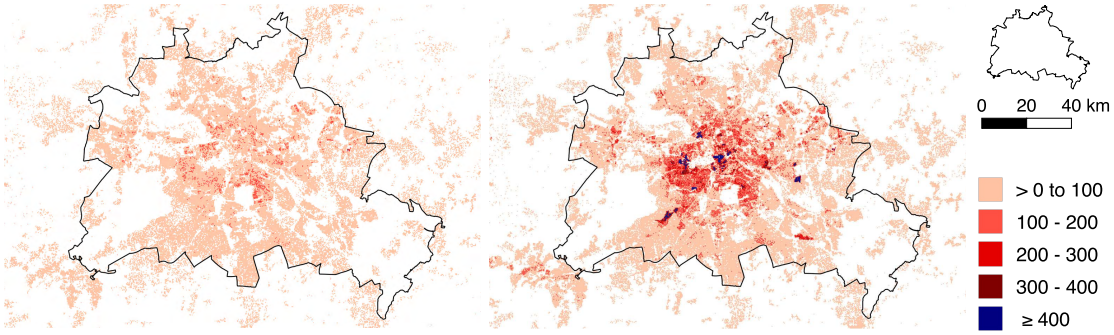

(a) home activities **(b)** home, work and education activities

Figure 5.5: Considered agent units between 10.00 and 11.00 a.m. for different assumptions regarding the considered activity types.

increases the number of considered agent units that may be exposed to noise, especially in the city center where many work and education activities are concentrated in small areas. This is also observed for other times during the day. However, during the evening and night, the number of considered agent units that may be exposed to noise is about the same for both assumptions, since the majority of the population is at home.

5.4.3 Exposure Analysis

In a first analysis, home locations are considered as the only activity locations where individuals may be affected by road traffic noise. Other activity locations, e.g., the work place, school or university, are excluded from the exposure analysis. Fig. 5.6 depicts the noise immissions between 10.00 and 11.00 a.m. for receiver points with different levels of affected agent units. In Fig. 5.6a, the noise immissions are displayed for all receiver points. Whereas, in Fig. 5.6b, for receiver points with 0 affected agent units, the noise immissions are faded out, and Fig. 5.6c only depicts the receiver points with more than 50 affected agent units. This illustration reveals that along most parts of the motorway, the population density between 10.00 and 11.00 a.m. is on a relative low level, i.e., along the motorways outside of the city center, which results in relatively small numbers of affected agents in these areas. However, for certain areas, mainly in the city center area, the noise level is high and the number of affected agent units is relatively large. For that reason, in the following, the city center area is investigated in more detail. Fig. 5.7 compares the noise immissions of the inner-city area of Berlin which are exposed to individuals who perform a “home” activity during the day (10.00 - 11.00 a.m., Fig. 5.7a) and in the evening (9.00 - 10.00 p.m., Fig. 5.7b). Noise

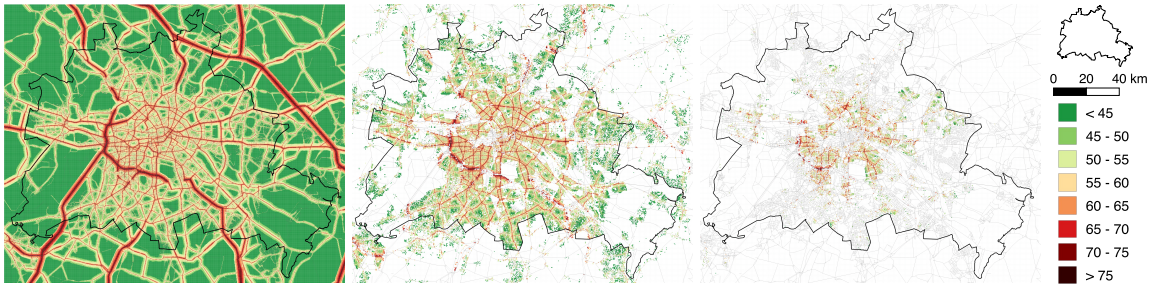

(a) all receiver points **(b)** > 0 affected agent units **(c)** > 50 affected agent units

Figure 5.6: Noise immissions in $dB(A)$ for different levels of affected agents between 10.00 and 11.00 a.m. (considered activity type: home).

immissions which do not affect any agent unit are faded out. For receiver points with less than 75 affected agent units, the transparency is set to 75%. It becomes apparent, that the within-day

(a) 10.00 to 11.00 a.m. **(b)** 9.00 to 10.00 p.m.

Figure 5.7: Temporal comparison of the most relevant inner-city noise immissions in $dB(A)$; considered activity type: home; receiver points with 0 affected agent units are not displayed; for receiver points with less than 75 affected agent units, the transparency is set to 75%.

dynamics of the population density have a significant impact on the overall noise exposures. During the day, less individuals are at home, and since further activity types are neglected, the number of affected agents is very small (Fig. 5.7a). Whereas, in the evening, most individuals are at home and the number of considered agent units that are exposed to noise is much larger (Fig. 5.7b). Along most parts of the inner-city motorway, the population density is relatively small. Therefore, in these areas, traffic noise does not cause substantial damage. However, in some areas, the noise level is high and the number of affected agent units is relatively large. During the day, mainly at the southern and western part of the inner-city motorway ring road A100 (see C2 and A5 in Fig. 5.7a), as well as along major corridors heading from the southern and western part of the A100 and the northeastern area of Berlin towards the city center (see B5, D4, H3 and H8 in Fig. 5.7a). In the evening, high noise levels and large numbers of affected agents are found in further areas along the southwestern part of the A100 (see B3 in Fig. 5.7b), as well as along main roads inside and outside the city center area.

Next, in addition to the activity type “home”, also “work” and “education” activities are assumed to be relevant and will therefore be considered in the calculation of affected agent units. Further steps towards an even more detailed exposure analysis are discussed in Sec. 5.5.3. Fig. 5.8 shows the noise immissions for areas with a large number of affected agent units in the time interval from

10.00 until 11.00 a.m. Again, receiver points with 0 affected agent units are not displayed. Since the absolute number of agent units is much larger compared to Fig. 5.7, and in order to point out the most relevant noise immissions, for receiver points with less than 200 affected agent units, the transparency is set to 75%. A comparison of Fig. 5.8 and Fig. 5.7a reveals a substantial change in

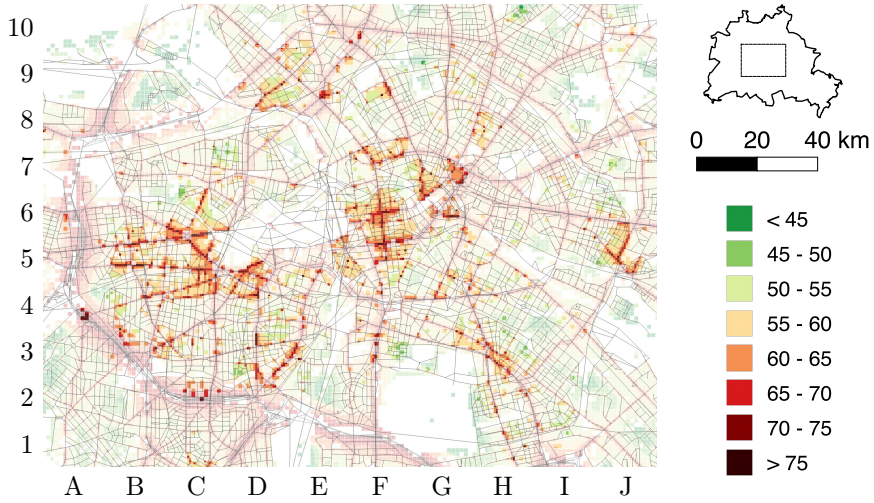

Figure 5.8: Most relevant inner-city noise immissions in $dB(A)$ between 10.00 and 11.00 a.m.; considered activity types: home, work, education; receiver points with 0 affected agent units are not displayed; for receiver points with less than 200 affected agent units, the transparency is set to 75%.

the results. In the previous consideration, the most affected population is identified along parts of the inner-city motorway ring-road (A100) as well as in residential areas at the inner-city side of the ring-road (see Fig. 5.7a). Whereas, now, high noise levels and many affected individuals are identified in the western business district and university campus in Berlin-Charlottenburg (e.g., Kurfürstendamm, Kantstraße, Ernst-Reuter-Platz, see C5 and D4 in Fig. 5.8) and the eastern business district and university campus in Berlin-Mitte (e.g., Friedrichstraße, Unter den Linden, see F6 and G7 in Fig. 5.8).

5.4.4 Noise Damages

Next, the noise level and the number of affected agent units are transferred into one dimension, namely the damage costs (see Sec. 5.2.4). The total damages per day amount to 812,591 *EUR* considering home activities only. Including work and education activities increases the total damage costs by 255,523 *EUR* (total damage costs: 1,068,114 *EUR*). Thus, the average noise damage while being at home amounts to 0.18 *EUR*, and respectively to 0.24 *EUR* while being at home and at work, university, school or kindergarten.

As described in Sec. 5.4.2, the difference between the two assumptions regarding the considered activity types, is most significant during the day. Fig. 5.9 depicts the noise damage cost in 1000 *EUR* per time of day for both assumptions regarding the considered activity types (blue: home; red: home, work, education). The fluctuations of the noise damages per time exhibit several peaks which are the result of an overlay of (i) changes in the noise immissions due to a varying traffic volumes, (ii) changing numbers of affected agents and (iii) different threshold values depending on the time of day. The peaks at around 08.00 a.m. and 3.00 p.m. correspond to the higher noise levels during

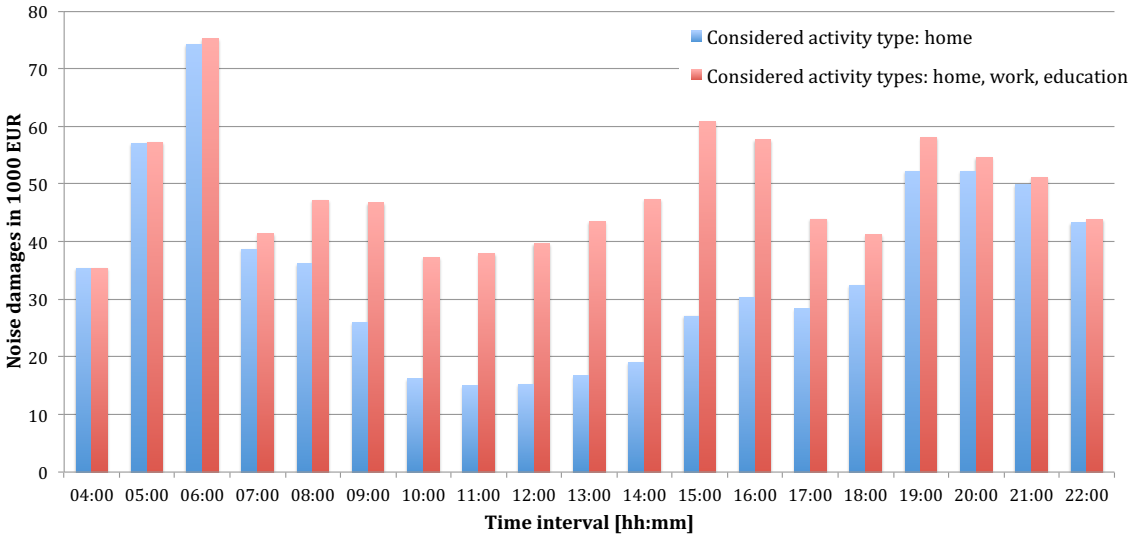

Figure 5.9: Noise damages in 1000 *EUR* per time bin (end time) for both assumptions regarding the considered activity types.

the morning and afternoon rush-hour. Between 06.00 a.m. and 6.00 p.m. higher noise levels are compensated by a higher threshold value of 50 $dB(A)$. Whereas, in the evening and night, lower thresholds values of 45 $dB(A)$ and 40 $dB(A)$ increase the damage costs even though the noise levels are on a lower level.

5.5 Discussion

5.5.1 Model Validation

In this study, an existing noise computation methodology is coupled with an activity-based and dynamic simulation model. Both approaches are separately validated against real-world data: The noise computation methodology is based on the German RLS-90 standard which is developed and validated using empirical data (FGSV, 1992). The simulation model of the Greater Berlin area was calibrated and validated against real-world traffic data (see Sec. 3, Neumann et al., 2014). Therefore, the results of the proposed methodology are as well considered as valid in the scope of the model.

Additionally, the results of the presented methodology, i.e., the simulation-based computation of noise levels for the Greater Berlin area, are compared to a noise computation by Krapf and Ibbeken (2012) for the Berlin Senate Department for Urban Development and the Environment (SenStadt, 2012b). The computation by Krapf and Ibbeken (2012) follows the German VBUS approach (BaSt, 2006) which is developed based on the German RLS-90 methodology (FGSV, 1992). In Krapf and Ibbeken (2012) noise immission levels are computed for facade points at residential buildings, schools and hospitals. In order to compare the two computation approaches, the presented methodology is applied to the facade points given in Krapf and Ibbeken (2012). Fig. 5.10 depicts for an exemplary inner-city area the difference of the day-evening-night noise level (L_{den}, see 2002/49/EC) between both models. Yellow dots indicate an absolute difference below two $dB(A)$. The value of two $dB(A)$ corresponds to the model accuracy given in Krapf and Ibbeken (2012). Orange and red dots indicate

Figure 5.10: L_{den} comparison: Presented methodology vs. Krapf and Ibbeken (2012); Map section: Southwestern Berlin area: Dahlem/Steglitz/Lichterfelde; Background map: © OpenStreetMap contributors (http://www.openstreetmap.org)

that in the model by Krapf and Ibbeken (2012) noise levels are higher compared to the proposed approach. Light green and dark green dots indicate that in the model by Krapf and Ibbeken (2012) noise levels are lower compared to the proposed approach. The comparison reveals that the noise values along most major roads are at the same level, i.e., the difference in L_{den} between both approaches is in the range of $+/-2$ $dB(A)$. However, along minor roads with speed levels below 50 km/h, the noise levels are much lower in the model by Krapf and Ibbeken (2012) compared to the proposed approach. This can be explained by the simplifications in both modeling approaches:

- The model by Krapf and Ibbeken (2012) neglects most of the minor roads in the inner-city area as noise sources. Consequently, noise levels along minor roads are underestimated. In contrast, the proposed methodology considers all roads as noise sources, including minor roads with speed levels below 50 km/h.
- As described in Sec. 5.2.1 and Sec. 5.2.2, in order to obtain a fast computational performance, the presented methodology applies some simplifications such as neglecting shielding effects of buildings. Hence, noise levels are overestimated behind the first row of buildings along main roads, i.e., at backyards and along minor roads in residential areas close to main roads. In contrast, the model by Krapf and Ibbeken (2012) accounts for shielding effects of buildings. Depending on the building density as well as the height and type of buildings the propagation of sound is hindered to a different extent. For a closed building structure (roads that are completely flanked by buildings), shielding effects of buildings may reduce noise levels by more than 20 $dB(A)$ from one row of buildings to the next one (see, e.g., SenStadt, 2012b).

Furthermore, along a few main roads with narrow facades, noise levels are observed to be much higher in the model by Krapf and Ibbeken (2012). The reason for this discrepancy is that Krapf and Ibbeken (2012) account for noise reflection at buildings and the presented approach neglects these effects in order to increase computational performance.

5.5.2 Model Simplifications

As described in Sec. 5.2.1 and Sec. 5.2.2, for reasons of simplification, i.e., to keep the amount of input data at a low level, and a better computational performance, several noise-related impacts are not accounted for, such as shielding effects of buildings, single and multiple reflections, the road surface and road gradients. Depending on the availability of data, the applied simulation approach may be extended to include additional corrections in the computation of noise emissions and immissions. However, the objective of this study is to enhance noise mapping standards by pointing out the importance of a more sophisticated consideration of the people that may be exposed to road traffic noise. That is, the focus is placed on the exposure analysis – an essential element of strategic noise mapping which is, however, neglected or strongly simplified in most studies (see Sec. 5.1). The presented methodology makes use of the detailed representation of the demand side in the applied transport model (see Sec. 1.5 and Sec. 5.2.3). And in return, the computation of noise propagation and immission is simplified to a reasonable level of complexity. The fast computational performance is in particular important for three reasons: noise maps can be drawn for large-scale areas (an entire city including the surrounding area), noise levels can be computed for all road types (minor and major roads), and the approach can be used for internalization studies which require an iterative computation of noise exposures (see Ch. 6 and Ch. 7).

5.5.3 Model Improvements

The noise computation may be improved by using more specific traffic data which may easily be obtained from the traffic model, such as traffic volumes for shorter time periods than 1 h. Since this study follows the RLS-90 approach, the speed correction is based on the maximum speed level instead of the actual speed level (see Sec. 5.2.1). By using the actual speed level, the impact of traffic congestion on the noise levels would be taken into account.

Furthermore, an even more detailed consideration of the population may improve the exposure analysis, e.g., work activities may be differentiated according to the work type; home activities may be differentiated based on person-specific attributes relevant for the noise sensitivity (e.g., children vs. adults); or additional activity types such as leisure activities may be incorporated. Neglecting additional activity types such as leisure activities may lead to an underestimation of noise exposures for specific land use types. This study also neglects on-road exposures that are particularly relevant for non-motorized transport users, e.g., cyclists, pedestrians or PT passengers waiting at transit stops. As a further limitation, the presented methodology neglects indoor sound sources and the indoor noise propagation, and assumes all people at the considered activity type to be exposed to the computed noise level. However, not all people may actually be affected by traffic noise, e.g., due to workplaces or bedrooms which are not located at the most exposed building facade (see, e.g., Murphy and King, 2010; Eriksson et al., 2013) or other noise sources at the activity location (e.g., a machine at the workplace or the TV at home). Also, the cost factors, which are used for the calculation of noise damages, are not differentiated according to the type of activity even though different noise limit values are given for different activities such as mental vs. repetitive activities.

5.6 Conclusion

Most noise maps do not include estimates for the people who are exposed to the computed noise levels. If, in such studies, exposures are taken into account, the evaluation is limited to the affected people in dwellings even though several regulations and studies indicate the importance of including further activity types such as working or being in school. Furthermore, the exposures are computed based on static resident numbers, thus neglecting spatial and temporal variations in the population. In this study, an activity-based and dynamic approach is presented to calculate road traffic noise damages and investigate population exposures. The contribution of this approach is that (1) affected people at the workplace and places of education are incorporated and (2) the within-day dynamics of varying population densities in different areas of the city is explicitly taken into account. The proposed methodology is applied to a real-world case study of the Greater Berlin area. The main findings of this study are listed below.

- It is shown that the number of affected people may be incorporated into a noise map by means of an additional layer (see e.g., Fig. 5.6). The overlay of noise level and number of affected people reveals that only a small number of people is exposed to the relatively high motorway noise emissions. In contrast, most of the individuals are found to be affected along major inner-city roads.
- It is important to account for the within-day dynamics of varying population densities in different areas of the city. As indicated by the temporal comparison (Fig. 5.7), in primary residential areas, less people are exposed to noise during the day compared to the evening or night. Thus, the use of static resident numbers would result in an overestimation of noise damages in residential areas during the day.
- The inclusion of further activity types has a substantial effect on the results. Assuming people at the workplace, university, school or kindergarten to be additionally affected by noise, as indicated by several studies and regulations, noise exposures are very large in the CBDs. Whereas, only assuming individuals at their home location to be affected by noise, the most significant noise damages are observed in more residential areas around the CBDs.

Overall, this study may be seen as a first step towards an enhancement of exposure analysis and noise mapping standards by explicitly considering the complexities and dynamics of people's travel behavior and daily activities. Hence, a more precise exposure analysis allows to provide better recommendations for policy makers and may therefore induce a more efficient use of noise control measures. This study forms the basis for further research projects, e.g., mapping back the noise damages to the causing transport users and investigating the changes in travel behavior (see e.g., Ch. 6, Ch. 7 or Ch. 8).

CHAPTER 6

Average Noise Cost Pricing

In this chapter, a first noise internalization approach is presented and successfully applied to a real-world case study of the Greater Berlin area. The proposed approach uses an activity-based transport simulation to compute noise levels and population densities as well as to assign noise damages back to road segments and transport users. This chapter is an edited version of an article that has been previously published (Kaddoura et al., 2017c).

6.1 Introduction and Problem Statement

Many studies prove that environmental noise causes cardiovascular diseases, tinnitus, cognitive impairment and sleep disturbances (see, e.g., Ising et al., 1996; Stassen et al., 2008; WHO Europe, 2009, 2011; Babisch et al., 2013). This negative impact on public health is addressed by a vast number of noise control measures. Encouraging the use of quieter vehicles (e.g., improved aerodynamics, tires or engines), the building of noise barriers, and improved road surfaces aim to reduce noise exposures. They do, however, not affect the origin of the sound, namely the travel behavior. Traffic control measures allow for a reduction in noise exposures by changing the travel behavior, e.g., the transport route, the mode of transportation or the departure time. Possible means to rearrange traffic flows towards a higher system efficiency are, for example, reduced speed levels, turn restrictions or pricing schemes. The economic principle of optimal price setting by means of internalizing external effects has been widely studied in the literature (Vickrey, 1969; Arnott et al., 1994; de Palma and Lindsey, 2004; Friesz et al., 2004, see also Sec. 1.2).

In order to prioritize various noise control measures and to quantify external noise cost which may be internalized, the number of individuals who are exposed to certain noise levels is of major importance. Traffic management strategies should ideally consider both the reduction in noise exposures and the avoidance costs such as increased travel times from driving detours (see, e.g., Lin et al., 2014). A review of several noise regulations reveals that estimates for the number of exposed individuals should not be limited to residents at their home location (see Sec. 5.1, see in particular Tab. 5.1 and Tab. 5.2). Several studies address the absence of a standardized methodology to calculate noise exposures and set priorities for action planning in the European Union (see, e.g., Murphy and King, 2010; Ruiz-Padillo et al., 2014, see also Sec. 5.1). Ruiz-Padillo et al. (2014) propose an approach to compute a road stretch-specific priority index that can be used for noise control action planning. The index sorts road stretches by their noise problems, i.e, taking into consideration the noise level as well as the number of exposed residents. Furthermore, the priority index considers the "occurrence of noise sensitive centers" such as educational, cultural or health facilities. Gühnemann et al. (2014) discuss optimal pricing strategies to protect sensitive areas. The authors find that prices should be regulated globally and account for all sensitive areas. Furthermore, the authors address the importance of considering the impact of noise on recreational activities. Lin et al. (2014) address traffic management strategies designed to meet hard environmental constraints. The authors present a criterion which can be used to assess traffic control measures regarding their impact on the network performance. In context of air pollution, Hatzopoulou and Miller (2010) and Kickhöfer and Kern (2015) have pointed out the importance of accounting for the temporal and spatial variability in air quality and population density. Similar to the latter study, this chapter presents an approach to compute noise exposures which explicitly considers the within-day dynamics of varying population densities in different areas of the city and incorporates individuals that may be affected at work, university or school, which is both found to have a substantial effect on the quantification of noise exposures.

In this chapter, a user-specific and dynamic pricing approach is proposed to internalize road traffic noise damages. The computation of noise exposures follows the methodology described in Sec. 5.2. The proposed pricing approach uses an activity-based transport simulation to compute noise levels and population densities as well as to assign noise damages back to road segments and transport users. Iteratively, road segment and time dependent noise exposure tolls are computed to which transport users can react. Since tolls correspond to the transport user's contribution to the overall noise exposures, incentives are given to change users' travel behavior towards a higher system efficiency. The presented approach can be used for noise control action planning, i.e, how to manage traffic to reduce noise exposures while keeping the avoidance costs low. Thereby, the proposed approach explicitly accounts for the temporal and spatial variation of the noise level and population density. Furthermore, noise exposures are quantified taking into consideration people who are exposed to traffic noise at work or educational activities. The innovative pricing approach is applied to the case study of the Greater Berlin area.

The remainder of this chapter is organized as follows: Sec. 6.2 describes the applied transport simulation framework and the noise internalization approach. Sec. 6.3 provides the setup of the Berlin case study which is used for two pricing experiments. The simulation outcome is analyzed and discussed in Sec. 6.4 and Sec. 6.5. Finally, Sec. 6.6 provides the conclusions for policy makers and an outlook on future research.

6.2 Methodology: Internalization of Road Traffic Noise Damages

The presented approach to compute and internalize road traffic noise damages is visualized in Fig. 6.1. In the first module, the noise emissions are calculated based on the traffic flow, HGV

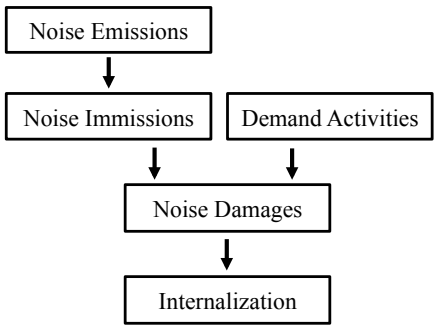

Figure 6.1: Computation modules

share and the speed level. The second module computes the noise immissions for a predefined set of receiver points. The third computation module follows all individuals' daily activities (locations and activity start and end times). Both the noise immissions and demand activities are required by the fourth module which computes individual damage costs. The fifth module assigns the damages back to the road segments and vehicles. A detailed description of the first four modules, i.e, how noise damages are calculated, is provided in Sec. 5.2 and App. A. This section describes the newly

introduced internalization module, i.e, how noise damages are mapped back to road segments and vehicles.

The applied approach to assign noise damage costs back to the causing agents is based on Gerike et al. (2012) in which the computation methods are provided, but where no numerical examples are presented. The approach considers the logarithmic scale of noise and computes the contribution of each road segment and vehicle to the overall noise damage costs. An overview of the internalization methodology applied in this study is given in Fig. 6.2. In a first step, the receiver points' damage

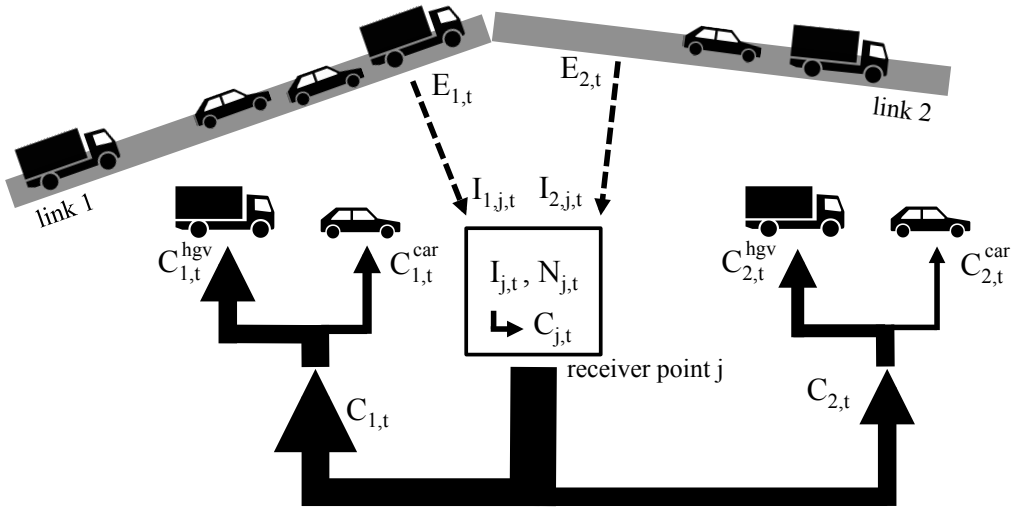

Figure 6.2: Back-mapping of noise damage costs to links and vehicles; the widths of the solid arrows represent the approximate assigned costs

costs are assigned to the road segments. Road segment i's total contribution to the overall noise damage costs is

$$C_{i,t} = \sum_j S_{i,j,t} \cdot C_{j,t} \ , \tag{6.1}$$

with

$$S_{i,j,t} = \left(\frac{10^{0.05 \cdot I_{i,j,t}}}{10^{0.05 \cdot I_{j,t}}} \right)^2 \ , \tag{6.2}$$

where $C_{i,t}$ is the total contribution of road segment i to the overall noise damages at the surrounding receiver points; and $S_{i,j,t}$ is the share of road segment i to the noise damage costs at receiver point j during time interval t (Gerike et al., 2012, Eq. 2).

In a second step, the road segment's total contribution is allocated to the different vehicle types (Gerike et al., 2012, Eq. 5 and 6). The costs assigned to each vehicle type are

$$C_{i,t}^{car} = S_{i,t}^{car} \cdot C_{i,t} \tag{6.3}$$

$$C_{i,t}^{hgv} = S_{i,t}^{hgv} \cdot C_{i,t} \ , \tag{6.4}$$

with

$$S_{i,t}^{car} = \frac{M_{i,t} \cdot (1 - \frac{p_{i,t}}{100}) \cdot 10^{0.1 \cdot E_i^{car}}}{M_{i,t} \cdot (1 - \frac{p_{i,t}}{100}) \cdot 10^{0.1 \cdot E_i^{car}} + M_{i,t} \cdot (\frac{p_{i,t}}{100}) \cdot 10^{0.1 \cdot E_i^{hgv}}} \tag{6.5}$$

$$S_{i,t}^{hgv} = \frac{M_{i,t} \cdot (\frac{p_{i,t}}{100}) \cdot 10^{0.1 \cdot E_i^{hgv}}}{M_{i,t} \cdot (1 - \frac{p_{i,t}}{100}) \cdot 10^{0.1 \cdot E_i^{car}} + M_{i,t} \cdot (\frac{p_{i,t}}{100}) \cdot 10^{0.1 \cdot E_i^{hgv}}} \ , \tag{6.6}$$

where $C_{i,t}^{car}$ and $C_{i,t}^{hgv}$ are the costs assigned to each vehicle type (passenger car or HGV); $S_{i,t}^{car}$ and $S_{i,t}^{hgv}$ are the noise shares for each vehicle type on road segment i during the time interval t; $M_{i,t}$ is the traffic volume; $p_{i,t}$ is the HGV share in %; and E_i^{car} and E_i^{hgv} are calculated as described in Eq. (A.3) and Eq. (A.4).

Finally, the costs allocated to single vehicles are

$$c_{i,t}^{car} = \frac{C_{i,t}^{car}}{M_{i,t} \cdot (1 - \frac{p_{i,t}}{100})} \tag{6.7}$$

$$c_{i,t}^{hgv} = \frac{C_{i,t}^{hgv}}{M_{i,t} \cdot (\frac{p_{i,t}}{100})} \ , \tag{6.8}$$

where $c_{i,t}^{car}$ is the costs assigned to each passenger car, and $c_{i,t}^{hgv}$ is the costs assigned to each HGV on road segment i during time interval t.

This internalizes *average* noise costs. *Marginal* noise costs will be investigated in Ch. 7.

6.3 Case Study: Berlin, Germany

6.3.1 Scenario Setup

The approach to internalize noise damages is applied to a real-world case study of the Greater Berlin area which was generated by Neumann et al. (2014, see also Sec. 3.3) who converted a trip-based model into an activity-based MATSim model. The transport users are modeled as "population-representative" agents based on SrV survey data (see Ahrens, 2009) and "non-population representative" agents to include additional traffic, e.g., freight, airport and tourist traffic. In this study, the agents' executed plans of the relaxed travel demand generated by Neumann et al. (2014) are used as input demand for the simulation experiments. For a better computational performance, a 10% sample of the population is used and road capacities are reduced accordingly. Both the demographic and traffic related data which are required to compute noise exposures are taken from the applied case study of the Greater Berlin area. The precision of noise exposures is therefore limited to the precision of the applied transport model.

6.3.2 Choice Dimensions and Simulation Setup

To allow for a comparison of the base case and the internalization policy, the transport network and simulation setup is the same as in Ch. 5. Each simulation is run for a total of 100 iterations. During the first 80 iterations, in each iteration, 10% of the agents are enabled to experience **new routes** (choice set generation). During the final 20 iterations, the agents' choice sets are fixed and the selection of travel alternatives is based on a multinomial logit model. The maximum number of travel alternatives per agent is set to 4 plans. Thus, each agent's choice set may consist of several

reasonable travel options. For instance, agents may use long routes with relatively low toll payments or short routes with relatively high toll payments. Applying a random utility model and allowing for more than one travel alternative per agent introduces day-to-day variability, which is found to result in an overall plausible travel behavior. In this study, the traffic flow model only accounts for road users, i.e, cars and HGV. Other transport modes, e.g., PT, bike and walking, are modeled in a simplified way calculating trip travel times between two activity locations based on the beeline distance. The applied methodology focuses on noise caused by passenger cars and HGV. Further noise sources such as buses, streetcars, trains, and air planes are neglected. Assuming the agents to perform activities for the predefined typical duration ($t_{typ} = t_{perf}$, see Sec. 1.5), the VTTS is 10 EUR/h. However, an agent's VTTS may be larger or smaller, depending on the agent's individual time pressure (see Ch. 3).

6.3.3 Simulation Experiments

As discussed in Ch. 5, traffic noise exposures may be computed for two different assumptions which have a substantial effect on the results.

- **Assumption *A*:** Noise damage costs are only incurred for individuals who are exposed to noise at their **home** activity.
- **Assumption *B*:** Noise damage costs are incurred for individuals who are exposed to noise at **home**, at **work** and **education** activities, i.e, school and university.

In this study, noise damage costs are mapped back to road segments and vehicle categories based on the method described in Sec. 6.2, and each causing agent is charged her contribution to the overall noise damages (internalization policy). These simulation experiments are carried out for both assumptions regarding the considered activity types, pricing policy A and B. The internalization policies are compared with the results given in Ch. 5 based on Kaddoura et al. (2017b), in which the simulation is run for the same case study but without pricing, thus the outcome is considered as the current traffic situation (base case).

6.4 Results

As shown in Tab. 6.1, both pricing experiments yield a reduction in noise damages of about 6% compared to the base case situation. The total travel time and travel distance are observed to increase since transport users take detours in order to avoid high toll payments on roads in residential areas. The numbers given in Tab. 6.1 refer to the entire day, whereas the relative changes are much higher during the morning, evening and night when noise immission thresholds are lower than during the day. The reduction in noise damage costs results from the transport users' ability to adjust their route choice decisions. That is, the network wide traffic volume, i.e, the number of starting trips per time, remains unaltered. Allowing for mode and departure time choice would presumably increase the effect. Considering all transport users within the car mode, the average toll per trip amounts to 0.17 EUR for assumption A, and 0.22 EUR for assumption B. The average toll per car user amounts to 0.15 EUR for assumption A, and 0.20 EUR for assumption B. Noise costs caused by HGV account for about a third of the total noise damages. The average toll payed per HGV amounts to 1.46 EUR for assumption A, and 1.93 EUR for assumption B. The average toll per person ("population representative" agents, see Sec. 6.3) is 0.13 EUR for assumption A,

Table 6.1: Changes in daily noise damages, travel time and driving distance due to the pricing policy. Note that for pricing policy B, the relative reduction in noise damage costs for B is smaller than for A despite the absolute reduction being larger. This is because the base value is larger. More information, such as user benefits, toll revenues and system welfare, are given in Ch. 7, see in particular Tab. 7.1.

	Pricing policy A	Pricing policy B
Change in noise damage costs	−51,436 EUR (−6.03%)	−63,925 EUR (−5.77%)
Change in travel time	+6,221 h (+0.44%)	+9,418 h (+0.66%)
Change in driving distance	+650,713 km (+0.82%)	+875,011 km (+1.11%)

and 0.16 EUR for assumption B. For trips below 10 km, the average noise cost is approximately 0.015 EUR/km for assumption A and 0.02 EUR/km for assumption B. However, for longer trips the average noise cost per km is found to decrease with the distance traveled. This is explained by the fact that for a longer trip distance, the proportion of motorway usage in typically less dense populated areas is greater, and consequently the caused noise exposures are lower.

6.4.1 Spatial Investigation of Pricing Policy *A*

Traffic Volumes Fig. 6.3 depicts the changes in traffic volumes during the afternoon peak between 3.00 and 4.00 p.m. as a result of the noise internalization policy A. Dark green and light green colored road segments indicate a decrease in traffic volume, whereas orange and red represent an increase in traffic. Furthermore, Fig. 6.3 incorporates the population density given in units of residents who perform a "home" activity during the considered time interval (3.00–4.00 p.m.). The changes in traffic volumes indicate two effects: First, transport users shift from minor to major roads such as to the inner-city ring road motorway. Second, indicated by the overlay of the traffic changes with the population units, transport users shift to roads in areas with lower population densities (see, e.g., the decrease in traffic in the densely populated area G4 in Fig. 6.3).

Noise Exposures For the same time period, Fig. 6.4 shows the changes in noise immission levels in $dB(A)$ between the base case and the internalization policy A. In Fig. 6.4a, all receiver points are shown, whereas in Fig. 6.4b, the changes in noise levels are only shown for receiver points where the number of considered population units between 3.00 and 4.00 p.m. is greater than 0. The overall noise level in the inner city area is found to decrease except for certain areas or corridors. Taking into consideration the number of affected population units, the results indicate an overall reduction in noise exposures due to the pricing policy. Overall, noise levels are observed to decrease in areas with relatively high population densities and to increase along parallel road stretches in areas with lower population densities. A decrease in noise for a relatively high population density is for example observed in Dahlem along the south-west corridor "Clayallee" which comes along with an increase in noise levels at the parallel road stretch "Onkel-Tom-Straße" leading through the forest "Grunewald" (see C4 in Fig. 6.4).[1] A noise reduction in areas with high population densities is also observed in Neukölln east of the green area "Tempelhofer Feld" (see F5 in Fig. 6.4) or in Tempelhof along the north-south road corridor "Manteuffelstraße" and "Boelckestraße" which in return involves an increase in noise at the parallel road stretch "Tempelhofer Damm" (see E5 in

[1] This effectively shifts noise from a residential area into a nature reserve. If this is politically undesirable, then it will be necessary to penalize this as well in the algorithm.

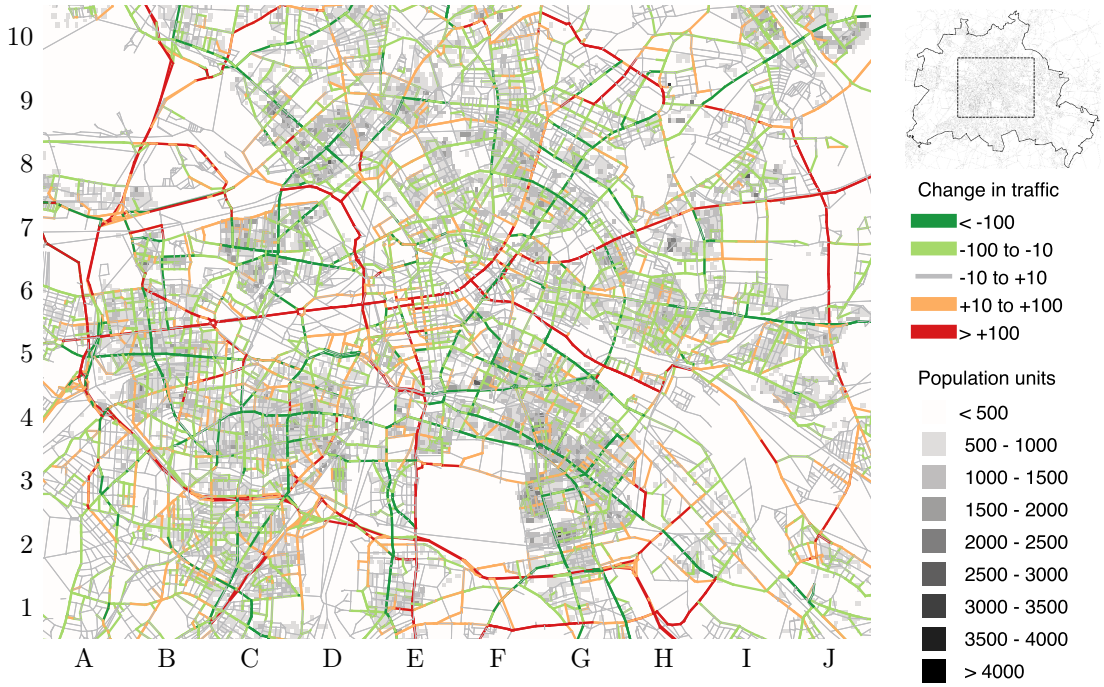

Figure 6.3: Absolute changes in traffic volumes due to the pricing policy and considered population units based on assumption A between 3.00 and 4.00 p.m.

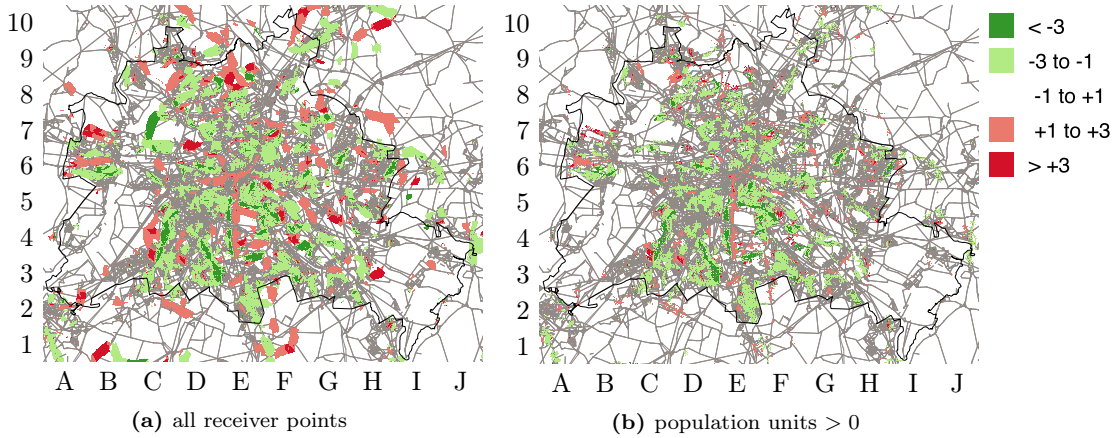

(a) all receiver points **(b)** population units > 0

Figure 6.4: Change in noise immission levels in $dB(A)$ between 3.00 and 4.00 p.m. as a result of the pricing policy A . Changes in noise immissions below 1 $dB(A)$ are not displayed.

Fig. 6.4). The changes in noise levels along the inner-city ring road and the outer city motorway are found to be very low which is explained by the logarithmic scale of noise, i.e, the declining impact of an additional vehicle on the overall noise level for larger traffic volumes.

Noise Damages As described in Sec. 5.2, noise exposures are translated into damage costs considering both the number of affected population units and the noise level. The changes in daily noise damage costs are shown in Fig. 6.5. As depicted in Fig. 6.4, the increase in traffic on motorways does not result in a significant increase in noise damage cost. Whereas, along other road stretches, mainly in residential areas and the inner-city area, changes in noise damage costs are

much larger. For several areas, a decrease in noise cost is observed to yield a smaller increase in noise cost along parallel corridors (see, e.g., F5 and E5 in Fig. 6.5).

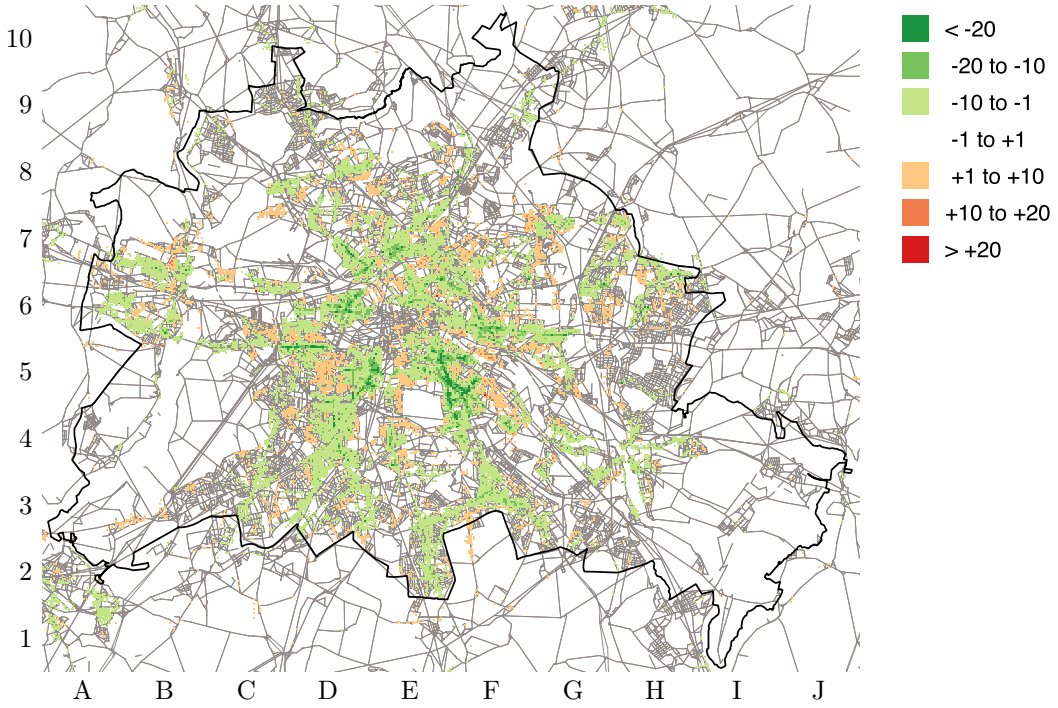

Figure 6.5: Change in daily noise cost in *EUR* as a result of the pricing policy A

6.4.2 Taking into Consideration Additional Activity Types

The assumption regarding the considered activity types is found to have a substantial effect on the policy recommendations to be derived from the changes in network utilization. Fig. 6.6 depicts the changes in traffic between 3.00 and 4.00 p.m. as a result of the noise internalization policy B. A comparison of Fig. 6.6 with Fig. 6.3 reveals how the two pricing policies A and B differ in terms of the suggested traffic flow changes. Assuming individuals at work, school or university to be additionally affected by noise (pricing policy B), in the CBDs, i.e, east and west of the inner-city green area "Tiergarten" (see E6 and C5 in Fig. 6.6), the traffic volume is much smaller than when only accounting for residential noise damages (pricing policy A).

6.4.3 Investigation for Different Times of the Day

Next, the changes in traffic resulting from the pricing policy are analyzed for different times of the day. A comparison of different time periods reveals that the dynamic approach is of major importance in both pricing policies. Applying pricing policy A, for most road stretches, e.g., the "Hermannstraße" and "Karl-Marx-Straße" in Neukölln, during the day, the predicted traffic volume is lower compared to the base case. This is explained by a large number of residents spending the day at home. During morning, evening and night periods, the route shift effects are even stronger compared to the daytime which is explained by a large number of residents returning to their home location and thus being at home in the evening. Nevertheless, for a few road stretches, e.g., the

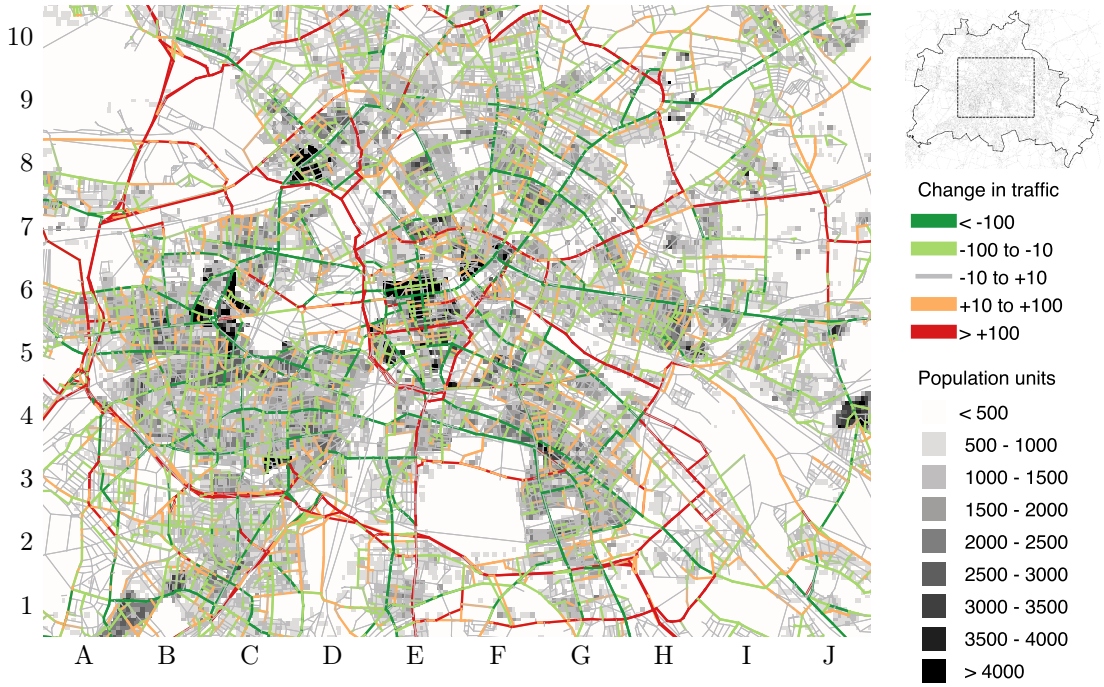

Figure 6.6: Absolute changes in traffic volumes due to the pricing policy and considered population units based on assumption *B* between 3.00 and 4.00 p.m.

"Hohenzollerndamm" in Wilmersdorf, an opposite change in traffic is observed for different times of the day, i.e, an increase in traffic volume during the day and a decrease in traffic in the evening, morning and night. This is explained by large temporal deviations of the population density, i.e, a small number of residents staying at home during the daytime and a large number of residents returning to their home location in the evening.

Applying pricing policy *B*, the time of day is found to have a very strong impact on the resulting traffic changes. As shown in Fig. 6.6, during the day, the system is improved by giving the incentive to drive around the CBDs, whereas, in the evening, morning and night, most individuals have left the CBDs. Consequently, the number of exposed individuals is very small and toll payments are very low during these time periods. Thus, in the morning, evening and night, the incentive of driving through the CBDs has the effect of reducing noise exposures in residential areas.

6.5 Discussion

A time-dependent and link-specific tolling system seems difficult to be implemented in the real world. Nevertheless, the proposed approach may be used to derive noise control strategies by means of traffic management. The proposed internalization approach induces changes on the demand side which reduce noise exposure costs. However, the desired demand changes may also be invoked by other means than pricing. A monetary toll can be as well interpreted as a correction term to be added to the transport user's generalized travel cost. Instead of charging a toll, for example, the speed limit could be reduced for certain roads while having the same effect on the transport users, e.g., encouraging users to take a different route. The results of the case study in this chapter allow to draw conclusions about the desired network utilization. In particular, for each time period, traffic flows could be rearranged by making certain road stretches less attractive. By applying the presented

methodology to case studies with further choice dimensions, the results would additionally indicate further demand reactions, such as temporal changes when enabling departure time choice, or modal shifts when enabling mode choice, which would further improve the overall system efficiency.

It is important to note that road priorities for action planning that are simply based on variables such as the noise level and the exposed population (see, e.g., Ruiz-Padillo et al., 2014) are difficult to be used for traffic management purposes. A road stretch may have a high priority index even though there is no meaningful alternative for the transport users, e.g., alternative route in a less densely populated area. That is, any kind of traffic management intending to reduce the noise level along a selected road stretch, for example a lower speed level or turn restrictions, may result in even higher noise exposures somewhere else. On the other hand, for less prioritized road stretches with a lower noise level and fewer residents, there may be good alternatives which allow for a reduction in noise exposures by means of traffic management, e.g., rearranging the traffic flow along parallel road stretches in less noise sensitive areas. In contrast, the presented approach accounts for the existence of meaningful alternatives. Each transport user can decide whether to avoid the toll payments by changing the travel behavior or to stick to the original travel behavior in case the travel alternatives involve even higher noise tolls or other travel costs. Hence, the presented noise internalization approach can be used to identify road priorities for action planning that include the existence of meaningful alternatives. A higher priority is indicated by road stretches with a predicted decrease in traffic due to noise pricing, whereas a lower priority for action planning is indicated by road stretches with no or only small changes in traffic.

In the applied pricing approach by Gerike et al. (2012), tolls are computed based on each transport user's contribution to the overall noise exposure costs and total noise damages are mapped back to the causing transport users. This means, tolls correspond to the (weighted) average noise costs. As indicated by Tab. 6.1 in Sec. 6.4, the simulation outcome confirms the economic theory which says that average cost pricing may not yield a maximization of social welfare. Accounting for the change in travel distance and travel time, in both pricing policies, the increase in travel related costs is much larger than the decrease in noise damages. In a related study, an optimal noise cost pricing approach is implemented in which noise tolls are computed based on the marginal noise damage cost (see Ch. 7). Nevertheless, the advantage of the average noise cost pricing policy by Gerike et al. (2012), which is applied in the present study, is that the toll revenues are equal to total noise damage costs. Hence, affected individuals could be compensated for their noise damages. In contrast, a marginal cost pricing approach does not yield full cost recovery. This is related to the logarithmic cost structure of noise (see Sec. 5.2), resulting in marginal noise cost that are below average noise cost (Maibach et al., 2008).

6.6 Conclusion

In this study, an innovative noise internalization approach is presented and successfully applied to a real-world case study of the Greater Berlin area in which transport users are enabled to adjust their route choice decisions. The contribution of the presented approach is that noise exposure tolls are computed by explicitly accounting for the temporal and spatial variation of the noise level and exposed population. Moreover, the activity-based simulation approach allows to go beyond residential noise exposures and additionally account for individuals who are exposed to traffic noise at work, school or university. Iteratively, transport users are enabled to react to local tolls which

correspond to the transport user's contribution to the overall noise exposures. Hence, the proposed approach can be used to investigate traffic control strategies.

Applying the pricing approach to the Berlin case study reveals that the overall noise exposures decrease by about 6% even though transport users are only enabled to adjust their routes and the number of trip departures per time remains unaltered. As a reaction to the pricing policy, transport users shift from minor to major roads and take detours in order to avoid high toll payments in areas with high population densities. Thus, the total travel time and travel distance increase. Consequently, noise levels are reduced in areas with high population densities, whereas noise levels in less dense populated areas increase. As indicated in Ch. 5, the assumption at which activities, individuals are affected by traffic noise is found to have a substantial effect on the policy recommendations. Going beyond residential noise exposures and assuming individuals at work, school or university to be additionally affected by noise, pricing significantly reduces the traffic volume in the CBDs. Moreover, the dynamic approach of calculating noise levels and population exposures is found to be of major importance for traffic management strategies. Accounting for noise exposures at work, school or university yields the incentive to drive around the CBDs during the daytime and to drive through the CBDs during the early morning, late evening and night. Overall, this study may be seen as a first step towards a more sophisticated noise control by means of intelligent traffic management.

The presented methodology can easily be extended towards differentiated cost rates and threshold values for various activity types or population subgroups, which would improve the quantification of noise exposure costs and noise tolls. As addressed by Gühnemann et al. (2014), recreational activities may be incorporated which is straightforward using an activity-based approach. Moreover, the model could be extended to account for on-road exposures which are in particular relevant for pedestrians and cyclists. A major task for future studies is to use the presented methodology to identify road stretches with high priorities for action planning. This prioritization can then be used to design a policy for certain areas or road stretches which should be evaluated based on the changes in noise damages and travel related cost. The following chapter presents an alternative noise pricing approach which computes toll levels based on the marginal effect.

CHAPTER 7

Marginal Noise Cost Pricing

In this chapter, a second noise pricing approach is presented which estimates optimal noise toll levels based on the marginal effect. Simulation experiments are carried out for the case study of the Greater Berlin area and results are compared to the average cost pricing methodology presented in Ch. 6. This chapter is an edited version of an article that has been previously published (Kaddoura and Nagel, 2016a).

7.1 Introduction and Problem Statement

Noise barriers, quieter road surfaces, improved tires or quieter engine types may reduce either noise emissions or immissions and consequently also population exposures to noise (see, e.g., Lloyd, 1998). An alternative approach is to reduce noise by means of intelligent traffic management, i.e., individual changes in travel behavior. Road pricing is one out of a variety of tools to manage traffic. In Ch. 6 average noise cost prices per road, time and vehicle are calculated following the approach by Gerike et al. (2012). In a first step, noise damage costs are assigned to the road segments. In a second step, the road segment's total contribution is allocated to the different vehicle types and vehicles. Average noise cost pricing seems a valid approach to reduce noise exposure costs and to obtain revenues which are sufficient to compensate everybody for incurred damages. However, the economically optimal solution is to charge marginal cost prices (see, e.g., Pigou, 1920; Maibach et al., 2008; Small and Verhoef, 2007, see also Sec. 1.2). In the case of noise, marginal costs are below average costs (Maibach et al., 2008). That is, average noise cost pricing results in too high prices which may result in welfare losses.

In this chapter, the advantages which come along with the activity-based simulation approach are combined with an economically optimal noise pricing methodology. An innovative simulation-based approach is presented which calculates vehicle-specific, dynamic and road-specific marginal noise costs. Based on the marginal cost, differentiated optimal noise tolls are calculated and charged from the transport users. Further external cost components such as congestion, air pollutants and accidents are neglected. The proposed marginal noise cost pricing methodology is based on the noise exposure computation approach presented in Sec. 5.2 and summarized in Sec. 7.2.1. Combining this approach with the economically optimal way of price setting provides new insights into improved traffic management.

Most noise action planning approaches use static resident numbers to investigate population exposures to noise (see, e.g., SenStadt, 2012a; DEFRA, 2015; Gulliver et al., 2015, see also Sec. 5.1). Differentiated noise limit values for hospitals, schools, residential areas and commercial areas (16. BImSchV, see also Tab. 5.1) as well as for different work activity types such as a conference room, a single office, an open space office or an industrial workspace (DIN EN ISO 11690-1, see also Tab. 5.2) indicate that noise exposure analysis should go beyond residential noise exposures and additionally account for traffic noise at the workplace or education activities. In this study, the computation of noise exposures and resulting marginal cost tolls accounts for the within-day dynamics of affected individuals for different activity types and locations.

7.2 Methodology

7.2.1 Computation of Traffic Noise Exposures

The noise computation methodology is based on the German RLS-90 approach ('Richtlinien für den Lärmschutz an Straßen', FGSV, 1992) applying the approach 'lange, gerade Fahrstreifen' ('long, straight lanes') and Nielsen et al. (1996) for the correction of the road segments' lengths. For each time interval, noise emissions are calculated on the basis of the traffic flow, the share of HGV and the speed level. Noise immissions are calculated for a predefined set of receiver points accounting for the noise emissions at the surrounding road segments and considering the decrease in noise due to air absorption. To allow for fast computational performance which is in particular relevant for the iterative optimization approach, in this study, further noise corrections such as ground attenuation, multiple reflections or shielding of buildings are not considered. Instead, the focus is placed on a detailed representation of the affected population. Applying the activity-based simulation methodology allow to track each individuals' daily activities (locations and activity start and end times) which are then used to compute dynamic population densities. Furthermore, the types of activities such as being at home, at work, school or university are known and can therefore be used for an activity-type specific computation of population densities. Both the noise immissions and demand activities are required to compute noise exposures. Hence, the computation of noise exposures accounts for the within-day dynamics of varying population densities in different areas of the city. Noise is converted into monetary units based on the avoidance costs and willingness to pay applying the threshold-based German EWS approach (FGSV, 1997) which defines a limit value of 40 $dB(A)$ for the night (6 p.m. to 6 a.m.) and 50 $dB(A)$ for the day (6 a.m. to 6 p.m.). In order to comply with the noise evaluation method defined by the European Union (2002/49/EC, Annex I), in this study, an evening period is introduced. Hence, the threshold immission values are set to 50 $dB(A)$ for during the day (6 a.m. to 6 p.m.), 45 $dB(A)$ for the evening (6 p.m. to 10 p.m.) and 40 $dB(A)$ for the night (10 p.m. to 6 a.m.). A detailed description of the applied computation methodology is provided in Sec. 5.2.

7.2.2 Computation of Marginal Noise Cost

For each receiver point and time interval, the superposition of noise from the surrounding links is computed applying the principle of energetic addition; the final noise immission level is

$$I_{j,t} := 10 \cdot \log_{10} \sum_i 10^{0.1 \cdot I_{i,j,t}(n_i^{car}, n_i^{hgv})} \tag{7.1}$$

where $I_{j,t}$ is the noise immission level in $dB(A)$ at receiver point j during the time interval t; $I_{i,j,t}$ denotes the immission level in $dB(A)$ at receiver point j resulting from link i, where $I_{i,j,t}$ is larger than 0 $dB(A)$; n_i^{car} is the number of cars; and n_i^{hgv} is the number of HGV. To improve the computational performance, in this study, only the links within a maximum radius of 500 m around each receiver point are taken into account.

The change in noise immission for an additional vehicle is computed as depicted in

Eq. (7.2) and Eq. (7.3). For computational reasons the terms are rearranged to avoid the repeated summation over the surrounding links of each receiver point and to use $I_{j,t}$ instead, which is computed in a previous step. The noise immission level for an additional car on link k is

$$\begin{aligned} I_{j,t}^{car,k} &:= 10 \cdot \log_{10} \left(10^{0.1 \cdot I_{k,j,t}(n_k^{car}+1, n_k^{hgv})} + \sum_{i \neq k} 10^{0.1 \cdot I_{i,j,t}(n_i^{car}, n_i^{hgv})} \right) \\ &= 10 \cdot \log_{10} \left(10^{0.1 \cdot I_{k,j,t}(n_k^{car}+1, n_k^{hgv})} - 10^{0.1 \cdot I_{k,j,t}(n_k^{car}, n_k^{hgv})} + 10^{0.1 \cdot I_{j,t}} \right) \\ &\{I_{i,j,t} > 0, I_{k,j,t}(n_k^{car}, n_k^{hgv}) > 0, I_{k,j,t}(n_k^{car}+1, n_k^{hgv}) > 0\} \end{aligned} \tag{7.2}$$

where $I_{j,t}^{car,k}$ is the noise immission level for one additional car on link k in $dB(A)$. The noise immission level for an additional HGV on link k is

$$\begin{aligned} I_{j,t}^{hgv,k} &:= 10 \cdot \log_{10} \left(10^{0.1 \cdot I_{k,j,t}(n_k^{car}, n_k^{hgv}+1)} + \sum_{i \neq k} 10^{0.1 \cdot I_{i,j,t}(n_i^{car}, n_i^{hgv})} \right) \\ &= 10 \cdot \log_{10} \left(10^{0.1 \cdot I_{k,j,t}(n_k^{car}, n_k^{hgv}+1)} - 10^{0.1 \cdot I_{k,j,t}(n_k^{car}, n_k^{hgv})} + 10^{0.1 \cdot I_{j,t}} \right) \\ &\{I_{i,j,t} > 0, I_{k,j,t}(n_k^{car}, n_k^{hgv}) > 0, I_{k,j,t}(n_k^{car}, n_k^{hgv}+1) > 0\} \end{aligned} \tag{7.3}$$

where $I_{j,t}^{hgv,k}$ is the noise immission level for one additional HGV on link k in $dB(A)$. Marginal noise exposure costs are

$$\begin{aligned} mc_t^{car,k} &:= \sum_j \left(C_{j,t}(I_{j,t}^{car,k}) - C_{j,t}(I_{j,t}) \right) \\ mc_t^{hgv,k} &:= \sum_j \left(C_{j,t}(I_{j,t}^{hgv,k}) - C_{j,t}(I_{j,t}) \right) \end{aligned} \tag{7.4}$$

where $mc_t^{car,k}$ are the marginal cost of an additional car on link k; $mc_t^{hgv,k}$ are the marginal cost of an additional HGV on link k; and $C_{j,t}$ are the cost as a function of a time-dependent threshold value, the number of exposed individuals and the noise immission level (see Sec. 5.2).

7.3 Case Study: Berlin, Germany

7.3.1 Scenario Setup

The marginal noise cost pricing approach is applied to a real-world case study of Berlin, Germany, generated by Neumann et al. (2014, see also Sec. 3.3). The transport network consists of all major and minor roads of the Greater Berlin area. The transport demand side is modeled as "population-representative" agents and "non-population representative" agents to account for additional traffic

such as freight, airport and tourist traffic. The executed plans of the relaxed system state by Neumann et al. (2014) are used as initial demand for the simulation experiments in this study. For a faster computation, a 10% population sample is used and the traffic flow model only accounts for cars and HGV. For other transport modes, i.e., PT, bike and walking, travel times are computed based on the beeline distance and the noise impact is neglected.

7.3.2 Choice Dimensions and Simulation Setup

Each simulation experiment is run for a total of 100 iterations. During each of the first 80 iterations, 10% of the transport users are allowed to experience new routes (choice set generation) and for the final 20 iterations, travel alternatives are selected based on a multinomial logit model (fixed choice sets). Each agent's choice set comprises a maximum of 4 travel alternatives. In this study, the traffic flow model only accounts for road users, i.e., cars and HGV.

7.3.3 Simulation Experiments

In this study, two noise pricing experiments are carried out for two assumptions:

- **Assumption *A*:** Marginal noise cost prices are computed based on the assumption that noise exposure costs are only incurred for residents who are exposed to traffic noise at their **home** location.
- **Assumption *B*:** Marginal noise cost prices are computed based on the assumption that noise exposure costs are incurred for individuals who are exposed to noise at their **home** location, and additionally at **work**, **school** or **university**.

In both experiments, marginal noise cost are computed as described in Sec. 7.2.2.

7.4 Results

In the following, the marginal noise cost pricing approach is compared to the average noise cost pricing approach. The case study is the same as in Ch. 6. For both pricing approaches welfare relevant parameters are compared to the base case situation in which the simulation is run for 100 iterations without pricing.

In Tab. 7.1 the changes in welfare relevant parameters are provided for assumption A and B and both average and marginal noise cost pricing. All noise pricing experiments result in higher benefits from reductions in noise exposures. Furthermore, noise pricing decreases travel related user benefits. This is explained by (i) toll payments and (ii) the reaction to avoid these toll payments, for example making a detour. For assumption A, the daily changes in social welfare are small (+1,263 *EUR*, +3,817 *EUR*), whereas, for assumption B, the changes in social welfare are on a much higher level. For assumption B, the average cost pricing approach results in lower daily system welfare compared to the base case (−47,889 *EUR*), whereas, marginal noise cost pricing strongly increases daily system welfare (+79,632 *EUR*). The reduction in noise exposures is considerably larger despite an overall lower level of toll payments when applying marginal noise cost prices compared to the average cost approach. Therefore, the overall price reaction is weaker, resulting in a slighter decrease of travel related user benefits. Overall, the positive welfare effect is rather small

Table 7.1: Daily changes welfare relevant parameters as a result of noise pricing: Average Cost Pricing (ACP) vs. Marginal Cost Pricing (MCP)

	Assumption *A*		Assumption *B*	
	ACP	MCP	ACP	MCP
Benefits from changes in noise exposures [*EUR*]	+51,436	+91,492	+63,925	+104,369
Benefits from changes in travel related cost (including toll payments) [*EUR*]	−852,026	−375,620	−1,156,701	−396,513
Changes in toll revenues [*EUR*]	+801,853	+287,945	+1,044,888	+371,775
Changes in system welfare [*EUR*]	+1,263	+3,817	−47,889	+79,632

compared to the large amount of required toll payments. This may be explained by the assumption regarding transport users' choice dimensions (route choice only).

Fig. 7.1 depicts the daily traffic volumes for the inner-city area of Berlin. Clearly visible is the inner-city highway in the south-western area as well as the main inner-city roads. A second layer depicts the aggregated daily population units for assumption *B*, with darker red tones indicating a higher population density. Areas with very low population densities such as parks are displayed in white. Fig. 7.2 depicts the absolute daily changes in traffic volume for the inner-city area of Berlin as a result of the marginal noise cost pricing approach for assumption *B*. For comparison, Fig. 7.3 depicts the absolute daily changes in traffic volume for the inner-city area of Berlin as a result of the average noise cost pricing approach. Green-colored road segments indicate a decrease in traffic, red-colored road segments indicate an increase in traffic volume. Overall, the structural changes

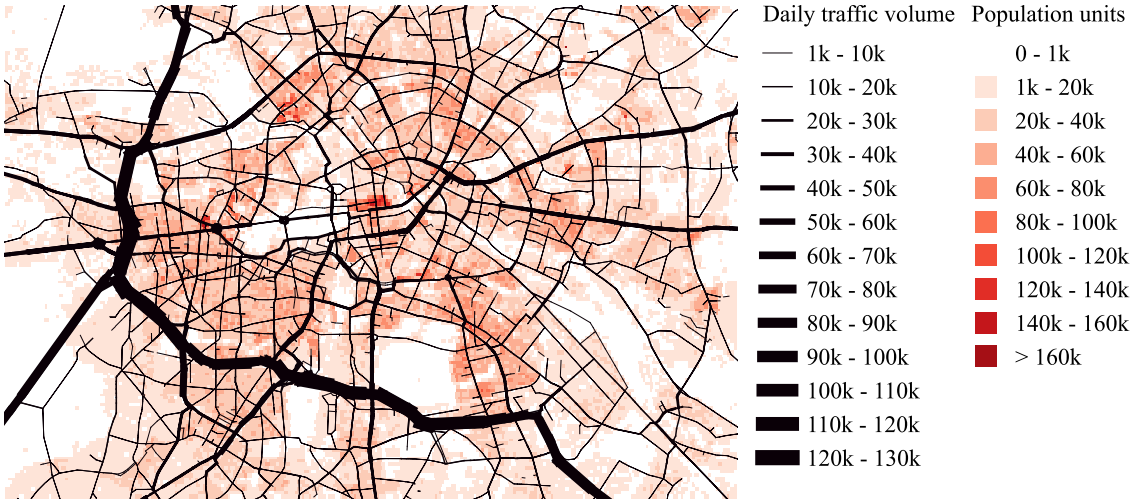

Figure 7.1: Base case: Daily traffic volume and population units (assumption B)

in traffic volumes are similar for both the average and the marginal noise cost pricing approach. Transport users avoid noise tolls by shifting to roads in areas with lower population densities. For most minor roads the traffic volume decreases, whereas on major road segments, such as the inner-city highway, the traffic volume typically increases. A comparison of both pricing approaches reveals that marginal noise cost pricing results in overall smaller changes in traffic volumes. Due to lower marginal noise cost prices, the changes in traffic volume are substantially smaller. By contrast,

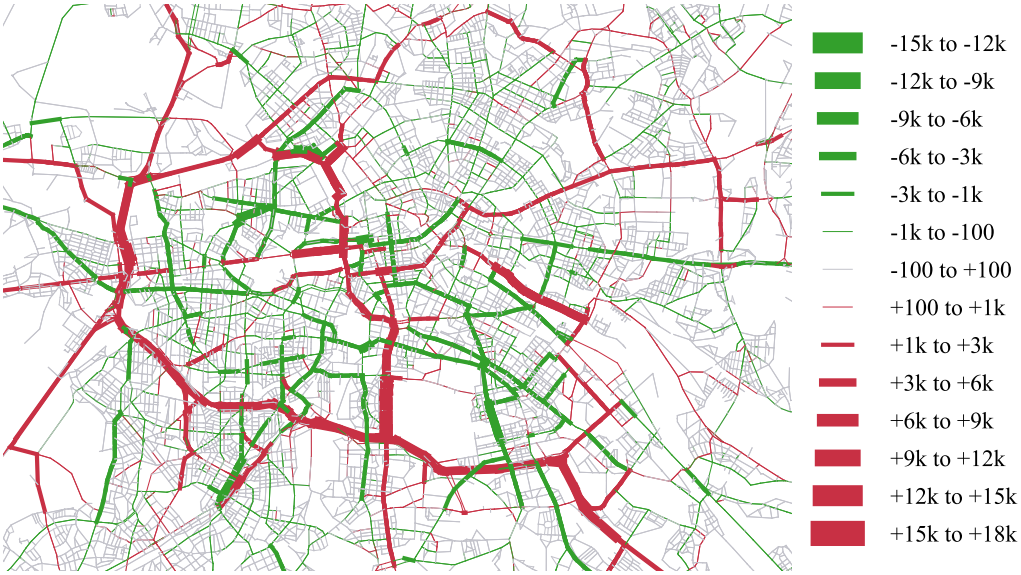

Figure 7.2: Marginal noise cost pricing: Changes in daily traffic volume (assumption B)

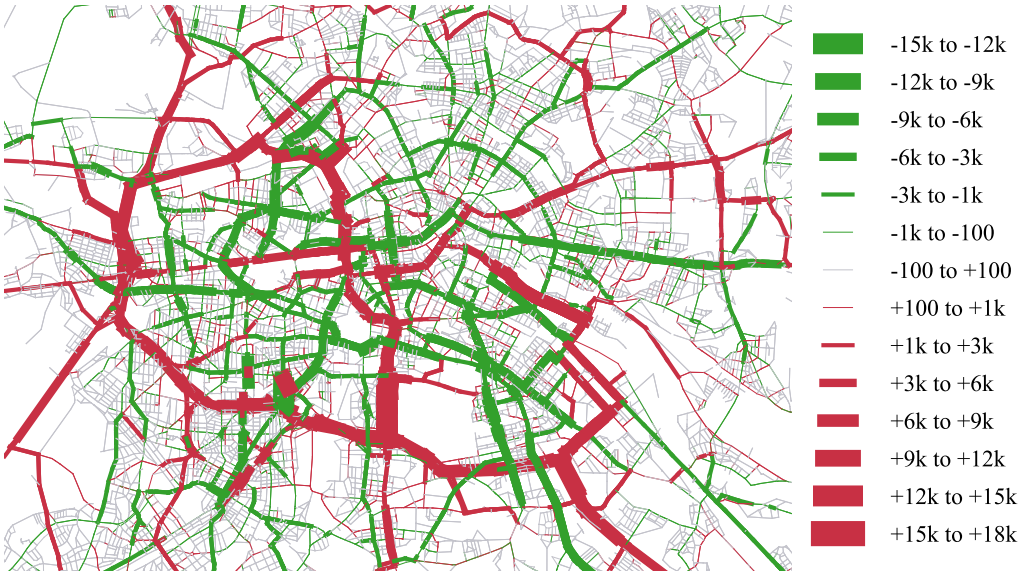

Figure 7.3: Average noise cost pricing: Changes in daily traffic volume (assumption B)

average noise cost pricing provokes a stronger reaction as exemplified by elevated traffic volume variations for a larger number of road segments.

For assumption *A*, the considered population units appear differently compared to assumption *B*. As work and educational activities are neglected pricing results in higher traffic volumes in CBD areas with a large number of work and educational activities. Due to the smaller number of population units, optimal tolls are considerably less for assumption *A* compared to assumption *B*.

Fig. 7.4 depicts the temporal distribution of the average toll per car trip for the average and marginal noise cost pricing experiments (Assumption *B*). Overall, marginal noise cost prices are lower than average cost prices. During daytime, the difference between average and marginal noise cost tolls is minimal, whereas in the morning, evening and night, due to lower traffic volumes, average noise cost prices are significantly higher than marginal noise cost tolls.

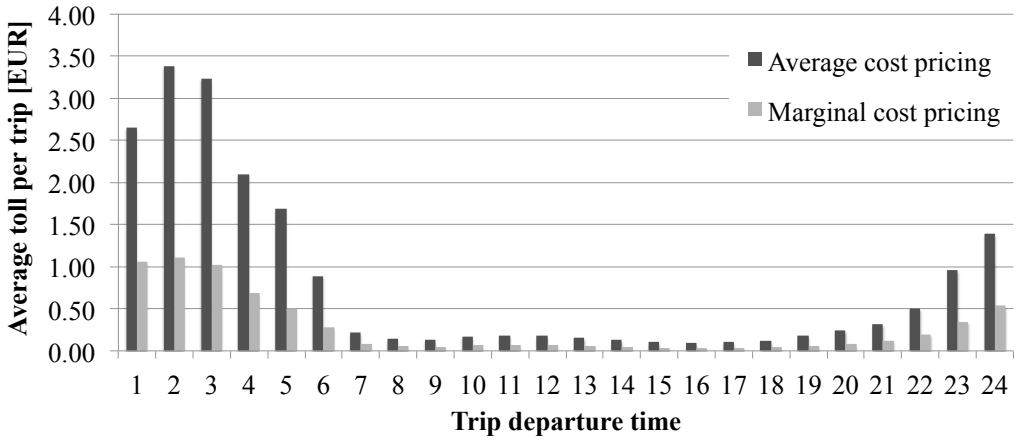

Figure 7.4: Average noise price per car trip over departure time

Marginal and average noise cost tolls are found to increase with the trip distance. However, for longer travel distances the toll level increases at a lesser degree. This can be explained by long stretches of travel routes which go through less densely populated areas. For assumption B with regard to all vehicle types, marginal noise cost tolls increase from 0.01 EUR for trips shorter than 1 km up until 0.10 EUR for trip distances between 19 and 20 km. In contrast, average noise cost tolls are on a higher level, ranging from 0.03 EUR (<1 km) until 0.28 EUR (19-20 km).

7.5 Conclusion and Outlook

In this study, an innovative simulation-based approach was presented to calculate marginal noise costs. The approach makes use of the simulation-based methodology to compute noise exposures described in Sec. 5.2. By making use of an activity-based transport simulation, the computation of noise exposures accounts for temporal and spatial differences of noise levels and population densities. Furthermore, the approach allows to account for individuals who are exposed to traffic noise at work or educational activities. Marginal noise cost can be converted into optimal time-, road- and vehicle-specific tolls to optimize the transport system - provided the transport users are enabled to adjust their travel behavior. The contribution of the proposed approach is that the economically optimal way of price setting is combined with the advantages of the activity-based simulation. The proposed optimization approach was applied to the large-scale case study of Berlin, Germany, in which transport users were enabled to change their transport route. The results were compared with a similar approach in which tolls are set based on average noise cost (see Ch. 6).

The results of the case study have shown that the proposed marginal noise cost pricing approach increases the overall system welfare. Nevertheless, the change in welfare is rather small compared to the large amount of toll revenues. This may be explained by the transport users' limited choice dimensions (route choice only). Transport users are found to avoid marginal noise cost payments by shifting to roads stretches in areas with lower population densities. For most minor roads the traffic volume decreases, whereas on most major road segments, such as the inner-city highway, the traffic volume increases. The assumption regarding which activity types are accounted for (assumption A vs. B) results in different optimal traffic flows. For road segments where the optimal traffic volume is lower than the existing one, instead of a toll, for example, the speed level can be reduced while

having the same effect on the transport users' travel decisions. For the marginal cost approach, the reduction in noise exposures is found to be larger than applying the average cost approach despite the fact that toll payments are lower. This indicates that the marginal cost approach works quite well for traffic noise. By contrast, the average noise cost approach results in smaller noise exposure reductions. Moreover, the average cost approach overprices the transport system. As a consequence, the transport users' changes in travel behavior is too strong which, for assumption *B*, leads to a substantial welfare loss.

Overall, the presented approach can be used to obtain optimal traffic flows which may be used to derive traffic control strategies. Definitely, in some cases, traffic management will not achieve the desired objectives and other noise control measures are more suitable. However, it is worth considering the rearrangement of traffic flows as one of the tools to control noise.

In the following chapters, the presented marginal noise cost pricing approach will be combined with existing pricing approaches for other external effects, in particular congestion (see Ch. 3 and Ch. 4) and exhaust emissions (Kickhöfer and Kern, 2015).

Part III

Simultaneous Pricing of Several External Effects

CHAPTER 8

Simultaneous Internalization of Traffic Congestion and Noise Costs: Investigation of Transport Users' Route Choice Decisions

This chapter elaborates on the interrelation of external effects, in particular road traffic congestion and noise. For traffic congestion and noise, single objective optimization is compared with multiple objective optimization. The simulation-based optimization approach is applied to the real-world case study of the Greater Berlin area. This chapter is an edited version of a previously published article (Kaddoura and Nagel, 2018).

8.1 Introduction and Problem Statement

Transport users do not only invest their own time and money, but impose so-called external costs on others, such as congestion, noise, air pollution, or accidents. If the users had to compensate for their external damages, they might behave differently, e.g., by using other routes, other time slots, switching to environmentally friendlier vehicles or modes, or travel less. The economic theory states that correct prices yield an optimal use of transport resources. However, due to the existence of external effects, prices only reflect parts of the full cost. Consequently, the wrong incentives are given which results in a typically too extensive usage of transport resources yielding welfare losses. Following the concept introduced by Pigou (1920), the social welfare optimum can be achieved by correcting the costs payed by the transport users according to the marginal external cost. Thus, external costs are internalized and prices reflect full cost. Hence, pricing can be understood as a decentralized (or market-based) instrument to change individual travel decisions towards an overall improved transport system (see, e.g., Maibach et al., 2008; Small and Verhoef, 2007, see also Sec. 1.2).

Many studies find that during peak times, congestion causes the largest part of all transport related external costs (see, e.g., Maibach et al., 2008; de Borger et al., 1996; Small and Verhoef, 2007; Parry and Small, 2009, p. 103). In particular, for HGV and during night times, noise is found to be a very important contribution to the total external costs (Maibach et al., 2008; Nash, 2003). In this chapter, the focus is placed on traffic congestion and noise exposures which both differ in many respects. Increased travel times due to traffic congestion mainly affect individuals within the transport system, i.e, the following road users. In contrast, traffic noise primarily affects individuals outside the transport system, for example local residents. Furthermore, traffic congestion and noise differ significantly in their cost structure. Marginal congestion cost are larger than average congestion cost (Maibach et al., 2008; Korzhenevych et al., 2014). In contrast, marginal noise cost are below average noise cost which is explained by the logarithmic characteristic of noise, i.e, that the impact of an additional vehicle is smaller for large traffic volumes compared to small traffic volumes (FGSV, 1992; Maibach et al., 2008).

Several studies indicate that external effects such as traffic congestion, noise, air pollution and accidents are interrelated with each other (see e.g., Calthrop and Proost (1998) for an analytical study, see e.g., Ghafghazi and Hatzopoulou (2014) for a simulation-based study, see e.g., Barth and Boriboonsomsin (2009) for an empirical study). That is, reducing one externality may increase or decrease other external effects. Noise computation models typically account for a road-specific free-flow speed level in that a higher speed level increases the noise level (see, e.g., FGSV, 1992). Makarewicz and Galuszka (2011) address the model-based prediction of road traffic noise using the speed-flow diagram and find that traffic congestion and noise are inversely related, i.e, that a reduced speed level due to increased traffic congestion reduces the annual average sound level. The interrelation between speed level and air pollution is empirically found to be "U"-shaped, with lower

speeds and higher speeds yielding larger emissions than middle-ranged speed levels (Barth and Boriboonsomsin, 2009). This relationship is taken into account by analytical and simulation-based air pollution emission models (see, e.g., Wismans et al., 2011; Kickhöfer et al., 2013). For the relation between congestion and accident costs, on the one hand, the number of interactions (and possible collisions) increase with the number of vehicles. On the other hand, for high traffic volumes, studies that are based on empirical data find that a reduced speed level due to congestion may lead to less severe accidents and decreasing accident costs (Shefer and Rietveld, 1997; High Level Group on Transport Infrastructure Charging, 1999; Maibach et al., 2008). Noland et al. (2008) analyze empirically the impact of the London congestion charge on road casualties and identify an increase in motorcycle casualties which is explained by the incentive to use motorcycles in order to avoid the congestion charge. However, Noland et al. (2008) do not find a significant change in road casualties. Also, the increase in speed levels is found to have no effect on the severity of accidents (Noland et al., 2008). In several studies, the overall benefits are analyzed by measuring changes in congestion costs as well as other external costs for different transport policies (see e.g., Beamon and Griffin (1999); Daniel and Bekka (2000); Proost and van Dender (2001); Beevers and Carslaw (2005) for model-based approaches, and see e.g., Percoco (2014, 2015) for empirical approaches). Wismans et al. (2011) use an analytical model to separately optimize single external effects and measure the impact on other externalities. For an illustrative case study, Wismans et al. (2011) find congestion and air pollution to be positively correlated, whereas congestion and air pollution are negatively correlated with noise and accidents.

The interrelation of external effects makes it difficult for transport planners to employ the right policy. Ideally, a transport policy should simultaneously reduce all external costs which, however, may not be easy to achieve. In particular, the reduction of one external effect may increase another external effect. This inverse relationship between different external effects puts policy makers in a dilemma. A combined optimization approach in which several external effects are simultaneously minimized provides a way out and may help to resolve the trade-off between different external effects. In a few recent studies, external effects are simultaneously optimized for a simplified network using analytical methods, see for example Chen and Yang (2012) and Wang et al. (2014) who minimize the combined external costs of congestion and air pollutants or Verhoef and Rouwendal (2003) who minimize congestion and accident costs. In Shepherd (2008), a single link model is used to compute optimal tolls for simple and more complex CO_2 and accident models. The author finds the complexity of the external cost model to have a significant impact on the optimal toll level. Because of their rather simplified nature, most analytical approaches are less appropriate to handle complex real-world networks or a more sophisticated representation of the transport demand side, for example multiple origin-destination points, non-deterministic behavior, complex user reactions, or user-user interactions such as dynamic congestion with spill-back. In contrast, Agarwal and Kickhöfer (2015) use an agent-based simulation framework to simultaneously optimize congestion and air pollution levels for a complex real-world scenario of the Munich metropolitan area. The authors find congestion and air pollution emissions to be positively correlated, that is, the internalization of one external effect also reduces the other one.

This study aims to investigate the interrelation of congestion and noise in order to implement effective policies that control both congestion and noise. The inverse relation between congestion and noise raises the question if or how it is possible to simultaneously reduce both externalities by means of intelligent traffic management. Similar to Agarwal and Kickhöfer (2015) who looked at congestion and air pollution, the present study applies an agent-based simulation approach to identify an approximation of the optimal congestion levels and road traffic noise exposures. A market-based

optimization approach is applied (see Sec. 8.2.1) which combines two external cost pricing tools, first, a congestion internalization approach which accounts for dynamic queueing and heterogenous users (see Sec. 8.2.2, see also Sec. 3.2.1 for a detailed description of the methodology) and, second, a marginal user-specific noise exposure pricing tool in which noise levels and population densities are dynamically computed (see Sec. 8.2.3, see also Sec. 7.2.2 for a more detailed description). The innovative optimization approach is applied to a real-world case study of the Greater Berlin area. Several simulation experiments are carried out which are analyzed with regard to the changes in travel behavior, congestion level, noise impact and overall system welfare (see Sec. 8.4).

8.2 Methodology

8.2.1 General Approach

The proposed methodology makes use of an iterative simulation of the market mechanism and follows the Pigouvian taxation principle (see Sec. 1.2). First, road-, user- and time-specific tolls are set to reflect marginal external costs. Second, the transport users are enabled to adjust their travel behavior to reduce toll payments. Since the prices that are paid by the users reflect full cost, specifically the private cost (own travel time) and the external cost (delays imposed on other travelers, noise exposures), the system changes towards a higher efficiency. That is, transport users adjust their travel behavior to reduce the sum of the private and the external cost. This will lead to a state where all users (approximately) pay for their marginal external costs. The road-, user, and time-specific tolls can also be interpreted as correction terms to be added to the users' generalized cost formulation in order to increase the system efficiency.

The proposed approach to approximate optimal toll levels uses the open-source transport model MATSim (see Sec. 1.5) to compute the external cost and to simulate the market mechanism, i.e, the changes in travel demand as a response to the external cost toll payments. In this study, the external costs are assumed to be composed of two cost components only, namely traffic congestion, i.e, delays imposed on other transport users (see Sec. 8.2.2), and noise damages, i.e, population exposures to traffic noise (see Sec. 8.2.3). However, the proposed market-based approach allows to easily add further cost components (see Sec. 8.6).

8.2.2 Congestion Pricing

In this study, external congestion effects are computed applying the methodology described in Ch. 3 which is based on Kaddoura and Kickhöfer (2014) and Kaddoura (2015). The computation of external congestion effects is directly linked to the queue model described in Sec. 1.5 (Traffic Flow Simulation). Whenever an agent is delayed at a bottleneck, the causing agents in the queue ahead are identified. Each of the causing agents has previously consumed a fraction of the bottleneck's flow capacity, i.e, c_{flow}^{-1}, and is therefore considered to be responsible for the delay equivalent to that amount of time. The delay is converted into monetary units accounting for the delayed transport user's value of travel time savings. Thereby, the pricing approach considers model-inherent heterogeneous values of travel time savings (see Ch. 3). Based on the delay costs imposed on other travelers, the causing agents have to pay a toll which corresponds to an approximation of marginal

external congestion cost. Hence, external congestion costs are internalized and transport users are enabled to change their travel behavior in order to avoid these tolls (see Sec. 8.2.1).

8.2.3 Noise Exposure Pricing

In this study, noise damages are internalized applying the marginal cost approach presented in Sec. 7.2.2. Road-, user- and time-specific tolls are set based on marginal noise exposure cost. For each road segment and time interval, the discretization of marginal noise exposure costs are computed by adding one additional car or HGV and computing the difference in noise damages in the surrounding area. The computation of noise damages is based on the German RLS-90 approach ('Richtlinien für den Lärmschutz an Straßen', FGSV, 1992) applying the approach 'lange, gerade Fahrstreifen' ('long, straight lanes') and Nielsen et al. (1996) for the correction of the road segments' lengths. In a first step, for each time interval and road segment, a basic noise emission level is calculated as a function of traffic volume and HGV share. In further computation steps, the noise level is corrected, in particular to account for the speed level. Next, noise immissions are calculated for each time interval and a predefined set of receiver points accounting for the noise emissions at the surrounding road segments. Finally, for each time interval, noise exposure costs are computed as a function of noise immission level and number of affected people. The number of affected people is computed for each time interval based on the simulated population density, i.e, the agents' activities (locations and activity start and end times). In residential areas, for example, the population density may decrease during the day since people go to work, school or other activities. In contrast, in CBDs, for example, the population density is very high during the day and very low during the night. The conversion into monetary units follows the threshold-based German EWS approach (FGSV, 1997). A detailed description of how noise damages are calculated, is provided in Sec. 5.2 and App. A. The translation of noise damages into marginal cost prices is provided in Sec. 7.2.2.

In Ch. 7, some results are presented regarding the model's sensitivity: marginal noise cost pricing is contrasted with much higher average noise cost pricing. Overall, the effects go into the same direction: reduction of traffic on smaller roads and concentration of volumes on already heavily used larger streets. However, while for marginal cost pricing the overall welfare goes up, the average cost pricing approach pushes so hard that the overall welfare goes down again, and ends up lower than the base case.

Extension: Actual speed instead of free-flow speed The RLS-90 noise computation approach ignores actual vehicle speeds. Instead, the RLS-90 only accounts for the maximum speed level in the range of 30 to 130 km/h for passenger cars and 30 to 80 km/h for HGV (FGSV, 1992). In this study, the noise computation methodology is modified in order to account for the interplay of noise and traffic congestion, i.e, reduced speed levels resulting in lower noise levels. Other than described in the RLS-90, in this study, noise emissions are computed based on the actual speed level instead of the free-flow speed level. Thus, the extended computation approach additionally requires the average speed level of each road segment and time interval which is provided by the dynamic traffic simulation, specifically the queue model described in Sec. 1.5 (Traffic Flow Simulation). For speeds below 30 km/h, noise levels are computed assuming the minimum speed of 30 km/h (FGSV, 1992). For speeds above the valid range, the speed level which is used to compute noise emissions is set to either 130 km/h for passenger cars or 80 km/h for HGV according to the maximum speed values considered by the RLS-90 approach (FGSV, 1992).

8.3 Case Study: Berlin, Germany

8.3.1 Scenario Setup

The simulation experiments described in Sec. 8.3.3 are applied to the real-world case study of the Greater Berlin region, Germany. The case study was generated by Neumann et al. (2014, see also Sec. 3.3) who converted a macroscopic and trip-based model into an activity- and agent-based MATSim scenario. As input demand for the simulation experiments, the agents' executed plans of the relaxed travel demand generated by Neumann et al. (2014) are used. To allow for a better computational performance, a 10% population sample is used. Furthermore, the PT mode is considered applying a simplified approach in which travel times are computed based on the linear distance. This study focuses on traffic congestion within the road network. Delay effects within the PT mode or interaction between cars and buses is neglect. The noise computation is limited to noise caused by passenger cars and HGV, other noise sources such as transit vehicles are not accounted for.

In this case study, the activity-related utility function is set as described in Eq. (1.2). The trip-related utility $V_{p,a}^{trip}$ is computed as follows:

$$V_{p,a}^{trip} = \beta_m^0 + \beta_m^d \cdot d_{p,a,m} + \beta_m^t \cdot t_{p,a,m} + \beta^c \cdot c_{p,a} \ , \tag{8.1}$$

where p denotes the person, a denotes the activity, m denotes the mode, β_m^0 is the alternative specific constant, $d_{p,a,m}$ is the travel distance, β_m^d is the marginal utility of the distance, $t_{p,a,m}$ is the travel time, β_m^t is the marginal utility of the travel time, $c_{p,a}$ is the sum of all monetary amounts paid during the trip to activity a and β^c is the marginal utility of monetary costs.

In this case study, an agent's approximate VTTS is

$$VTTS \approx \frac{\beta^{act} - \beta_m^t}{-\beta^c} = 10 \ EUR/h \tag{8.2}$$

However, depending on the agent's individual time pressure, actual VTTS may be higher or lower (see Ch. 3).

8.3.2 Choice Dimensions and Simulation Setup

In each pricing experiment, transport users are enabled to adjust their route choice decisions in order to avoid toll payments. In this study, further user reactions such as departure time and mode choice are deactivated. New transport routes are identified based on the least cost path. Vehicle-specific generalized travel costs are discretized and computed for 15 *min* time bins. To improve the computational performance, noise levels and population densities are computed for a time bin size of 1 *h*. Each simulation experiment is run for a total of 100 iterations. During each of the first 80 iterations, 10% of the agents experience new routes. During the final 20 iterations, agents' choice sets are fixed and travel plans are selected based on a multinomial logit model. The utility which is relevant for a travel plan's probability to be chosen is computed as described in Eq. (1.1). To keep the required amount of memory low, the number travel alternatives per agent is limited to 4 plans.

8.3.3 Simulation Experiments

In this study, the following simulation experiments are carried out. The first two experiments investigate both of the above described pricing approaches separately. The third simulation experiment combines the two pricing approaches and traffic congestion and noise exposures are simultaneously optimized. In simulation experiment 4a, 4b and 4c, a cordon pricing scheme is investigated for different toll levels.

1. **Isolated congestion pricing:** External congestion effects are internalized applying the methodology described in Sec. 8.2.2. Road-, user- and time-specific tolls only reflect the congestion cost.
2. **Isolated noise exposure pricing:** Noise exposure costs are internalized applying the methodology described in Sec. 8.2.3. Road-, user- and time-specific tolls are set equal to the marginal noise exposure cost. In order to properly account for the interplay of congestion and noise, noise emissions are calculated applying the extension, i.e, using the actual speed level instead of the free-flow speed level. Noise exposure costs are computed assuming that noise damages are incurred for individuals who are exposed to noise at **home**, at **work** and **education** activities, i.e, school and university.
3. **Simultaneous congestion and noise exposure pricing:** Prices are simultaneously set based on the external noise and congestion cost applying the methodology described in Sec. 8.2.2 and Sec. 8.2.3. Road-, user- and time-specific tolls are composed of two additive terms, one reflecting the congestion cost and the other one reflecting the noise exposure cost. For the computation of noise exposure costs, again, noise damages are assumed to be incurred for individuals at **home**, **work** and **education** activities.
4. **Cordon pricing:** Each time a vehicle enters the cordon area a monetary amount has to be payed. The cordon area is defined as the inner-city area of Berlin by setting the cordon line according to the circular urban railway line and the inner-city motorway ring road A100. The inner-city motorway ring road is situated outside the cordon area.
   (a) The cordon toll is set to 1 *EUR*.
   (b) The cordon toll is set to 10 *EUR*.
   (c) The cordon toll is set to 100 *EUR*.

8.4 Results

8.4.1 The Interplay of Congestion and Noise

In this section, the extension described in Sec. 8.2.3 is compared to the previously existing approach. The extended noise computation approach accounts for reduced speed levels due to traffic congestion. Fig. 8.1 depicts the changes in noise immissions for the city center area of Berlin between 3.00 and 4.00 p.m. as a result of the new computation approach. For certain road segments, actual speed levels are lower compared to the free-flow speed level which directly translates into lower noise emissions. However, for some road segments traffic congestion is very low resulting in very small differences between the model extension and the existing approach. The differences in noise levels are found to be much larger along motorways during peak times. This is explained by the higher free-flow speed level and therefore larger differences between the free-flow speed and the actual speed level in the case of congestion.

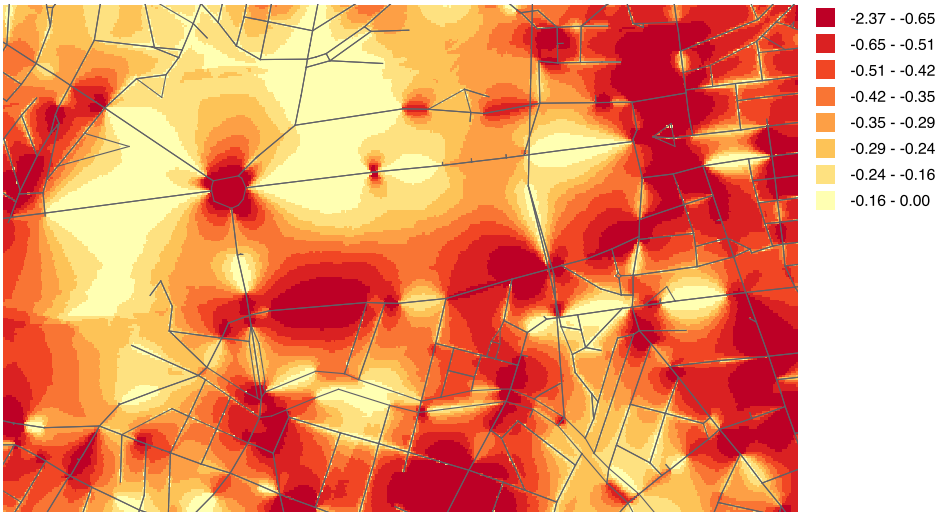

Figure 8.1: Change in noise levels in $dB(A)$ as a result of traffic congestion (City center area of Berlin, 3.00 - 4.00 p.m.)

8.4.2 Simultaneous versus Isolated Noise and Congestion Pricing

Aggregated Results Tab. 8.1 provides aggregated results for pricing experiments 1, 2 and 3. In simulation experiment 1, tolls are set based on the external congestion costs, whereas noise damages are neglected (isolated congestion cost pricing). In simulation experiment 2 tolls are set based on marginal external noise exposure costs, whereas external congestion costs are not accounted for (isolated noise cost pricing). In experiment 3, the optimization methodology is simultaneously applied to both congestion and noise. The pricing experiments are compared with the base case in which no pricing scheme is applied.

Table 8.1: Comparison of simulation Exp. 1 (isolated congestion cost pricing), 2 (isolated noise cost pricing) and 3 (simultaneous congestion and noise pricing) with the base case

	Experiment 1	Experiment 2	Experiment 3
Changes in travel distance	+22,899 *km*	+633,070 *km*	+667,146 *km*
Changes in travel time	−17,012 *h*	+4,486 *h*	−9,971 *h*
Benefits from changes in noise damage costs	−1,147 *EUR*	+110,867 *EUR*	+110,413 *EUR*
Changes in travel related user benefits (including toll payments)	−1,033,819 *EUR*	−373,970 *EUR*	−1,507,082 *EUR*
Changes in toll revenues	+1,484,971 *EUR*	+367,007 *EUR*	+1,883,735 *EUR*
Changes in system welfare	+450,006 *EUR*	+103,903 *EUR*	+487,066 *EUR*

In all pricing experiments, transport users are enabled to adjust their route choice decisions. In order to avoid highly tolled roads, transport users are even willing to take detours. Consequently, the total travel distance is found to increase for all pricing experiments compared to the base case (no pricing). In the isolated congestion pricing policy (Exp. 1), the change in travel behavior results in a congestion relief effect indicated by a decrease in total travel time. In contrast, the isolated noise pricing policy (Exp. 2) results in a much larger increase in total travel distance and an increase in total travel time. The noise damage costs are observed to slightly increase in the

isolated congestion pricing policy (Exp. 1). In contrast, isolated noise pricing (Exp. 2) results in a large decrease of noise damage costs.

The system welfare is defined as the sum of the transport users' travel related benefits (including toll payments), the toll revenues and the population's noise damages. Each of the three pricing experiments results in an increase in system welfare compared to the base case (no pricing). In the simultaneous congestion and noise pricing policy (Exp. 3), both the total travel time and noise damage costs are found to decrease. Consequently, the increase in system welfare is larger compared to the isolated pricing studies (Exp. 1 or 2). However, in all three internalization pricing experiments the change in travel related user benefits is negative. That is, without returning toll revenues to transport users, the population is in total worse off. This is in line with findings from other studies (see, e.g., Levinson, 2010).

A comparison of the aggregated numbers for simulation experiment 1 and 2 reveals that congestion and noise tolling have an opposite effect. Each isolated pricing policy is found to reduce one external effect but to increase the other one. This explains why in the simultaneous congestion and noise pricing policy, the increase in system welfare is below the sum of the increase in welfare in the two isolated pricing policies (see Tab. 8.1, last row).

Spatial and Temporal Analysis

Isolated Pricing Policies Fig. 8.2 depicts the changes in daily traffic volumes as a result of the different internalization policies. A comparison of Fig. 8.2a and Fig. 8.2b illustrates the conflicting route shift effects resulting from congestion and noise tolling. Isolated congestion pricing results in route shifts from major to minor roads. In particular, transport users avoid the heavily congested and tolled inner-city motorway and use alternative routes along smaller roads (see Fig. 8.2a). Thereby, the simulation captures the following effects on the noise level:

- Because of the logarithmic computation of noise, a shift from a busy road to a less busy road translates into higher noise levels.
- Overall, the population density along the motorway is rather low, whereas the population density is much higher along smaller roads. Thus, shifting from less densely populated areas to very densely populated areas increases the level of noise exposures.
- Reduced traffic congestion is linked to a higher speed level which in turn increases the noise level (see Sec. 8.4.1).

In contrast, isolated noise pricing results in an increase in traffic volume on the inner-city motorway and on main corridors in less densely populated areas. In return, the traffic volume decreases on smaller inner-city roads (see Fig. 8.2b). This has the following impact on traffic congestion:

- Transport users avoid densely populated areas by taking detours (longer travel distances and travel times) which increases the traffic volume and the congestion level.
- Due to the logarithmic structure of noise, marginal noise cost tolls are lower on very busy roads. As a result, transport users are concentrated along major roads resulting in a higher level of congestion.

Fig. 8.3 depicts the resulting change in L_{den}, the day-evening-night noise index proposed by the Environmental Noise Directive of the European Union 2002/49/EC. As indicated by Tab. 8.1, in the isolated congestion pricing policy (Exp. 1), the increase in noise damages is rather small. Fig. 8.3a reveals a small decrease in noise along certain corridors and a small increase in noise

(a) Isolated congestion pricing (Exp. 1)

(b) Isolated noise pricing (Exp. 2)

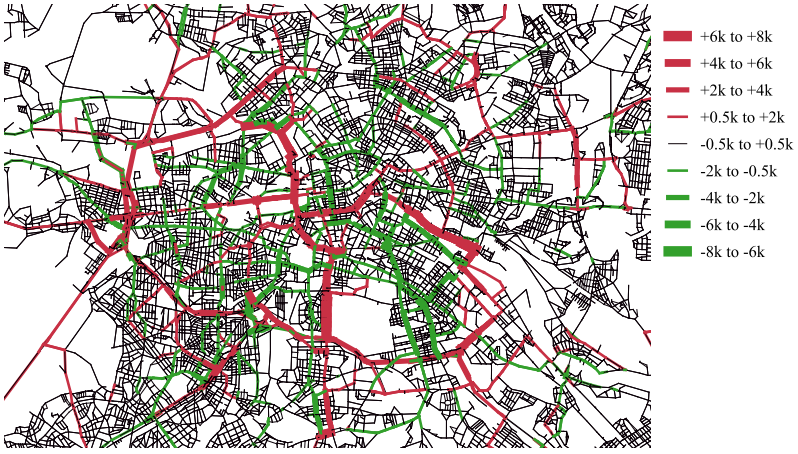

(c) Simultaneous congestion and noise pricing (Exp. 3)

Figure 8.2: Changes in daily traffic volume

in a wider area. That is, the increase in noise damages is due to the larger number of exposed people rather than an overall increase in noise levels. In contrast, in the isolated noise pricing policy (Exp. 2), overall noise damages are found to decrease significantly. Fig. 8.3b reveals that in a very wide area, noise levels are significantly reduced, whereas along certain corridors with few exposed individuals, noise levels significantly increase. A detailed investigation of spatial equity is provided in Ch. 6 for a noise pricing scheme and in Kaddoura (2015) for a congestion pricing scheme.

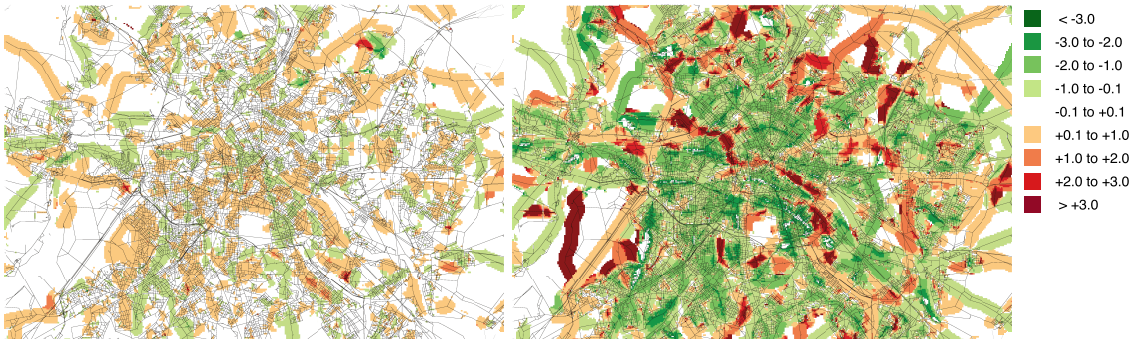

(a) Isolated congestion pricing (Exp. 1) **(b)** Isolated noise pricing (Exp. 2)

Figure 8.3: Change in noise levels in $dB(A)$ as a result of the pricing policy (L_{den}, see Environmental Noise Directive of the European Union 2002/49/EC)

Simultaneous Pricing Policy In the simultaneous congestion and noise pricing policy (Exp. 3), the changes in daily traffic volume depicted in Fig. 8.2c seem to correspond to the overlay of Fig. 8.2a and Fig. 8.2b. Moreover, in the simultaneous pricing policy, the change in noise levels is similar to the isolated noise pricing policy shown in Fig. 8.3b.

Fig. 8.4 and Fig. 8.5 depict the relevance of congestion and noise for the overall toll level in simulation experiment 3 depending on the time of the day.[1] Fig. 8.4 shows the average delay imposed

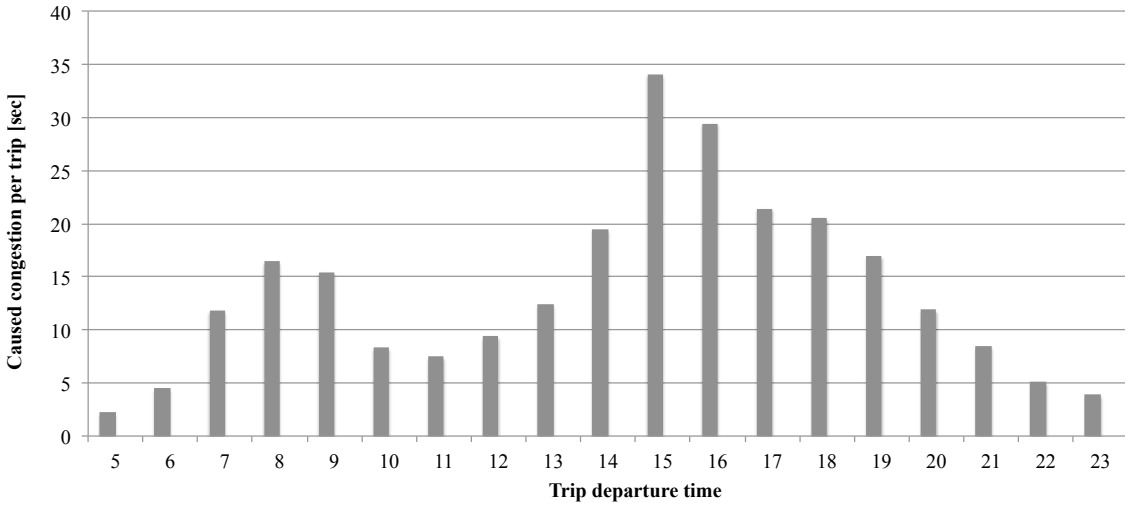

Figure 8.4: Caused congestion effect per trip departure time (Exp. 3, population representative agents)

on other travelers which increases during the peak periods, in particular during the afternoon-peak. In contrast, Fig. 8.5 shows the opposite effect: Marginal noise cost are observed to increase during off-peak times, in particular during the early morning and late evening when noise threshold values are higher and overall traffic volumes are on a lower level. Consequently, the congestion externality results in high toll levels during the day and low toll levels during early morning and late evening. In contrast, the noise externality results in high toll levels during the early morning and late evening and low toll levels during the peak periods. That is, in the simultaneous congestion and noise pricing study (Exp. 3), depending on the time of the day, road prices result from different effects. During the day, in particular during peak times, travel behavior is dominated by the reaction to

[1] The analysis only refers to the "population-representative" agents. "Non-population-representative" agents such as HGV, commercial traffic and tourists are excluded from the analysis.

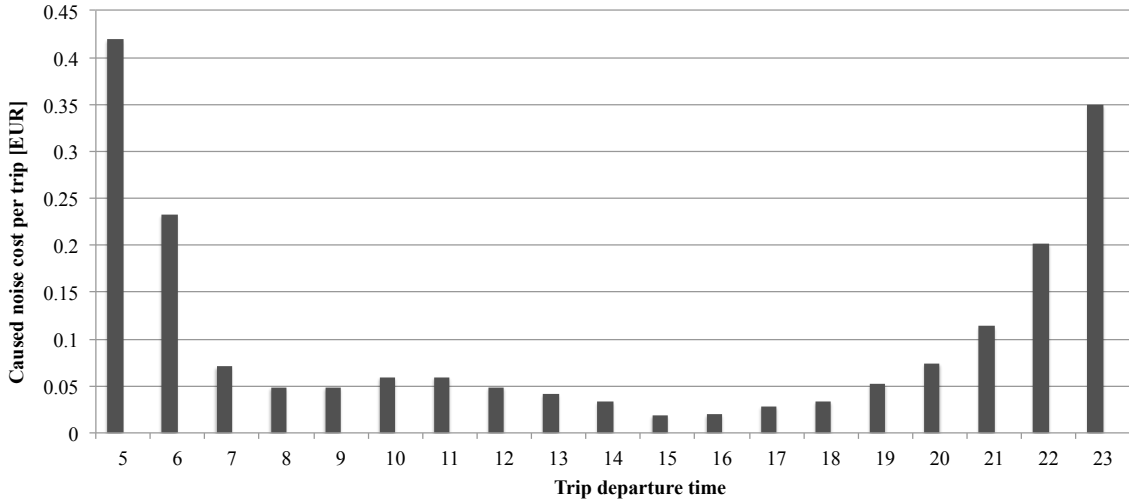

Figure 8.5: Caused noise cost per trip departure time (Exp. 3, population representative agents)

avoid congestion prices. In contrast, during the early morning and late evening, travel behavior is dominated by the reaction to avoid noise prices.

Fig. 8.6 depicts the changes in traffic volume as a result of the simultaneous congestion and noise pricing policy for a time period during the day (3 p.m.–4 p.m.) and for an off-peak time period (8 p.m.–9 p.m.). As indicated by Fig. 8.4 and Fig. 8.5, a comparison of Fig. 8.6a and Fig. 8.6b reveals different route shift effects for different times of the day. During the afternoon peak, the changes in traffic volume are similar to the isolated congestion pricing policy, i.e, transport users are observed to shift from major to minor roads. In contrast, in the evening, the demand changes are similar to the isolated noise pricing, i.e, transport users are observed to shift from minor to major roads.

8.4.3 Sensitivity Analysis

To investigate the model sensitivity, the toll levels are systematically varied. In the simultaneous congestion and noise pricing experiment (Exp. 3), the road-, user- and time-specific toll is composed of two cost components: a monetary amount which approximates marginal external congestion costs (congestion toll) and a monetary amount which approximates marginal external noise damage costs (noise toll). In different simulation experiments, the congestion and the noise toll level are increased by 10% and +30%.

Fig. 8.7 depicts the changes in total travel distance, travel time and noise damages of the simultaneous pricing scheme (Exp. 3) compared to the base case (no pricing) for different congestion and noise toll levels. The results of the sensitivity analysis show that for all toll levels, the simultaneous congestion and noise pricing experiment results in an increase in travel distance, a reduction in car travel time and a reduction in noise damages. The comparison with the base case (no pricing) reveals that a higher congestion toll level yields a larger reduction in total travel time compared to the base case (no pricing). Furthermore, the results show that increasing the congestion toll component reduces the benefits from changes in noise damages. This is explained by the change in the weighting of the different cost components. The noise cost component becomes more and more irrelevant for the transport users' routing decisions compared to the congestion cost component. Increasing the noise toll level reveals the opposite effect: The noise cost component

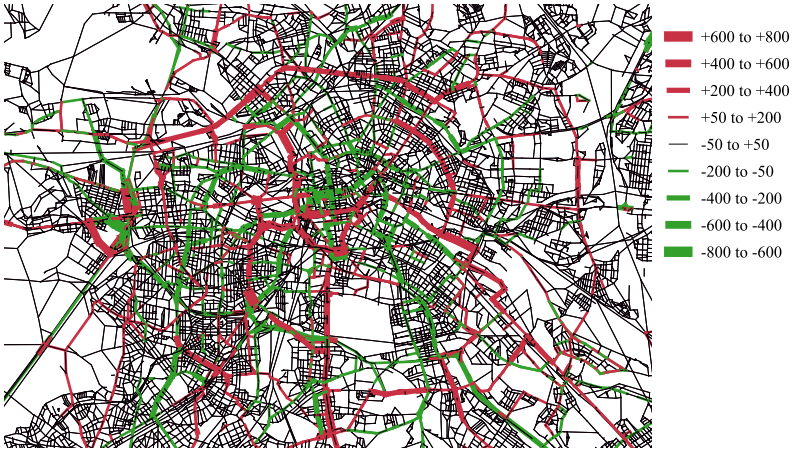

(a) Peak: 3 p.m.–4 p.m.

(b) Off-peak: 8 p.m.–9 p.m.

Figure 8.6: Changes in traffic volume: Simultaneous congestion and noise pricing (Exp. 3)

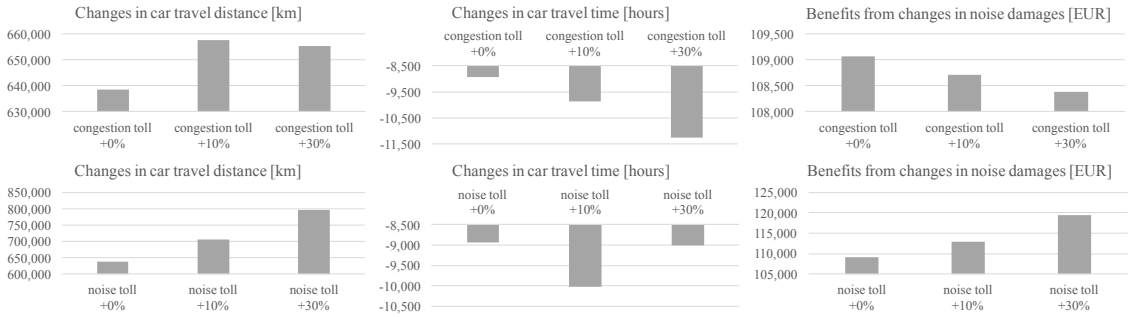

Figure 8.7: Sensitivity analysis: Variation of the congestion and noise toll level; Comparison of the simultaneous congestion and noise pricing experiment with the base case (no pricing)

becomes more and more relevant and dominates the transport users' behavior, i.e, the agents take long detours indicated by the large increase in changes in total travel distance compared to the base case (no pricing). Consequently, for higher noise toll levels, the benefits from changes in noise damage costs increase.

8.4.4 Analyzing the Effects of a Cordon Toll

This section provides the results of the cordon pricing scheme described in Sec. 8.3.3 (Exp. 4a, 4b and 4c). Tab. 8.2 provides the aggregated parameters for the different cordon toll levels (1 *EUR*, 10 *EUR* and 100 *EUR*). Transport users are only enabled to avoid the toll payments by adjusting their route choice decisions, i.e, not crossing the cordon.

For all cordon toll levels, the travel time and travel distance are found to increase. For the 1 *EUR* cordon toll (Exp. 4a), the changes on the demand side are rather small. For higher cordon toll levels (Exp. 4b and 4c), the user reactions are stronger, indicated by a larger increase in travel time and travel distance. The benefits from changes in noise damages are rather small in all cases. A comparison of the cordon toll with experiment 2 and 3 (see Tab. 8.1), reveals that both of these schemes result in a much larger reduction of noise damages than the cordon toll. Additionally, while experiments 1, 2 and 3 the overall welfare effect is positive, the cordon pricing scheme (Exp. 4a, 4b and 4c) decreases the system welfare. This is related to the assumption that transport users are only enabled to adjust their transport routes. That is, the simulation experiments neglects additional possible user reactions such as switching to alternative modes.

Table 8.2: Comparison of simulation Exp. 4a, 4b and 4c (cordon pricing) with the base case

	Experiment 4a	Experiment 4b	Experiment 4c
Cordon toll	1 *EUR*	10 *EUR*	100 *EUR*
Changes in travel distance	+82,476 *km*	+382,609 *km*	+432,386 *km*
Changes in travel time	+1,828 *h*	+7,883 *h*	+8,687 *h*
Benefits from changes in noise damage costs	+312 *EUR*	+3,349 *EUR*	+3,481 *EUR*
Changes in travel related user benefits (including toll payments)	−730,179 *EUR*	−6,046,062 *EUR*	−58,065,791 *EUR*
Changes in toll revenues	+683,150 *EUR*	+5,876,100 *EUR*	+57,782,000 *EUR*
Changes in system welfare	−46,718 *EUR*	−166,613 *EUR*	−280,311 *EUR*

A spatial plot of the changes in daily traffic volume due to the cordon toll of 10 *EUR* compared to the base case is provided in Fig. 8.8. Since the inner-city motorway ring road is located outside of the cordon area, transport users rather take the motorway than driving through the city center. The overall effect of the cordon pricing scheme is that transport demand decreases in the inner-city area and increases outside the cordon area. However, along a few inner-city road stretches travel demand slightly increases compared to the base case. This can be explained by transport users that avoid to exit and reenter the cordon area for trips starting and ending within the cordon area. Fig. 8.9 shows the change in L_{den} resulting from the cordon pricing scheme (cordon toll = 10 *EUR*; Exp. 4b). Along the inner-city motorway ring road and outside of the cordon area, noise levels are observed to increase. In contrast, along most roads in the inner-city area, noise levels are observed to decrease. Overall, the changes in noise levels resulting from the cordon tolling scheme are at a lower level compared to the noise internalization approach.

8.5 Discussion

This study evaluates the trade-offs between traffic congestion and noise reduction strategies. Taking into account further external cost components in the price setting may have a considerable effect

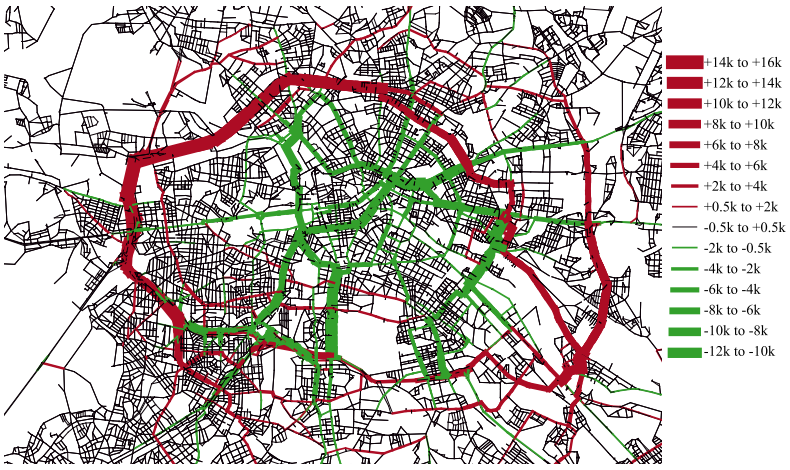

Figure 8.8: Changes in daily traffic volume: Cordon toll = 10 *EUR*

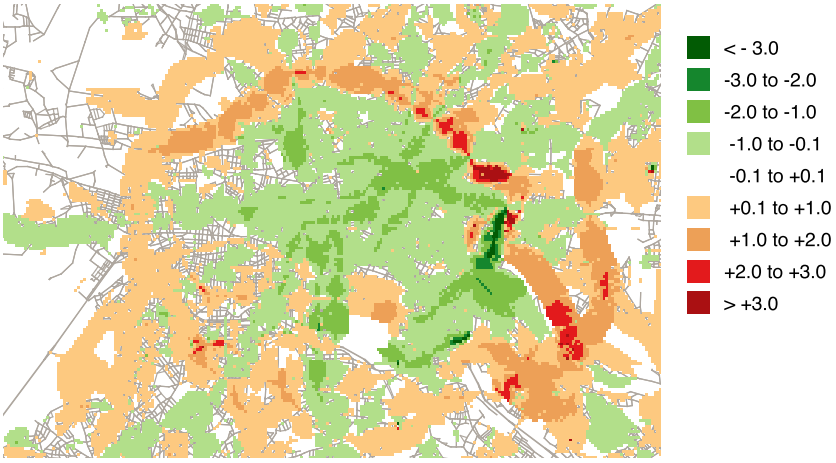

Figure 8.9: Change in L_{den} in $dB(A)$ as a result of the cordon pricing scheme (Exp. 4b, cordon toll = 10 *EUR*)

on the observed results. Including the cost of greenhouse gases such as CO_2 presumably pushes towards shorter travel distances to reduce global emission cost (see, e.g., Kickhöfer and Nagel, 2016). In contrast, accounting for local air pollutants such as particulates and nitrogen oxides, may have an effect similar to noise since damages depend on the number of locally affected people. Hence, accounting for local air pollution cost will presumably shift transport users to even longer distances to avoid trips through densely populated areas (see, e.g., Kickhöfer and Kern, 2015). The external effects' cost structure is of major importance. As described above, marginal noise costs are very low for busy roads during peak times which is found to result in traffic concentration effects. In contrast, in the case of air pollution and human health, the dose response function is linear and marginal costs are similar to average costs (Maibach et al., 2008) which is expected to result in cost levels that are more likely decision-relevant for travelers on busy roads during peak times. Additionally, emissions of air pollutants increase for high speed levels and low speed levels compared to medium speed levels (Barth and Boriboonsomsin, 2009; Maibach et al., 2008) which provides an additional incentive to avoid heavily congested roads during peak times.

In the applied case study of the Greater Berlin area, transport users are only enabled to adjust their transport routes. Hence, the simulation experiments may underestimate the real-world effects,

i.e, the aggregate increase in system welfare. Indeed, the presented methodology allows for more complex user reactions; transport users may for example be enabled to adjust their mode of transportation. In this context, the presented methodology may also be combined with existing optimization approaches for the PT mode (see Ch. 2).

The results confirm the well-known result that toll revenue redistribution is important in order to generate overall positive benefits for road users (see, e.g., Levinson, 2010). On the damages side, the approach is equitable by design: Each person-h spent at an activity is valued equally when negatively affected by noise. This section does not look at, say, income-differentiated reactions to the tolls. The approach itself is capable to do this (Kickhöfer et al., 2011); in contrast, this section investigates the interaction between congestion and noise tolls without having to disentangle the results from additional effects. Still, the present study is an important milestone on the way to a simulation package that is able to both model behavior and to assess benefits and damages by individual synthetic person.

8.6 Conclusion

This study elaborates on the interrelation of external effects. For congestion and noise, single objective optimization is compared with multiple objective optimization. The optimization methodology follows an iterative market-based approach. An agent-based simulation framework is used to compute and internalize external congestion effects and noise exposures. The applied internalization approach accounts for dynamic congestion and heterogeneous values of travel time savings. Tolls are computed for each transport user, road segment and time interval. For the case study of the Greater Berlin area, several simulation experiments are carried out, (1) isolated congestion pricing, (2) isolated noise pricing, (3) simultaneous congestion and noise pricing and (4) cordon pricing. In each pricing experiment, transport users are enabled to adjust their route choice decisions in order to avoid toll payments.

The results reveal a negative correlation between congestion and noise since the internalization of one effect increases the other one. This interrelation of congestion and noise is consistent with the findings of other studies (Wismans et al., 2011; Makarewicz and Galuszka, 2011, see Sec. 8.1). Nevertheless, the multiple objective optimization shows that it is possible to simultaneously reduce congestion costs and noise damages. Going beyond the scope of most existing studies, the results are analyzed for a large-scale network and a detailed representation of the population. A detailed investigation of temporal and spatial effects reveals that the interrelation of congestion and noise is very low. Depending on the time of day, travel behavior primarily results from avoiding either one externality or the other one. During peak times, congestion is the more relevant external effect, whereas during off-peak times, in particular during the night, noise is the more relevant externality. During peak times, transport users are observed to shift from the inner-city motorway to smaller roads. In contrast, during off-peak times, transport users shift from minor to main roads, in particular to the inner-city motorway. The comparison with different cordon pricing schemes reveals that the simultaneous congestion and noise pricing methodology is more effective in terms of welfare maximization, i.e, reduction of noise damages and congestion costs.

The presented methodology provides important implications for policy makers. The results of the Berlin case study indicate that it is possible to simultaneously reduce congestion and noise. The key factor is to follow a dynamic traffic management approach and temporally change the incentives during the course of the day:

- During the evening, night and morning, transport policies should aim at reducing noise exposures in residential areas. This objective may be achieved by concentrating traffic flows or providing incentives to use roads in less densely populated areas. The through traffic may for example be banned in residential areas inducing transport users to take detours. The resulting increase in traffic congestion is minor compared to the reduction in noise exposures.
- During the day, the results of the simulation experiments indicate that system welfare is increased by reducing congestion, i.e, by motivating a shift from congested motorways to smaller roads and spreading the demand within the network. Due to higher noise threshold values during the day compared to the morning, evening and night, as well as due to the logarithmic scale of noise and the overall high demand levels during the day, the increase in noise damages is minor compared to the reduction in congestion costs.

This neglects the impact of further external effects. Considering additional external cost components, the policy recommendations for the evening, night and morning presumably hold. In contrast, the results observed during the day, in particular the shift from motorways to minor roads in more densely populated areas is presumably associated with an increase in air pollution exposure and accident costs yielding a decrease in system welfare.

In the following chapter, the proposed market-based optimization approach will be extended to simultaneously account for air pollution (Kickhöfer and Kern, 2015). As discussed in Sec. 8.5 and shown in Ch. 3, the applied simulation framework allows for additional choice dimensions. Pricing experiments in the following chapters will also account for more complex user reactions, in particular transport users' mode choice decisions.

CHAPTER 9

Simultaneous Internalization of Congestion, Noise and Air Pollution Costs: Investigation of Mode and Route Choice Decisions

In this chapter, the interrelation of congestion, noise and air pollution is investigated for the real-world case study of the Greater Munich area. Simulation experiments are carried out for different assumptions regarding transport users choice dimensions. This chapter is an edited version of an article that has been previously published (Kaddoura et al., 2017a).

9.1 Introduction and Problem Statement

Following the concept of Pigouvian taxation, the system welfare is maximized by charging a toll which is equivalent to the marginal external effect (see Sec. 1.2). During peak times, most studies find traffic congestion to be the most significant transport related external effect (see, e.g., Maibach et al., 2008; de Borger et al., 1996). During off-peak times, environmental effects such as noise and air pollution exposures are more significant external cost components, in particular for heavy good vehicles (Maibach et al., 2008).

Several studies focus on a single external effect, i.e., traffic congestion, and address strategies, e.g., dynamic pricing, to increase the overall system efficiency (see, e.g., Vickrey, 1969; Arnott et al., 1994; Friesz et al., 2004; de Palma and Lindsey, 2004).

Some studies go beyond the consideration of a single external effect and address the correlation of transport related external effects (see, e.g., Calthrop and Proost, 1998; Ghafghazi and Hatzopoulou, 2014). Makarewicz and Galuszka (2011) use a speed-flow diagram to predict road traffic noise levels and find traffic congestion and noise to be inversely related, i.e., a reduction in traffic congestion increases the average noise level. In several studies, the correlation of speed level and air pollution is described as "U"-shaped, with high emission costs for low and high speed levels and low emission costs for intermediate speed levels (Barth and Boriboonsomsin, 2009; Wismans et al., 2011). The HBEFA[1] provides emission factors and differentiates, inter alia, between different area types, speed limits and the traffic states "free flow", "heavy", "saturated" and "stop-and-go". For urban roads and the traffic state "stop-and-go", emission factors are approximately twice as high compared to the other traffic states.

Only few studies address the simultaneous optimization of several externalities. Shefer and Rietveld (1997) address the simultaneous optimization of congestion level and accident costs. Shefer and Rietveld (1997) highlight the importance of accounting for the interdependence of different external effects in cost-benefit analyses. Verhoef and Rouwendal (2003) develop a model in which car drivers optimize their speeds taking into consideration congestion and accident costs. Shepherd (2008) investigates the simultaneous pricing of acrshortco2 emissions and accident costs. Shepherd (2008) finds model assumptions for external effects to have a crucial effect on the policy recommendations. Li et al. (2014) develop an analytical model to address the optimal design of a cordon pricing scheme which simultaneously accounts for traffic congestion and air pollution. Li et al. (2014) find that ignoring the congestion externality, dramatically decreases the cordon toll level.

Most of the existing studies on the simultaneous optimization of several externalities make use of analytical models that are applied to illustrative and rather simplistic case studies. In few recent studies, a simulation-based optimization methodology is developed and applied to real-world case studies: Agarwal and Kickhöfer (2015) propose simultaneous internalization of traffic congestion and air pollution costs. The approach is applied to the Munich metropolitan area. The authors

[1] Handbook Emission Factors for Road Transport, Version 3.2 (INFRAS, 2010)

find that the two externalities are positively correlated and the combined pricing scheme yields the highest gain in system welfare. In a following study, Agarwal and Kickhöfer (2016) identify the amplitude of the correlation of externalities between the two externalities and provide the corrected average toll levels for peak and off-peak hours. The reduction in emission costs found in Agarwal and Kickhöfer (2015) is lower compared to a later study by Agarwal and Kickhöfer (2016). This is triggered by providing a more realistic (fast) PT alternative to commuters and reverse commuters. This emphasize the need of a detailed investigation of transport users' choice dimensions. The computation of air pollution costs by Agarwal and Kickhöfer (2016) follows a simplified approach in which actual population exposures are neglected and an average cost factor is used to convert emissions into costs. This emission cost calculation approach is extended by Kickhöfer and Kern (2015) who explicitly account for population exposures to local air pollutants. In Ch. 6, noise damages caused by road users are internalized and traffic volumes on main arterial routes are found to increase which indicates an increase in traffic congestion. In Ch. 8 traffic congestion and noise damages in the Greater Berlin area are simultaneously internalized. Despite the observation that traffic congestion and noise are negatively correlated, i.e., internalizing one effect increases the other one, the simultaneous pricing policy reveals a reduction in both external effects; with traffic congestion being the more significant external cost component during peak times; and noise exposure costs being the more significant external cost component during off-peak times. In the study described in Ch. 8, possible user reactions are limited to route choice, neglecting e.g., demand elasticity resulting from mode choice. Solé-Ribalta et al. (2017) simulate the effects of a congestion pricing scheme in the city center region of Madrid and find a local reduction of air pollutants, in particular during peak times. However, Solé-Ribalta et al. (2017) only account for route choice and do not compute the system wide effects, e.g., the change in global pollution.

This study provides several extensions compared to previous simulation-based external cost studies:

- Previous simulation-based pricing studies only address the internalization of a single external effect (see, e.g., Ch. 6 or Kickhöfer and Kern (2015)), or only two external effects, e.g., traffic congestion and air pollution (Agarwal and Kickhöfer, 2016), or traffic congestion and noise (see Ch. 8). In contrast to previous studies, this study addresses the investigation and internalization of all three external effects, i.e., traffic congestion, noise damages and air pollution costs.
- In previous simultaneous internalization studies, the population density which is used to compute emission exposure costs, is assumed to be equally distributed in the study area, i.e., average factors are used to convert emissions to monetary costs (Agarwal and Kickhöfer, 2016). In contrast, this study accounts for the person-specific exposures to exhaust, integrating the approach by Kickhöfer and Kern (2015) into the simultaneous congestion and noise internalization framework.
- In previous simultaneous external cost pricing studies, the computation of congestion charges follows the methodology described in Ch. 3 in which person-specific road charges depend on the position in the queue, in particular the number of following road users. In this study, an improved congestion pricing approach is used, which computes road-specific and time interval-based congestion charges that are updated from one iteration to the next one based on the level of traffic congestion (see Sec. 4.3.2).
- Going beyond the scope of previous studies, this study explicitly investigates the impact of transport users' choice dimensions in the context of external cost pricing. All simulation

experiments are carried out for two different assumptions regarding transport users' choice dimensions: In a first simulation setup, transport users are only allowed to adjust their transport routes. In a second simulation setup, transport users are allowed to adjust their transport route *and* mode of transportation.

- In contrast to previous studies, this study provides a more detailed look into the spatial network effects resulting from the simultaneous pricing scheme.

This chapter is structured as follows: Sec. 9.2 describes the applied transport simulation framework as well as the simulation-based external cost pricing approaches. Sec. 9.3 describes the case study of the Munich municipality region and Sec. 9.3.3 lists the simulation experiments. Sec. 9.4 provides the simulation results and discussion. The simulation outcome is analyzed with regard to the enabled choice dimensions both at the aggregated and spatially and temporally disaggregated level. Finally, Sec. 9.5 briefly summarizes the main findings.

9.2 Methodology: Internalization of Congestion, Noise and Air Pollution Costs

The Pigouvian taxation principle is applied as follows: MATSim is used to iteratively compute and adjust an approximation of the optimal toll levels: In a first step, toll levels are computed based on the external congestion, noise and air pollution costs. In a second step, transport users are enabled to react to these road charges by adjusting their transport route and/or travel mode. Then, the toll levels are adjusted based on the updated external costs, and so on.

For each road segment, user, and time of day, the toll is computed as the sum of a congestion charge, marginal noise cost and marginal air pollution cost. A detailed description of the applied external cost pricing approaches is provided below.

Congestion Pricing The computation of congestion charges follows the interval-based list pricing approach presented in Sec. 4.3.2. For each road segment and time bin, the congestion charge is computed based on the congestion level and adjusted from iteration to iteration. In this study, the congestion charge is set to a value proportional to the average delay. All agents traveling on the same road segment and within the same time interval are charged the same amount. The price per road segment is adjusted as follows:

$$m_{r,t,k} = K_p \cdot d_{r,t,k} \ , \tag{9.1}$$

where $m_{r,t,k}$ denotes the toll per link r and time interval t, k is the iteration in which the toll is adjusted, K_p is a tuning parameter and $d_{r,t,k}$ is the average delay per transport user. K_p is set to twice the VTTS which in previous simulation experiments produces good results in terms welfare maximization and may economically interpreted as an approximation of the marginal congestion costs (see Sec. 4.6).

Noise Pricing The computation of noise levels follows the methodology described in Sec. 5.2. In a first step, hourly noise levels are calculated based on the German RLS-90 approach ('Richtlinien

für den Lärmschutz an Straßen', FGSV, 1992) taking into account the traffic volume, the share of heavy goods vehicles and the speed level. In a second step, the potentially affected individuals are dynamically computed, making use of the dynamic and activity-based simulation framework. The resulting population densities account for all agents performing any type of activity (e.g., home, work, leisure); on-road exposures are not considered. In a third step, the population densities and noise levels are used to compute noise damages following the methodology described in the German EWS approach which suggests a time-dependent, threshold-based monetization (FGSV, 1997). In a final step, for each road segment, time interval and vehicle type, marginal noise damage costs are computed following the methodology described in Sec. 7.2.2: Marginal noise exposure costs are

$$\begin{aligned} mc_t^{car,r} &:= \sum_j \left(C_{j,t}(I_{j,t}^{car,r}) - C_{j,t}(I_{j,t})\right) \\ mc_t^{hgv,r} &:= \sum_j \left(C_{j,t}(I_{j,t}^{hgv,r}) - C_{j,t}(I_{j,t})\right) \end{aligned} \tag{9.2}$$

where $mc_t^{car,r}$ are the marginal costs of an additional car on link r in time interval t; $mc_t^{hgv,r}$ are the marginal costs of an additional HGV on link r; and $C_{j,t}$ are the noise costs at receiver point j; $I_{j,t}^{car,r}$ is the noise level resulting from an additional car on link r; $I_{j,t}^{car,r}$ is the noise level resulting from an additional HGV on link r; and $I_{j,t}$ is the current noise level.

Air Pollution Pricing The applied air pollution emission modelling tool is developed by Hülsmann et al. (2011) and, further improved and extended by Kickhöfer et al. (2013). In a first step, vehicle characteristics (vehicle type, age, cubic capacity, fuel type etc.), dynamic attributes (parking duration, distance travelled, speed) and road types are used to get the cold (during warm up phase of vehicle) and warm emissions from the Handbook on Emission Factors for Road Transport (HBEFA) database (Version 3.1, INFRAS, 2010). In a second step, the exhaust emissions are converted to monetary units using the average emission cost factors (see Tab. 9.1) given by Maibach et al. (2008). In this study, for local air pollutants, SO_2 (sulfur dioxide), $PM2.5$ (particulate matter 2.5), NO_x (nitrogen oxides), $NMHC$ (non-methane hydrocarbons), population exposures are computed based on the methodology proposed by Kickhöfer and Kern (2015). For this, the network is divided into discrete cells of size $l = 250\ m$. The effect of air pollution is distributed to the neighboring cells using Eq. (9.3).

$$d_j = F \cdot \exp(-\frac{x_j^2}{2l^2}) \tag{9.3}$$

where x_j is the distance between the center of the cell in which a vehicle is causing emissions (source-cell) and the center of the cell j where agents perform activities (receptor-cell). F is a normalization factor such that distribution factors for all neighboring cells sum up to unity. The resulting costs are then charged from the causing agent. Since CO_2 is a global air pollutant, the CO_2 emission costs are charged from the causing agent using the average cost factor by Maibach et al. (2008) without any computation of population exposures.

Table 9.1: Emission cost factors. Source: Maibach et al. (2008).

Emission type	Cost factor (EUR/ton)
CO_2	70
$NMHC$	1,700
NO_x	9,600
PM	384,500
SO_2	11,000

9.3 Case Study: Munich, Germany

9.3.1 Scenario Setup

The case study of the Greater Munich area was initially generated by Kickhöfer and Nagel (2016) and further improved by Agarwal and Kickhöfer (2016). The MATSim network is generated based on a VISUM[2] data (RSB, 2005) model. The demand for the Greater Munich area is categorized into three parts. (a) The inner urban demand is created using detailed survey data (Follmer et al., 2004, MiD 2002) which contains more than 1.4 million individuals. (b) Commuters and reverse commuters are synthesized using data provided by Böhme and Eigenmüller (2006) in which about 0.3 million are commuters and about 0.2 million are reverse commuters. (c) About 0.15 million freight trips are generated using data provided by German Ministry of Transport (ITP and BVU, 2007).

9.3.2 Simulation Setup

To improve the computational performance, in this study, the sample size is reduced to 1% of the total population. Each link's flow and storage capacity (see Sec. 1.5) is reduced accordingly; the flow capacity is reduced to 1% and the storage capacity is reduced to 3% which in previous studies is found to provide more realistic traffic congestion patterns. That is, the underlying queue model accounts for the reduced sample size (see, e.g., Agarwal et al., 2017) and produces realistic congestion patterns.

9.3.3 Choice Dimensions and Simulation Experiments

In this study, different pricing schemes, i.e., no pricing, isolated congestion pricing (Exp. C), isolated noise pricing (Exp. N), isolated air pollution pricing (Exp. A), and simultaneous congestion, noise and air pollution pricing (Exp. CNA), are applied to the case study of Munich. Each pricing scheme is investigated for two different assumptions regarding the transport users' choice dimensions, i.e., route choice only vs. mode and route choice. A summary of all simulation experiments is provided in Tab. 9.2.

[2] 'Verkehr In Städten UMlegung', see www.ptv.de

Table 9.2: Simulation experiments

	Route choice only	Mode and route choice
Base case continued (No Pricing)	✓	✓
Exp. C	✓	✓
Exp. N	✓	✓
Exp. A	✓	✓
Exp. CNA	✓	✓

9.4 Results and Discussion

9.4.1 Aggregated Effects

Tab. 9.3 provides the simulation outcome for the pricing experiments with and without mode choice. The system welfare is computed as

$$W = V^{users} + R - C^{noise} - C^{air} \tag{9.4}$$

where W is the system welfare per day, R are the total daily toll revenues, C^{noise} are the total daily noise costs, C^{air} are the total daily air pollution costs and V_{users} are the daily user benefits which include the congestion costs and are computed as

$$V^{users} = \frac{1}{\beta_m} \cdot \sum_p \sum_a V_{p,a} - \sum_p C_p^{trip} \tag{9.5}$$

where $V_{p,a}$ is a person's p positive utility for performing an activity a (see Eq. (1.2)), β_m is the marginal utility of money and C_p^{trip} are the person's trip-related costs including the monetary toll payments. All pricing experiments are found to yield a positive change in system welfare compared to the base case (no pricing). The simultaneous pricing experiment (Exp. CNA) results in the largest increase in system welfare (see Tab. 9.3).

The additional choice dimension of transport users adjusting their mode of transportation is observed to increase the absolute change in external costs. That is, allowing for mode choice reinforces the impact of pricing. The increase in system welfare resulting from the pricing policy is much larger for the simulation experiments with mode choice compared to the simulation experiments without mode choice (see Tab. 9.3). In the simulation experiments with mode choice, the toll revenues are much lower compared to the simulation experiments without mode choice. This is explained by the additional choice dimension, i.e., transport users with high toll payments and no meaningful alternative route are now enabled to avoid the toll payments by switching to the toll-free PT mode. Also, the increase in system welfare in relation to the toll revenues becomes much larger.

Allowing transport users to switch to an alternative mode of transportation, in the simultaneous pricing experiment, the number of car trips decreases by 4.6% (shift towards the PT mode). An interesting observation is that in the isolated congestion pricing scheme (Exp. C) the number of car trips increase by 2.56%, yet, the total car travel distance and delays within the car mode are reduced (see Tab. 9.3). This is explained by a capacity relief effect in the city area, i.e., long distance

Table 9.3: Changes in aggregated simulation results compared to the base case; scaled to full population; typical work day.

Only route choice

Change in ...	Exp. C	Exp. N	Exp. A	Exp. CNA
number of car trips	0 (0.00%)	0 (0.00%)	0 (0.00%)	0 (0.00%)
average travel distance per car trip [*km*]	≈ 0 (1.14%)	≈ 0 (0.02%)	≈ 0 (-0.03%)	≈ 0 (1.11%)
average travel time per car trip [*sec*]	-287 (-11.40%)	-11 (-0.45%)	-15 (-0.61%)	-273 (-10.84%)
delay [*h*]	-139,631 (-29.68%)	-5,474 (-1.16%)	-3,564 (-0.76%)	-135,446 (-28.79%)
noise costs [*EUR*]	-9,488 (-1.66%)	-19,168 (-3.35%)	-26,127 (-4.57%)	-31,721 (-5.55%)
air pollution costs [*EUR*]	-90,133 (-2.64%)	-50,506 (-1.48%)	-262,964 (-7.72%)	-290,147 (-8.51%)
toll revenues [*EUR*]	5,242,709	187,370	3,145,114	8,632,478
system welfare [*EUR*]	3,123,797	75,051	653,041	3,187,310

Mode and route choice

Change in ...	Exp. C	Exp. N	Exp. A	Exp. CNA
number of car trips	51,500 (2.56%)	-500 (-0.02%)	-103,300 (-5.13%)	-92,500 (-4.60%)
average travel distance per car trip [*km*]	-2 (-6.31%)	≈ 0 (-0.69%)	-2 (-5.01%)	-4 (-10.54%)
average travel time per car trip [*sec*]	-404 (-16.12%)	-42 (-1.66%)	-275 (-10.99%)	-555 (-22.18%)
delay [*h*]	-141,292 (-30.34%)	-16,003 (-3.44%)	-111,480 (-23.94%)	-203,817 (-43.77%)
noise costs [*EUR*]	-3,550 (-0.63%)	-18,991 (-3.38%)	-42,026 (-7.49%)	-58,185 (-10.37%)
air pollution costs [*EUR*]	-74,070 (-2.23%)	-71,563 (-2.15%)	-521,652 (-15.71%)	-606,226 (-18.25%)
toll revenues [*EUR*]	4,769,564	187,522	2,799,642	6,926,436
system welfare [*EUR*]	3,523,119	421,959	2,610,615	5,087,305

commuters switch from car to alternative modes which reduces traffic congestion and makes the car mode more attractive for short distance inner urban travelers. A similar finding is reported by Agarwal and Kickhöfer (2016) in which emission pricing results in an increase in urban car trips.

In the only route choice simulation setup, toll payments can only be avoided by switching to alternative roads. Changes in average travel distance per car trip slightly increases in experiment C, N and CNA and slightly decreases in experiment A.

For both assumptions regarding the users' choice dimensions, isolated external cost pricing results in a reduction of the internalized effect, i.e., a decrease in total delay for experiment C, a decrease in noise costs for experiment N, and a decrease in air pollution costs for experiment A. Furthermore, simultaneous pricing (Exp. CNA) results in an overall reduction of all three internalized external effects. In Tab. 9.3, the delay is defined as the excess travel time for all road segments (similar to the delay definition in Sec. 4.3.2). This definition does not cover the delay effect resulting from users taking a longer but uncongested transport route.[3]

For all pricing experiments with and without mode choice, there is a positive correlation between the different external costs, i.e., pricing one effect results in a reduction of all external effects. Similar positive effects at the aggregated level are also observed in Agarwal and Kickhöfer (2016) and Agarwal and Kickhöfer (2015). For the simulation experiment with mode choice this intuitively makes sense since transport users switch from car to alternative modes. For the simulation experiment without mode choice, this observation may be explained by the spatial structure in the Munich region, in particular a positive correlation of congested roads and densely populated areas with potentially large air pollution and noise exposure costs.

The positive correlation observed in Tab. 9.3 in only valid at the aggregated level. At the spatially disaggregated level, the correlation effects are observed to be different, see below in Sec. 9.4.5.

9.4.2 Resulting Toll Payments

In the simultaneous pricing experiments, the average toll per trip varies between 3.00 *EUR* and 5.40 *EUR* (without mode choice), and 2.50 *EUR* and 4.80 *EUR* (with mode choice), depending on the time of the day. Fig. 9.1 provides a temporal analysis of each external effects' contribution to the average toll per trip. Noise-related toll payments are observed to be at a very low level, in particular during peak times. This may be related to the logarithmic scale of noise, i.e., marginal noise cost tolls decrease for higher traffic volumes. The congestion externality seems to be the most significant externality; during the day, congestion charges are higher compared to air pollution charges. Congestion-related toll payments increase during the morning and afternoon/evening peak which can be explained by the overall larger congestion level. The contribution of noise charges to the average toll is slightly larger in the early morning, late evening and the night. This is explained by lower cost thresholds, larger population exposures and higher marginal noise cost due to lower absolute traffic volumes. The contribution of air pollution charges to the average toll level decreases during peak times which can be explained by the higher relevance of congestion charges during these times as well as a reduced number of exposed people (on-road exposures are not considered[4]).

[3] An alternative approach is to compare the travel time of the chosen route (actual travel time) with the travel time of the route which would have been chosen in an empty network (free speed travel time) for each trip.

[4] For a study which explicitly accounts for on-road exposures, see Agarwal and Kaddoura (2019).

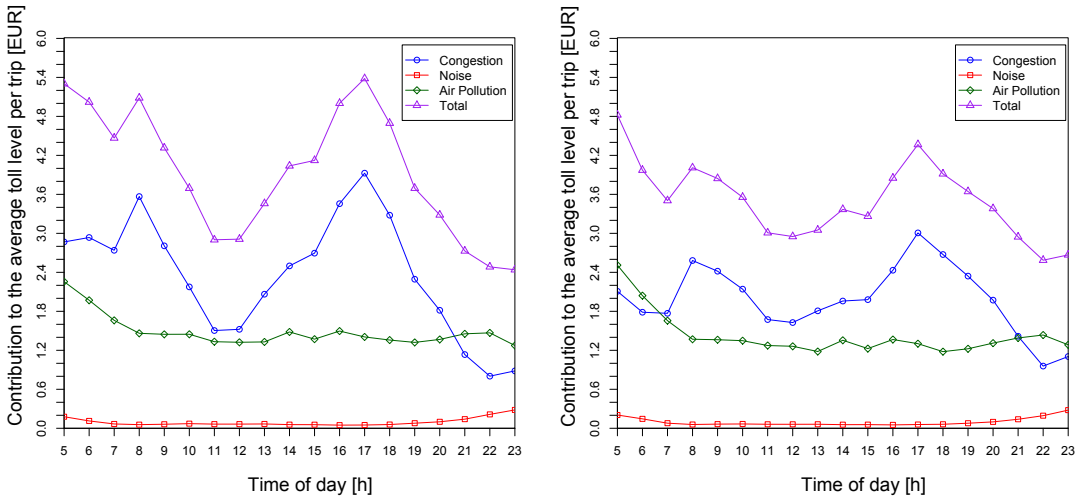

(a) only route choice

(b) Route and mode choice

Figure 9.1: Munich: Tolls per time of day (Exp. CNA)

9.4.3 Mode Switch Analysis

In Tab. 9.4, the simultaneous pricing experiment without mode choice is analyzed for two different user types: "car retainers" and "car to non-car switchers". The user type is identified by looking into the simulation outcome of the pricing experiment with mode and route choice. Average toll

Table 9.4: Average toll per trip (Exp. CNA; only route choice)

	Contribution of each external effect			
Considered users	Congestion	Noise	Air pollution	$\sum$
Car retainers	2.11	0.06	1.33	3.50
Car to non-car switchers	2.89	0.12	1.55	4.55

payments by "car retainers" are observed to be much lower compared to the average toll payments by "car to non-car switchers". That is, "car retainers" prefer to pay the relatively low tolls rather than switching to an alternative mode. In contrast, "car to non-car switchers" prefer to avoid the relatively high tolls by switching the mode of transportation—in case they are allowed to do so (simulation experiments with mode and route choice).

9.4.4 Changes in Traffic Volume

Fig. 9.2 depicts the changes in daily traffic volumes resulting from the simultaneous pricing experiment. In the only route choice simulation setup, transport users shift from the densely populated inner-city area to the western inner-city ring road as well as to the outer-city motorway ring road. In contrast, with mode and route choice, overall traffic volumes are reduced on most roads including the outer-city motorway ring road. Only for some roads in the city center area an increase in traffic volume is observed.

Fig. 9.3 shows the change in traffic volume per user type resulting from the simultaneous pricing experiment in the route choice only setup (Fig. 9.3a: change in freight vehicles, Fig. 9.3b: change

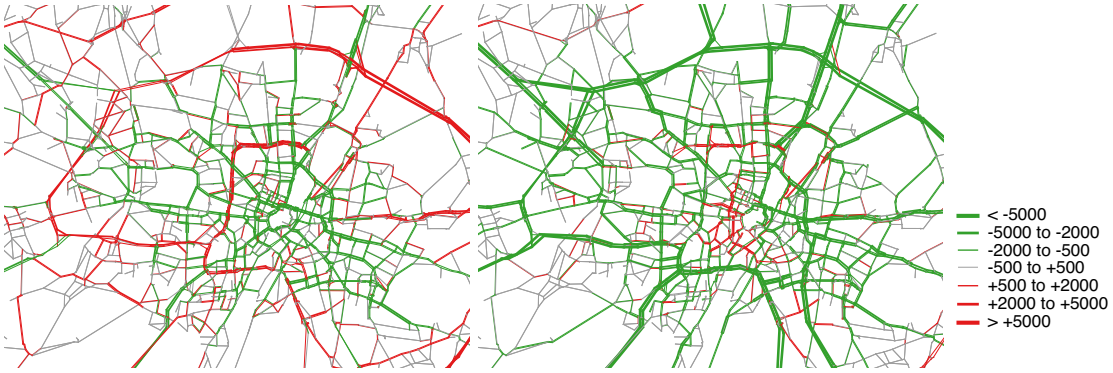

(a) Only route choice **(b)** Mode and route choice

Figure 9.2: Total changes in daily traffic volumes resulting from the simultaneous pricing experiment (Exp. CNA).

(a) Freight traffic **(b)** Inner urban traffic + commuters

Figure 9.3: A more detailed look into Fig. 9.2a: Changes in daily traffic volumes per user type resulting from the simultaneous pricing experiment (Exp. CNA- route choice only).

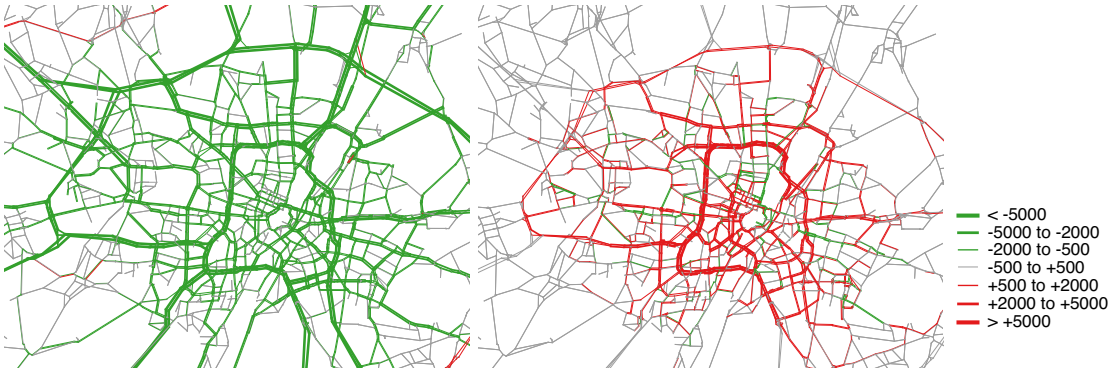

(a) Freight traffic + commuters **(b)** Inner urban traffic

Figure 9.4: A more detailed look into Fig. 9.2b: Changes in daily traffic volumes per user type resulting from the simultaneous pricing experiment (Exp. CNA- with mode and route choice.

in inner urban traffic and commuters). Fig. 9.3a points out that the number of freight vehicles decreases on the western inner city ring road. In contrast, the number of inner urban travelers

and commuters increases (see Fig. 9.3a) which yields the increase in overall traffic volume on the western inner city ring road observed in Fig. 9.2a.

The increase in traffic on inner-city roads in the route and mode choice simulation setup observed in Fig. 9.2b is explained by the overall lower level of traffic congestion caused by long-distance commuters, which makes the car mode more attractive for short distance trips in the inner-city center area. This effect is visualized in Fig. 9.4 which provides the changes in daily traffic volumes resulting from the simultaneous pricing scheme (Exp. CNA) filtered by user type. The number of freight vehicles and commuters decrease for most road segments (see Fig. 9.4a). In contrast, inner urban traffic increases on most road segments (see Fig. 9.4b). This spatial observation is supported by the reduction in average trip distance which decreases by 4 km compared to the base case (see Tab. 9.3).

Fig. 9.5 depicts two layers: the changes in traffic volumes per road segment between 3.00 and 4.00 p.m. resulting from the simultaneous pricing scheme (Exp. CNA) without mode choice and the population density in the base case for the same time bin. Overall, transport users avoid the city

(a) Greater Munich area **(b)** Munich city center area

Figure 9.5: Changes in traffic volumes resulting from the simultaneous pricing experiment (Exp. CNA) without mode choice; 3-4 p.m.; Map layer: © OpenStreetMap contributors.

center area by taking the outer-city motorway ring road, where (i) population densities are very low and (ii) congestion effects are at an overall lower level. A closer look into the city center area reveals the same effects: transport users avoid (i) areas with high and very high population densities and (ii) typically congested roads, e.g., in Munich, by using the inner-city ring road around the city center area instead of direct routes through the city center area.

Fig. 9.6 depicts the changes in daily traffic volume resulting from the isolated pricing experiments with mode and route choice. The effects observed in the isolated pricing experiments may help to understand the changes in traffic volume resulting from the simultaneous pricing experiment shown in Fig. 9.2b. An interesting observation is that experiment C and A show a contrary effect regarding the changes in traffic volume. Congestion pricing increases the usage of the inner- and outer city ring roads. In contrast, air pollution pricing yields reduced traffic volumes on the inner- and outer city ring roads.

9.4.5 Changes in Air Pollution and Noise

Fig. 9.7 depicts the changes in daily NO_x and L_{den} levels resulting from the simultaneous pricing scheme (Exp. CNA). With and without mode choice the NO_x and noise level is significantly reduced

(a) Exp. C **(b)** Exp. N **(c)** Exp. A

Figure 9.6: Change in daily traffic volume resulting from the isolated pricing schemes; Simulation setup with mode and route choice.

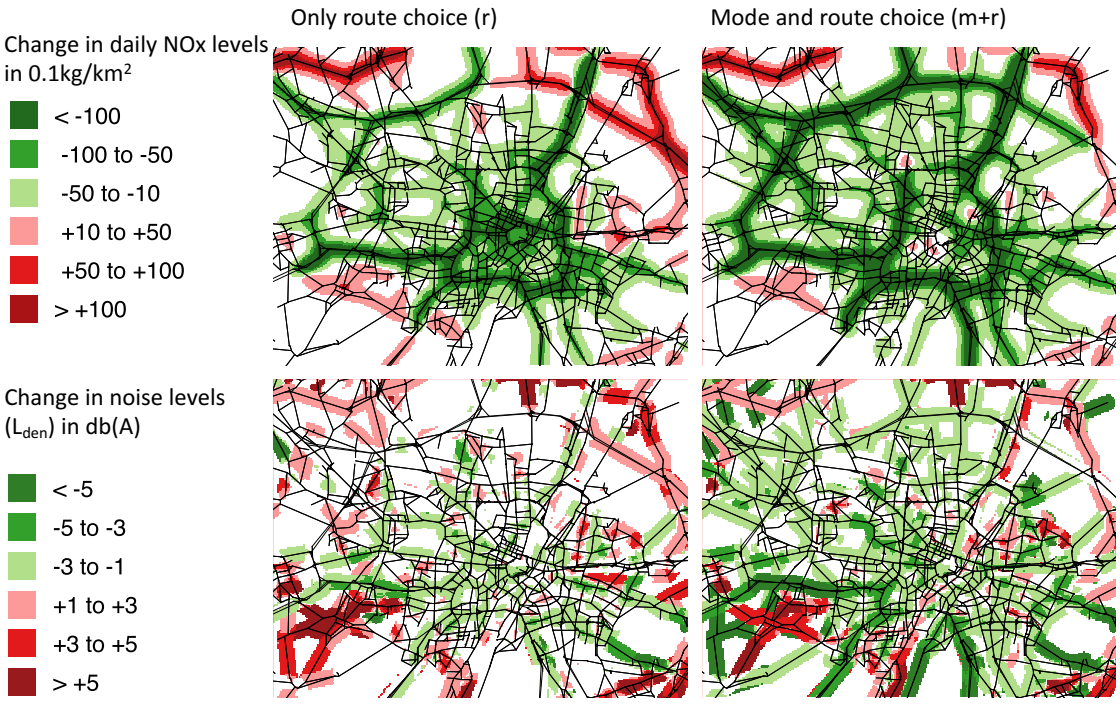

Figure 9.7: Changes in air pollution exposures and noise levels resulting from the simultaneous pricing scheme (Exp. CNA) with and without mode choice.

in the inner-city area. For NO_x levels, similar results are also observed in Agarwal and Kickhöfer (2016). In the simulation setup with mode choice, this effect is stronger compared to the simulation setup without mode choice. This is explained by the reduction in number of car trips and average car travel distance.

A comparison of Fig. 9.7 with Fig. 9.2 reveals that for some roads the change in NO_x and noise levels do not correlate with the change in traffic volume (see, e.g., the western inner-city ring road in the route choice only case). This is explained by Fig. 9.3 which shows the change in traffic volume per user type resulting from the simultaneous pricing experiment in the route choice only setup (left: change in freight vehicles, right: change in inner urban traffic and commuters). Fig. 9.3a points out that the number of freight vehicles decreases which causes the observed reduction in NO_x emissions.

Changes in noise levels are observed to be very large even though changes in daily traffic volumes are minor (see, e.g., in the southwestern Greater Munich area). This may be explained by the

logarithmic scale of noise. Also, the temporal distribution of travel demand plays an important role, i.e., the L_{den} noise index adds a penalty of several $dB(A)$ to noise levels in the evening and night time periods.

Fig. 9.8 and Fig. 9.9 depict the changes in NO_x and noise L_{den} level for each isolated pricing experiments. Local changes in NO_x are observed to be very different in experiment C, N and A.

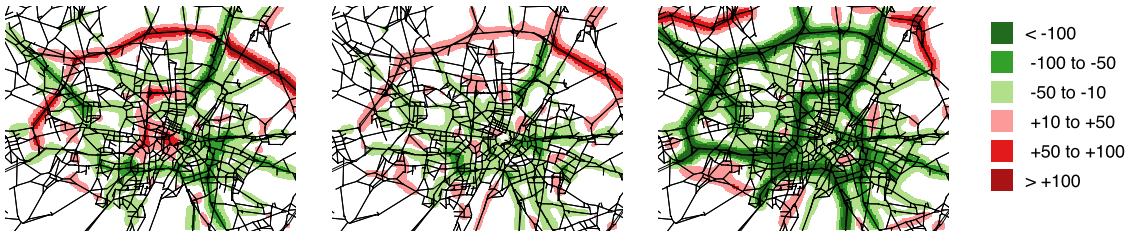

(a) Exp. C **(b)** Exp. N **(c)** Exp. A

Figure 9.8: Change in daily NO_x levels in $0.1kg/sqkm$ resulting from the isolated pricing schemes; Simulation setup with mode and route choice.

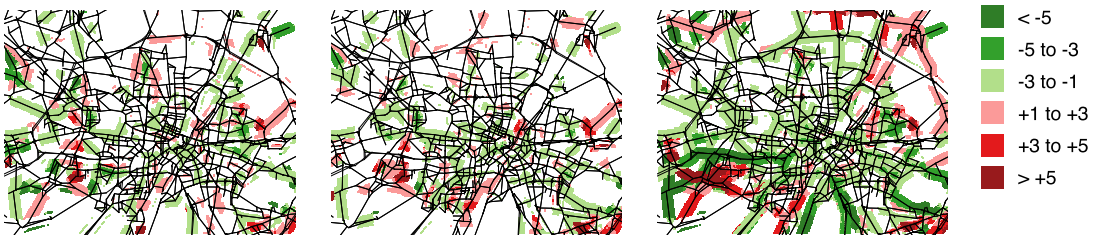

(a) Exp. C **(b)** Exp. N **(c)** Exp. A

Figure 9.9: Change in noise L_{den} levels in $dB(A)$ resulting from the isolated pricing schemes; Simulation setup with mode and route choice.

Isolated congestion pricing yields an increase in NO_x in the outer city ring road as well as in the city center area which is explained by the increase in inner urban traffic. Isolated noise pricing yields slight reduction in NO_x in the city center area and increase in NO_x along the outer city ring road. Isolated air pollution pricing yields an overall reduction in NO_x in the city center area as well as along the outer city ring road. Changes in noise levels are observed to be very low in the isolated congestion (Exp. C) and noise pricing (Exp. N) scheme. In the isolated air pollution pricing scheme (Exp. A), the changes in noise levels are similar to the changes in experiment CNA.

9.4.6 Discussion

At the aggregated level, congestion, noise and air pollution are found to be positively correlated. For the simulation setup with mode choice, this is in line with previous studies (see, e.g., Agarwal and Kickhöfer, 2015, 2016) and intuitively makes sense since the internalization of a single externality is expected to make the car mode less attractive and to yield a shift from the car mode to alternative modes. The simulation outcome reveals that this speculation is only partly correct. In the isolated congestion pricing scheme a rebound effect is observed, i.e., the number of long-distance car trips (commuters) are replaced by a larger number of short distance car trips (inner urban traffic). Yet, the overall level of traffic congestion is significantly reduced.

One of the finding is, that in the Munich case study, the positive correlation of congestion, noise and air pollution is also observed in the simulation setup without mode choice. This stands in contrast to the simulation outcome in Ch. 8 for the case study of the Greater Berlin area, where the correlation of congestion and noise was found to be negative. An explanation for this may be a different spatial structure in the Berlin and Munich case study. The positive correlation indicates that traffic congestion occurs in areas with high population densities where the number of people potentially exposed to air pollution and noise is high.

A further finding is that the positive correlation which is observed at the aggregated level is not confirmed by the spatially disaggregated effects, i.e., the changes in traffic volume per road segment and the resulting changes in traffic congestion, air pollution and noise. That is, isolated external cost pricing yields an overall reduction in total traffic congestion, noise and air pollution costs in the entire study area, however, spatially the effects are significantly different yielding some parts of the population better off and other parts worse off. With mode choice one might have speculated that mode shift effects from car to alternative modes result in reduced noise and air pollution levels in the entire area. This is, however, not the case and may be explained by the rebound effect described above, i.e., some parts of the population (in particular long distance commuters) shift from car to the PT which makes the car mode more attractive for other parts of the population (in particular inner urban travelers) with spatially different travel patterns (origins, destinations and routes).

The effect of noise tolling is found to be rather low in the Munich case study. In contrast, in previous studies for the Greater Berlin area, the impact on transport users' route choice decisions was much larger (see Ch. 7 and Ch. 8). This may be explained by the network resolution: In previous studies for the Greater Berlin area, the road network contains all road types, including minor roads where traffic volumes are rather low and consequently marginal cost noise tolls are at a higher level. In contrast, the present case study of the Greater Munich area only accounts for the main road network where traffic volumes are higher and consequently marginal noise toll levels are rather low, in particular during peak times.

In this study, the alternative modes of transportation, i.e., bicycle and PT, are simulated in a simplified way, i.e., transport users are teleported with a predefined speed from one activity location to the next one. That is, spatial or temporal differences in the PT mode are not accounted for. Furthermore, capacity constraints and external effects, such as delays imposed on other travelers within the PT mode (see Ch. 2), are neglected. Accounting for capacity constraints and extending the external cost pricing scheme to all alternative modes is expected to make the alternative modes less attractive and weaken the observed mode shift effects.

This study neglects the fact that transport users may have some flexibility in their activity scheduling decisions and may travel earlier or later. Departure time choice allows travelers to remain within the car mode but still to avoid congested peak times or high toll payments, e.g., congestion charges during peak times or noise charges in the early morning or late evening. That is, departure time choice increases the attractiveness of the car mode. This, in consequence, may weaken the observed mode shift effects and reduction in external costs: Car travelers will rather travel earlier or later in order to reduce their external cost toll payments than switching to an alternative mode where their external cost payments would have been zero.

This study also neglects mode-specific operating and maintenance costs which vary depending on the level of usage. Adding these cost components to the system welfare may have a substantial effect on the overall results.

This study only focuses on congestion, noise and air pollution. Accounting for further external effects, such as accident costs, may have an impact on the optimal route and mode choice decisions.

Assuming marginal external accident costs to correlate with the population density, accident cost pricing may push towards the same direction as the air pollution and noise pricing schemes, where costs are also computed accounting for the population density. Since accident costs may be assumed to be larger for higher speed levels (Shefer and Rietveld, 1997; High Level Group on Transport Infrastructure Charging, 1999), without mode choice, there might be a negative correlation with congestion pricing, which reduces congestion and increases the speed level. In contrast, with mode choice, accident cost pricing is expected to be positively correlated with the other external cost pricing schemes since the overall car toll level increases and pushes further towards alternative modes of transportation.

9.5 Conclusion

In this study, the Pigouvian taxation principle is applied to an agent-based simulation framework. In a number of different external cost pricing simulation experiments, the interrelation of isolated congestion pricing (Exp. C), isolated noise pricing (Exp. N), isolated air pollution pricing (Exp. A) and simultaneous congestion, noise and air pollution pricing (Exp. CNA) is investigated for the real-world case study of the Greater Munich area for two different assumptions regarding the transport users choice dimensions, only route choice as well as mode and route choice.

Overall, this study contributes to a better understanding of the interrelation of transport related external effects both at the aggregated and disaggregated level. For both assumptions regarding the transport users choice dimensions (with and without mode choice) the simultaneous congestion, noise and air pollution pricing scheme reduces all external effects and increases the overall system efficiency. At the aggregated level, the isolated external cost pricing experiments are found to reduce all other external effects (positive correlation of external effects). This is even found for the simulation setup without mode choice which indicates that traffic congestion occurs in areas with high population densities where the number of people potentially exposed to air pollution and noise is at a higher level. In contrast to previous studies, this study also looks into the spatially disaggregated effects. Even in the simulation experiments with mode choice, for certain areas the correlation in traffic congestion, noise and NO_x is found to be negative, yielding different parts of the population better off and worse off. Nevertheless, at the aggregated level, the correlation of external effects is positive and pricing a single external effect reduces all other external effects.

Furthermore, this study highlights the importance of correctly accounting for all relevant choice dimensions. Only accounting for route choice and neglecting the fact that transport users also adjust their mode of transportation in order to react to a transport policy may underestimate the great potential of pricing. On the other hand, as discussed in Sec. 9.4.6, neglecting further choice dimensions such as departure time choice, may overestimate the mode shift effects and the resulting increase in system welfare.

Based on these findings, the overall policy recommendation is that transport policies should be designed very carefully. Transport policies that only address a single externality may have a positive effect at the aggregated level, however, may lead to a negative effect at the disaggregated level, e.g., an increase in air pollution in some areas, which leaves some parts of the population worse off. Designing a policy which accounts for all external effects seems to be a good strategy to keep the local negative side effects low, however, does not provide a guarantee to reduce all external effects in the entire study area or prevent undesired rebound effects. To prevent such undesired

rebound effects (here: increase in inner-urban traffic), it seems reasonable to combine the concept of external cost pricing with further transport policies.

Part IV

External Cost Pricing in a World of Shared Autonomous Vehicles

CHAPTER 10

External Cost Pricing in a World of Shared Autonomous Vehicles

AVs create new opportunities to traffic planners and policy-makers. In the case of SAVs, dynamic pricing, vehicle routing and dispatch strategies may aim for the maximization of the overall system welfare instead of the operator's profit. In this chapter, an existing congestion pricing methodology is applied to the SAV transport mode. On the SAV operator's side, the routing- and dispatch-relevant cost are extended by the time and link-specific congestion charge. On the users' side, the congestion costs are added to the fare. Simulation experiments are carried out for Berlin, Germany in order to investigate the impact of SAVs and different pricing setups on the transport system. This chapter is an edited version of Kaddoura et al. (2018).

10.1 Introduction and Problem Statement

In the last few years, research on AVs has increased substantially and several companies have started the development and real-world application of AVs (Harris, 2015; Hsu, 2016). A broad market introduction of SAVs, also referred to as *autonomous taxis* or *autonomous car-sharing*, is expected in the coming years. According to most studies, one SAV is capable to replace up to approximately 10 conventional CCs trips at a high service quality; the total mileage is found to increase caused by empty trips to pick up passengers (Spieser et al., 2014; Fagnant and Kockelman, 2014; Martinez et al., 2014; Burghout et al., 2015; Bischoff and Maciejewski, 2016a). In the case of pooling (ride sharing) and depending on the fleet size, even more CC trips may be replaced by one SAV and total mileage may decrease (see, e.g., Burghout et al., 2015).

Analyzing the overall welfare effects of introducing an SAV mode needs to account for both the transport users and operators. On the operator's side, several cost components need to be considered, e.g., depreciation, fuel, cleaning, navigation fees, maintenance and wear (see, e.g., Bösch et al., 2018; Litman, 2017a). The estimation of average vehicle costs is addressed in several studies with lower-bound estimates in the range of 0.30 to 0.38 EUR per passenger-km (Bösch et al., 2018; Trommer et al., 2016) and upper-bound estimates between 0.40 and 2.00 EUR per passenger-km (Litman, 2017a). Bösch et al. (2018) find the average costs per passenger-km to be lower for SAVs compared to CCs or private AVs. In contrast, Litman (2017a) estimates SAVs to cost more than CCs or private AVs.

On the users' side, increased total mileage may translate into a higher level of traffic congestion which increases generalized travel costs. The increase in total mileage may result from empty pick-up trips, vehicle relocations (Fagnant and Kockelman, 2016), mode shift effects and newly generated trips (Truong et al., 2017; Harb et al., 2018). On the other hand, SAVs are expected to increase the level of comfort and, thus, to decrease the marginal costs of traveling. The VTTS is expected to be reduced by 30-35% (Litman, 2017b; Childless et al., 2015). Furthermore, travel time may be saved by eliminating parking search (Litman, 2017a). Also, a more fluent flow of autonomous vehicles, platooning as well as intelligent routing may reduce traffic congestion (Fagnant and Kockelman, 2015; Litman, 2017a). Shared vehicles are expected to reduce car ownership (Litman, 2017a) which translates into a reduction of daily fixed costs for owning a CC (or a private AV) . By avoiding the human error, AVs have the potential to reduce accident costs (Fagnant and Kockelman, 2015; Litman, 2017a). In case SAVs are considered to be non-electric vehicles, on the one hand, the increase in total mileage may increase air pollution costs (Litman, 2017a). On the other hand, eliminated parking search, reduced cold starts and environmental friendly vehicles (shortened vehicle lifespan) may decrease air pollution costs (Fagnant and Kockelman, 2014). Furthermore, SAVs, or

AVs in general, may reduce the demand for nearby parking which allows for a new usage of public space (Fagnant and Kockelman, 2015). On the other hand, additional space may be required for pick-up and drop-off activities.

Considering mobility as a "normal good", lower travel costs are expected to increase total vehicle-*km*, i.e, the number of trips and/or the trip distances (see, e.g., Litman, 2017a). The expected increase in traffic may result in an inefficient usage of resources and a loss in system welfare. This study investigates optimal price setting strategies for SAVs and CCs in order to prevent an excessive use of transport resources. Following the concept of Pigouvian taxation, the system welfare is maximized by internalizing so-called external effects (Pigou, 1920). By adding the external costs to the generalized travel costs, the decision-relevant travel costs are corrected and reflect the full costs associated with the usage of transport resources (see Sec. 1.2). For decisions which routes to take, marginal external costs vary with the road segment and time of day. Consequently, a first-best optimal tolling scheme to optimize the road usage may be difficult to be fully understood by the transport users, resulting in failing incentives and welfare losses. Furthermore, the required tolling technology may be very costly. A more simplified second-best tolling scheme may reduce tolling costs and be more comprehensible for the transport users, however, also involve a loss in welfare compared to the first-best solution. A world with SAVs, or AVs in general, creates new opportunities to traffic planners and policy-makers. Instead of providing incentives to private car users by means of optimal pricing, traffic management may directly control the AV operation. In particular, in the case of SAVs, dynamic vehicle routing and dispatch strategies may aim for the maximization of the overall system welfare instead of the operator's profit. This offers a crucial advantage over existing pricing schemes for CCs. For transport users' decisions to use the SAV mode or an alternative mode of transportation, trip-specific marginal external costs may be added to the base fare paid by SAV users.

There are several studies in which the Pigouvian taxation principle is applied in the context of road traffic (see, e.g., Vickrey, 1969; Arnott et al., 1993; Verhoef and Small, 2004, see also Ch. 3, Ch. 6 and Ch. 9) or PT (see, e.g., Turvey and Mohring, 1975; Kraus, 1991, see also Ch. 2). External cost pricing in the context of innovative mobility concepts, e.g., SAVs, is investigated to a lesser extent. Sharon et al. (2017) present a welfare improving tolling approach and discuss its potentials in the context of AV technology, i.e, computer-controlled route choice, however, neglect transport users' mode choice decisions. Most existing studies neglect transport users mode choice reactions and assume a fixed amount of SAV trips (see, e.g., Maciejewski and Bischoff, 2015; Bischoff and Maciejewski, 2016a,b; Fagnant and Kockelman, 2016). In contrast, Liu et al. (2017) account for transport users' mode choice reactions and investigate different fare levels. The SAV fares are, however, static and not related to the level of traffic congestion. Liu et al. (2017) also discuss the impact of SAVs on air pollutant emissions and estimate a reduction of emitted air pollutants, however, without looking into the spatial effects. Simoni et al. (2019) investigate different congestion pricing schemes for an AV-oriented and an SAV-oriented scenario with different assumptions regarding cost parameters and SAV fleet sizes. In Simoni et al. (2019), different types of congestion pricing schemes are applied to all user segments, environmental effects are not analyzed and car ownership rates are a model input. In contrast, in the present study, different pricing schemes are applied to different user segments (only SAVs vs. all user segments), the car ownership rate is a model inherent and the impact of SAVs and different pricing setups is investigated. The present study picks up the lack of research and investigates optimal price setting strategies for SAV and CC users. An agent-based simulation framework is used to model transport users' reactions to a newly introduced SAV mode in Berlin, Germany. Transport users are enabled to adjust the

departure time, transport route and mode of transportation, which includes the decision to own a CC. This is the first study in which different congestion pricing strategies are investigated in the context of SAVs, the environmental impact is simulated and transport users' mode choice decisions, including the decision to own a CC, are explicitly taken into account. This study analyzes the impact of SAVs and the pricing strategy on air pollution and noise levels, and provides a detailed look into the mode switch effects.

The remainder of this chapter is organized as follows. Sec. 10.2 briefly describes the agent-based simulation framework and presents the SAV pricing methodology. Sec. 10.3 describes the Berlin case study, simulation setup and experiments. Sec. 10.4 describes the simulation results, Sec. 10.5 provides the discussion and Sec. 10.6 concludes this study.

10.2 Methodology: Shared Autonomous Vehicle Optimization Approach

This study proposes an optimal SAV operation approach which builds on the Pigouvian taxation principal, i.e, the internalization of congestion costs. The congestion charge is computed for each road segment and 900 *sec* time interval. The computation of dynamic congestion prices follows the iterative interval-based list pricing methodology described in Sec. 4.3.2. A discrete Proportional Controller is applied which sets the congestion charge proportionally to the average delay. The trip-specific costs are then taken into account by the SAV operator *and* users:

- On the SAV operator's side, the routing- and dispatch-relevant cost are extended by the time and link-specific congestion costs.
- On the user side, the trip-related congestion costs caused by the SAV are added to the base fare to be charged from the SAV user. The trip-related congestion costs also include the external costs incurred during the pick-up trip.

SAV operators are allowed to adjust their vehicle dispatching and routing in order to avoid the congestion charge. Transport users are enabled to adjust their mode of transportation, their departure time as well as their transport route. In each iteration the road- and time-specific congestion cost term is (re-)computed based on the updated delay level applying the method of successive averages.

10.3 Case Study: Berlin, Germany

10.3.1 Scenario Setup

The transport supply side contains all roads and PT lines in the Greater Berlin area. Travel demand consists of commuters and non-commuters using the car, PT, bicycle, ride and walk mode. The synthetic population is calibrated against real-world traffic data, i.e, car counts, modal split infas and DLR (2010) and trip-distances Ahrens (2009). A more detailed description of the applied case study is provided in Sec. 4.5.1 and Ziemke et al. (2019).

SAV Setup: Adding SAVs as an Additional Mode of Transportation A fleet of 10,000 SAVs is added to the existing modes of transportation and may be used for trips starting and ending within the service area. To speed up computational performance, in this study, a 10% sample is used and the SAV fleet size and road capacities are reduced accordingly. The service area is set to the inner-city Berlin area (see Fig. 10.1). In the first iteration, all vehicles are randomly distributed in the service area, in all further iterations, vehicles remain on the link where the last passenger was dropped off. The vehicle fleet size is set in a way that there are no capacity-related effects, i.e, there are always vehicles available to serve all passengers.

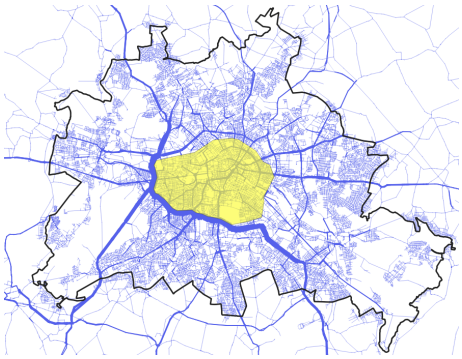

Figure 10.1: Case study: Greater Berlin area. Black line: Berlin city boundary. Blue lines: Road network, the line width corresponds to the relative traffic volume in the base case. Yellow area: SAV service area.

10.3.2 Choice Dimensions and Simulation Setup

All transport users are allowed to change their transport routes and departure times in order to avoid traffic congestion or toll payments. In addition, all users are allowed to change their mode of transportation. For each sub-tour, i.e, trip chains starting and ending at the same activity location, the transport mode may be changed to only car, only bicycle (chain-based modes) or a combination of PT and walk. The ride mode is fixed, i.e, transport users are not enabled to switch from or to the ride mode. Each agent's choice sets is limited to 5 travel plans. All simulation experiments are run for a total of 200 iterations. During choice set generation (first 160 iterations), in each iteration the share of agents who change their mode, route and departure time is set to 10%, 5% and 5%. In the final 40 iterations, all agents select from their choice sets based on a multinomial logit model.

Transport Modes **CC** users' travel times result from the simulated traffic flows, including the interaction of SAVs and CCs.

The **SAV** fleet size is set to 10,000 SAVs (scaled up to 100%). The SAV service area is set to the inner-city Berlin area, a trip request starting and/or ending outside the service area is rejected and the agent gets stuck. In this study, the service does not allow for pooling (ride-sharing). In the first iteration, the vehicles are randomly distributed in the inner-city Berlin area. Then, vehicles remain on the link where the last drop off took place. The pick-up duration is set to 2 *min*, the drop off duration is set to 1 *min*. SAVs interact with other SAVs as well as CCs. Assuming mixed traffic conditions, traffic flow parameters for SAVs are considered to be equal to CCs.

Travel times within the **PT** mode result from walking times from and to the transit stop, waiting times and in-vehicle times based on the schedule. In this simulation setup, buses and tramways do not interact with SAVs, CCs or bicycles.

The **walk**, **bicycle** and **ride** mode are simulated in a simplified way, i.e, teleported from one activity to the next one. That is, transport users do not interact with each other or users of other modes. For walk and bicycle, the travel times are computed based on a mode-specific speed (walk: 4 km/h; bicycle: 12 km/h) and a trip distance resulting from the beeline distance and a beeline distance factor (walk: 1.5; bicycle: 1.4). For ride, the travel time is computed based on the least cost network route taking into consideration the (congested) car travel time.

10.3.3 Simulation Experiments

The following simulation experiments are carried out.

- **Base case (bc-0):** There is no SAV mode and there is no congestion charge applied to any transport mode.
- **SAV base fare pricing (SAV-0):** The SAV mode is added as an additional mode of transportation (see Sec. 10.3.1). SAV users only have to pay the base fare. There is no congestion charge applied to any transport mode.
- **SAV base fare + external cost pricing (SAV-1):** The SAV mode is added as an additional mode of transportation (see Sec. 10.3.1). The congestion charge is applied to the SAV mode only. That is, SAV users have to pay the base fare plus road and time-specific congestion prices.
- **SAV base fare + external cost pricing; CC external cost pricing (SAV-2):** The SAV mode is added as an additional mode of transportation (see Sec. 10.3.1). The congestion charge is applied to both the SAV and CC mode. That is, SAV users have to pay the base fare plus road and time-specific congestion prices and also CC users have to pay road and time-specific congestion prices.

10.3.4 Cost Parameters

System welfare is computed as

$$W = V + \Pi + C_{toll}^{CC} + C_{toll}^{SAVo} \ , \tag{10.1}$$

where V is the user benefits, Π is the profit of the SAV operator, and C_{toll}^{SAVo} and C_{toll}^{CC} are the toll revenues earned by the regulator, e.g., the state. The user benefits are

$$V = \sum_i \left(V_{i,activity} \cdot \beta_{money}^{-1} - C_{i,travel} \right) \ , \tag{10.2}$$

where i denotes the person, $V_{i,activity}$ is the positive utility from performing activities, $beta_{money}$ is the marginal utility of money and $C_{i,travel}$ are the travel related costs computed as

$$\begin{aligned} C_{i,travel} = {} & c_{trip}^{CC} \cdot n_i^{CC} + c_{km}^{CC} \cdot d_i^{CC} + c_{hour}^{CC} \cdot t_i^{CC} + C_{i,toll}^{CC} \\ & + r_{day}^{SAVu} + c_{trip}^{SAVu} \cdot n_i^{SAVu} + c_{km}^{SAVu} \cdot d_i^{SAVu} + c_{hour}^{SAVu} \cdot t_i^{SAVu} + C_{i,fare}^{SAVu} \end{aligned} \tag{10.3}$$

Table 10.1: Cost parameters

CC	trip-related fixed cost	c_{trip}^{CC}	1.5 *EUR* per trip (Ziemke et al., 2019)
	km-based operating cost rate	c_{km}^{CC}	0.20 *EUR*/vehicle-*km* (Ziemke et al., 2019)
	private time cost	c_h^{CC}	$= beta_{perf}$ (opportunity cost of time) = 6.0 *EUR* per person-hour (Ziemke et al., 2019)
	total congestion and noise road charges	C_{toll}^{CC}	see Sec. 10.2
Walk	trip-related fixed cost	c_{trip}^{walk}	0.00 *EUR* per trip (Ziemke et al., 2019)
	private time cost	c_h^{walk}	$= beta_{perf}$ = 6.0 *EUR*/*h* (Ziemke et al., 2019)
Bicycle	trip-related fixed cost	c_{trip}^{bike}	1.85 *EUR* per trip (Ziemke et al., 2019)
	private time cost	c_h^{bike}	$= beta_{perf}$ = 6.0 *EUR*/*h* (Ziemke et al., 2019)
PT	trip-related fixed cost	c_{trip}^{PT}	0.60 *EUR* per trip (Ziemke et al., 2019)
	private time cost	c_h^{PT}	$= beta_{perf}$ = 6.0 *EUR*/*h* (Ziemke et al., 2019)
SAV users	trip-related fixed cost	c_{trip}^{SAVu}	0 *EUR* per trip
	daily profit for no longer owning a CC	r_{day}^{SAVu}	5.3 *EUR* (per SAV user who (i) used a CC in the base case and (ii) has no other CC trip). In (Tab. 8-32 Planco et al., 2015), for an electric vehicle, i.e, a Citroen C-Zero, vehicle-specific fixed costs (without costs for the driver) ["Feste Kosten (ohne Lohn)"] are 1,930 *EUR* per year; divided by 365 days per year results in 5.3 *EUR* per day.
	private time cost	c_h^{SAVu}	$= c_h^{CC} \cdot 70\%$ (Litman, 2017b; Childless et al., 2015) = 4.2 *EUR* per person-*h*
	user price (base fare)	c_o^{SAVu}	= 0.35 *EUR*/*km* (estimated user costs based on Trommer et al. (2016) and Bösch et al. (2018))
	total fare payments	C_{fare}^{SAVu}	see Sec. 10.3.3
SAV operator	total congestion road charges	C_{toll}^{SAVo}	see Sec. 10.2
	total fare revenues	C_{fare}^{SAVu}	equal to the amount paid by the SAV users

The profit Π is computed as

$$\Pi = C_{fare}^{SAVu} - C_{toll}^{SAVo} - C^{SAVo} \,, \tag{10.4}$$

where C_{fare}^{SAVu} are the revenues, C_{toll}^{SAVo} are the toll payments paid by the operator and C^{SAVo} are the SAV operating costs. Inserting Eq. 10.4 into Eq. 10.1 yields the following:

$$W = V + C_{fare}^{SAVu} + C_{toll}^{CC} - C^{SAVo} \tag{10.5}$$

The mode-specific cost parameters are given in Tab. 10.1.

10.4 Results

10.4.1 Average Tolls and Fares

Tab. 10.2 depicts the resulting average toll and fare per trip and per *km* traveled for the SAV and CC mode. The SAV base fare amounts to 0.35 *EUR*/*km* and depending on the simulation experiment a dynamic congestion charge (see Sec. 10.2) is added to these costs. For CC users, the operating costs are set to 0.20 *EUR*/*km* (see Tab. 10.1) and only in simulation experiment SAV-2, a dynamic congestion charge has to be paid. Low average CC toll payments per *km* are explained by

relatively uncongested, long-distance trips starting and/or ending outside of Berlin. The congestion

Table 10.2: Tolls and fares paid by CC and SAV users (trip-based analysis)

	SAV-0	SAV-1	SAV-2
Base fare (SAV mode) [EUR/km]	0.35	0.35	0.35
Average fare (SAV mode) [EUR/km]	0.35	0.46	0.45
Average fare per SAV trip [EUR]	1.00	1.24	1.23
Average toll (CC mode) [EUR/km]	0.00	0.00	0.04
Average toll per CC trip [EUR]	0.00	0.00	0.44

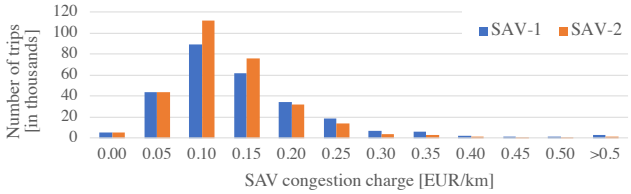

Figure 10.2: Trip frequency for the resulting SAV congestion charges

charges depend on the level of traffic congestion. Consequently, during peak times and on heavily congested road segments, the congestion charge is at a higher level. Fig. 10.2 depicts the trip frequency for the resulting SAV congestion charges. For a few trips, SAV users only pay the base fare and the congestion charge is zero. For approximately 95% of all trips, the congestion charge ranges from 0.05 EUR/km to 0.30 EUR/km. For some trips the congestion charge is even much higher and reaches up to a maximum of 7.16 EUR/km (Exp. SAV-1) or 5.03 EUR/km (Exp. SAV-2).

10.4.2 Mode Shift Effects

The aggregated mode shift effect is depicted in Tab. 10.3. For each simulation experiment, the

Table 10.3: Modal split analysis

	bc-0	SAV-0	SAV-1	SAV-2
Total CC trip share [%]	43.2	42.5	42.6	39.4
Total PT trip share [%]	14.0	13.6	13.7	14.8
Total Bicycle trip share [%]	13.4	13.3	13.3	15.2
Total Walk trip share [%]	20.2	19.6	19.7	19.8
Total Ride trip share [%]	9.2	9.2	9.2	9.2
Total SAV trip share [%]	-	1.8	1.5	1.6
SAV trip share within service area [%]	-	17.7	14.8	15.8
SAV trips (upscaled to full population size)	-	326,420	272,620	292,080

mode-specific trip share is given taking into consideration all trips (i.e, trips inside and outside of Berlin). The overall low total SAV trip shares are explained by the small service area and relatively small number of SAV trips compared to the total trip number. With respect to a total of 1,847,310 trips starting and ending within the SAV service area (see Fig. 10.1), the SAV trip share amounts to 17.7% in experiment SAV-0, 14.8% in experiment SAV-1 and 15.8% in experiment SAV-2.

Fig. 10.3 depicts the person-specific mode shift effects in two simulation experiments. The line width is proportional to the number of users that have switched from one mode to the other or

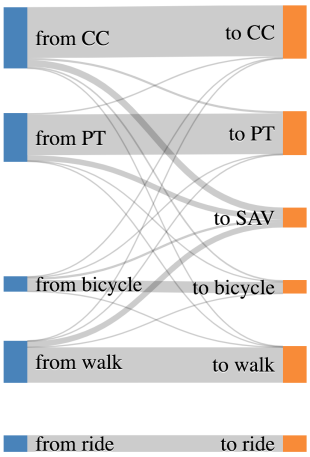

(a) bc-0 → SAV-0

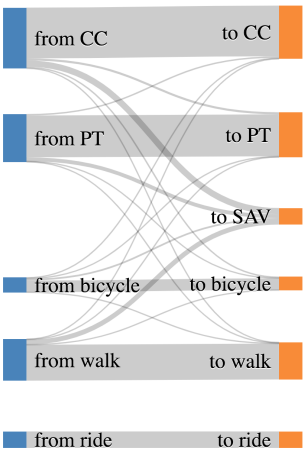

(b) bc-0 → SAV-1

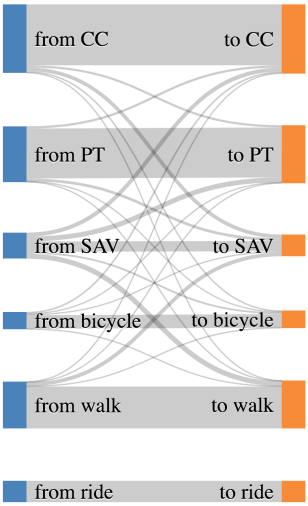

(c) SAV-0 → SAV-1

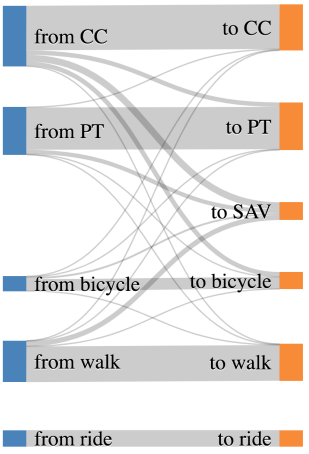

(d) bc-0 → SAV-2

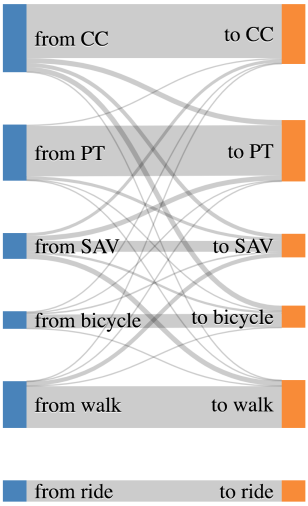

(e) SAV-0 → SAV-2

Figure 10.3: Mode switch analysis (all trips by potential SAV users)

that have used the same mode of transportation in both cases. All figures refer to the potential SAV users, i.e, individuals with at least one trip starting and ending inside the service area.

Comparing simulation experiment SAV-0 and bc-0 (Fig. 10.3a), the overall observation is that the SAV mode attracts users from all possible modes of transportation (CC, PT, bicycle, walk), in particular from the CC, walk and PT mode. A comparison of simulation experiment SAV-1 and SAV-0 (Fig. 10.3c) reveals that SAV pricing pushes users from the SAV mode to other modes. The simultaneous SAV and CC congestion pricing scheme pushes transport users from both the CC and SAV mode to other modes, in particular to the PT and bicycle mode. The disaggregated analysis reveals that there are always mode shift effects into both directions, e.g., from the CC to the PT mode and vice versa. Comparing experiment SAV-0 and bc-0, a closer look into the numbers reveals that there are slightly more users switching from CC to PT and bicycle compared to the users switching from PT and bicycle to CC. This indicates that the SAV mode is not only attracting transport users from the CC mode but also makes the CC mode relatively less attractive and pushes towards the PT and bicycle mode. A comparison of Fig. 10.3c and Fig. 10.3e reveals the change in mode switch patterns in the different pricing experiments. Comparing experiment SAV-1 and SAV-0 (Fig. 10.3c), the most dominant mode switch effect is from SAV (back) to CC as well as to PT and walk. In contrast, comparing experiment SAV-2 to SAV-0 (Fig. 10.3e), the most dominant mode switch effect from SAV to PT and walk. That is, the additional pricing of the CC mode, makes the CC mode less attractive for users switching from the SAV mode to alternative modes.

10.4.3 Travel Time

For each mode switch effect described in the previous section, Fig. 10.4 depicts the change in average beeline speed. The beeline speed is computed as the beeline distance between the trip's origin and destination divided by the travel time. A first observation is that changes in the beeline

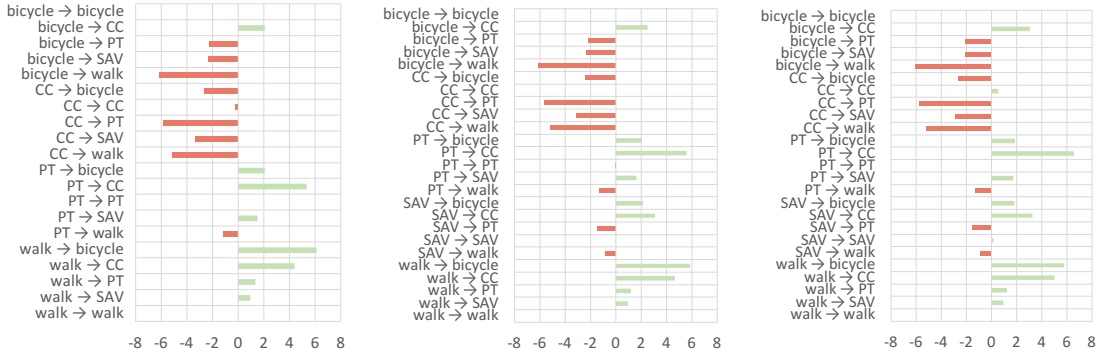

(a) bc-0 → SAV-0 **(b)** SAV-0 → SAV-1 **(c)** SAV-0 → SAV-2

Figure 10.4: Change in average beeline speed per trip for each mode switch effect [km/h]; only potential SAV users

speed are mainly related to the mode switch type, i.e, the currently and previously used mode of transportation. Transport users switching from the bicycle and CC mode to the SAV mode decrease their beeline speed, whereas, users switching from PT and walk to the SAV mode increase their travel speed (Exp. SAV-0 vs. bc-0, Fig. 10.4a). Changes in beeline speed of transport users remaining within the same transport mode are much smaller compared to users switching between different modes. For users remaining within the CC and SAV mode, the change in average beeline speed and travel time per trip are provided in Tab. 10.4 and may be used as an indicator for

the traffic congestion level. The introduction of the SAV mode is observed to increase the traffic

Table 10.4: Changes in average beeline speed and travel time per trip; transport users remaining within their transport modes; only potential SAV users

mode switch type	bc-0 → SAV-0	SAV-0 → SAV-1	SAV-0 → SAV-2
	Change in average beeline speed [km/h]		
CC → CC	−0.16 (−1.13%)	+0.02 (+0.15%)	+0.56 (+4.03%)
SAV → SAV	-	+0.02 (+0.32%)	+0.16 (+2.30%)
	Change in average travel time [sec]		
CC → CC	+16 (+1.22%)	-2 (-0.14%)	-65 (-4.51%)
SAV → SAV	-	-4 (-0.41%)	-25 (-2.54%)

congestion level (SAV-0 vs. bc-0). The pricing schemes counteract this effect and reduce the traffic congestion level compared to the unregulated SAV market (increase in beeline speed in SAV-1 vs. SAV-0 and SAV-2 vs. SAV-0). Applying the congestion charge to the SAV mode only (Exp. SAV-1) yields a very small reduction in traffic congestion (increase in beeline speed below 1% for both the CC and SAV mode). In contrast, applying the congestion charge to both the SAV and CC mode (Exp. SAV-2) yields a very strong reduction in traffic congestion.

Next, the change in average beeline distance of all potential SAV users is analyzed over all mode switch types. Introducing the SAV mode increases the beeline speed by 0.82 km/h (+9.24%) compared to the base case (SAV-0 vs. bc-0). This may be explained by the mode shift effect from slow modes (e.g., walk and PT) to the much faster SAV mode. Simulation experiment SAV-1 reduces the beeline speed by 0.07 km/h (−0.72%) compared to experiment SAV-0 since transport users are pushed (back) to slower modes. Simulation experiment SAV-2 increases the average beeline speed by 0.05 km/h (+0.48%) compared to experiment SAV-0 which may be explained by the increase in overall system efficiency.

10.4.4 Traffic Volume

Fig. 10.5 depicts the changes in daily traffic volume (sum of CCs and SAVs) per road segment. Overall, introducing the SAV mode (Exp. SAV-0) increases the traffic volume in the inner-city area compared to the base case (see Fig. 10.5a). Charging a congestion charge from SAV users reduces this effect and fewer individuals use the SAV mode which translates into a reduced number of SAV vehicles in the service area compared to experiment SAV-0 (see Fig. 10.5b and 10.5c). Additionally applying the congestion charge to CC users yields a significant reduction in daily traffic volume on most road segments compared to the base case. However, on some road segments, in particular in the city center area, traffic volumes increase (see Fig. 10.5d and 10.5e). Fig. 10.6 investigates this effect in more detail and depicts the change in traffic volume for different vehicle types. This shows that the observed increase in daily traffic volume in the inner-city center area is caused by SAV operations. The number of CCs are observed to decrease for most road segments, also in the inner-city center area which is explained by the overall reduction in CC users.

10.4.5 Shared Autonomous Vehicle Performance

Fig. 10.7 depicts the SAV operation performance parameters during the course of the day. In all simulation experiments, throughout the day, approximately half of the SAV fleet is available and

(a) Exp. SAV-0 vs. bc-0.

(b) Exp. SAV-1 vs. bc-0.

(c) Exp. SAV-1 vs. SAV-0.

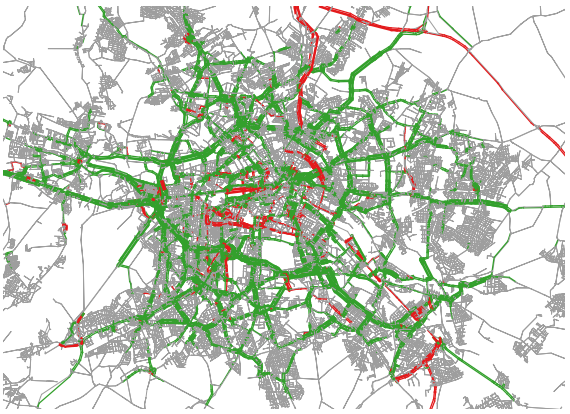

(d) Exp. SAV-2 vs. bc-0.

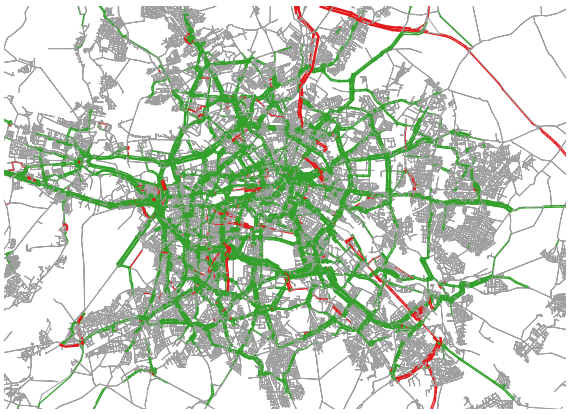

(e) Exp. SAV-2 vs. SAV-0

Figure 10.5: Change in daily traffic volume (sum of CCs and SAVs) per road segment

waits for a trip request. That is, there are no trip request rejections caused by capacity constraint effects and waiting times are rather short compared to a reduced fleet size. In simulation experiment SAV-0, the average waiting time per SAV trip amounts to 185 *sec* and the average in-vehicle time per SAV trip amounts to 740 *sec*. A reduced number of SAV users and less traffic congestion translates into a decrease in average waiting time (169 *sec* in experiment SAV-1; 170 *sec* in experiment SAV-2).

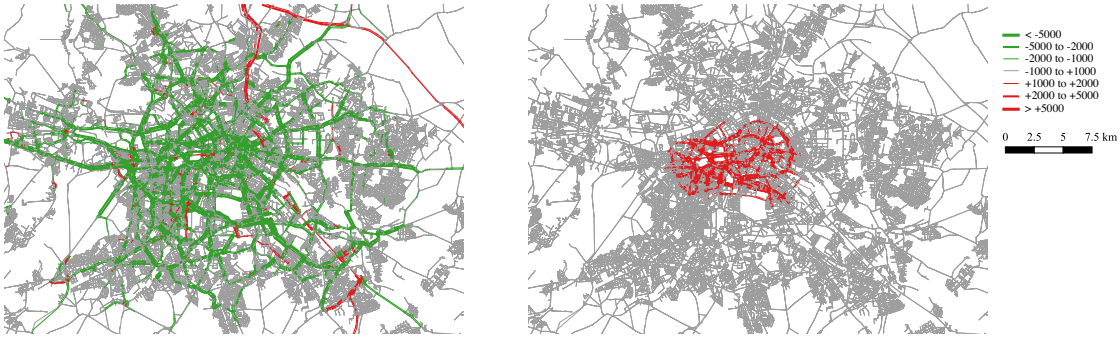

(a) Change in CCs **(b)** Change in SAV

Figure 10.6: Change in traffic volume per vehicle type; Exp. SAV-2 vs. bc-0.

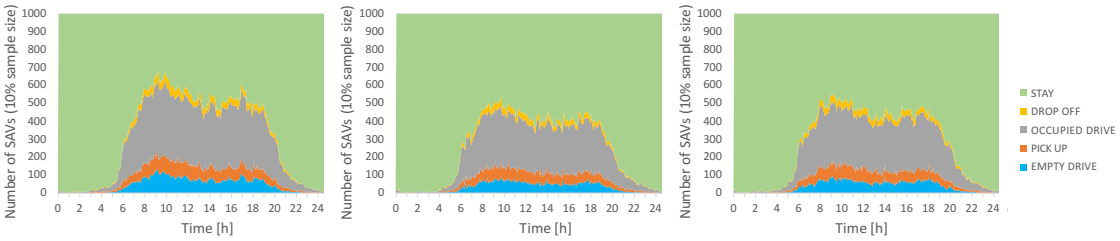

(a) Exp. SAV-0 **(b)** Exp. SAV-1 **(c)** Exp. SAV-2

Figure 10.7: SAV time profile: Number of SAVs (10% sample size) per time of day. Green: stay and wait for a trip request. Yellow: passenger drop off. Gray: occupied drive. Orange: passenger pick up. Blue: empty drive.

10.4.6 System Welfare

Tab. 10.5 depicts the changes in system welfare compared to the base case (bc-0). System welfare is defined as the sum of the travel related user benefits, monetary payments and SAV operating costs. Environmental effects are separately analyzed in Sec. 10.4.7 and not accounted for in the aggregated welfare analysis. In all simulation experiments with SAVs, system welfare increases compared to

Table 10.5: Aggregated results: Change in system welfare; comparison with the base case; upscaled to full population size

Change in...	SAV-0 vs. bc-0	SAV-1 vs. bc-0	SAV-2 vs. bc-0
travel related user benefits (incl. tolls/fares) [*k EUR*]	323.67	201.82	-2440.20
monetary payments [*k EUR*]	329.00	338.94	3590.01
change in SAV operating costs [*k EUR*]	389.85	303.33	331.76
system welfare [*k EUR*]	262.81	237.44	818.06

the base case (bc-0). In simulation experiment SAV-1, system welfare decreases compared to the unregulated SAV market (Exp. SAV-0). Regulating both the CC and SAV market (simulation experiment SAV-2) yields the largest increase in system welfare.

10.4.7 Environmental Effects

This section analyzes the air pollution, in particular NO_x emissions and noise L_{den} effects caused by road traffic. The **air pollution emission computation** follows the methodology described

in Hülsmann et al. (2011) and Kickhöfer et al. (2013). The computation approach accounts for vehicle characteristics (vehicle type, age, cubic capacity, fuel type etc.), dynamic attributes (parking duration, distance travelled, speed, traffic state) and road types to get the cold and warm emissions from the HBEFA database (Version 3.2, INFRAS, 2010). The computation of air pollution emissions is based on the assumption that all CCs have combustion engines and all SAVs are electric. For the propagation of air pollution to the surrounding area, a Gaussian distance weighting function is used (Agarwal, 2017, Appendix A). The **noise computation** follows the methodology described in Sec. 5.2 which is based on the German RLS-90 approach ('Richtlinien für den Lärmschutz an Straßen', FGSV, 1992) taking into account the traffic volume, the share of heavy goods vehicles and the speed level (see App. A). For speed levels above 30 km/h, an electric vehicle is assumed to have an effect approximately similar to a vehicle with a combustion engine. Therefore, the applied noise computation does not differentiate between SAVs and CCs. The absolute environmental effect in the base case (Exp. bc-0) is shown in Fig. 10.8. Overall, along the inner-city motorway as well as

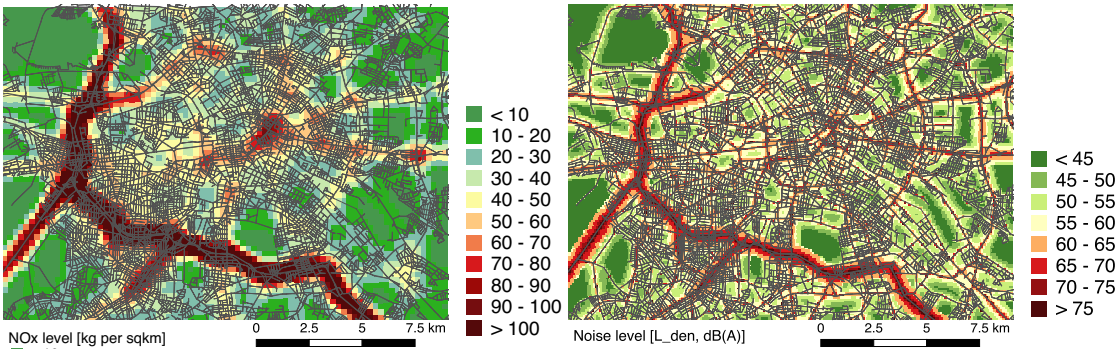

Figure 10.8: Absoulte NO_x and noise L_{den} levels; City center area

main roads, absolute NO_x and noise levels are much higher compared to areas along smaller roads.

Impact on Air Pollution Fig. 10.9 depicts the changes in NO_x levels resulting from the different simulation experiments. In experiment SAV-0 some users are shifted from the CC mode to the electric SAV mode (see Sec. 10.4.2). Consequently, NO_x levels are observed to decrease in the inner-city area (see Fig. 10.9a). In experiment SAV-1, a more expensive SAV mode decreases the number SAV users, thus, the previous effect is reduced (see Fig. 10.9b) and NO_x levels slightly increase compared to experiment SAV-0 (see Fig. 10.9c). Additionally applying the congestion charge to CC users significantly reduces the air pollution levels in the entire Berlin area, in particular along the inner-city motorway and main roads as well as in the inner-city center area (see Fig. 10.9d and 10.9e).

Impact on Noise Fig. 10.10 depicts the changes in noise (L_{den}) levels resulting from the different simulation experiments. Therefore, the increase in traffic volume (see Fig. 10.5a) translates into slightly higher noise levels in the inner-city Berlin area (Exp. SAV-0 vs. bc-0; see Fig. 10.10a). The logarithmic scale of noise yields a much higher elasticity for roads with lower traffic volumes. Thus, experiment SAV-1 only has a minor effect on the noise levels and changes in noise levels compared to experiment SAV-0 are indiscernible (see Fig. 10.10b and 10.10c). The large reduction in CC users in experiment SAV-2 yields a strong reduction in noise levels compared to the base case (see Fig. 10.10d) and experiment SAV-0 (see Fig. 10.10e) along several road corridors. Nevertheless, the increase in noise resulting from the additional SAV traffic is only partly compensated and overall noise levels still increase along minor roads in the inner-city area (see Fig. 10.10d).

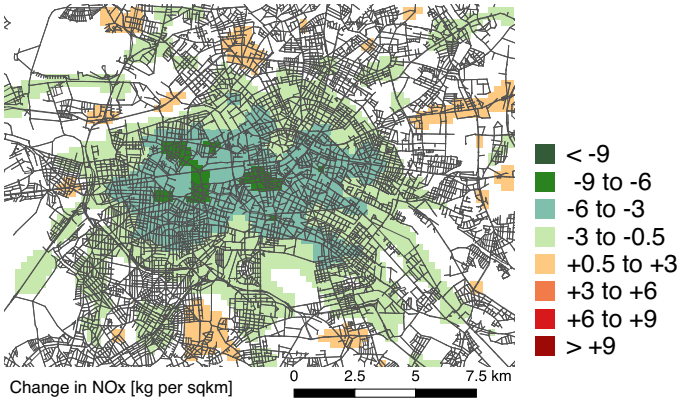

(a) Exp. SAV-0 vs. bc-0.

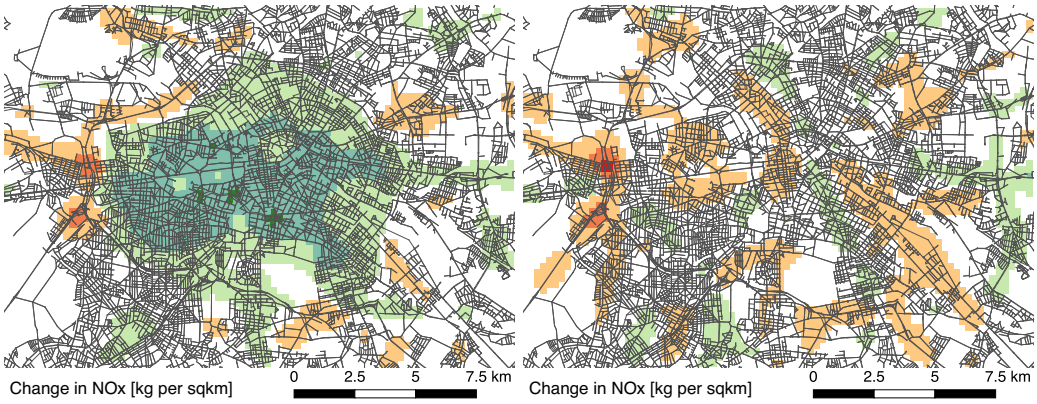

(b) Exp. SAV-1 vs. bc-0. **(c)** Exp. SAV-1 vs. SAV-0.

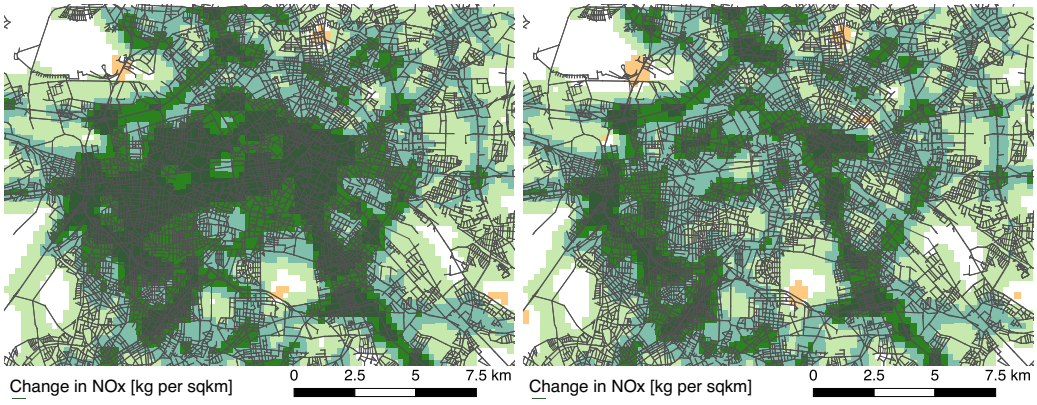

(d) Exp. SAV-2 vs. bc-0. **(e)** Exp. SAV-2 vs. SAV-0.

Figure 10.9: Change in daily NO_x levels [$kg/sqkm$]; City center area

10.5 Discussion

In this study, the applied pricing scheme only accounts for the traffic congestion externality. Further external effects such as air pollution and noise are analyzed, but not included into the pricing. This could be easily changed if of interest. Adding noise damage costs to the SAV pricing scheme for example would probably push traffic from minor roads in residential areas to major roads, to less densely populated areas, or to other modes of transportation (see Ch. 8).

The SAV fleet size is deliberately set to a very high level of 10,000 SAVs in order to avoid rejections of trip requests caused by fleet size constraint effects. As shown in previous studies, above a certain threshold value, changing the vehicle fleet size only yields a minor change in service

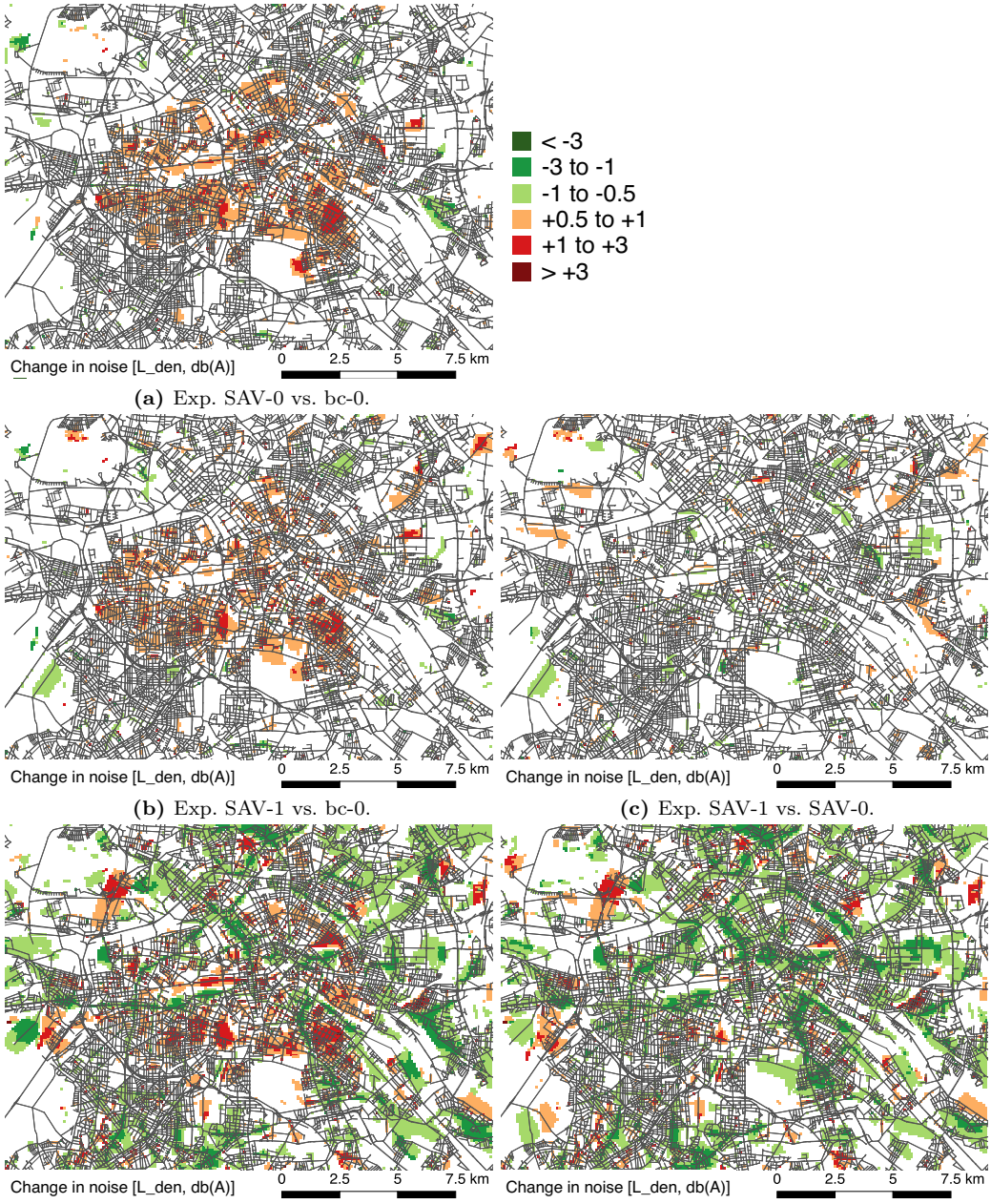

(a) Exp. SAV-0 vs. bc-0.

(b) Exp. SAV-1 vs. bc-0.

(c) Exp. SAV-1 vs. SAV-0.

(d) Exp. SAV-2 vs. bc-0.

(e) Exp. SAV-2 vs. SAV-0.

Figure 10.10: Change in noise (L_{den}); City center area

quality, see, e.g., Maciejewski and Bischoff (Fig. 5, demand-supply-balancing strategy, 2015) and Bischoff (Fig. 6.1, 2019). Thus, reducing the vehicle fleet size to the maximum level of simultaneously required vehicles (5,000−6,000 SAVs, see Fig. 10.7) would not have a significant effect on the overall service quality and simulation outcome.

The applied German RLS-90 methodology does not explicitly account for speed levels below 30 km/h where engine noise dominates over rolling and aerodynamic noise and, thus, the vehicle engine type may have a significant effect on the noise level. Considering SAVs to be electric, the observed increase in noise levels caused by SAV traffic (see Fig. 10.10a) may be overestimated, in particular along smaller roads with speed levels below or around 30 km/h. Further research is required to develop or apply a more suitable noise computation approach in order to correctly account for electric vehicles and predict the impact on the environmental noise.

In the existing base scenario of the Greater Berlin area, daily mode-specific fixed costs such as for owning a car or a PT annual ticket are not explicitly accounted for. In order to compensate for this, a reward for no longer owning a car was instead implemented for the present study (see Tab. 10.1). Future base scenarios should rather include a separate parameter for daily fixed cost if a certain mode is used at all. In an updated and calibrated version of the Berlin case study by Ziemke et al. (2019), available at `https://github.com/matsim-vsp/matsim-berlin`, version number 5.3, for the CC mode, the daily cost of owning a vehicle is set to 5.3 *EUR* (Tab. 8-32, Planco et al., 2015, see also Tab. 10.1). For the PT mode, daily monetary costs is set to the daily share of an annual ticket, e.g., 2.1 *EUR* (761.00 *EUR* annual ticket fare Berlin; divided by 365 days per year).

10.6 Conclusion and Outlook

In this study, congestion pricing is applied to the SAV transport mode. Several simulation experiments (see Sec. 10.3.3) are carried out in order to investigate the effects of different pricing setups on the overall transport system and the environment. In experiment SAV-0, SAV users only have to pay the base fare of 0.35 *EUR*/*km*. In experiment SAV-1, SAV users additionally have to pay a congestion charge. In experiment SAV-2, both the SAV and CC users have to pay a congestion charge.

For SAV-0, where SAV users only pay the base fare of 0.35 *EUR*/*km* and there is no congestion charge added to the user costs, the model predicts an SAV share of 17.7% within the service area (inner-city Berlin area, see Fig. 10.1). This number is higher compared to Trommer et al. (2016) who estimate an SAV trip share of 10% by the year 2035, however, referring to all of Germany. Thus, a higher SAV trip share in an urban area seems plausible.

With congestion pricing, the SAV trip share amounts to 14.8% (Exp. SAV-1; congestion pricing for SAV users only) and 15.8% (Exp. SAV-2; congestion pricing for SAV and CC users) of all trips within the service area (inner-city center area).

Introducing the SAV mode yields an increase in traffic in the in the inner-city Berlin area. Consequently, the level of traffic congestion increases. Since SAVs are assumed to be electric and CCs to have a combustion engine, a mode shift from CCs to SAVs translates into lower air pollution concentrations in the inner-city area. In contrast, noise levels slightly increase in the inner-city area, in particular along minor roads in residential areas.

Applying a congestion charge to the SAV mode (Exp. SAV-1) only slightly reduces the level of traffic congestion compared to the case where SAV users only pay the base fare. A significant reduction in travel time is only obtained in the case where the congestion charge is applied to both the SAV and CC mode (Exp. SAV-2). The latter pricing scheme also significantly reduces air pollution levels in the entire Berlin area. Along certain corridors, noise levels are observed to decrease, however, still increase along smaller roads in residential areas.

Overall, this study highlights the importance of controlling *both*, the SAV and CC mode, in order to improve a city's transport system. Charging congestion prices from both SAV and CC users (Exp. SAV-2) results in the largest increase in system welfare and strongest reduction in environmental effects. Regulating no or only one transport mode (Exp. s SAV-0 and SAV-1) increases system welfare compared to the base case (bc-0), however, results in a lower system welfare compared to experiment SAV-2. Charging congestion cost fees from SAV users but not from CC users (Exp. SAV-1) even results in a lower system welfare compared to the unregulated SAV and CC mode (Exp. SAV-0).

This study recommends pricing policies to develop integrated pricing schemes for *all* modes of transportation, in particular the CC *and* the SAV mode. A fare above operating costs will decrease the number of transport users switching from bicycle and walk to the SAV mode which may be a desired effect. However, without an increase in costs for CC users, a higher SAV fare also pushes users from the SAV to the CC mode. Furthermore, to tackle the increase in traffic volume on minor roads in residential areas, SAV operators or regulators should re-think door-2-door service, and instead possibly define virtual pick-up points that are located conveniently for users and well accessible for SAV operators. Both BerlKönig by BVG (BVG, 2019) in Berlin and MOIA (MOIA, 2019) in Hamburg and Hannover show tendencies in this direction.

Future studies may address the model's sensitivity regarding changes in cost parameters, e.g., the daily profit for no longer owning a CC (r_{day}^{SAVu}) and the VTTS for using the SAV (c_h^{SAVu}), as well as SAV operation parameters, i.e, the service area and the SAV fleet size. Furthermore, existing studies on regulative measures, e.g., a ban on private cars in the city center area (Bischoff and Maciejewski, 2016b), should be extended and combined with different pricing schemes as well as analyzed with regard to mode switch effects and the environmental impact.

CHAPTER 11

Conclusion and Outlook

11.1 Conclusion

This thesis investigates the use of simulated dynamic pricing for the optimization of transport systems. The applied simulation-based optimization approach contains both the computation of optimal user prices as well as the prediction of user reactions to these prices. A mechanistic approach is developed which calculates dynamic and road-specific prices to be added to each user's generalized travel cost in order to provide corrected incentives to transport users and improve the overall transport system. The pricing strategies are incorporated into the agent-based transport simulation framework Multi-Agent Transport Simulation (MATSim), which allows for a real-world application, complex user reactions, dynamic traffic congestion and a detailed analysis of the pricing scheme's effects.

Overall, the simulation studies conducted in this thesis indicate that the simulation-based internalization approach provides a useful method for investigating optimal pricing strategies. Applying an agent-based approach with heterogeneous transport users who are differently pressed for time and have varying activity locations and trip patterns, transport users react differently to the pricing scheme. Transport users may for example either accept the increase in monetary costs and benefit from improved travel conditions or try to avoid high monetary costs by switching to cheaper alternatives (e.g., modes, routes or times). The enabled choice dimensions are found to have a significant effect on the overall change in travel behavior and system efficiency.

The first part of this thesis addresses the pricing of delay effects within the Public Transport (PT) and private car mode. Ch. 2 shows that the microscopic simulation of user interactions at transit stops may be a useful tool to estimate optimal user-specific PT fares. The developed methodology provides insights into potentially relevant external delay effects in the PT mode and allows to investigate the relationship between optimal fare and, e.g., time of day, travel distance and service level. The next two chapters address traffic congestion effects in the private car mode. Two congestion pricing approaches are developed and investigated. The first one (Queue based Congestion Pricing (QCP), see Ch. 3) is similar to the microscopic PT user pricing approach, introduced in Ch. 2 and directly builds on the Pigouvian taxation principle: Marginal external congestion costs are computed based on the simulated queuing dynamics at the bottleneck links and resulting toll payments differ from agent to agent depending on the position in the queue and the delayed users' Values of Travel Time Savings (VTTS). The second congestion pricing approach (List Pricing (LP), see Ch. 4) uses control-theoretical elements to adjust toll levels depending on the congestion level in order to reduce or eliminate traffic congestion: Resulting toll payments are the same for all travelers per time bin and road segment. The pricing approaches are applied to Vickrey's bottleneck model and the case study of the Greater Berlin area. Both congestion pricing approaches significantly reduce traffic congestion and increase overall system welfare compared to the base case (no pricing). For different assumptions regarding transport users choice dimensions (with and without mode and departure time choice), the second and rather simple approach (LP) results in a higher system welfare compared to the first one (QCP) which may be explained by a better consideration of the system's dynamics and the agents' stochastic learning behavior. This highlights the importance of investigating optimal pricing strategies under realistic conditions, in particular accounting for the complexity in user behavior. The applied simulation framework MATSim accounts for stochastic user behavior and only approximates the user equilibrium, which may be considered closer to the real world compared to a model where transport users have perfect knowledge of all travel alternatives, behave completely rationally and travel behavior strictly corresponds to the user equilibrium. It is also highlighted that optimal toll

levels have to be computed *mutatis mutandis*, i.e, taking into consideration the transport users' reactions, and not *ceteris paribus*. Pricing schemes should for example rather slowly adjust the time-specific toll levels from one time period (day/week/month) to the next one to allow transport demand to adjust to the prices.

The second part of this thesis addresses the simulation-based internalization of noise damages. Ch. 5 describes the simulation-based computation of noise damages, which includes the computation of noise emissions, immissions and population densities. The application to the real-world case study of the Greater Berlin area demonstrates the importance of accounting for the spatial and temporal variation in the population since the use of static resident numbers would result in an overestimation of residential noise damages and an underestimation of noise exposures at work, education and other activities, in particular in the Central Business Districts (CBDs). In Ch. 6 and Ch. 7, the noise damages are mapped back to the causing individuals. Iteratively, road segment and time dependent noise exposure tolls are computed to which transport users may react by adjusting their route choice decisions. The overall observed effect is that transport users shift from minor to major roads and take detours in order to avoid areas with high population densities. Depending on the time of day and depending on which population groups or activity types are considered, the methodology proposes different tolling schemes (drive around vs. through CBDs). In Ch. 6, tolls are set based on average noise damages, whereas, in Ch. 7 a methodology is introduced which computes tolls based on the marginal damage costs. Simulation experiments for Berlin reveal that both approaches reduce noise damages, however, an increase in system welfare is only achieved by the marginal cost pricing approach. For the marginal cost approach, the reduction in noise exposures is found to be larger than applying the average cost approach despite the fact that toll payments are lower. This indicates that the marginal cost approach works quite well for traffic noise.

The third part of this thesis elaborates on the interrelation of external effects. Ch. 8 investigates the interrelation of road traffic congestion and noise damages by comparing single objective optimization (isolated pricing of an external effect) with multiple objective optimization (simultaneous pricing of external effects). Simulation experiments for Berlin in which transport users are, similar to Ch. 6 and Ch. 7, only enabled to adjust their route choice decisions, reveal a negative correlation between congestion and noise (isolated pricing of one effect increases the other one). Nevertheless, the multiple objective optimization shows that it is possible to simultaneously reduce congestion costs and noise damages. The explanation is that during peak times, congestion is the more relevant cost component, whereas, during the evening, night and morning, noise is the more relevant effect. Thus, the pricing methodology reveals a key element for policy making and highlights the importance of following a dynamic approach to focus on the more relevant external cost component. Ch. 9 elaborates on the interrelation of congestion, noise and air pollution. Simulation experiments are carried out for the case study of the Greater Munich area and, similar to Ch. 4, for different assumptions regarding transport users choice dimensions (route choice only vs. mode and route choice). With and without mode choice, the simultaneous congestion, noise and air pollution pricing scheme reduces all external effects and increases the overall system efficiency. With and even without mode choice, the isolated external cost pricing yields a reduction of all three external effects and an increase in overall system welfare (positive correlation). However, looking at the spatially disaggregated effects reveals that even in the simulation experiments with mode choice, for certain areas, the correlation in traffic congestion, noise and NO_x is found to be negative, yielding different parts of the population better off and worse off. The pricing experiments also highlight the importance of correctly accounting for all relevant choice dimensions, in particular, neglecting

the fact that transport users may also adjust their mode of transportation in order to react to a transport policy may underestimate the full potential of pricing. As discussed in Sec. 9.4.6, the observed aggregated positive correlation of congestion and noise even in the case without mode choice is in contrast to Ch. 8, where for the case study of the Greater Berlin area the aggregated correlation of congestion and noise was found to be negative. This may be explained by a different spatial structure in the Berlin and Munich case study. The positive correlation in the Munich case study indicates that traffic congestion occurs in areas with a high population density and a potentially large number of exposed individuals. Consequently, in the Munich case study, pricing any of the external effects encourages some travelers to avoid the city center area and switch to the less congested motorway ring road (A99) which is also an area with a relatively low population density and a smaller number of potentially exposed individuals. In contrast, in the Berlin case study, traffic congestion occurs in areas with lower population densities, e.g., the inner-city motorway ring road (A100), and congestion pricing encourages some travelers to switch to smaller roads in the city-center area and a more densely populated area compared to the area along the motorway. The effect of noise tolling is found to be rather low in the Munich case study which stands in contrast to the studies for the Greater Berlin area in Ch. 7 and Ch. 8. This may be explained by the coarse network resolution which concentrates traffic on arterial roads and consequently results in rather low marginal noise toll levels (see Sec. 9.4.6). The observed differences in the Berlin and Munich case study reveal that findings regarding aggregated effects should rather carefully be generalized and highlights the importance of an adequate model setup and a case-specific investigation of optimal pricing strategies.

The last part of this thesis looks to the future and addresses optimal pricing strategies in regard to the prospect of Shared Autonomous Vehicles (SAVs). In Ch. 10, the congestion pricing approach, introduced in Ch. 4 (LP), is applied to the SAV mode. On the SAV operator's side, the routing- and dispatch-relevant cost are extended by the time and link-specific congestion charge. On the users' side, the congestion costs are added to the fare. Simulation experiments are carried out for the Berlin case study allowing transport users to adjust their mode, route and departure time decisions. The impacts of SAVs and different pricing schemes on the transport system and the environment are investigated. For the pricing setup, where SAV users only pay the base fare and there is no congestion charge added to the user costs, the model predicts an SAV share of 17.7% within the inner-city Berlin service area which is considered plausible. The level of traffic congestion increases, air pollution levels decrease and noise levels slightly increase in the inner-city area. The SAV congestion charge pushes users from SAVs to the walk, bicycle and Conventional (driver-controlled) private Car (CC) mode. This effect is avoided by applying the same congestion charge also to CC users. The simulation results highlight the importance of controlling *both*, the SAV and CC mode to improve a city's transport system. Charging congestion prices from both SAV and CC users results in the largest increase in system welfare and strongest reduction in environmental effects. Overall, Ch. 10 shows that simulated dynamic pricing is not only a useful approach for the optimization of conventional transport modes but also for innovative transport modes such as SAVs.

Tab. 11.1 summarizes the observed main user reactions with and without mode choice. Tab. 11.2 provides an overview of the observed interrelation of external effects; "+" indicates a positive correlation, i.e., reducing one effect by means of pricing also reduces the other effect; "−" indicates a negative correlation, i.e., reducing one effect by means of pricing increases the other one; and "+/−" indicates either a positive or negative correlation. Finally, a more detailed summary of the different policies' impacts on the external cost components for the simulation setup with and without mode choice is given in Tab. 11.3 and Tab. 11.4, respectively. The observed positive correlation in the

simulation experiments with mode choice is highly relevant for policy makers; a transport policy which tackles a single external effect is very likely to also have a positive effect on all other external effects. A main finding for transport modelers is the importance to account for transport users' mode choice reactions; a transport model without mode choice should rather carefully be used for policy evaluation.

Table 11.1: Primary user reactions

Internalized effect	Without mode choice	With mode choice
Congestion	Switch to less congested roads (Berlin: smaller roads; Munich: motorway ring road)	Switch to alternative modes of transportation
Noise	Switch to main roads; Switch to roads in less densely populated areas	
Global Air Pollutants	Switch to shorter routes	
Local Air Pollutants	Switch to roads in less densely populated areas	

Table 11.2: Interrelation of external effects

Effect 1	Effect 2	Without mode choice	With mode choice
Congestion	Noise	+/−	+
Congestion	Air Pollution	+/−	+
Noise	Air Pollution	+	+

Table 11.3: Policy impact (without mode choice)

Policy	Congestion	Noise	Air Pollution
Congestion pricing	**decrease** (Berlin, Munich)	**increase** (Berlin), **decrease** (Munich)	**decrease** (Munich)
Noise pricing	**increase** (Berlin), **decrease** (Munich)	**decrease** (Berlin, Munich)	**decrease** (Munich)
Air Pollution pricing	**decrease** (Munich)	**decrease** (Munich)	**decrease** (Munich)
Simultaneous external cost pricing	**decrease** (Berlin, Munich)	**decrease** (Berlin, Munich)	**decrease** (Munich)

Table 11.4: Policy impact (with mode choice)

Policy	Congestion	Noise	Air Pollution
Congestion pricing	**decrease** (Berlin, Munich)	**decrease** (Munich)	**decrease** (Munich)
Noise pricing	**decrease** (Munich)	**decrease** (Munich)	**decrease** (Munich)
Air Pollution pricing	**decrease** (Munich)	**decrease** (Munich)	**decrease** (Munich)
Simultaneous external cost pricing	**decrease** (Munich)	**decrease** (Munich)	**decrease** (Munich)
Introducing SAVs	**increase** (Berlin)	**increase** (Berlin)	**decrease** (Berlin)
Introducing SAVs and Congestion pricing	**decrease** (Berlin)	**increase** (Berlin)	**decrease** (Berlin)

11.2 Outlook

The proposed pricing methodology uses various software modules that have been developed over the last few years, including some modules that have been developed in the context of this thesis (MATSim's noise contribution, see https://github.com/matsim-org/matsim/tree/master/contribs/noise; MATSim's decongestion contribution, see https://github.com/matsim-org/matsim/tree/master/contribs/decongestion). The applied simulation framework MATSim and the external cost pricing approaches are open source and publicly available which allows for an easy and a well organized extension or improvement of the proposed methodology. Model improvements may for example address the simulation-based computation of road traffic noise. A first step has been taken by Kühnel et al. (2019) who incorporate noise shielding effects of buildings into the simulation framework. Further steps may address additional correction terms provided in the Richtlinien für den Lärmschutz an Straßen (RLS-90), e.g., for reflection effects at building facades or the impact of the road surface (FGSV, 1992). A challenging task for future research projects is to extend existing noise computation rules by a detailed consideration of different vehicle types, in particular electric vs. combustion engines, including noise computation rules for speed levels below 30 kilometer (km)/hour (h).

In future research projects, the presented pricing methodology may be extended by additional external effects associated with road traffic (e.g., accidents) or PT users (e.g., the disutility of crowded vehicles). An integrated simulated dynamic pricing study may be carried out in which pricing strategies for the private car mode are coupled with pricing strategies for the PT mode (see Ch. 2). Further research studies may also address the interrelation of external effects between different modes of transportation, e.g., reduced traffic congestion within the car mode vs. crowded vehicles and/or delays within the PT mode. Innovative technologies and transport modes such as SAVs raise several questions in the context of transport system optimization that may be addressed by simulated dynamic pricing. Further pricing studies may for example investigate optimal dynamic pricing strategies for different assumptions regarding the SAV service area, the SAV fleet size and the SAV market share. Overall, the presented pricing methodology should be applied to further case studies, i.e, other models for specific regions or future scenarios, to investigate whether the policy recommendations and observed effects hold for a different spatial and temporal structure of transport supply and demand.

APPENDIX A

Noise Computation based on the RLS-90

The initial average sound level $E_{i,t}^{25}$ is computed as

$$E_{i,t}^{25} = 37.3 + 10 \cdot \log_{10} \left[M_{i,t} \cdot (1 + 0.082 \cdot p_{i,t}) \right] , \tag{A.1}$$

where i denotes the road segment; t is the time bin; $M_{i,t}$ is the traffic volume; and $p_{i,t}$ is the Heavy Goods Vehicles (HGV) share in %.

The additive correction term for deviations from a maximum speed of 100 km/h is calculated as follows.

$$D_{i,t}^{v} = E_i^{car} - 37.3 + 10 \cdot \log_{10} \left[\frac{100 + (10^{0.1 \cdot (E_i^{hgv} - E_i^{car})} - 1) \cdot p_{i,t}}{100 + 8.23 \cdot p_{i,t}} \right] , \tag{A.2}$$

where $D_{i,t}^{v}$ is the speed correction in $dB(A)$; and E_i^{car} and E_i^{hgv} are calculated as described in Eq. (A.3) and Eq. (A.4).

$$E_i^{car} = 27.7 + 10 \cdot \log_{10} \left[1 + (0.02 \cdot v_i^{car})^3 \right] , \tag{A.3}$$

where v_i^{car} denotes the maximum speed level in km/h for passenger cars.

$$E_i^{hgv} = 23.1 + 12.5 \cdot \log_{10} \left(v_i^{hgv} \right) , \tag{A.4}$$

where v_i^{hgv} denotes the maximum speed level in km/h for HGV.

The decrease in noise with the distance due to air absorption is calculated as follows:

$$D_{i,j}^{d} = 15.8 - 10 \cdot \log_{10}\left(d_{i,j}\right) - 0.0142 \cdot d_{i,j}^{0.9}\,, \tag{A.5}$$

where $d_{i,j}$ is the distance between road segment i and receiver point j.

List of Units and Acronyms

AUD Australian Dollar; 1 Australian Dollar (*AUD*) = 0.64 Euro (*EUR*) (December, 2017).

CO_2 carbon dioxide.

DM Deutsche Mark.

EUR Euro.

L_{den} noise day-evening-night index.

NMHC non-methane hydrocarbons.

NO_x nitrogen oxides.

PM particulate matter.

SO_2 sulfur dioxide.

$dB(A)$ A-weighted decibel; unit of relative loudness; corrects the sound pressure level for the relative loudness perceived by the human ear for different frequencies..

dB decibel; in acoustics: unit of sound pressure level.

h hour, 60 *min*.

kg kilogram, the SI base unit of mass.

km kilometer, 1000 *m*.

k thousand, 1×10^3.

min minute, 60 *sec*.

m meter, the SI base unit of length.

sec second, the SI base unit for time.

sqkm square kilometer, km^2.

util utility unit.

ACP Average Cost Pricing. xv, 94

AV Autonomous Vehicle. 7, 140, 141

CBD Central Business District. 15, 76, 85, 86, 88, 95, 105, 159

CC Conventional (driver-controlled) private Car. xiii, xvi, 8, 140–146, 148–152, 155, 156, 160

EWS Empfehlungen für Wirtschaftlichkeitsuntersuchungen an Straßen. 67, 91, 105, 123

HBEFA Handbook on Emission Factors for Road Transport, see `www.hbefa.net`. 123, 152

HGV Heavy Goods Vehicles. 35, 64, 65, 68, 79, 81, 82, 91–93, 102, 105, 106, 111, 163

LP List Pricing. xi, xii, 45–49, 51–58, 158, 160

MATSim Multi-Agent Transport Simulation, see `www.matsim.org`. xv, 6–9, 14, 16, 19, 20, 26, 30, 35, 43, 46, 50, 68, 81, 104, 106, 122, 124, 158, 162

MCP Marginal Cost Pricing. xv, 94

MiD Mobilität in Deutschland. 50, 124

MPC Marginal Private Cost. xi, 3

MSC Marginal Social Cost. xi, 3

OD Origin-Destination. 3, 4

PT Public Transport. 2, 5, 7–9, 14–16, 18–24, 26, 27, 50, 53, 68, 75, 82, 93, 106, 116, 121, 125, 133, 141–143, 145, 146, 148, 149, 155, 158, 162

QCP Queue based Congestion Pricing. 16, 31, 37, 38, 44, 45, 47–49, 51–53, 56–58, 158

RLS-90 Richtlinien für den Lärmschutz an Straßen. 62, 64, 65, 73, 75, 91, 105, 152, 154, 162

SAV Shared Autonomous Vehicle. xiii, xiv, xvi, xvii, 5, 7–9, 140–156, 160–162

SD Standard Deviation. 24

SrV System repräsentativer Verkehrsbefragungen, Mobilität in Städten. 50, 81

VTTS Value of Travel Time Savings. xi, xv, 4, 6, 9, 19, 20, 30, 31, 33–38, 42–44, 50, 56, 82, 106, 122, 140, 156, 158

Bibliography

16. BImSchV. Verkehrlärmschutzverordnung vom 12. Juni 1990 (BGBI. I S. 1036), die durch Artikel 1 der Verordnung vom 18. Dezember 2014 (BGBI I S. 2269) geändert worden ist. 16. Verordnung zur Durchführung des Bundes-Immissionsschutzgesetzes. (cited on pp. xv, 63, 90).

2002/49/EC. Directive of the European Parliament and of the Council of 25 June 2002 relating to the assessment and management of environmental noise. Official Journal of the European Communities. (cited on pp. xiii, 62, 73, 91, 109, 111).

2006 No. 2238. Environmental Protection, England: The Environmental Noise (England) Regulations 2006. URL http://www.legislation.gov.uk/uksi/2006/2238/pdfs/uksi_20062238_en.pdf. (cited on p. 62).

34. BImSchV. Verordnung über die Lärmkartierung vom 6. März 2006 (BGBl. I S. 516). 34. Verordnung zur Durchführung des Bundes-Immissionsschutzgesetzes. (cited on p. 62).

Agarwal, A. *Mitigating negative transport externalities in industrialized and industrializing countries*. PhD thesis, TU Berlin, Berlin, Germany, 2017. (cited on p. 152).

Agarwal, A. and I. Kaddoura. On-road air pollution exposure to cyclists in an agent-based simulation framework. *Periodica Polytechnica Transportation Engineering*, 2019. doi: 10.3311/PPtr.12661. (cited on p. 127).

Agarwal, A. and B. Kickhöfer. Agent-based simultaneous optimization of congestion and air pollution: A real-world case study. *Procedia Computer Science*, 52(C):914–919, 2015. ISSN 1877-0509. doi: 10.1016/j.procs.2015.05.165. (cited on pp. 41, 103, 120, 121, 127, 132).

Agarwal, A. and B. Kickhöfer. The correlation of externalities in marginal cost pricing: lessons learned from a real-world case study. *Transportation*, 2016. doi: 10.1007/s11116-016-9753-z. (cited on pp. 10, 121, 124, 127, 131, 132).

Agarwal, A., M. Zilske, K. Rao, and K. Nagel. An elegant and computationally efficient approach for heterogeneous traffic modelling using agent based simulation. *Procedia Computer Science*, 52(C): 962–967, 2015. ISSN 1877-0509. doi: 10.1016/j.procs.2015.05.173. (cited on p. 7).

Agarwal, A., G. Lämmel, and K. Nagel. Incorporating within link dynamics in an agent-based computationally faster and scalable queue model. *Transportmetrica A: Transport Science*, 2017. doi: 10.1080/23249935.2017.1364802. (cited on p. 124).

Ahrens, G.-A. Endbericht zur Verkehrserhebung Mobilität in Städten – SrV 2008 in Berlin. Technical report, Technische Universität Dresden, 2009. URL http://www.stadtentwicklung.berlin.de/verkehr/politik_planung/zahlen_fakten/download/2_SrV_endbericht_tudresden_2008_berlin.pdf. (cited on pp. 35, 50, 68, 81, 142).

Arnott, R., A. de Palma, and R. Lindsey. Economics of a bottleneck. *Journal of Urban Economics*, 27(1): 111–130, 1990. ISSN 0094-1190. doi: 10.1016/0094-1190(90)90028-L. (cited on pp. 3, 6, 46, 56).

Arnott, R., A. de Palma, and R. Lindsey. A structural model of peak-period congestion: A traffic bottleneck with elastic demand. *The American Economic Review*, 83(1):161–179, 1993. ISSN 00028282. (cited on pp. 4, 16, 40, 41, 44, 46, 141).

Arnott, R., A. de Palma, and R. Lindsey. The welfare effects of congestion tolls with heterogeneous commuters. *Journal of Transport Economics and Policy*, 28:139–161, 1994. (cited on pp. 78, 120).

ATC. National Guidelines for Transport System Management in Australia. Technical report, Australian Transport Council, 2006. URL http://www.transportinfrastructurecouncil.gov.au/publications/files/National_Guidelines_Volume_4.pdf. (cited on pp. xv, 20, 21).

Babisch, W., G. Pershagen, J. Selander, D. Houthuijs, O. Breugelmans, E. Cadum, F. Vigna-Taglianti, K. Katsouyanni, A. S. Haralabidis, K. Dimakopoulou, P. Sourtzi, S. Floud, and A. L. Hansell. Noise annoyance – A modifier of the association between noise level and cardiovascular health? *Science of The Total Environment*, 452–453:50–57, 2013. doi: 10.1016/j.scitotenv.2013.02.034. (cited on pp. 62, 78).

Barth, M. and K. Boriboonsomsin. Traffic congestion and greenhouse gases. *ACCESS Magazine, University of California Transportation Center*, 35, 2009. (cited on pp. 102, 103, 115, 120).

BaSt. Vorläufige Berechnungsmethode für den Umgebungslärm an Strassen VBUS, May 2006. Bundesanstalt für Strassenwesen. (cited on p. 73).

Beamon, B. M. and P. M. Griffin. A simulation-Based methodology for analyzing congestion and emissions on a transportation network. *Simulation*, 72(2):105–114, 1999. doi: 10.1177/003754979907200204. (cited on p. 103).

Beckers, T., C. von Hirschhausen, J. Klatt, and M. Winter. Effiziente Verkehrspolitik für den Straßensektor in Ballungsräumen, 2007. Abschlussbericht zu dem FoPS-Forschungsvorhaben 73.326/2004: Instrumente zur nachhaltigen Sicherung der Verkehrsinfrastruktur in Städten und Ballungsräumen; Auftraggeber: Bundesministerium für Verkehr, Bau und Stadtentwicklung. (cited on pp. 2, 5).

Beevers, S. D. and D. C. Carslaw. The impact of congestion charging on vehicle emissions in London. *Atmospheric Environment*, 39:1–5, 2005. doi: 10.1016/j.atmosenv.2004.10.001. (cited on p. 103).

Bischoff, J. *Mobility as a Service and the transition to driverless systems*. PhD thesis, TU Berlin, Berlin, Germany, 2019. in preparation. (cited on p. 154).

Bischoff, J. and M. Maciejewski. Simulation of City-wide Replacement of Private Cars with Autonomous Taxis in Berlin. *Procedia Computer Science*, 83:237–244, 2016a. ISSN 1877-0509. doi: 10.1016/j.procs.2016.04.121. (cited on pp. 8, 140, 141).

Bischoff, J. and M. Maciejewski. Autonomous taxicabs in Berlin – a spatiotemporal analysis of service performance. *Transportation Research Procedia*, 19:176–186, 2016b. doi: 10.1016/j.trpro.2016.12.078. (cited on pp. 141, 156).

Böhme, S. and L. Eigenmüller. Pendlerbericht Bayern. Technical report, IAB, 2006. (cited on p. 124).

Burghout, W., P.-J. Rigole, and I. Andreasson. Impacts of Shared Autonomous Taxis in a Metropolitan Area. In *Transportation Research Board 94th Annual Meeting*, number 15-4000, 2015. (cited on p. 140).

Button, K. *Transport economics*. Edward Elgar Publishing Limited, 2nd edition, 1993. (cited on pp. 3, 43).

Button, K. The Rationale for Road Pricing: Standard Theory and Latest Advances. *Research in Transportation Economics*, 9(Supplement C):3–25, 2004. ISSN 0739-8859. doi: 10.1016/S0739-8859(04)09001-8. (cited on pp. 16, 40, 44).

BVG. Webpage with fare overview (1 January 2019) provided by Berliner Verkehrsbetriebe (BVG), 2019. URL https://shop.bvg.de/uploads/files/Tarifinformationen___Preise_ab_1._Januar_2019.pdf. Accessed 15 March 2019. (cited on p. 5).

BVG. Webpage of the ride-pooling service BerlKönig provided by Berliner Verkehrsbetriebe (BVG) and ViaVan, 2019. URL https://www.berlkoenig.de. Accessed 15 March 2019. (cited on p. 156).

BVU, IVV, and PLANCO. Bundesverkehrswegeplan 2003 – Die gesamtwirtschaftliche Bewertungsmethodik. Technical Report FE-Nr. 96.0790/2003, Beratergruppe Verkehr+Umwelt, Ingenieurgruppe IVV, Planco Consulting GmbH, 2003. (cited on p. 63).

Bösch, P. M., F. Becker, H. Becker, and K. W. Axhausen. Cost-based analysis of autonomous mobility services. *Transport Policy*, 64:76–91, May 2018. doi: 10.1016/j.tranpol.2017.09.005. (cited on pp. 140, 145).

Calthrop, E. and S. Proost. Road Transport Externalities. *Environmental and Resource Economics*, 11 (3–4):335–348, 1998. doi: 10.1023/A:1008267917001. (cited on pp. 102, 120).

Charypar, D. and K. Nagel. Generating complete all-day activity plans with genetic algorithms. *Transportation*, 32(4):369–397, 2005. ISSN 0049-4488. doi: 10.1007/s11116-004-8287-y. (cited on p. 8).

Chen, L. and H. Yang. Managing congestion and emissions in road networks with tolls and rebates. *Transportation Research Part B: Methodological*, 46:933–948, 2012. doi: 10.1016/j.trb.2012.03.001. (cited on p. 103).

Childless, S., B. Nichols, B. Charlton, and S. Coe. Using an activity-based model to explore possible impacts of automated vehicles. Annual Meeting Preprint 15-5118, Transportation Research Board, Washington, D.C., Jan. 2015. (cited on pp. 140, 145).

Daganzo, C. *Fundamentals of Transportation and Traffic Operations*. Pergamon, 1997. ISBN 9780080427850. (cited on p. 43).

Daniel, J. I. and K. Bekka. The environmental impact of highway congestion pricing. *Journal of Urban Economics*, 47:180–215, 2000. doi: 10.1006/juec.1999.2135. (cited on p. 103).

de Borger, B., I. Mayeres, S. Proost, and S. Wouters. Optimal pricing of urban passenger transport: A simulation exercise for Belgium. *Journal of Transport Economics and Policy*, 30(1):31–54, 1996. (cited on pp. 2, 14, 102, 120).

de Palma, A. and R. Lindsey. Congestion pricing with heterogeneous travelers: A general-equilibrium welfare analysis. *Networks and Spatial Economics*, 4(2):135–160, 2004. doi: 10.1023/B:NETS.0000027770.27906.82. (cited on pp. 30, 78, 120).

DEFRA. Environmental Noise Directive: Implementation of Round 1 Noise Action Plans: Progress Report. Technical report, Department for Environment, Food and Rural Affairs, London, UK, 2014. URL http://www.gov.uk/defra. (cited on p. 62).

DEFRA. Noise Mapping England. Department for Envirionment, Food and Rural Affairs, 2015. URL http://services.defra.gov.uk/wps/portal/noise/maps. Accessed 27 January 2015. (cited on pp. 62, 90).

Department of Transport. *Calculation of Road Traffic Noise (CoRTN)*. Her Majesty's Stationery Office, London, United Kingdom, 1988. URL http://www.noiseni.co.uk/calculation_of_road_traffic_noise.pdf. (cited on p. 62).

Dhondt, S., C. Beckx, B. Degraeuwe, W. Lefebvre, B. Kochan, T. Bellemans, L. I. Panis, C. Macharis, and K. Putman. Health impact assessment of air pollution using a dynamic exposure profile: Implications for exposure and health impact estimates. *Environmental Impact Assessment Review*, 36:42–51, 2012. doi: 10.1016/j.eiar.2012.03.004. (cited on p. 64).

DIN 4109, Beiblatt 1. Schallschutz im Hochbau; Ausführungsbeispiele und Rechenverfahren. Deutsches Institut für Normung e.V. 11/1989. (cited on p. 64).

DIN EN ISO 11690-1. Acoustics – Recommended practice for the design of low-noise workplaces containing machinery – Part 1: Noise control strategies (ISO 11690-1:1996); German version EN ISO 11690-1:1996 [Akustik – Richtlinien für die Gestaltung lärmarmer maschinenbestückter Arbeitsstätten – Teil 1: Allgemeine Grundlagen (ISO 11690-1:1996), Deutsche Fassung EN ISO 11690-1:1996]. Deutsches Institut für Normung e.V. 02/1997. (cited on pp. xv, 64, 90).

Douglas, N. and G. Karpouzis. Estimating the cost to passengers of station crowding. In *28th Australasian Transport Research Forum (ATRF), Sydney*, 2005. (cited on p. 15).

Eliasson, J. and L. Jonsson. The unexpected "yes": Explanatory factors behind the positive attitudes to congestion charges in Stockholm. *Transport Policy*, 18(4):636–647, 2011. ISSN 0967-070X. doi: 10.1016/j.tranpol.2011.03.006. (cited on p. 5).

Eriksson, C., M. Nilsson, D. Stenkvist, T. Bellander, and G. Pershagen. Residential traffic noise exposure assessment: application and evaluation of European Environmental Noise Directive maps. *Journal of Exposure Science and Environmental Epidemiology*, 23:531–538, 2013. doi: 10.1038/jes.2012.60. (cited on pp. 62, 75).

European Commission. Annual Accident Report 2018. Technical report, European Road Safety Observatory, 2018. (cited on p. 2).

Fagnant, D. and K. Kockelman. Preparing a nation for autonomous vehicles: opportunities, barriers and policy recommendations. *Transportation Research Part A*, 77:167–181, 2015. doi: /10.1016/j.tra.2015.04.003. (cited on pp. 140, 141).

Fagnant, D. J. and K. M. Kockelman. The travel and environmental implications of shared autonomous vehicles, using agent-based model scenarios. *Transportation Research Part C: Emerging Technologies*, 40:1–13, 2014. ISSN 0968-090X. doi: 10.1016/j.trc.2013.12.001. (cited on p. 140).

Fagnant, D. J. and K. M. Kockelman. Dynamic ride-sharing and fleet sizing for a system of shared autonomous vehicles in Austin, Texas. *Transportation*, pages 1–16, 2016. ISSN 1572-9435. doi: 10.1007/s11116-016-9729-z. (cited on pp. 140, 141).

FGSV. *Richtlinien für den Lärmschutz an Straßen (RLS), Ausgabe 1990, Berichtigte Fassung.* Forschungsgesellschaft für Straßen- und Verkehrswesen, 1992. URL http://www.fgsv.de. (cited on pp. 62, 65, 73, 91, 102, 105, 123, 152, 162).

FGSV. *Empfehlungen für Wirtschaftlichkeitsuntersuchungen an Straßen (EWS). Aktualisierung der RAS-W 86.* Forschungsgesellschaft für Straßen- und Verkehrswesen, 1997. URL http://www.fgsv.de. (cited on pp. 63, 67, 91, 105, 123).

Follmer, R., U. Kunert, J. Kloas, and H. Kuhfeld. Mobilität in Deutschland – Ergebnisbericht. Technical report, infas/DIW, Bonn, 2004. URL www.kontiv2002.de. (cited on p. 124).

Fosgerau, M. Congestion in the bathtub. *Economics of Transportation*, 4(4):241–255, 2015. ISSN 2212-0122. doi: 10.1016/j.ecotra.2015.08.001. (cited on p. 41).

Friesz, T. L., D. Bernstein, and N. Kydes. Dynamic congestion pricing in disequilibrium. *Networks and Spatial Economics*, 4(2):181–202, 2004. doi: 10.1023/B:NETS.0000027772.43771.94. (cited on pp. 78, 120).

Garg, N. and S. Maji. A Critical review of principal traffic noise models: Strategies and implications. *Environmental Impact Assessment Review*, 46:68–81, Apr. 2014. (cited on p. 62).

Gawron, C. An Iterative Algorithm to Determine the Dynamic User Equilibrium in a Traffic Simulation Model. *International Journal of Modern Physics C*, 9(3):393–407, 1998. (cited on pp. 6, 7).

Gerike, R., F. Hülsmann, F. Heidegger, J. Friedemann, and T. Becker. Quantification and mapping external noise costs back to transport users - development of an integrated urban modelling approach. In *Proceedings of the European Conference on Noise Control (EURONOISE)*, 2012. (cited on pp. 80, 87, 90).

Ghafghazi, G. and M. Hatzopoulou. Simulating the environmental effects of isolated and area-wide traffic calming schemes using traffic simulation and microscopic emission modeling. *Transportation*, 41: 633–649, Feb. 2014. (cited on pp. 102, 120).

Gühnemann, A., A. Koh, and S. Shepherd. Optimal Charging Strategies under Conflicting Objectives for the Protection of Sensitive Areas: A Case Study of the Trans-Pennine Corridor. *Networks and Spatial Economics*, pages 1–28, 2014. doi: 10.1007/s11067-013-9211-9. (cited on pp. 78, 88).

Gulliver, J., D. Morley, D. Vienneau, F. Fabbri, M. Bell, P. Goodman, S. Beevers, D. Dajnak, F. J. Kelly, and D. Fecht. Development of an open-source road traffic noise model for exposure assessment. *Environmental Modelling & Software*, 2015. doi: http://dx.doi.org/10.1016/j.envsoft.2014.12.022. (cited on pp. 62, 90).

Harb, M., Y. Xiao, G. Circella, P. L. Mokhtarian, and J. L. Walker. Projecting travelers into a world of self-driving vehicles: estimating travel behavior implications via a naturalistic experiment. *Transportation*, 45(6):1671–1685, Nov. 2018. ISSN 1572-9435. doi: 10.1007/s11116-018-9937-9. (cited on p. 140).

Harris, M. Uber Could Be First to Test Completely Driverless Cars in Public. IEEE Spectrum, 14.09.2015, 2015. URL http://spectrum.ieee.org/cars-that-think/transportation/self-driving/uber-could-be-first-to-test-completely-driverless-cars-in-public. (cited on p. 140).

Hatzopoulou, M. and E. J. Miller. Linking an activity-based travel demand model with traffic emission and dispersion models: Transport's contribution to air pollution in Toronto. *Transportation Research Part D: Transport and Environment*, 15(6):315–325, 2010. ISSN 1361-9209. doi: 10.1016/j.trd.2010.03.007. (cited on pp. 63, 78).

Haywood, L. and M. Koning. Estimating crowding costs in public transport. Discussion Papers of DIW Berlin 1293, DIW Berlin, German Institute for Economic Research, Apr. 2013. (cited on p. 15).

Hensher, D. A. The valuation of commuter travel time savings for car drivers: Evaluating alternative model specifications. *Transportation*, 28:101–118, 2001. (cited on p. 30).

Hensher, D. A. and J. M. Rose. Developement of commuter and non-commuter mode choice models for the assessment of new public transport infrastructure projects: A case study. *Transportation Research Part A: Policy and Practice*, 41:428–443, 2007. ISSN 0965-8564. doi: 10.1016/j.tra.2006.09.006. (cited on p. 30).

Hess, S., A. Erath, and K. W. Axhausen. Zeitwerte im Personenverkehr: Wahrnehmungs- und Distanzabhängigkeit. Report for research project 2005/007, Vereinigung Schweizerischer Verkehrsingenieure (SVI), 2008. See www.astra.admin.ch. (cited on p. 30).

High Level Group on Transport Infrastructure Charging. Calculating Transport Accident Costs. Final report of the expert advisors to the high level group on infrastructure charging, 1999. URL http://ec.europa.eu/transport/infrastructure/doc/crash-cost.pdf. (cited on pp. 103, 134).

Holland, J. *Adaptation in Natural and Artificial Systems*. Bradford Books, 1992. Reprint edition. (cited on p. 45).

Horni, A., K. Nagel, and K. W. Axhausen, editors. *The Multi-Agent Transport Simulation MATSim*. Ubiquity, London, 2016. doi: 10.5334/baw. URL http://matsim.org/the-book. (cited on pp. 8, 9, 68, 173, 175).

Hsu, J. GM and Lyft Team Up for Robot Taxi Service. IEEE Spectrum, 04.01.2016, Jan. 2016. URL http://spectrum.ieee.org/cars-that-think/transportation/self-driving/gm-and-lyft-team-up-for-robot-taxi-service. (cited on p. 140).

Hülsmann, F., R. Gerike, B. Kickhöfer, K. Nagel, and R. Luz. Towards a multi-agent based modeling approach for air pollutants in urban regions. In *Conference on "Luftqualität an Straßen"*, pages 144–166. Bundesanstalt für Straßenwesen, FGSV Verlag GmbH, 2011. ISBN 978-3-941790-77-3. (cited on pp. 123, 152).

infas and DLR. Mobilität in Deutschland 2008 – Ergebnisbericht. Technical Report FE Nr. 70.801/2006, Institut für angewandte Sozialwissenschaft, Deutsches Zentrum für Luft- und Raumfahrt, 2010. URL http://daten.clearingstelle-verkehr.de/223/. (cited on pp. 50, 142).

INFRAS. Handbook Emission Factors for Road Transport 3.1. Technical report, INFRAS Zurich Switzerland, 2010. URL http://www.hbefa.net. (cited on pp. 120, 123, 152).

Ising, H., T. Günther, C. Havestedt, C. Krause, B. Markert, H. U. Melchert, G. Schoknecht, W. Thefeld, and K. W. Tietze. Lärmbeurteilung – Extra-aurale Wirkungen. Arbeitswissenschaftliche Erkenntnisse Nr. 98, Bundesanstalt für Arbeitsschutz und Arbeitsmedizin, Dortmund, 1996. (cited on pp. 62, 78).

ITP and BVU. Prognose der deutschlandweiten Verkehrsverflechtungen 2025. Technical report, Intraplan Consult GmbH, Beratergruppe Verkehr+Umwelt GmbH, 2007. URL http://daten.clearingstelle-verkehr.de/220/. (cited on p. 124).

ITP and VWI. Standardisierte Bewertung. Technical report, Intraplan Consult GmbH, Verkehrswissenschaftliches Institut Stuttgart GmbH, 2006. (cited on p. 63).

Jansson, K. Optimal Public Transport Price and Service Frequency. *Journal of Transport Economics and Policy*, 27(1):33–50, 1993. (cited on p. 15).

Kaddoura, I. Marginal Congestion Cost Pricing in a Multi-Agent Simulation: Investigation of the Greater Berlin Area. *Journal of Transport Economics and Policy*, 49(4):560–578, 2015. (cited on pp. xi, 7, 30, 31, 32, 33, 42, 104, 110).

Kaddoura, I. and B. Kickhöfer. Optimal Road Pricing: Towards an Agent-based Marginal Social Cost Approach. VSP Working Paper 14-01, TU Berlin, Transport Systems Planning and Transport Telematics, 2014. URL http://www.vsp.tu-berlin.de/publications. (cited on pp. 31, 33, 42, 104).

Kaddoura, I. and K. Nagel. Activity-based computation of marginal noise exposure costs: Implications for traffic management. *Transportation Research Record*, 2597, 2016a. doi: 10.3141/2597-15. (cited on p. 90).

Kaddoura, I. and K. Nagel. Agent-based congestion pricing and transport routing with heterogeneous values of travel time savings. *Procedia Computer Science*, 83:908–913, 2016b. doi: 10.1016/j.procs.2016.04.184. (cited on pp. 7, 30).

Kaddoura, I. and K. Nagel. Simultaneous internalization of traffic congestion and noise exposure costs. *Transportation*, 45(5):1579–1600, 2018. doi: 10.1007/s11116-017-9776-0. (cited on pp. 7, 102).

Kaddoura, I. and K. Nagel. Congestion pricing in a real-world oriented agent-based simulation context. *Research in Transportation Economics*, 74:40–51, 2019. doi: 10.1016/j.retrec.2019.01.002. (cited on pp. 7, 40).

Kaddoura, I., B. Kickhöfer, A. Neumann, and A. Tirachini. Agent-based optimisation of public transport supply and pricing: Impacts of activity scheduling decisions and simulation randomness. *Transportation*, 42(6):1039–1061, 2015a. ISSN 0049-4488. doi: 10.1007/s11116-014-9533-6. (cited on pp. 7, 14, 15, 18, 21).

Kaddoura, I., B. Kickhöfer, A. Neumann, and A. Tirachini. Optimal public transport pricing: Towards an agent-based marginal social cost approach. *Journal of Transport Economics and Policy*, 49(2):200–218, 2015b. (cited on p. 14).

Kaddoura, I., A. Agarwal, and B. Kickhöfer. Simulation-based optimization of congestion, noise and air pollution costs: the impact of transport users' choice dimensions. In *ITEA Annual Conference and School on Transportation Economics*, 2017a. (cited on p. 120).

Kaddoura, I., L. Kröger, and K. Nagel. An activity-based and dynamic approach to calculate road traffic noise damages. *Transportation Research Part D: Transport and Environment*, 54:335–347, 2017b. ISSN 1361-9209. doi: 10.1016/j.trd.2017.06.005. (cited on pp. 62, 82).

Kaddoura, I., L. Kröger, and K. Nagel. User-specific and dynamic internalization of road traffic noise exposures. *Networks and Spatial Economics*, 17(1):153–172, 2017c. doi: 10.1007/s11067-016-9321-2. (cited on pp. 7, 78).

Kaddoura, I., J. Bischoff, and K. Nagel. Towards welfare optimal operation of innovative mobility concepts: External cost pricing in a world of shared autonomous vehicles. VSP Working Paper 18-01, TU Berlin, Transport Systems Planning and Transport Telematics, 2018. URL http://www.vsp.tu-berlin.de/publications. (cited on pp. 7, 140).

Kickhöfer, B. and J. Kern. Pricing local emission exposure of road traffic: An agent-based approach. *Transportation Research Part D: Transport and Environment*, 37(1):14–28, 2015. ISSN 1361-9209. doi: 10.1016/j.trd.2015.04.019. (cited on pp. 78, 97, 115, 117, 121, 123).

Kickhöfer, B. and K. Nagel. Towards High-Resolution First-Best Air Pollution Tolls. *Networks and Spatial Economics*, 16(1):175–198, 2016. doi: 10.1007/s11067-013-9204-8. (cited on pp. 115, 124).

Kickhöfer, B., D. Grether, and K. Nagel. Income-contingent user preferences in policy evaluation: application and discussion based on multi-agent transport simulations. *Transportation*, 38(6):849–870, 2011. ISSN 0049-4488. doi: 10.1007/s11116-011-9357-6. (cited on pp. 19, 30, 116).

Kickhöfer, B., F. Hülsmann, R. Gerike, and K. Nagel. Rising car user costs: comparing aggregated and geo-spatial impacts on travel demand and air pollutant emissions. In Vanoutrive, T. and A. Verhetsel, editors, *Smart Transport Networks: Decision Making, Sustainability and Market structure*, NECTAR Series on Transportation and Communications Networks Research, pages 180–207. Edward Elgar Publishing Ltd, 2013. ISBN 978-1-78254-832-4. doi: 10.4337/9781782548331.00014. (cited on pp. 19, 103, 123, 152).

Korzhenevych, A., N. Dehnen, J. Bröcker, M. Holtkamp, H. Meier, G. Gibson, A. Varma, and V. Cox. Update of the Handbook on External Costs of Transport. Technical report, European Commission – DG Mobility and Transport, 2014. (cited on p. 102).

Krapf, K.-G. and S. Ibbeken. Lärmkartierung 2012 für den Ballungsraum Berlin. Technical report, Wölfel Beratende Ingenieure GmbH und Co. KG in Zusammenarbeit mit Lärmkontor GmbH, 2012. (cited on pp. xii, 73, 74).

Kraus, M. Discomfort externalities and marginal cost transit fares. *Journal of Urban Economics*, 29: 249–259, 1991. (cited on pp. 14, 15, 26, 141).

Krzyzanowski, M., B. Kuna-Dibbert, and J. Schneider. Health effects of transport-related air pollution. Technical report, World Health Organization (WHO), 2005. ISBN 92 890 1373 7. (cited on p. 2).

Kühnel, N., I. Kaddoura, and Möckel. Incorporation of noise shielding in an agent-based transport model by using volunteered geographic data. *Procedia Computer Science*, 151:808–813, 2019. doi: 10.1016/j.procs.2019.04.110. (cited on p. 162).

Lam, K. and Y. T. Chung. Exposure of urban populations to road traffic noise in Hong Kong. *Transportation Research Part D: Transport and Environment*, 17:466–472, 2012. doi: 10.1016/j.trd.2012.05.003. (cited on p. 63).

Lam, W. H. K., C.-Y. Cheung, and C. F. Lam. A study of crowding effects at the Hong Kong light rail transit stations. *Transportation Research Part A*, 33:401–415, 1999. (cited on p. 15).

Lämmel, G. and G. Flötteröd. Towards system optimum: Finding optimal routing strategies in time-tependent networks for large-scale evacuation problems. In Mertsching, B., M. Hund, and Z. Aziz, editors, *KI 2009: Advances in Artificial Intelligence*, volume 5803 of *LNCS (LNAI)*, pages 532–539. Springer, Berlin, 2009. doi: 10.1007/978-3-642-04617-9_67. (cited on p. 41).

Levinson, D. Equity effects of road pricing: a review. *Transport Reviews*, 30(1):33–57, 2010. (cited on pp. 109, 116).

Levinson, D. M. and P. Rafferty. Delayer Pays Principle: Examining Congestion Pricing With Compensation. *International Journal of Transport Economics*, 31(3):295–311, 2004. (cited on p. 41).

Li, Z., Y. Wang, W. H. K. Lam, A. Sumalee, and K. Choi. Design of Sustainable Cordon Toll Pricing Schemes in a Monocentric City. *Networks and Spatial Economics*, 14(2):133–158, 2014. ISSN 1572-9427. doi: 10.1007/s11067-013-9209-3. (cited on p. 120).

Lin, X., C. M. J. Tampère, F. Viti, and B. Immers. The Cost of Environmental Constraints in Traffic Networks: Assessing the Loss of Optimality. *Networks and Spatial Economics*, pages 1–21, 2014. doi: 10.1007/s11067-014-9228-8. (cited on p. 78).

Litman, T. Autonomous Vehicle Implementation Predictions. *Victoria Transport Policy Institute*, 2017a. URL http://www.vtpi.org/avip.pdf. (cited on pp. 140, 141).

Litman, T. Transportation Cost and Benefit Analysis II - Travel Time Costs. Technical report, Victoria Transport Policy Institut, 2017b. (cited on pp. 140, 145).

Liu, J., K. M. Kockelman, P. M. Boesch, and F. Ciari. Tracking a system of shared autonomous vehicles across the Austin, Texas network using agent-based simulation. *Transportation*, 44(6):1261–1278, Nov. 2017. ISSN 1572-9435. doi: 10.1007/s11116-017-9811-1. (cited on p. 141).

Lloyd, A. H. Analysis of Strategies To Control Traffic Noise at the Source: Implications for Policy Makers. *Transportation Research Record*, 1626:41–48, 1998. (cited on p. 90).

Lyft. Webpage of the on-demand mobility service provider Lyft, Inc., 2019. URL https://www.lyft.com. Accessed 15 March 2019. (cited on p. 5).

Maciejewski, M. Dynamic Transport Services. In Horni et al. (2016), chapter 23. doi: 10.5334/baw. URL http://matsim.org/the-book. (cited on p. 8).

Maciejewski, M. and J. Bischoff. Large-scale Microscopic Simulation of Taxi Services. *Procedia Computer Science*, 52:358–364, 2015. ISSN 1877-0509. doi: 10.1016/j.procs.2015.05.107. (cited on pp. 141, 154).

Maciejewski, M., J. Bischoff, S. Hörl, and K. Nagel. Towards a Testbed for Dynamic Vehicle Routing Algorithms. In Bajo, J., Z. Vale, K. Hallenborg, A. P. Rocha, P. Mathieu, P. Pawlewski, E. Del Val, P. Novais, F. Lopes, N. D. Duque Méndez, V. Julián, and J. Holmgren, editors, *Highlights of Practical Applications of Cyber-Physical Multi-Agent Systems: International Workshops of PAAMS 2017, Porto, Portugal, June 21-23, 2017, Proceedings*, pages 69–79. Springer International Publishing, 2017. ISBN 978-3-319-60285-1. doi: 10.1007/978-3-319-60285-1. (cited on p. 8).

Maibach, M., D. Schreyer, D. Sutter, H. van Essen, B. Boon, R. Smokers, A. Schroten, C. Doll, B. Pawlowska, and M. Bak. Handbook on estimation of external costs in the transport sector. Technical report, CE Delft, 2008. URL http://ec.europa.eu/transport/sites/transport/files/themes/sustainable/doc/2008_costs_handbook.pdf. Internalisation Measures and Policies for All external Cost of Transport (IMPACT). (cited on pp. xvi, 2, 3, 15, 43, 56, 87, 90, 102, 103, 115, 120, 123, 124).

Makarewicz, R. and M. Galuszka. Road traffic noise prediction based on speed-flow diagram. *Applied Acoustics*, 72(4):190–195, 2011. (cited on pp. 102, 116, 120).

Marshall, A. *Principles of Economics*. London: Macmillan and Co., Ltd., 1920. URL http://www.econlib.org/library/Marshall/marP.html. (cited on p. 3).

Martinez, L. M., G. H. A. Correia, and J. M. Viegas. An agent-based simulation model to assess the impacts of introducing a shared-taxi system: an application to Lisbon (Portugal). *Journal of Advanced Transportation*, 49(3):475–495, July 2014. doi: 10.1002/atr.1283. (cited on p. 140).

MATSim-VSP. Webpage of the MATSim Open Berlin Scenario provided by the Department of Transportation System Planning and Telematics (VSP) at Technische Universität Berlin, 2019. URL https://github.com/matsim-vsp/matsim-berlin. Accessed 15 March 2019. (cited on p. 50).

Mohring, H. Optimization and Scale Economics in Urban Bus Transportation. *American Economic Review*, 62(4):591–604, 1972. ISSN 0002-8282. (cited on pp. 14, 15, 25).

MOIA. Webpage of the ride-pooling service provided by MOIA GmbH, 2019. URL https://www.moia.io/. Accessed 15 March 2019. (cited on p. 156).

MoT. Webpage of the Ministry of Transport (MoT) by the Government of Singapore about Electronic Road Pricing (ERP), 2019. URL https://www.mot.gov.sg/about-mot/land-transport/motoring/erp. Accessed 15 March 2019. (cited on p. 5).

Murphy, E. and E. A. King. Strategic environmental noise mapping: Methodological issues concerning the implementation of the EU Environmental Noise Directive and their policy implications. *Environment International*, 36(3):290–298, 2010. doi: 10.1016/j.envint.2009.11.006. (cited on pp. 63, 75, 78).

Nagel, K. and G. Flötteröd. Agent-based traffic assignment: Going from trips to behavioural travelers. In Pendyala, R. and C. Bhat, editors, *Travel Behaviour Research in an Evolving World – Selected papers from the 12th international conference on travel behaviour research*, pages 261–294. International Association for Travel Behaviour Research, 2012. ISBN 978-1-105-47378-4. (cited on p. 9).

Nagel, K., D. Grether, U. Beuck, Y. Chen, M. Rieser, and K. Axhausen. Multi-agent transport simulations and economic evaluation. *Journal of Economics and Statistics (Jahrbücher für Nationalökonomie und Statistik)*, 228(2+3):173–194, 2008. (cited on p. 41).

Nagel, K., B. Kickhöfer, and J. W. Joubert. Heterogeneous tolls and values of time in multi-agent transport simulation. *Procedia Computer Science*, 32:762–768, 2014. ISSN 1877-0509. doi: 10.1016/j.procs.2014.05.488. (cited on pp. 34, 37).

Nash, C. UNIfication of accounts and marginal costs for Transport Efficiency (UNITE). Final Report for Publication, Funded by 5th Framework RTD Programme, 2003. (cited on pp. 2, 15, 102).

Neumann, A., M. Balmer, and M. Rieser. Converting a Static Trip-Based Model Into a Dynamic Activity-Based Model to Analyze Public Transport Demand in Berlin. In Roorda, M. and E. Miller, editors, *Travel Behaviour Research: Current Foundations, Future Prospects*, chapter 7, pages 151–176. International Association for Travel Behaviour Research (IATBR), 2014. ISBN 9781304715173. (cited on pp. xi, 10, 35, 36, 68, 73, 81, 92, 93, 106).

Neumann, A., I. Kaddoura, and K. Nagel. Mind the gap – Passenger arrival patterns in multi-agent simulations. *International Journal of Transportation*, 4(1):27–40, 2016. doi: 10.14257/ijt.2016.4.1.02. (cited on pp. 7, 23, 57).

Nielsen, H. L., H. Bendtsen, J. Kielland, E. Bechmann, S. Ljunggren, C. Göransson, K. Strömmer, S.-L. Paikkala, A. Jansson, P. Tómasson, J. Kragh, H. Jonasson, U. Sandberg, S. Storheier, and J. Parmanen. *Road Traffic Noise. Nordic Prediction Method.* TemaNord. The Nordic Council of Ministers, 1996. (cited on pp. 62, 64, 66, 91, 105).

Noland, R., M. Quddus, and W. Ochieng. The effect of the London congestion charge on road casualties: an intervention analysis. *Transportation*, 35(1):73–91, 2008. ISSN 0049–4488. doi: 10.1007/s11116-007-9133-9. (cited on p. 103).

de Palma, A., R. Lindsey, and E. Quinet. Time-Varying Road Pricing and Choice of Toll Locations. *Research in Transportation Economics*, 9(Supplement C):107–131, 2004. ISSN 0739-8859. doi: 10.1016/S0739-8859(04)09005-5. (cited on p. 41).

de Palma, A., M. Kilani, and S. Proost. Discomfort in mass transit and its implication for scheduling and pricing. *Transportation Research Part B*, 71:1–18, 2015a. doi: http://dx.doi.org/10.1016/j.trb.2014.10.001. (cited on p. 15).

de Palma, A., R. Lindsey, and N. Picard. Trip-timing decisions and congestion with household scheduling preferences. *Economics of Transportation*, 4(1):118–131, 2015b. ISSN 2212-0122. doi: 10.1016/j.ecotra.2015.02.001. (cited on p. 41).

Parry, I. and K. Small. Does Britain or the United States Have the Right Gasoline Tax? *The American Economic Review*, 95(4):1276–1289, 2005. doi: 10.1257/0002828054825510. (cited on p. 2).

Parry, I. W. H. and K. A. Small. Should urban transit subsidies be reduced? *American Economic Review*, 99:700–724, 2009. (cited on pp. 2, 15, 102).

Percoco, M. The effect of road pricing on traffic composition: Evidence from a natural experiment in Milan, Italy. *Transport Policy*, 31(0):55–60, 2014. ISSN 0967-070X. doi: 10.1016/j.tranpol.2013.12.001. (cited on p. 103).

Percoco, M. Heterogeneity in the reaction of traffic flows to road pricing: a synthetic control approach applied to Milan. *Transportation*, 42(6):1063–1079, 2015. ISSN 0049–4488. doi: 10.1007/s11116-014-9544-3. (cited on p. 103).

Pigou, A. *The Economics of Welfare*. MacMillan, New York, 1920. (cited on pp. 3, 40, 90, 102, 141).

Planco, ITP, and TUBS. Grundsätzliche Überprüfung und Weiterentwicklung der Nutzen-Kosten-Analyse im Bewertungsverfahren der Bundesverkehrswegeplanung. Endbericht FE Projekt Nr. 960974/2011, Planco GmbH, Intraplan Consult GmbH, TU Berlin Service GmbH, 2015. Im Auftrag des BMVI. (cited on pp. 145, 155).

Proost, S. and K. van Dender. The welfare impacts of alternative policies to address atmospheric pollution in urban road transport. *Regional Science and Urban Economics*, 31(4):383–411, 2001. ISSN 0166-0462. doi: 10.1016/S0166-0462(00)00079-X. (cited on pp. 4, 14, 103).

Prud'homme, R., M. Koning, L. Lenormand, and A. Fehr. Public transport congestion costs: The case of the Paris subway. *Transport Policy*, 21(C):101–109, 2012. (cited on p. 15).

Rau, G., K. Roßner, and P. van den Brulle. Bildschirmarbeit – Lärmminderung in Mehrpersonenbüros. Arbeitswissenschaftliche Erkenntnisse Nr. 124, Bundesanstalt für Arbeitsschutz und Arbeitsmedizin, Dortmund, 2003. ISSN 0720-1699. (cited on p. 64).

Reed, T. and J. Kidd. 2018 Global Traffic Scorecard Report. Technical report, INRIX, Feb. 2019. (cited on p. 2).

Rieser, M. *Adding Transit to an Agent-Based Transportation Simulation: Concepts and Implementation*. PhD thesis, 2010. (cited on p. 8).

Rieser, M. Modeling Public Transport with MATSim. In Horni et al. (2016), chapter 16. doi: 10.5334/baw. URL http://matsim.org/the-book. (cited on p. 8).

RPS. Roma to Brisbane Pipeline - Dalby Compressor Station Upgrade: Environmental Management Plan. Technical report, RPS Australia East Pty Ltd, Sonus Pty Ltd, 2011. (cited on p. 64).

RSB. Municipality of Munich: Referat für Stadtplanung und Bauordnung, 2005. (cited on p. 124).

Rückert-John, J., I. Bormann, and R. John. Umweltbewusstsein in Deutschland 2012. Technical report, Bundesministerium für Umwelt, Naturschutz und Reaktorsicherheit, 2013. URL http://www.umweltbundesamt.de/publikationen/umweltbewusstsein-in-deutschland-2012. (cited on p. 62).

Ruiz-Padillo, A., A. J. Torija, A. Ramos-Ridao, and D. P. Ruiz. A methodology for classification by priority for action: Selecting road stretches for network noise action plans. *Transportation Research Part D: Transport and Environment*, 29:66–78, 2014. doi: 10.1016/j.trd.2014.04.002. (cited on pp. 63, 78, 87).

Schade, J. and B. Schlag. Acceptability of urban transport pricing. Research Report 72, VATT, Helsinki, 2000. URL www.vatt.fi/en/publications. ISBN 951-561-354-X. (cited on p. 4).

Schlechte, T. and A. Tanner. Railway capacity auctions with dual prices. Technical Report 10-10, Konrad-Zuse-Zentrum für Informationstechnik Berlin (ZIB), 2010. (cited on p. 45).

SenStadt. Umweltatlas Berlin; Strategische Lärmkarten (Ausgabe 2012) / Berechnungsergebnisse / tabellarische Auswertungen. Senatsverwaltung für Stadtentwicklung Berlin, 2012a. URL http://www.stadtentwicklung.berlin.de/umwelt/umweltatlas/e_tab/ta705_04-06.xls. Accessed 26 January 2015. (cited on pp. 62, 90).

SenStadt. Umweltatlas Berlin; Strategische Lärmkarten; Straßenverkehr; Lärmindex LDEN. Senatsverwaltung für Stadtentwicklung Berlin, 2012b. URL http://www.stadtentwicklung.berlin.de. (cited on pp. 62, 73, 74).

Sharon, G., M. W. Levin, J. P. Hanna, T. Rambha, S. D. Boyles, and P. Stone. Network-wide adaptive tolling for connected and automated vehicles. *Transportation Research Part C: Emerging Technologies*, 84:142–157, 2017. doi: 10.1016/j.trc.2017.08.019. (cited on p. 141).

Shefer, D. and P. Rietveld. Congestion and Safety on Highways: Towards an Analytical Model. *Urban Studies*, 34(4):679–692, 1997. (cited on pp. 103, 120, 134).

Shepherd, S. P. The effect of complex models of externalities on estimated optimal tolls. *Transportation*, 35 (4):559–577, 2008. ISSN 0049–4488. doi: 10.1007/s11116-007-9157-1. (cited on pp. 103, 120).

Simoni, M. D., K. M. Kockelman, K. M. Gurumurthy, and J. Bischoff. Congestion Pricing in a World of Self-driving vehicles: an Analysis of Different Strategies in Alternative Future Scenarios. *Transportation Research Part C: Emerging Technologies*, 98:167–185, Jan. 2019. doi: 10.1016/j.trc.2018.11.002. (cited on p. 141).

Small, K. A. and E. T. Verhoef. *The economics of urban transportation*. Routledge, 2007. ISBN 9780415285148. (cited on pp. 2, 3, 4, 14, 90, 102).

Solé-Ribalta, A., S. Gómez, and A. Arenas. Decongestion of Urban Areas with Hotspot Pricing. *Networks and Spatial Economics*, pages 1–18, 2017. ISSN 1572-9427. doi: 10.1007/s11067-017-9349-y. (cited on p. 121).

Spieser, K., K. Treleaven, R. Zhang, E. Frazzoli, D. Morton, and M. Pavone. Toward a systematic approach to the design and evaluation of automated mobility-on-demand systems: A case study in Singapore. In *Road Vehicle Automation*, pages 229–245. Springer, 2014. URL http://hdl.handle.net/1721.1/82904. (cited on p. 140).

Stassen, K. R., P. Collier, and R. Torfs. Environmental burden of disease due to transportation noise in Flanders (Belgium). *Transportation Research Part D: Transport and Environment*, 13:355–358, 2008. doi: 10.1016/j.trd.2008.04.003. (cited on pp. 62, 78).

Tanner, A. and K. Mitusch. Trassenvermarktung: Auktion versus Listenpreisverfahren. *Internationales Verkehrswesen*, 63(3):15–19, 2011. (cited on p. 45).

Tenailleau, Q. M., N. Bernard, S. Pujol, H. Houot, D. Joly, and F. Mauny. Assessing residential exposure to urban noise using environmental models: does the size of the local living neighborhood matter? *Journal of Exposure Science and Environmental Epidemiology*, 25:89–96, 2015. doi: 10.1038/jes.2014.33. (cited on p. 63).

TfL. Wepbage of the integrated transport authority Transport for London (TfL), 2019. URL https://tfl.gov.uk/fares/. Accessed 15 March 2019. (cited on p. 5).

Tirachini, A. The economics and angineering of bus stops: Spacing, design and congestion. *Transportation Reserach Part A*, 59:37–57, 2014. (cited on p. 15).

Tirachini, A. and D. A. Hensher. Multimodal Transport Pricing: First Best, Second Best and Extensions to Non-motorized Transport. *Transport Reviews*, 32:181–202, 2012. (cited on p. 4).

Tirachini, A., D. A. Hensher, and J. M. Rose. Multimodal pricing and optimal design of urban public transport: The interplay between traffic congestion and bus crowding. *Transportation Research Part B: Methodological*, 61:33–54, 2014. ISSN 0191-2615. doi: 10.1016/j.trb.2014.01.003. (cited on pp. xv, 15, 19, 20).

Trommer, S., V. Kolarova, F. E., L. Kröger, B. Kickhöfer, T. Kuhnimhof, B. Lenz, and P. Phleps. Autonomous Driving: The Impact of Vehicle Automation on Mobility Behaviour. Institute for Mobility Research (ifmo), 2016. (cited on pp. 140, 145, 155).

Truong, L. T., C. De Gruyter, G. Currie, and A. Delbosc. Estimating the trip generation impacts of autonomous vehicles on car travel in Victoria, Australia. *Transportation*, 44(6):1279–1292, Nov. 2017. ISSN 1572-9435. doi: 10.1007/s11116-017-9802-2. (cited on p. 140).

Turvey, R. and H. Mohring. Optimal Bus Fares. *Journal of Transport Economics and Policy*, 9(3):280–286, 1975. (cited on pp. 14, 15, 17, 26, 141).

Uber. Webpage of the on-demand mobility service provider Uber Technologies Inc., 2019. URL https://www.uber.com/. Accessed 15 March 2019. (cited on p. 5).

van den Berg, V. and E. Verhoef. Winning or Losing from Dynamic Bottleneck Congestion Pricing?: The Distributional Effects of Road Pricing with Heterogeneity in Values of Time and Schedule Delay. *Journal of Public Economics*, 95(7–8):983–992, 2011. doi: 10.1016/j.jpubeco.2010.12.003. (cited on p. 30).

van den Berg, V. A. *Congestion Pricing With Heterogeneous Travellers*. PhD thesis, Tinbergen Institute, 2011. (cited on pp. 7, 41).

van Essen, H., B. Boon, A. Schroten, M. Otten, M. Maibach, C. Schreyer, C. Doll, P. Jochem, M. Bak, and B. Pawlowska. Internalisation measures and policy for the external cost of transport. Technical report, Delft, CE, 2008. (cited on p. 14).

Verhoef, E. Marginal Cost Based Pricing in Transport. Key Implementation Issues from the Economic Perspective, 2001. Paper presented at Seminar One of IMPRINT-EUROPE. (cited on pp. 2, 4, 14).

Verhoef, E. Inside the queue: hypercongestion and road pricing in a continuous time?continuous place model of traffic congestion. *Journal of Urban Economics*, 54:531–565, 2003. (cited on p. 41).

Verhoef, E. T. and J. Rouwendal. A Structural Model of Traffic Congestion: Endogenizing speed choice, traffic safety and time losses. Technical report, Department of Spatial Economics, Free University Amsterdam, 2003. (cited on pp. 103, 120).

Verhoef, E. T. and K. A. Small. Product Differentiation on Roads: Constrained Congestion Pricing with Heterogeneous Users. *Journal of Transport Economics and Policy*, 38(1):127–156, 2004. (cited on pp. 30, 141).

Vickrey, W. Congestion Theory and Transport Investment. *The American Economic Review*, 59(2): 251–260, 1969. (cited on pp. 3, 30, 41, 46, 56, 57, 78, 120, 141).

Vickrey, W. Pricing, metering and the efficient use of urban transportation facilities. *Highway Research Record*, 476:36–48, 1973. (cited on pp. 4, 30).

Walton, H. and et al. Understanding the Health Impacts of Air Pollution in London. Technical report, King's College London, 2015. URL https://www.london.gov.uk/sites/default/files/HIAinLondon_KingsReport_14072015_final_0.pdf. (cited on p. 2).

Wang, J., L. Chi, X. Hu, and H. Zhou. Urban traffic congestion pricing model with the consideration of carbon emissions cost. *Sustainability*, 6(2):676–691, 2014. doi: 10.3390/su6020676. (cited on p. 103).

Wardman, M. and G. Whelan. Twenty years of rail crowding valuation studies: Evidence and lessons from British experience. *Transport Reviews*, 31(3):379–398, 2011. (cited on p. 15).

WG-AEN. Good Practice Guide for Strategic Noise Mapping and the Production of Associated Data on Noise Exposure. Technical report, European Commission Working Group Assessment of Exposure to Noise, 2006. Position Paper, Version 2, Final Draft. (cited on p. 62).

WHO Europe. Night Noise Guidelines for Europe. Technical report, World Health Organization, 2009. URL http://www.euro.who.int/__data/assets/pdf_file/0017/43316/E92845.pdf. (cited on pp. 62, 63, 64, 78).

WHO Europe. Burden of Disease from Environmental Noise. Quantification of Health Life Years Lost in Europe. Technical report, World Health Organisation, 2011. URL http://www.euro.who.int/__data/assets/pdf_file/0008/136466/e94888.pdf. (cited on pp. 2, 62, 78).

Wismans, L., E. van Berkum, and M. Bliemer. Dynamic Traffic Management Measures to Optimize Air Quality, Climate, Noise, Traffic Safety and Congestion: Effects of a Single Objective Optimization. In van Nunen, J. A., P. Huijbregts, and P. Rietveld, editors, *Transitions Towards Sustainable Mobility*, pages 297–313. Springer Berlin Heidelberg, 2011. doi: 10.1007/978-3-642-21192-8_16. (cited on pp. 103, 116, 120).

Wright, L. and W. Hook. Bus Rapid Transit Planning Guide. Technical report, ITDP, Institute for Transportation and Development Policy, New York, 2007. (cited on p. 18).

Xiong, C. and L. Zhang. A positive model of departure time choice under road pricing and uncertainty. *Transportat Research Record*, (2345):117–125, 2013. (cited on p. 57).

Ziemke, D., K. Nagel, and C. Bhat. Integrating CEMDAP and MATSim to increase the transferability of transport demand models. *Transportation Research Record*, 2493:117–125, 2015. doi: 10.3141/2493-13. (cited on p. 50).

Ziemke, D., I. Kaddoura, and K. Nagel. The MATSim Open Berlin Scenario: A multimodal agent-based transport simulation scenario based on synthetic demand modeling and Open Data. *Procedia Computer Science*, 151:870–877, 2019. doi: 10.1016/j.procs.2019.04.120. (cited on pp. 10, 50, 142, 145, 155).